DNA damage responses in mammalian cells : focus on signaling and repair

Vrouwe, M.G.

DNA DAMAGE RESPONSES IN MAMMALIAN CELLS
FOCUS ON SIGNALING AND REPAIR

Mischa G. Vrouwe

Lay-out and printing: Off Page, www.offpage.nl

DNA DAMAGE RESPONSES IN MAMMALIAN CELLS
FOCUS ON SIGNALING AND REPAIR

proefschrift
ter verkrijging van
de graad van Doctor aan de Universiteit Leiden
op gezag van de Rector Magnificus prof. mr. P.F. van der Heijden,
volgens het besluit van het College voor Promoties
te verdedigen op dinsdag 20 november 2012
klokke 15.00 uur

door

Mischa G. Vrouwe
geboren te Ter Aar
in 1975

PROMOTIECOMMISSIE:

Promotor:	Prof. Dr. L.H.F. Mullenders
Overige leden:	Prof. Dr. J. Brouwer
	Dr. W. Vermeulen (Erasmus MC)
	Dr. J.P. de Winter (VUmc)

TABLE OF CONTENTS

1

Introduction

1.1 DNA DAMAGE AND REPAIR

Since the discovery of DNA in 1869 by Friedrich Miescher our understanding of its function has grown considerably. Initially the importance of DNA might not have been appreciated but subsequent experimentation, amongst others by Fredrick Griffith (Griffith, 1928) and Oswald Avery and co-workers (Avery et al., 1944), laid the foundation for our current understanding of DNA being the carrier of genetic, hereditary information. Conservation of the genetic information is of great importance as changes, in the form of DNA mutations, have the potential to contribute to the development of disease. It can be easily perceived that genomic mutations can lead to hereditary illnesses but also cancer, a common non-inherited disease caused by genetic alterations.

One factor that contributes to mutagenesis is damage to the DNA. DNA can be damaged through various processes which can be of endogenous or exogenous origin. Examples of endogenous processes that damage DNA are spontaneous deamination of bases or depurination of DNA as well as damage inferred through reactions involving reactive cellular metabolites such as reactive oxygen species (ROS). In addition to the endogenous processes environmental agents can also damage DNA, either through exposure to certain chemical compounds or by exposure to ultraviolet (UV) or ionizing radiation (IR). Damaged DNA may be toxic for the cell as it can interfere with metabolic processes such as transcription and replication which can lead to cell death (Ljungman et al., 1999;Kaina, 2003). However, perhaps more dangerous is the conversion of DNA damage to a mutation, a process that primarily depends on DNA replication. Once a DNA lesion has been converted into a mutation all information required to restore the original DNA sequence is lost. In contrast to mutations, damaged DNA often represents a reversible situation as the damage can be removed in order to reconstitute the original DNA configuration.

Given the importance of DNA for the health of an organism it is important to realize that chemical moieties of DNA are prone to DNA damage formation either by spontaneous degradation or attacks by endogenous agents. Although the frequency at which DNA lesions are formed within a cell depends to some extend on its environment it has been estimated that a human cell is subject to approximately 10.000 depurination events per day (Lindahl and Nyberg, 1972) as well as around 10.000 ROS induced DNA adducts (Ames and Shigenaga, 1992). Despite these high lesion frequencies the intergeneration mutation rate in humans was found to be low at approximately 1.1×10^{-8} per base pair per generation, which equates to approximately 70 *de novo* mutations per diploid genome (The 1000 Genomes Consortium, 2010;Roach et al., 2010). To maintain such high level of genome integrity cells rely on DNA damage signaling pathways as well as DNA repair mechanisms for efficient removal of DNA lesions. Several pathways have been identified which respond to different types of DNA lesions (Figure1) (Hoeijmakers, 2001).

Nucleotide excision repair (NER) is a mechanism that is capable of removing a wide range of structurally unrelated DNA adducts, including solar UV-induced lesions as well as endogenously induced oxidative DNA lesions. The autosomal recessive disorders xeroderma pigmentosum, Cockayne syndrome, UV sensitivity syndrome and trichothiodystrophy are associated with defects in NER. An overview of NER is given in chapter 2.

Base excision repair (BER) is a pathway that is responsible for removing endogenous base lesions as well as repairing similar lesions generated by environmental agents. Among the base damages that are repaired by BER are ROS induced damages as well as base deaminations and depurinations. Also single strand DNA breaks are repaired via this pathway. Two subpathways have been identified: short-patch BER which depends on polβ for resynthesizing a single nucleotide (Kubota et al., 1996) and long-patch BER which utilizes polδ or polε for repairing a two to eight nucleotide gap (Klungland and Lindahl, 1997). Defects in DNA end processing factors have been associated with the neurological diseases ataxia with oculomotor apraxia type-1 (AOA1) and spinocerebellar ataxia with axonal neuropathy (SCAN1). The BER protein uracil-DNA glycosylase (UNG) also functions in immunoglobulin development and mutation induction in the respective gene can lead to hyper-IgM syndrome (Imai et al., 2003).

Mismatch repair is a pathway that is central to ensuring the fidelity of DNA replication (Hsieh and Yamane, 2008). Its function is to correct base substitution mismatches as well as insertion-deletion mismatches that are formed as a result of replication errors. Mutations in mismatch repair genes cause Lynch syndrome, a hereditary condition that is associated with a high risk of developing colorectal cancer.

Non-homologous end joining (NHEJ) is one of two major pathways that exist for the repair of double strand DNA breaks (DSBs). It functions by detecting and tethering DNA ends, processing of damaged DNA ends and ligation (Lieber, 2008). This method of rejoining broken DNA is regarded as being error prone as it does not require a template

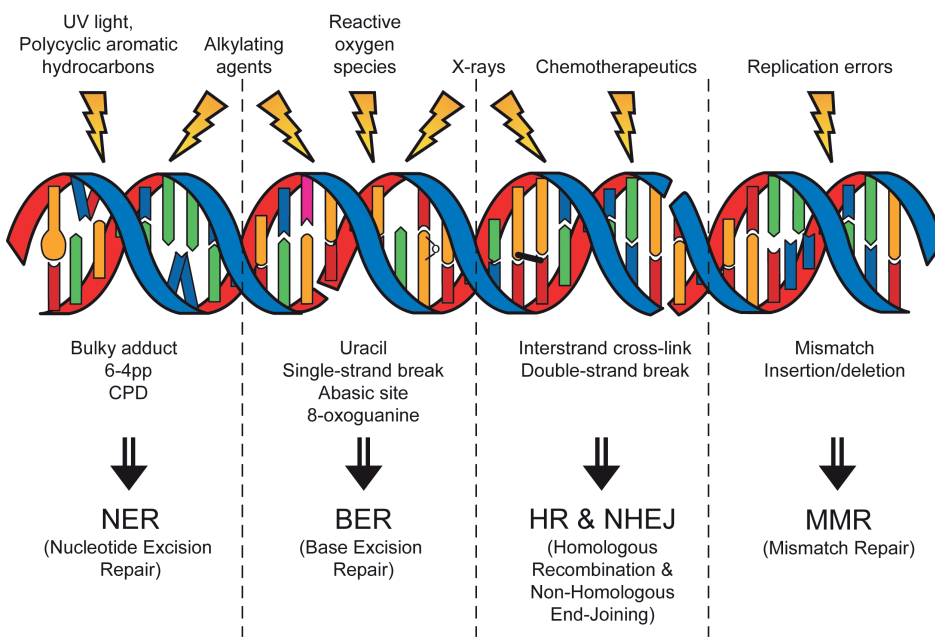

Figure 1: Overview of damage causing agents and resulting DNA adducts along with their respective repair pathway.

DNA for repair. As a result, small insertions or deletions can be found at the ligated break site. In mammalian cells NHEJ is the dominant pathway for repairing DSBs, in particular when cells are in the non-cycling G0/G1 state. Although DSBs can be induced by exogenous factors such as ionizing radiation, they are also created during immunoglobulin development. Consequently, defects in NHEJ can lead to radiation-sensitive severe combined immunodeficiency (RS-SCID) as well as ligase IV syndrome.

Homologous recombination (HR) is the second major pathway for repairing DSBs (Li and Heyer, 2008). Lesions that are repaired by HR include IR-induced DSBs, interstrand crosslinks and collapsed replication forks. HR repair is dependent on a sister chromatid to act as a DNA template and is therefore considered to be relatively error free. The requirement for a sister chromatid consequently restricts this form of repair to the S and G2 phases of the cell cycle where the chromatids are held in proximity by sister chromatid cohesion (Watrin and Peters, 2006). Defects in the HR genes BRCA1 and BRCA2 are linked to hereditary breast cancer.

Complementing these repair pathways are the DNA damage signaling cascades which regulate processes such as cell cycle progression and apoptosis (see also chapter 5). Although DNA repair and DNA damage signaling are distinct entities there exist proteins that function in both processes, for example ATM (Lobrich and Jeggo, 2005), the Mre11/Nbs1/Rad50 complex (Stracker and Petrini, 2011) and the cohesion complex (Yazdi et al., 2002;Kim et al., 2002b). While defects in cell cycle checkpoints are an important and easily measured consequence of defects in DNA damage signaling, the importance of the pathway is likely to reach beyond cell cycle regulation. Phosphoproteomic screens have revealed many proteins with diverse functions to be phosphorylated upon DNA damage, suggesting their functions may be modulated by DNA damage. One example being the regulation of DSB repair through the phosphorylation of Kap1 by the ATM kinase, which is a critical event for the repair of breaks in heterochromatinized DNA (Goodarzi et al., 2008).

1.2 DNA DAMAGE AND SIGNALING

There is overwhelming evidence that recognition of aberrant DNA structures by cellular surveillance proteins can initiate DNA damage signaling. Although damage signaling is often thought of to be synonymous with DNA damage induced checkpoint activation, it should be considered in a broader context of cellular responses to DNA damage. Most notably and in addition to checkpoint activation, DNA damage signaling can lead to induction of processes such as DNA damage repair, to changes in chromatin structure, transcriptional responses and apoptosis. To regulate these processes cells use a plethora of different post-translational modifications (PTM). Here those events most relevant for NER are described.

It has been long recognized that the checkpoint protein p53 becomes upregulated in response to DNA damaging agents such as UV light. In fact, as early as in 1984 it was reported by Maltzman and Czyzyk that p53 becomes stabilized in response to both UV and 4NQO treatment (Maltzman and Czyzyk, 1984). Moreover, these authors noted that while cycling cells were particularly efficient in their p53 response, also non-cycling cells were

able to induce p53 upon DNA damage, an effect that could be enhanced through the use of the DNA synthesis inhibitor hydroxyurea. Back then it was difficult to interpret these data, not least because p53 was thought to be an activator of replication rather than a checkpoint protein that is frequently mutated in tumours. However, ongoing research over the years has given new insights into the molecular mechanisms of both NER (chapter 4) and checkpoint activation allowing us to understand, in part, how these processes are linked.

ATR dependent signaling

ATR is a serine/threonine protein kinase that is part of the PI(3) kinase-like kinase family to which also the ATM, DNA-PKcs, mTOR and SMG1 protein kinases belong (Durocher and Jackson, 2001;Yamashita et al., 2001;Brumbaugh et al., 2004). ATR together with ATM are considered to be the key kinases that orchestrate DNA damage signaling. Moreover there is evidence that each kinase is activated by a distinct DNA structure. For ATM it is the DNA double strand break (DSB) that is considered to be main activating DNA lesion (Lee and Paull, 2005), although other stressors can activate ATM as well (Bakkenist and Kastan, 2003;Kanu and Behrens, 2007;Soutoglou and Misteli, 2008). ATR in contrast is activated by single stranded DNA (ssDNA) containing ssDNA/dsDNA junctions (Zou and Elledge, 2003;MacDougall et al., 2007;Costanzo and Gautier, 2003).

Activation of ATR is particularly important in sensing DNA replication stress (Guo et al., 2000) and to prevent untimely entry into mitosis (Cliby et al., 1998;Nghiem et al., 2001). Detection of ssDNA and initiation of the DNA damage checkpoint is, however, a process that requires several other proteins in addition to ATR itself (figure 1). ATR forms an obligate dimer with ATRIP (Cortez et al., 2001) and it is the latter subunit of the complex that can interact with ssDNA bound RPA (Zou et al., 2003). However, recruitment of ATR to ssDNA is by itself insufficient for kinase activation (MacDougall et al., 2007) as ATR signaling was found to be dependent on the RAD9-RAD1-HUS1 complex (known as 9-1-1) (Bao et al., 2004). The 9-1-1 complex has a heterotrimeric structure bearing similarities with the homotrimeric PCNA complex (Parrilla-Castellar et al., 2004). Analogous to the loading of PCNA onto DNA by the replication factor C (RFC) complex the 9-1-1 complex is loaded onto DNA by an RFC complex containing RAD17 (Majka and Burgers, 2003). Loading of either PCNA or 9-1-1 complexes requires ssDNA/dsDNA junctions but, whereas PCNA is loaded at recessed 3' ends, 9-1-1 is preferentially loaded at 5' template junctions (Ellison and Stillman, 2003). The presence of ssDNA bound RPA is important here as well as this complex directs the loading of 9-1-1 towards the 5' primed DNA (Ellison and Stillman, 2003;Majka et al., 2006).

Both ATR-ATRIP and the 9-1-1 complex are recruited to signaling competent DNA structures independently of one another yet the presence of both complexes still does not suffice for kinase activation. To achieve activation a direct interaction between ATR and its activator TopBP1 (Kumagai et al., 2006;Mordes et al., 2008) is required. A phosphorylation site on RAD9, one of the 9-1-1 complex members, facilitates the interaction with the BRCT domains of TopBP1 and has been proposed to recruit the protein towards the ATR complex (Lee et al., 2007;Delacroix et al., 2007;Furuya et al., 2004;St Onge et al., 2003). However, other reports suggest that recruitment of TopBP1 is mediated directly via ATR-ATRIP (Choi et al., 2010;Yan and Michael, 2009;Rendtlew Danielsen et al., 2009).

Once activated, ATR can phosphorylate checkpoint proteins like H2AX, p53 and CHK1 (Tibbetts et al., 1999;Liu et al., 2000;Ward and Chen, 2001) which can initiate a cell cycle arrest. Also proteins that are crucial for ATR activation like ATRIP, TopBP1 and RAD17 are themselves targets for phosphorylation (Cimprich and Cortez, 2008). The importance of these phosphorylation events is, however, not known. Moreover, large scale phosphoproteomic screens for targets of ATR and ATM have revealed several hundreds of different proteins to be targets for these kinases after DNA damage suggesting that the DNA damage signaling response might effect many additional processes that are still unexplored (Matsuoka et al., 2007;Stokes et al., 2007).

The MDC1 protein complex

A prominent feature of DNA damage mediated ATM/ATR activation, by virtue of H2AX phosphorylation, is the assembly of a multiprotein complex at or near the site of DNA damage in the vicinity of the kinase. Proteins that have thus far been identified as complex members include MDC1, the MRE11/RAD50/NBS1 subcomplex, 53BP1/ULP28, the BRCA1 complex (BRCA1, BARD1, BRCC36, ABRA1, RAP80), the ubiquitin ligases RNF8/HERC1 and RNF168, the sumo ligases PIAS1 and PIAS4, as well as UBC9 and UBC13 (reviewed in Panier and Durocher, 2009;Zlatanou and Stewart, 2010;Ciccia and Elledge, 2010). Complex assembly is achieved through the sequential recruitment of proteins and is regulated by post translational modifications like phosphorylation, ubiquitination and SUMOylation. Recruitment of the first factor, MDC1, is facilitated by the interaction of the MDC1 BRCT domain with phosphorylated H2AX. Subsequent ubiquitination and SUMOylation steps are then essential for full complex assembly i.e. the recruitment of 53BP1 and the BRCA1 complex. Thus far H2A type histones have been identified as targets for ubiquitin modification while BRCA1 was found to be modified by SUMO, however, it is well possible that additional proteins might be subject to these modifications.

The biological significance and functions of this multifactorial complex is perhaps not fully understood, but it is evident that proteins like BRCA1 and 53BP1 function in the DSB repair and checkpoint pathways (FitzGerald et al., 2009;Moynahan et al., 1999;Xu et al., 1999;Wang et al., 2002;Dimitrova et al., 2008). Furthermore, deficiency in H2AX, MDC1, 53BP1, RNF8 and RNF168 all result in immunodeficiency (Manis et al., 2004;Ward et al., 2004;Lou et al., 2006;Stewart et al., 2007;Ramachandran et al., 2010;Celeste et al., 2002).

DNA damage signaling in UV-irradiated cells

In addition to the response to DSB, several components of the MDC1 complex, including MDC1, RNF8 and 53BP1 have been shown to respond to UV-induced DNA damage in an ATR dependent manner (Marteijn et al., 2009;Jowsey et al., 2007). This response is not restricted to replicating cells but also occurs in non-cycling (G0/G1) cells where it depends on functional NER (Marteijn et al., 2009). It should, however, be noted that the complex composition differs in quiescent cells when compared to replicating cells as at least one of its components (BRCA1) is expressed at very low levels in non-dividing cells (Chen et al., 1996;Choudhury et al., 2004; chapter 4). The functional importance of the UV-induced MDC1 complex in quiescent cells has yet to be established. It is clear that ATR dependent

signaling does not affect NER dependent removal of 6-4PP (Auclair et al., 2008; chapter 4) although it is very likely that repair of 6-4PP triggers this response.

Better understanding of which factors contribute to UV mediated checkpoint signaling came from studies using cells with genetic defects in various NER genes. It was demonstrated that impairment of TC-NER results in high p53 expression following treatment with either UV or inhibitors of transcription elongation. These observations led to the conclusion that most probably persistent stalling of RNA polymerase II initiated this signaling response (Ljungman and Zhang, 1996;Ljungman et al., 1999;Yamaizumi and Sugano, 1994). However, it has also been demonstrated that repair of DNA lesions by GG-NER could itself contribute to checkpoint signaling (Matsumoto et al., 2007;Marti et al., 2006). Surprisingly, even in the absence of both GG-NER and persistent RNA polymerase stalling DNA damage checkpoints are still activated through an alternative mechanism involving the endonuclease APE1 (chapter 4). It is surprising that although the DNA damage checkpoint can be induced through distinct mechanisms, they all depend on the ATR kinase to transduce the signal (chapter 4; O'Driscoll et al., 2003;Derheimer et al., 2007).

Poly(ADP-ribosylation) (PAR) is a post translational modification that plays key roles in a wide variety of processes (reviewed in Krishnakumar and Kraus, 2010) including DNA repair. The PAR modification is catalyzed by members of the poly(ADP-ribose) polymerase (PARP) family to which currently 17 proteins are ascribed. Of these the founding member, PARP1 as well as PARP2 have been implicated in DNA repair (de Murcia et al., 1997;Wang et al., 1997;Schreiber et al., 2002).The PAR modification is thought to assert its function through two different mechanisms. Firstly, the addition of ADP-ribose moieties might directly modulate the activities of the target protein through both steric as well as charge effects. Secondly, PAR structures can promote the recruitment of other proteins that contain PAR-specific binding motifs. Currently 3 such sequences have been identified: an 8 amino acid basic residue rich cluster (Gagne et al., 2008), the PAR-binding zincfinger (PBZ) (Ahel et al., 2008) and the macrodomain (Timinszky et al., 2009). A variety of DDR proteins contains PAR-binding motifs, although the significance of these motifs for the protein function in many cases has not been determined. For some of these proteins, however, PAR-dependent recruitment to sites of DNA damage has been observed, for example XRCC1 (Okano et al., 2003), CHFR (Ahel et al., 2008), APLF (Rulten et al., 2008;Kanno et al., 2007;Bekker-Jensen et al., 2007) and ALC1 (Gottschalk et al., 2009; Ahel et al., 2009; chapter 3).

Several DNA repair pathways utilize the PAR modification, most notably SSB repair and DSB repair (both microhomology mediated end joining and homologous recombination) (Wang et al., 2006;Hochegger et al., 2006), although a role in NER has also been proposed (Ghodgaonkar et al., 2008;Berger et al., 1980). The mechanisms by which PARP activity enhances NER are not fully understood but involve both TCR protein CSB as well as GGR (Flohr et al., 2003; chapter 3). The role of PARP in GGR is dependent on UV-DDB, although it is unclear whether UV-DDB directly activates PARP or whether other proteins are involved. The consequence of PARP activation and subsequent PAR synthesis is the recruitment of the chromatin remodeling protein ALC1, which is necessary for efficient repair of CPD lesions (chapter 3). The implication of PARP1 in CSB dependent repair of DNA lesions is based on

the epistatic relationship between the two proteins (Flohr et al., 2003). How PARP1 regulates CSB function or visa versa is currently unknown. CSB has a putative PAR binding site (Gagne et al., 2008); however, it is unclear if and how this contributes to the proteins function.

1.3 COHESINOPATHIES AND DNA DAMAGE

The term cohesinopathy is used to indicate diseases that affect the function of the cohesin complex. To date three such syndromes have been described i.e. Cornelia de Lange Syndrome (CdLS), Roberts Syndrome / SC phocomelia (RBS) and Warsaw Breakage Syndrome (WABS). Disease causing mutations have been identified for all three syndromes and are predicted to affect sister chromatid cohesion (SCC). The establishment and dissolution of SCC has been studied in some detail and it is clear that defects in this process compromise chromosome segregation. In little over a decade it has, however, become apparent that the function of cohesin reaches beyond its role in mitosis by participating in gene regulation (Rollins et al., 1999), DNA repair (Klein et al., 1999) and DNA damage signaling (Kim et al., 2002b). The underlying mechanisms for these diverse processes are not understood in detail, but it is likely that the unique ability for cohesin to shape chromatin topology has led to diversification of its function.

The cohesion complex consists of four subunits: Smc1, Smc3, Rad21 and either one of the SA1 or SA2 paralogues. Both Smc1 and Smc3 are members of a family of proteins known as the structural maintenance of chromosomes superfamily. Smc1 and Smc3 form long antiparallel intramolecular coiled coils by folding back on themselves at a central hinge domain, allowing the N- and C- termini of the protein to interact and form a functional ATPase (Losada and Hirano, 2005). The ATPase heads of Smc1 and Smc3 are linked by the Rad21-SA1/SA2 heterodimer which, combined with the interaction between the Smc1 and Smc3 hinge domains results in a ring-like structure. How cohesin rings interact with chromosomes in order to establish SCC is not exactly known. One model, known as the embrace model, sees both sister chromatids encircled by a single cohesin ring (figure 2) (Gruber et al., 2003). An alternative model, the handcuff model, envisions that both sister chromatids are individually encircled by a cohesin ring, which than are linked together via SA1/SA2 (Zhang et al., 2008b).

In addition to cohesin ring components, several accessory factors are required for cohesion regulation. Loading of cohesin onto chromatin requires the NIPBL-Scc4 complex (also referred to as Scc2-Scc4) (Ciosk et al., 2000). Although SCC can only be established during or after replication, cohesin is already bound to chromatin in G1 phase cells. It is, however, during S phase that cohesin becomes associated with chromatin in a far more stable manner (Gerlich et al., 2006). It is probable that this increased stability is the result of SCC establishment during replication, a process that requires Ctf18 (Lengronne et al., 2006;Terret et al., 2009) and the Esco1 and Esco2 paralogues (Skibbens et al., 1999;Toth et al., 1999). The latter two proteins both have acetyltransferase activity and acetylation of Smc3 is a critical event for establishing SCC (Zhang et al., 2008a;Rolef Ben-Shahar et al., 2008;Unal et al., 2008). Acetylation of Smc3 decreases the association of Wapl and Pds5 with cohesin and hence might regulate stability of the ring (Rowland et al., 2009;Terret et

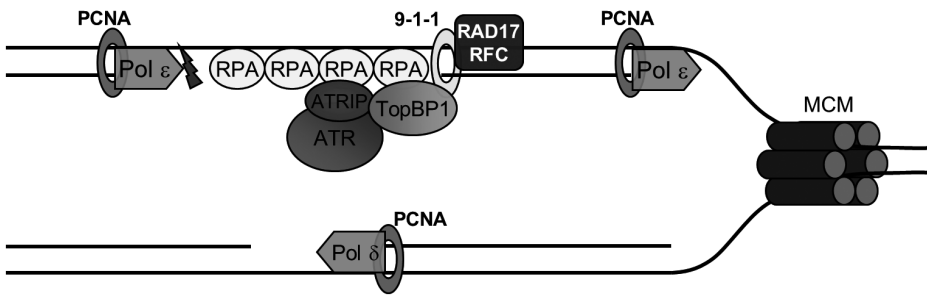

Figure 2:Model of replication fork stalling and ATR activation. DNA lesions can stall replicative DNA polymerases δ and ε. When the helicase becomes uncoupled from the arrested leading strand polymerase ε continuous unwinding of the parental DNA duplex by the MCM helicase creates a stretch of RPA bound ssDNA. Downstream reinitiating replication creates an 5'primer ssDNA/dsDNA junction that allows loading of the 9-1-1 complex by RAD17-RFC. Independently, the ATR-ATRIP complex is recruited to ssDNA through the interaction of ATRIP with RPA. Recruitment of TopBP1, which interacts both with RAD9 as well as ATR-ATRIP, promotes the activation of the ATR kinase activity.

al., 2009). Another, rather enigmatic, factor implicated in establishing SCC is DDX11 (ChlR1). The DDX11 homologue in *S. cerevisiae* was shown to physically and genetically interact with Eco1, the yeast Esco1/2 homologue (Skibbens, 2004;Parish et al., 2006). Depletion of DDX11 in human cells resulted in abnormal SCC, although it is unclear how the protein contributes to cohesion. The fact that it has DNA dependent helicase activity and interacts with replication associated proteins like Ctf18-RFC and Timeless would indicate it functions in cohesion establishment rather than maintenance (Farina et al., 2008;Leman et al., 2010).

Defects in various genes can cause cohesinopathy in humans. CdLS was originally found to be associated with heterozygous mutations in the NIPBL gene (Krantz et al., 2004;Tonkin et al., 2004), responsible for cohesin loading. Also the structural cohesin components SMC1 and SMC3 were found to be affected in CdLS (Musio et al., 2006;Deardorff et al., 2007). RBS on the other hand is caused by mutations in ESCO2 (Vega et al., 2005), whereas DDX11 was found to be defective in WABS (van der Lelij et al., 2010). While on the cellular level defects in SCC are evident in all three syndromes, clinical features such as growth and mental retardation, craniofacial anomalies and limb deformities indicate normal development is disrupted, possibly due to altered gene expression and cell differentiation (Dorsett, 2007). This suspected link between cohesin and gene regulation was strengthened when it was found that cohesin binds to the same genomic regions as the CCCTC-binding factor (CTCF) (Stedman et al., 2008;Wendt et al., 2008;Parelho et al., 2008;Rubio et al., 2008). CTCF has been implicated in diverse regulatory functions including transcriptional activation/repression and imprinting (Phillips and Corces, 2009). It has now emerged that cohesin shapes local chromatin topology at specific loci which is likely to modulate gene activity (Nativio et al., 2009;Hadjur et al., 2009;Hou et al., 2010;Mishiro et al., 2009) and thus would provide a basis for the observed developmental abnormalities in cohesinopathies.

Studies in *S. pombe* initially identified RAD21 as an important factor in DNA double strand break (DSB) repair (Birkenbihl and Subramani, 1992). However, subsequent studies

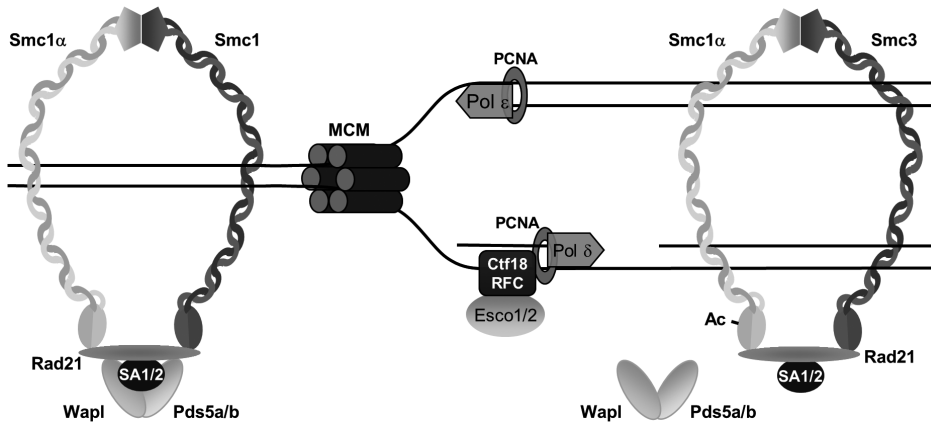

Figure 3: Model for cohesin establishment at the replication fork. During the cell cycle cohesion can dynamically interact with chromatin aided by NIPBL-Scc2 (not shown). Sister chromatid cohesion is established during S-phase in a replication dependent manner requiring the Ctf18-RFC complex and Esco1/2. Acetylation of Smc3 by the Esco1 or 2 proteins destabilizes the interaction of Pds5a or its paralog Pds5b with Wapl, causing a transition of cohesion to a more stable chromatin binding state.

demonstrated that other cohesin subunits are also important for this process when it became clear that establishing SSC was crucial for efficient DSB repair (Sjogren and Nasmyth, 2001). When it was found that CdLS was caused by defects in NIPBL, the question was how patient derived cells would respond to DNA damaging agents. As described in chapter 6 CdLS cells are indeed sensitive for DNA damage, in particular for the crosslinking agent mitomycin C. A similar sensitivity towards DNA damage was also observed in RBS (Van den Berg and Francke, 1993;Gordillo et al., 2008;van der Lelij et al., 2009) and WABS (van der Lelij et al., 2010) cells.

The reason why a deficiency in SCC results in sensitivity for DNA damaging agents is thought to lay in defective homologous recombination. When a DSB is created cohesin is recruited to the break site and establishes *de novo* cohesion (Kim et al., 2002a;Strom et al., 2004;Unal et al., 2004). This increased SCC is believed to bring the sister chromatids into close proximity thereby enhancing repair. Surprisingly, however, when a single DSB was introduced this not only led to increased SCC near the break site, but also on undamaged chromosomes (Strom et al., 2007;Unal et al., 2007). In yeast damage induced recruitment of cohesin near break sites is dependent on components of the DSB repair and signaling pathways such as Mre11, Mec1 and Tel1 (ATR and ATM in human) as well as H2AX phosphorylation (γH2AX). Establishing cohesion at the DNA break site also requires the acetyltransferase activity of Eco1. In undamaged cells the activity of this protein is impaired once S phase induced SCC has been established (Strom et al., 2007;Unal et al., 2007); a DSB would therefore need to activate the protein. This is achieved via phosphorylation of serine 83 of Mcd1 (Scc1) by the Chk1 kinase (Heidinger-Pauli et al., 2008). Chk1 is an effector kinase in the Mec1/Tel1 signaling pathway and is activated upon DNA damage.

Once phosphorylated, Mcd1 is acetylated by Eco1 generating a cohesin complex capable of establishing SCC (Heidinger-Pauli et al., 2009). Interestingly, as activity of the Chk1 kinase, once activated, is unlikely to be restricted to the break site it is possible that Mcd1 on other chromosomes is also targeted for phosphorylation, explaining the *trans* effect for *de novo* SCC after DNA damage.

Currently it is unclear if damage induced cohesion establishment is regulated in a similar manner in human cells. It is, however, without question that the that the ATM/ATR kinases play an important role in cohesin function as SMC1 and SMC3 are targets for damage induced phosphorylation (Yazdi et al., 2002;Kim et al., 2002b;Luo et al., 2008). Failure to phosphorylate SMC1 results in both checkpoint and repair defects (Kitagawa et al., 2004). Although the role of cohesin in checkpoint activation is independent of sister chromatid cohesion (Watrin and Peters, 2009), it is unclear whether the ability to establish damage induced cohesion is compromised when SMC1 or SMC3 cannot be phosphorylated. From phospho-proteomic screens designed to identify ATM/ATR targets it is also evident that SMC1 and SMC3 are not the only proteins in the cohesion pathway that are phosphorylated (Matsuoka et al., 2007;Stokes et al., 2007). Both CTF18 and ESCO1 were found to be modified following DNA damage, contributing to the complexity of this response.

REFERENCE LIST

1. Ahel,D., Z.Horejsi, N.Wiechens, S.E.Polo, E.Garcia-Wilson, I.Ahel, H.Flynn, M.Skehel, S.C.West, S.P.Jackson, T.Owen-Hughes, and S.J.Boulton. 2009. Poly(ADP-ribose)-dependent regulation of DNA repair by the chromatin remodeling enzyme ALC1. *Science* **325**: 1240-1243.
2. Ahel,I., D.Ahel, T.Matsusaka, A.J.Clark, J.Pines, S.J.Boulton, and S.C.West. 2008. Poly(ADP-ribose)-binding zinc finger motifs in DNA repair/checkpoint proteins. *Nature* **451**: 81-85.
3. Ames,B.N. and M.K.Shigenaga. 1992. Oxidants are a major contributor to aging. *Ann. N. Y. Acad. Sci.* **663**: 85-96.
4. Auclair,Y., R.Rouget, e.B.Affar, and E.A.Drobetsky. 2008. ATR kinase is required for global genomic nucleotide excision repair exclusively during S phase in human cells. *Proc. Natl. Acad. Sci. U. S. A* **105**: 17896-17901.
5. Avery,O.T., C.M.Macleod, and M.McCarty. 1944. Studies on the chemical nature of the substance inducing transformation of Pneumococcal types: Induction of transformation by a desoxyribonucleic acid fraction isolated from Pneumococcus type III. *J. Exp. Med.* **79**: 137-158.
6. Bakkenist,C.J. and M.B.Kastan. 2003. DNA damage activates ATM through intermolecular autophosphorylation and dimer dissociation. *Nature* **421**: 499-506.
7. Bao,S., T.Lu, X.Wang, H.Zheng, L.E.Wang, Q.Wei, W.N.Hittelman, and L.Li. 2004. Disruption of the Rad9/Rad1/Hus1 (9-1-1) complex leads to checkpoint signaling and replication defects. *Oncogene* **23**: 5586-5593.
8. Bekker-Jensen,S., K.Fugger, J.R.Danielsen, I.Gromova, M.Sehested, J.Celis, J.Bartek, J.Lukas, and N.Mailand. 2007. Human Xip1 (C2orf13) is a novel regulator of cellular responses to DNA strand breaks. *J. Biol. Chem.* **282**: 19638-19643.
9. Berger,N.A., G.W.Sikorski, S.J.Petzold, and K.K.Kurohara. 1980. Defective poly(adenosine diphosphoribose) synthesis in xeroderma pigmentosum. *Biochemistry* **19**: 289-293.
10. Birkenbihl,R.P. and S.Subramani. 1992. Cloning and characterization of rad21 an essential gene of Schizosaccharomyces pombe involved in DNA double-strand-break repair. *Nucleic Acids Res.* **20**: 6605-6611.
11. Brumbaugh,K.M., D.M.Otterness, C.Geisen, V.Oliveira, J.Brognard, X.Li, F.Lejeune, R.S.Tibbetts, L.E.Maquat, and R.T.Abraham. 2004. The mRNA surveillance protein hSMG-1 functions in genotoxic stress response pathways in mammalian cells. *Mol. Cell* **14**: 585-598.
12. Celeste,A., S.Petersen, P.J.Romanienko, O.Fernandez-Capetillo, H.T.Chen, O.A.Sedelnikova, B.Reina-San-Martin, V.Coppola, E.Meffre, M.J.Difilippantonio, C.Redon, D.R.Pilch, A.Olaru, M.Eckhaus, R.D.Camerini-Otero, L.Tessarollo, F.Livak, K.Manova, W.M.Bonner, M.C.Nussenzweig, and A.Nussenzweig. 2002. Genomic instability in mice lacking histone H2AX. *Science* **296**: 922-927.
13. Chen,Y., A.A.Farmer, C.F.Chen, D.C.Jones, P.L.Chen, and W.H.Lee. 1996. BRCA1 is a 220-kDa nuclear phosphoprotein that is expressed and phosphorylated in a cell cycle-dependent manner. *Cancer Res.* **56**: 3168-3172.
14. Choi,J.H., L.A.Lindsey-Boltz, M.Kemp, A.C.Mason, M.S.Wold, and A.Sancar. 2010. Reconstitution of RPA-covered single-stranded DNA-activated ATR-Chk1 signaling. *Proc. Natl. Acad. Sci. U. S. A* **107**: 13660-13665.
15. Choudhury,A.D., H.Xu, and R.Baer. 2004. Ubiquitination and proteasomal degradation of the BRCA1 tumor suppressor is regulated during cell cycle progression. *J. Biol. Chem.* **279**: 33909-33918.
16. Ciccia,A. and S.J.Elledge. 2010. The DNA damage response: making it safe to play with knives. *Mol. Cell* **40**: 179-204.
17. Cimprich,K.A. and D.Cortez. 2008. ATR: an essential regulator of genome integrity. *Nat. Rev. Mol. Cell Biol.* **9**: 616-627.
18. Ciosk,R., M.Shirayama, A.Shevchenko, T.Tanaka, A.Toth, A.Shevchenko, and K.Nasmyth. 2000. Cohesin's binding to chromosomes depends on a separate complex consisting of Scc2 and Scc4 proteins. *Mol. Cell* **5**: 243-254.
19. Cliby,W.A., C.J.Roberts, K.A.Cimprich, C.M.Stringer, J.R.Lamb, S.L.Schreiber, and S.H.Friend. 1998. Overexpression of a kinase-inactive ATR protein causes sensitivity to DNA-damaging agents and defects in cell cycle checkpoints. *EMBO J.* **17**: 159-169.
20. Cortez,D., S.Guntuku, J.Qin, and S.J.Elledge. 2001. ATR and ATRIP: partners in checkpoint signaling. *Science* **294**: 1713-1716.

21. Costanzo,V. and J.Gautier. 2003. Single-strand DNA gaps trigger an ATR- and Cdc7-dependent checkpoint. *Cell Cycle* **2**: 17.

22. de Murcia,J.M., C.Niedergang, C.Trucco, M.Ricoul, B.Dutrillaux, M.Mark, F.J.Oliver, M.Masson, A.Dierich, M.LeMeur, C.Walztinger, P.Chambon, and M.G.de. 1997. Requirement of poly(ADP-ribose) polymerase in recovery from DNA damage in mice and in cells. *Proc. Natl. Acad. Sci. U. S. A* **94**: 7303-7307.

23. Deardorff,M.A., M.Kaur, D.Yaeger, A.Rampuria, S.Korolev, J.Pie, C.Gil-Rodriguez, M.Arnedo, B.Loeys, A.D.Kline, M.Wilson, K.Lillquist, V.Siu, F.J.Ramos, A.Musio, L.S.Jackson, D.Dorsett, and I.D.Krantz. 2007. Mutations in cohesin complex members SMC3 and SMC1A cause a mild variant of cornelia de Lange syndrome with predominant mental retardation. *Am. J. Hum. Genet.* **80**: 485-494.

24. Delacroix,S., J.M.Wagner, M.Kobayashi, K.Yamamoto, and L.M.Karnitz. 2007. The Rad9-Hus1-Rad1 (9-1-1) clamp activates checkpoint signaling via TopBP1. *Genes Dev.* **21**: 1472-1477.

25. Derheimer,F.A., H.M.O'Hagan, H.M.Krueger, S.Hanasoge, M.T.Paulsen, and M.Ljungman. 2007. RPA and ATR link transcriptional stress to p53. *Proc. Natl. Acad. Sci. U. S. A* **104**: 12778-12783.

26. Dimitrova,N., Y.C.Chen, D.L.Spector, and L.T.de. 2008. 53BP1 promotes non-homologous end joining of telomeres by increasing chromatin mobility. *Nature* **456**: 524-528.

27. Dorsett,D. 2007. Roles of the sister chromatid cohesion apparatus in gene expression, development, and human syndromes. *Chromosoma* **116**: 1-13.

28. Durocher,D. and S.P.Jackson. 2001. DNA-PK, ATM and ATR as sensors of DNA damage: variations on a theme? *Curr. Opin. Cell Biol.* **13**: 225-231.

29. Ellison,V. and B.Stillman. 2003. Biochemical characterization of DNA damage checkpoint complexes: clamp loader and clamp complexes with specificity for 5' recessed DNA. *PLoS. Biol.* **1**: E33.

30. Farina,A., J.H.Shin, D.H.Kim, V.P.Bermudez, Z.Kelman, Y.S.Seo, and J.Hurwitz. 2008. Studies with the human cohesin establishment factor, ChlR1. Association of ChlR1 with Ctf18-RFC and Fen1. *J. Biol. Chem.* **283**: 20925-20936.

31. FitzGerald,J.E., M.Grenon, and N.F.Lowndes. 2009. 53BP1: function and mechanisms of focal recruitment. *Biochem. Soc. Trans.* **37**: 897-904.

32. Flohr,C., A.Burkle, J.P.Radicella, and B.Epe. 2003. Poly(ADP-ribosyl)ation accelerates DNA repair in a pathway dependent on Cockayne syndrome B protein. *Nucleic Acids Res.* **31**: 5332-5337.

33. Furuya,K., M.Poitelea, L.Guo, T.Caspari, and A.M.Carr. 2004. Chk1 activation requires Rad9 S/TQ-site phosphorylation to promote association with C-terminal BRCT domains of Rad4TOPBP1. *Genes Dev.* **18**: 1154-1164.

34. Gagne,J.P., M.Isabelle, K.S.Lo, S.Bourassa, M.J.Hendzel, V.L.Dawson, T.M.Dawson, and G.G.Poirier. 2008. Proteome-wide identification of poly(ADP-ribose) binding proteins and poly(ADP-ribose)-associated protein complexes. *Nucleic Acids Res.* **36**: 6959-6976.

35. Gerlich,D., B.Koch, F.Dupeux, J.M.Peters, and J.Ellenberg. 2006. Live-cell imaging reveals a stable cohesin-chromatin interaction after but not before DNA replication. *Curr. Biol.* **16**: 1571-1578.

36. Ghodgaonkar,M.M., N.Zacal, S.Kassam, A.J.Rainbow, and G.M.Shah. 2008. Depletion of poly(ADP-ribose) polymerase-1 reduces host cell reactivation of a UV-damaged adenovirus-encoded reporter gene in human dermal fibroblasts. *DNA Repair (Amst)* **7**: 617-632.

37. Goodarzi,A.A., A.T.Noon, D.Deckbar, Y.Ziv, Y.Shiloh, M.Lobrich, and P.A.Jeggo. 2008. ATM signaling facilitates repair of DNA double-strand breaks associated with heterochromatin. *Mol. Cell* **31**: 167-177.

38. Gordillo,M., H.Vega, A.H.Trainer, F.Hou, N.Sakai, R.Luque, H.Kayserili, S.Basaran, F.Skovby, R.C.Hennekam, M.L.Uzielli, R.E.Schnur, S.Manouvrier, S.Chang, E.Blair, J.A.Hurst, F.Forzano, M.Meins, K.O.Simola, A.Raas-Rothschild, R.A.Schultz, L.D.McDaniel, K.Ozono, K.Inui, H.Zou, and E.W.Jabs. 2008. The molecular mechanism underlying Roberts syndrome involves loss of ESCO2 acetyltransferase activity. *Hum. Mol. Genet.* **17**: 2172-2180.

39. Gottschalk,A.J., G.Timinszky, S.E.Kong, J.Jin, Y.Cai, S.K.Swanson, M.P.Washburn, L.Florens, A.G.Ladurner, J.W.Conaway, and R.C.Conaway. 2009. Poly(ADP-ribosyl)ation directs recruitment and activation of an ATP-dependent chromatin remodeler. *Proc. Natl. Acad. Sci. U. S. A* **106**: 13770-13774.

40. Griffith,F. 1928. The Significance of Pneumococcal Types. *J. Hyg. (Lond)* **27**: 113-159.

41. Gruber,S., C.H.Haering, and K.Nasmyth. 2003. Chromosomal cohesin forms a ring. *Cell* **112**: 765-777.

42. Guo,Z., A.Kumagai, S.X.Wang, and W.G.Dunphy. 2000. Requirement for Atr in phosphorylation of Chk1 and cell cycle regulation in response to DNA replication blocks and UV-damaged DNA in Xenopus egg extracts. *Genes Dev.* **14**: 2745-2756.

43. Hadjur,S., L.M.Williams, N.K.Ryan, B.S.Cobb, T.Sexton, P.Fraser, A.G.Fisher, and M.Merkenschlager. 2009. Cohesins form chromosomal cis-interactions at the developmentally regulated IFNG locus. *Nature* **460**: 410-413.

44. Hanahan,D. and R.A.Weinberg. 2011. Hallmarks of cancer: the next generation. *Cell* **144**: 646-674.

45. Heidinger-Pauli,J.M., E.Unal, V.Guacci, and D.Koshland. 2008. The kleisin subunit of cohesin dictates damage-induced cohesion. *Mol. Cell* **31**: 47-56.

46. Heidinger-Pauli,J.M., E.Unal, and D.Koshland. 2009. Distinct targets of the Eco1 acetyltransferase modulate cohesion in S phase and in response to DNA damage. *Mol. Cell* **34**: 311-321.

47. Hochegger,H., D.Dejsuphong, T.Fukushima, C.Morrison, E.Sonoda, V.Schreiber, G.Y.Zhao, A.Saberi, M.Masutani, N.Adachi, H.Koyama, M.G.de, and S.Takeda. 2006. Parp-1 protects homologous recombination from interference by Ku and Ligase IV in vertebrate cells. *EMBO J.* **25**: 1305-1314.

48. Hoeijmakers,J.H. 2001. Genome maintenance mechanisms for preventing cancer. *Nature* **411**: 366-374.

49. Hou,C., R.Dale, and A.Dean. 2010. Cell type specificity of chromatin organization mediated by CTCF and cohesin. *Proc. Natl. Acad. Sci. U. S. A* **107**: 3651-3656.

50. Hsieh,P. and K.Yamane. 2008. DNA mismatch repair: molecular mechanism, cancer, and ageing. *Mech. Ageing Dev.* **129**: 391-407.

51. Imai,K., G.Slupphaug, W.I.Lee, P.Revy, S.Nonoyama, N.Catalan, L.Yel, M.Forveille, B.Kavli, H.E.Krokan, H.D.Ochs, A.Fischer, and A.Durandy. 2003. Human uracil-DNA glycosylase deficiency associated with profoundly impaired immunoglobulin class-switch recombination. *Nat. Immunol.* **4**: 1023-1028.

52. Jowsey,P., N.A.Morrice, C.J.Hastie, H.McLauchlan, R.Toth, and J.Rouse. 2007. Characterisation of the sites of DNA damage-induced 53BP1 phosphorylation catalysed by ATM and ATR. *DNA Repair (Amst)* **6**: 1536-1544.

53. Kaina,B. 2003. DNA damage-triggered apoptosis: critical role of DNA repair, double-strand breaks, cell proliferation and signaling. *Biochem. Pharmacol.* **66**: 1547-1554.

54. Kanno,S., H.Kuzuoka, S.Sasao, Z.Hong, L.Lan, S.Nakajima, and A.Yasui. 2007. A novel human AP endonuclease with conserved zinc-finger-like motifs involved in DNA strand break responses. *EMBO J.* **26**: 2094-2103.

55. Kanu,N. and A.Behrens. 2007. ATMIN defines an NBS1-independent pathway of ATM signalling. *EMBO J.* **26**: 2933-2941.

56. Kim,J.S., T.B.Krasieva, V.LaMorte, A.M.Taylor, and K.Yokomori. 2002a. Specific recruitment of human cohesin to laser-induced DNA damage. *J. Biol. Chem.* **277**: 45149-45153.

57. Kim,S.T., B.Xu, and M.B.Kastan. 2002b. Involvement of the cohesin protein, Smc1, in Atm-dependent and independent responses to DNA damage. *Genes Dev.* **16**: 560-570.

58. Kitagawa,R., C.J.Bakkenist, P.J.McKinnon, and M.B.Kastan. 2004. Phosphorylation of SMC1 is a critical downstream event in the ATM-NBS1-BRCA1 pathway. *Genes Dev.* **18**: 1423-1438.

59. Klein,F., P.Mahr, M.Galova, S.B.Buonomo, C.Michaelis, K.Nairz, and K.Nasmyth. 1999. A central role for cohesins in sister chromatid cohesion, formation of axial elements, and recombination during yeast meiosis. *Cell* **98**: 91-103.

60. Klungland,A. and T.Lindahl. 1997. Second pathway for completion of human DNA base excision-repair: reconstitution with purified proteins and requirement for DNase IV (FEN1). *EMBO J.* **16**: 3341-3348.

61. Krantz,I.D., J.McCallum, C.DeScipio, M.Kaur, L.A.Gillis, D.Yaeger, L.Jukofsky, N.Wasserman, A.Bottani, C.A.Morris, M.J.Nowaczyk, H.Toriello, M.J.Bamshad, J.C.Carey, E.Rappaport, S.Kawauchi, A.D.Lander, A.L.Calof, H.H.Li, M.Devoto, and L.G.Jackson. 2004. Cornelia de Lange syndrome is caused by mutations in NIPBL, the human homolog of Drosophila melanogaster Nipped-B. *Nat. Genet.* **36**: 631-635.

62. Krishnakumar,R. and W.L.Kraus. 2010. The PARP side of the nucleus: molecular actions, physiological outcomes, and clinical targets. *Mol. Cell* **39**: 8-24.

63. Kubota,Y., R.A.Nash, A.Klungland, P.Schar, D.E.Barnes, and T.Lindahl. 1996. Reconstitution of DNA base excision-repair with purified human proteins: interaction between DNA polymerase beta and the XRCC1 protein. *EMBO J.* **15**: 6662-6670.

64. Kumagai,A., J.Lee, H.Y.Yoo, and W.G.Dunphy. 2006. TopBP1 activates the ATR-ATRIP complex. *Cell* **124**: 943-955.

65. Lee,J., A.Kumagai, and W.G.Dunphy. 2007. The Rad9-Hus1-Rad1 checkpoint clamp regulates interaction of TopBP1 with ATR. *J. Biol. Chem.* **282**: 28036-28044.

66. Lee,J.H. and T.T.Paull. 2005. ATM activation by DNA double-strand breaks through the Mre11-Rad50-Nbs1 complex. *Science* **308**: 551-554.

67. Leman,A.R., C.Noguchi, C.Y.Lee, and E.Noguchi. 2010. Human Timeless and Tipin stabilize replication forks and facilitate sister-chromatid cohesion. *J. Cell Sci.* **123**: 660-670.

68. Lengronne,A., J.McIntyre, Y.Katou, Y.Kanoh, K.P.Hopfner, K.Shirahige, and F.Uhlmann. 2006. Establishment of sister chromatid cohesion at the S. cerevisiae replication fork. *Mol. Cell* **23**: 787-799.

69. Li,X. and W.D.Heyer. 2008. Homologous recombination in DNA repair and DNA damage tolerance. *Cell Res.* **18**: 99-113.

70. Lieber,M.R. 2008. The mechanism of human nonhomologous DNA end joining. *J. Biol. Chem.* **283**: 1-5.

71. Lindahl,T. and B.Nyberg. 1972. Rate of depurination of native deoxyribonucleic acid. *Biochemistry* **11**: 3610-3618.

72. Liu,Q., S.Guntuku, X.S.Cui, S.Matsuoka, D.Cortez, K.Tamai, G.Luo, S.Carattini-Rivera, F.DeMayo, A.Bradley, L.A.Donehower, and S.J.Elledge. 2000. Chk1 is an essential kinase that is regulated by Atr and required for the G(2)/M DNA damage checkpoint. *Genes Dev.* **14**: 1448-1459.

73. Ljungman,M. and F.Zhang. 1996. Blockage of RNA polymerase as a possible trigger for u.v. light-induced apoptosis. *Oncogene* **13**: 823-831.

74. Ljungman,M., F.Zhang, F.Chen, A.J.Rainbow, and B.C.McKay. 1999. Inhibition of RNA polymerase II as a trigger for the p53 response. *Oncogene* **18**: 583-592.

75. Lobrich,M. and P.A.Jeggo. 2005. The two edges of the ATM sword: co-operation between repair and checkpoint functions. *Radiother. Oncol.* **76**: 112-118.

76. Losada,A. and T.Hirano. 2005. Dynamic molecular linkers of the genome: the first decade of SMC proteins. *Genes Dev.* **19**: 1269-1287.

77. Lou,Z., K.Minter-Dykhouse, S.Franco, M.Gostissa, M.A.Rivera, A.Celeste, J.P.Manis, D.J.van, A.Nussenzweig, T.T.Paull, F.W.Alt, and J.Chen. 2006. MDC1 maintains genomic stability by participating in the amplification of ATM-dependent DNA damage signals. *Mol. Cell* **21**: 187-200.

78. Luo,H., Y.Li, J.J.Mu, J.Zhang, T.Tonaka, Y.Hamamori, S.Y.Jung, Y.Wang, and J.Qin. 2008. Regulation of intra-S phase checkpoint by ionizing radiation (IR)-dependent and IR-independent phosphorylation of SMC3. *J. Biol. Chem.* **283**: 19176-19183.

79. MacDougall,C.A., T.S.Byun, C.Van, M.C.Yee, and K.A.Cimprich. 2007. The structural determinants of checkpoint activation. *Genes Dev.* **21**: 898-903.

80. Majka,J., S.K.Binz, M.S.Wold, and P.M.Burgers. 2006. Replication protein A directs loading of the DNA damage checkpoint clamp to 5'-DNA junctions. *J. Biol. Chem.* **281**: 27855-27861.

81. Majka,J. and P.M.Burgers. 2003. Yeast Rad17/Mec3/Ddc1: a sliding clamp for the DNA damage checkpoint. *Proc. Natl. Acad. Sci. U. S. A* **100**: 2249-2254.

82. Maltzman,W. and L.Czyzyk. 1984. UV irradiation stimulates levels of p53 cellular tumor antigen in nontransformed mouse cells. *Mol. Cell Biol.* **4**: 1689-1694.

83. Manis,J.P., J.C.Morales, Z.Xia, J.L.Kutok, F.W.Alt, and P.B.Carpenter. 2004. 53BP1 links DNA damage-response pathways to immunoglobulin heavy chain class-switch recombination. *Nat. Immunol.* **5**: 481-487.

84. Marteijn,J.A., S.Bekker-Jensen, N.Mailand, H.Lans, P.Schwertman, A.M.Gourdin, N.P.Dantuma, J.Lukas, and W.Vermeulen. 2009. Nucleotide excision repair-induced H2A ubiquitination is dependent on MDC1 and RNF8 and reveals a universal DNA damage response. *J. Cell Biol.* **186**: 835-847.

85. Marti,T.M., E.Hefner, L.Feeney, V.Natale, and J.E.Cleaver. 2006. H2AX phosphorylation within the G1 phase after UV irradiation depends on nucleotide excision repair and

not DNA double-strand breaks. *Proc. Natl. Acad. Sci. U. S. A* **103**: 9891-9896.

86. Matsumoto,M., K.Yaginuma, A.Igarashi, M.Imura, M.Hasegawa, K.Iwabuchi, T.Date, T.Mori, K.Ishizaki, K.Yamashita, M.Inobe, and T.Matsunaga. 2007. Perturbed gap-filling synthesis in nucleotide excision repair causes histone H2AX phosphorylation in human quiescent cells. *J. Cell Sci.* **120**: 1104-1112.
87. Matsuoka,S., B.A.Ballif, A.Smogorzewska, E.R.McDonald, III, K.E.Hurov, J.Luo, C.E.Bakalarski, Z.Zhao, N.Solimini, Y.Lerenthal, Y.Shiloh, S.P.Gygi, and S.J.Elledge. 2007. ATM and ATR substrate analysis reveals extensive protein networks responsive to DNA damage. *Science* **316**: 1160-1166.
88. Mishiro,T., K.Ishihara, S.Hino, S.Tsutsumi, H.Aburatani, K.Shirahige, Y.Kinoshita, and M.Nakao. 2009. Architectural roles of multiple chromatin insulators at the human apolipoprotein gene cluster. *EMBO J.* **28**: 1234-1245.
89. Mordes,D.A., G.G.Glick, R.Zhao, and D.Cortez. 2008. TopBP1 activates ATR through ATRIP and a PIKK regulatory domain. *Genes Dev.* **22**: 1478-1489.
90. Moynahan,M.E., J.W.Chiu, B.H.Koller, and M.Jasin. 1999. Brca1 controls homology-directed DNA repair. *Mol. Cell* **4**: 511-518.
91. Musio,A., A.Selicorni, M.L.Focarelli, C.Gervasini, D.Milani, S.Russo, P.Vezzoni, and L.Larizza. 2006. X-linked Cornelia de Lange syndrome owing to SMC1L1 mutations. *Nat. Genet.* **38**: 528-530.
92. Nativio,R., K.S.Wendt, Y.Ito, J.E.Huddleston, S.Uribe-Lewis, K.Woodfine, C.Krueger, W.Reik, J.M.Peters, and A.Murrell. 2009. Cohesin is required for higher-order chromatin conformation at the imprinted IGF2-H19 locus. *PLoS. Genet.* **5**: e1000739.
93. Negrini,S., V.G.Gorgoulis, and T.D.Halazonetis. 2010. Genomic instability--an evolving hallmark of cancer. *Nat. Rev. Mol. Cell Biol.* **11**: 220-228.
94. Nghiem,P., P.K.Park, Y.Kim, C.Vaziri, and S.L.Schreiber. 2001. ATR inhibition selectively sensitizes G1 checkpoint-deficient cells to lethal premature chromatin condensation. *Proc. Natl. Acad. Sci. U. S. A* **98**: 9092-9097.
95. O'Driscoll,M., V.L.Ruiz-Perez, C.G.Woods, P.A.Jeggo, and J.A.Goodship. 2003. A splicing mutation affecting expression of ataxia-telangiectasia and Rad3-related protein (ATR) results in Seckel syndrome. *Nat. Genet.* **33**: 497-501.
96. Okano,S., L.Lan, K.W.Caldecott, T.Mori, and A.Yasui. 2003. Spatial and temporal cellular responses to single-strand breaks in human cells. *Mol. Cell Biol.* **23**: 3974-3981.
97. Panier,S. and D.Durocher. 2009. Regulatory ubiquitylation in response to DNA double-strand breaks. *DNA Repair (Amst)* **8**: 436-443.
98. Parelho,V., S.Hadjur, M.Spivakov, M.Leleu, S.Sauer, H.C.Gregson, A.Jarmuz, C.Canzonetta, Z.Webster, T.Nesterova, B.S.Cobb, K.Yokomori, N.Dillon, L.Aragon, A.G.Fisher, and M.Merkenschlager. 2008. Cohesins functionally associate with CTCF on mammalian chromosome arms. *Cell* **132**: 422-433.
99. Parish,J.L., J.Rosa, X.Wang, J.M.Lahti, S.J.Doxsey, and E.J.Androphy. 2006. The DNA helicase ChlR1 is required for sister chromatid cohesion in mammalian cells. *J. Cell Sci.* **119**: 4857-4865.
100. Parrilla-Castellar,E.R., S.J.Arlander, and L.Karnitz. 2004. Dial 9-1-1 for DNA damage: the Rad9-Hus1-Rad1 (9-1-1) clamp complex. *DNA Repair (Amst)* **3**: 1009-1014.
101. Phillips,J.E. and V.G.Corces. 2009. CTCF: master weaver of the genome. *Cell* **137**: 1194-1211.
102. Ramachandran,S., R.Chahwan, R.M.Nepal, D.Frieder, S.Panier, S.Roa, A.Zaheen, D.Durocher, M.D.Scharff, and A.Martin. 2010. The RNF8/RNF168 ubiquitin ligase cascade facilitates class switch recombination. *Proc. Natl. Acad. Sci. U. S. A* **107**: 809-814.
103. Rendtlew Danielsen,J.M., D.H.Larsen, K.B.Schou, R.Freire, J.Falck, J.Bartek, and J.Lukas. 2009. HCLK2 is required for activity of the DNA damage response kinase ATR. *J. Biol. Chem.* **284**: 4140-4147.
104. Roach,J.C., G.Glusman, A.F.Smit, C.D.Huff, R.Hubley, P.T.Shannon, L.Rowen, K.P.Pant, N.Goodman, M.Bamshad, J.Shendure, R.Drmanac, L.B.Jorde, L.Hood, and D.J.Galas. 2010. Analysis of genetic inheritance in a family quartet by whole-genome sequencing. *Science* **328**: 636-639.
105. Rolef Ben-Shahar,T., S.Heeger, C.Lehane, P.East, H.Flynn, M.Skehel, and F.Uhlmann. 2008. Eco1-dependent cohesin acetylation during establishment of sister chromatid cohesion. *Science* **321**: 563-566.
106. Rollins,R.A., P.Morcillo, and D.Dorsett. 1999. Nipped-B, a Drosophila homologue

of chromosomal adherins, participates in activation by remote enhancers in the cut and Ultrabithorax genes. *Genetics* **152**: 577-593.

107. Rowland,B.D., M.B.Roig, T.Nishino, A.Kurze, P.Uluocak, A.Mishra, F.Beckouet, P.Underwood, J.Metson, R.Imre, K.Mechtler, V.L.Katis, and K.Nasmyth. 2009. Building sister chromatid cohesion: smc3 acetylation counteracts an antiestablishment activity. *Mol. Cell* **33**: 763-774.
108. Rubio,E.D., D.J.Reiss, P.L.Welcsh, C.M.Disteche, G.N.Filippova, N.S.Baliga, R.Aebersold, J.A.Ranish, and A.Krumm. 2008. CTCF physically links cohesin to chromatin. *Proc. Natl. Acad. Sci. U. S. A* **105**: 8309-8314.
109. Rulten,S.L., F.Cortes-Ledesma, L.Guo, N.J.Iles, and K.W.Caldecott. 2008. APLF (C2orf13) is a novel component of poly(ADP-ribose) signaling in mammalian cells. *Mol. Cell Biol.* **28**: 4620-4628.
110. Salk,J.J., E.J.Fox, and L.A.Loeb. 2010. Mutational heterogeneity in human cancers: origin and consequences. *Annu. Rev. Pathol.* **5**: 51-75.
111. Schreiber,V., J.C.Ame, P.Dolle, I.Schultz, B.Rinaldi, V.Fraulob, M.J.Menissier-de, and M.G.de. 2002. Poly(ADP-ribose) polymerase-2 (PARP-2) is required for efficient base excision DNA repair in association with PARP-1 and XRCC1. *J. Biol. Chem.* **277**: 23028-23036.
112. Sjogren,C. and K.Nasmyth. 2001. Sister chromatid cohesion is required for postreplicative double-strand break repair in Saccharomyces cerevisiae. *Curr. Biol.* **11**: 991-995.
113. Skibbens,R.V. 2004. Chl1p, a DNA helicase-like protein in budding yeast, functions in sister-chromatid cohesion. *Genetics* **166**: 33-42.
114. Skibbens,R.V., L.B.Corson, D.Koshland, and P.Hieter. 1999. Ctf7p is essential for sister chromatid cohesion and links mitotic chromosome structure to the DNA replication machinery. *Genes Dev.* **13**: 307-319.
115. Soutoglou,E. and T.Misteli. 2008. Activation of the cellular DNA damage response in the absence of DNA lesions. *Science* **320**: 1507-1510.
116. St Onge,R.P., B.D.Besley, J.L.Pelley, and S.Davey. 2003. A role for the phosphorylation of hRad9 in checkpoint signaling. *J. Biol. Chem.* **278**: 26620-26628.
117. Stedman,W., H.Kang, S.Lin, J.L.Kissil, M.S.Bartolomei, and P.M.Lieberman. 2008. Cohesins localize with CTCF at the KSHV latency control region and at cellular c-myc and H19/Igf2 insulators. *EMBO J.* **27**: 654-666.
118. Stewart,G.S., T.Stankovic, P.J.Byrd, T.Wechsler, E.S.Miller, A.Huissoon, M.T.Drayson, S.C.West, S.J.Elledge, and A.M.Taylor. 2007. RIDDLE immunodeficiency syndrome is linked to defects in 53BP1-mediated DNA damage signaling. *Proc. Natl. Acad. Sci. U. S. A* **104**: 16910-16915.
119. Stokes,M.P., J.Rush, J.Macneill, J.M.Ren, K.Sprott, J.Nardone, V.Yang, S.A.Beausoleil, S.P.Gygi, M.Livingstone, H.Zhang, R.D.Polakiewicz, and M.J.Comb. 2007. Profiling of UV-induced ATM/ATR signaling pathways. *Proc. Natl. Acad. Sci. U. S. A* **104**: 19855-19860.
120. Stracker,T.H. and J.H.Petrini. 2011. The MRE11 complex: starting from the ends. *Nat. Rev. Mol. Cell Biol.* **12**: 90-103.
121. Strom,L., C.Karlsson, H.B.Lindroos, S.Wedahl, Y.Katou, K.Shirahige, and C.Sjogren. 2007. Postreplicative formation of cohesion is required for repair and induced by a single DNA break. *Science* **317**: 242-245.
122. Strom,L., H.B.Lindroos, K.Shirahige, and C.Sjogren. 2004. Postreplicative recruitment of cohesin to double-strand breaks is required for DNA repair. *Mol. Cell* **16**: 1003-1015.
123. Terret,M.E., R.Sherwood, S.Rahman, J.Qin, and P.V.Jallepalli. 2009. Cohesin acetylation speeds the replication fork. *Nature* **462**: 231-234.
124. The 1000 Genomes Consortium. 2010. A map of human genome variation from population-scale sequencing. *Nature* **467**: 1061-1073.
125. Tibbetts,R.S., K.M.Brumbaugh, J.M.Williams, J.N.Sarkaria, W.A.Cliby, S.Y.Shieh, Y.Taya, C.Prives, and R.T.Abraham. 1999. A role for ATR in the DNA damage-induced phosphorylation of p53. *Genes Dev.* **13**: 152-157.
126. Timinszky,G., S.Till, P.O.Hassa, M.Hothorn, G.Kustatscher, B.Nijmeijer, J.Colombelli, M.Altmeyer, E.H.Stelzer, K.Scheffzek, M.O.Hottiger, and A.G.Ladurner. 2009. A macrodomain-containing histone rearranges chromatin upon sensing PARP1 activation. *Nat. Struct. Mol. Biol.* **16**: 923-929.
127. Tonkin,E.T., T.J.Wang, S.Lisgo, M.J.Bamshad, and T.Strachan. 2004. NIPBL, encoding a homolog of fungal Scc2-type sister chromatid cohesion proteins and fly Nipped-B, is mutated in Cornelia de Lange syndrome. *Nat. Genet.* **36**: 636-641.

128. Toth,A., R.Ciosk, F.Uhlmann, M.Galova, A.Schleiffer, and K.Nasmyth. 1999. Yeast cohesin complex requires a conserved protein, Eco1p(Ctf7), to establish cohesion between sister chromatids during DNA replication. *Genes Dev.* **13**: 320-333.

129. Unal,E., A.Arbel-Eden, U.Sattler, R.Shroff, M.Lichten, J.E.Haber, and D.Koshland. 2004. DNA damage response pathway uses histone modification to assemble a double-strand break-specific cohesin domain. *Mol. Cell* **16**: 991-1002.

130. Unal,E., J.M.Heidinger-Pauli, W.Kim, V.Guacci, I.Onn, S.P.Gygi, and D.E.Koshland. 2008. A molecular determinant for the establishment of sister chromatid cohesion. *Science* **321**: 566-569.

131. Unal,E., J.M.Heidinger-Pauli, and D.Koshland. 2007. DNA double-strand breaks trigger genome-wide sister-chromatid cohesion through Eco1 (Ctf7). *Science* **317**: 245-248.

132. Van den Berg,D.J. and U.Francke. 1993. Sensitivity of Roberts syndrome cells to gamma radiation, mitomycin C, and protein synthesis inhibitors. *Somat. Cell Mol. Genet.* **19**: 377-392.

133. van der Lelij,P., K.H.Chrzanowska, B.C.Godthelp, M.A.Rooimans, A.B.Oostra, M.Stumm, M.Z.Zdzienicka, H.Joenje, and J.P.de Winter. 2010. Warsaw breakage syndrome, a cohesinopathy associated with mutations in the XPD helicase family member DDX11/ChlR1. *Am. J. Hum. Genet.* **86**: 262-266.

134. van der Lelij,P., B.C.Godthelp, Z.W.van, G.D.van, A.B.Oostra, J.Steltenpool, G.J.de, R.J.Scheper, R.M.Wolthuis, Q.Waisfisz, F.Darroudi, H.Joenje, and J.P.de Winter. 2009. The cellular phenotype of Roberts syndrome fibroblasts as revealed by ectopic expression of ESCO2. *PLoS. One.* **4**: e6936.

135. Vega,H., Q.Waisfisz, M.Gordillo, N.Sakai, I.Yanagihara, M.Yamada, G.D.van, H.Kayserili, C.Xu, K.Ozono, E.W.Jabs, K.Inui, and H.Joenje. 2005. Roberts syndrome is caused by mutations in ESCO2, a human homolog of yeast ECO1 that is essential for the establishment of sister chromatid cohesion. *Nat. Genet.* **37**: 468-470.

136. Wang,B., S.Matsuoka, P.B.Carpenter, and S.J.Elledge. 2002. 53BP1, a mediator of the DNA damage checkpoint. *Science* **298**: 1435-1438.

137. Wang,M., W.Wu, W.Wu, B.Rosidi, L.Zhang, H.Wang, and G.Iliakis. 2006. PARP-1 and Ku compete for repair of DNA double strand breaks by distinct NHEJ pathways. *Nucleic Acids Res.* **34**: 6170-6182.

138. Wang,Z.Q., L.Stingl, C.Morrison, M.Jantsch, M.Los, K.Schulze-Osthoff, and E.F.Wagner. 1997. PARP is important for genomic stability but dispensable in apoptosis. *Genes Dev.* **11**: 2347-2358.

139. Ward,I.M. and J.Chen. 2001. Histone H2AX is phosphorylated in an ATR-dependent manner in response to replicational stress. *J. Biol. Chem.* **276**: 47759-47762.

140. Ward,I.M., B.Reina-San-Martin, A.Olaru, K.Minn, K.Tamada, J.S.Lau, M.Cascalho, L.Chen, A.Nussenzweig, F.Livak, M.C.Nussenzweig, and J.Chen. 2004. 53BP1 is required for class switch recombination. *J. Cell Biol.* **165**: 459-464.

141. Watrin,E. and J.M.Peters. 2006. Cohesin and DNA damage repair. *Exp. Cell Res.* **312**: 2687-2693.

142. Watrin,E. and J.M.Peters. 2009. The cohesin complex is required for the DNA damage-induced G2/M checkpoint in mammalian cells. *EMBO J.* **28**: 2625-2635.

143. Wendt,K.S., K.Yoshida, T.Itoh, M.Bando, B.Koch, E.Schirghuber, S.Tsutsumi, G.Nagae, K.Ishihara, T.Mishiro, K.Yahata, F.Imamoto, H.Aburatani, M.Nakao, N.Imamoto, K.Maeshima, K.Shirahige, and J.M.Peters. 2008. Cohesin mediates transcriptional insulation by CCCTC-binding factor. *Nature* **451**: 796-801.

144. Xu,X., Z.Weaver, S.P.Linke, C.Li, J.Gotay, X.W.Wang, C.C.Harris, T.Ried, and C.X.Deng. 1999. Centrosome amplification and a defective G2-M cell cycle checkpoint induce genetic instability in BRCA1 exon 11 isoform-deficient cells. *Mol. Cell* **3**: 389-395.

145. Yamaizumi,M. and T.Sugano. 1994. U.v.-induced nuclear accumulation of p53 is evoked through DNA damage of actively transcribed genes independent of the cell cycle. *Oncogene* **9**: 2775-2784.

146. Yamashita,A., T.Ohnishi, I.Kashima, Y.Taya, and S.Ohno. 2001. Human SMG-1, a novel phosphatidylinositol 3-kinase-related protein kinase, associates with components of the mRNA surveillance complex and is involved in the regulation of nonsense-mediated mRNA decay. *Genes Dev.* **15**: 2215-2228.

147. Yan,S. and W.M.Michael. 2009. TopBP1 and DNA polymerase-alpha directly recruit the 9-1-1 complex to stalled DNA replication forks. *J. Cell Biol.* **184**: 793-804.

148. Yazdi,P.T., Y.Wang, S.Zhao, N.Patel, E.Y.Lee, and J.Qin. 2002. SMC1 is a downstream effector in the ATM/NBS1 branch of the human S-phase checkpoint. *Genes Dev.* **16**: 571-582.

149. Zhang,J., X.Shi, Y.Li, B.J.Kim, J.Jia, Z.Huang, T.Yang, X.Fu, S.Y.Jung, Y.Wang, P.Zhang, S.T.Kim, X.Pan, and J.Qin. 2008a. Acetylation of Smc3 by Eco1 is required for S phase sister chromatid cohesion in both human and yeast. *Mol. Cell* **31**: 143-151.

150. Zhang,N., S.G.Kuznetsov, S.K.Sharan, K.Li, P.H.Rao, and D.Pati. 2008b. A handcuff model for the cohesin complex. *J. Cell Biol.* **183**: 1019-1031.

151. Zlatanou,A. and G.S.Stewart. 2010. A PIAS-ed view of DNA double strand break repair focuses on SUMO. *DNA Repair (Amst)* **9**: 588-592.

152. Zou,L. and S.J.Elledge. 2003. Sensing DNA damage through ATRIP recognition of RPA-ssDNA complexes. *Science* **300**: 1542-1548.

153. Zou,L., D.Liu, and S.J.Elledge. 2003. Replication protein A-mediated recruitment and activation of Rad17 complexes. *Proc. Natl. Acad. Sci. U. S. A* **100**: 13827-13832.

2

NUCLEOTIDE EXCISION REPAIR FROM DNA DAMAGE PROCESSING TO HUMAN DISEASE

Mischa G. Vrouwe and Leon H.F. Mullenders

Adapted from K. K. Khanna and Y. Shiloh (Eds.),
The DNA Damage Response: Implications on Cancer Formation and Treatment
(pp. 235-259). Springer

ABSTRACT

A network of DNA damage surveillance systems warrants genomic stability under conditions where cells and organisms are continuously exposed to DNA damaging agents. This network includes DNA repair pathways, but also signaling pathways that activate cell cycle checkpoints, apoptosis, transcription, and chromatin remodeling. Among the various repair pathways, nucleotide excision repair (NER) is a highly versatile and evolutionary conserved pathway with an intriguing wide substrate specificity; this pathway removes structurally unrelated bulky DNA lesions from the genome such as sunlight induced photolesions, bulky adducts formed by polycyclic aromatic hydrocarbons, cisplatin intrastrand crosslinks and alkylation products. The common features of these lesions are the variable degree of DNA helix distortion inflicted and their potency to block replication and transcription. The importance of functional NER for human health is highlighted by the existence of rare autosomal recessive human disorders such as xeroderma pigmentosum (XP). Affected individuals, characterized by a defect in NER, suffer from hypersensitivity to sunlight and display strongly enhanced cancer susceptibility in sunlight exposed parts of the skin. Mammalian NER involves multiple proteins (in excess of 30) and carries out the repair reaction in a highly orchestrated fashion.

In this book chapter we discuss the current knowledge of the molecular mechanisms underlying NER, its relation with human disease and the translation of knowledge to clinical use.

INTRODUCTION

Through evolution a network of DNA damage surveillance systems has evolved to warrant genomic stability under conditions where cells and organisms are continuously exposed to genotoxic agents present within the environment or exerted by endogenous processes. This network not only includes DNA repair pathways, but also signaling pathways that activate cell cycle checkpoints, apoptosis, transcription, and chromatin remodelling. The mechanisms by which eukaryotic cells sense DNA damage and activate signaling pathways are still poorly understood. One of the challenges is to understand how cells are capable to sense, recognize and repair low levels of different DNA lesions in their genomes at various stages of the cell cycle and in different chromatin environments.

A limited set of DNA repair pathways is capable to repair the large variety of structurally different DNA lesions that are formed in the genome. Nucleotide excision repair (NER) is a highly versatile and evolutionary conserved repair pathway that removes structurally unrelated bulky DNA lesions from the genome such as bulky adducts formed by polycyclic aromatic hydrocarbons, cisplatin intrastrand crosslinks and alkylation products. The common features of these lesions are the variable degree of DNA helix distortion inflicted and their potency to block replication and transcription elongation. In fact, NER is the only repair pathway in humans to remove the toxic and mutagenic photodimers from sunlight exposed parts of the skin. Mammalian NER involves multiple proteins (in excess of 30) and carries out the repair reaction in a highly orchestrated fashion involving a number of defined steps: (I) lesion recognition, (II) DNA unwinding and lesion demarcation, (III) dual incision and release of the incised fragment and (IV) gap filling by repair synthesis and ligation.

Two mechanistically distinct NER subpathways have been identified: Global genome NER (GG-NER) is capable of repairing DNA lesions in chromatin of different compaction levels and different functional states throughout the cell cycle. A subpathway of NER designated transcription-coupled repair (TC-NER) enables efficient repair of RNA polymerase II (RNAPII) blocking DNA lesions and allows quick resumption of transcription. The existence of three rare autosomal recessive human disorders i.e. xeroderma pigmentosum (XP), Cockayne syndrome (CS) and trichothiodystrophy (TTD) all associated with sensitivity to sunlight and NER deficiency, highlights the importance of functional NER for human health. Cells from XP patients are sensitive to UV (ultraviolet)-light and chemicals inducing bulky DNA lesions, and complementation studies revealed eight genes involved in the disease (XPA–XPG and XP Variant; see also chapter by A Lehmann). Complementation studies have revealed two CS complementation groups, CS-A and CS-B. In addition to XP and CS patients, a third group of UV sensitive and cancer prone patients has been identified that encompasses individuals exhibiting both XP and CS symptoms.

Although NER removes a variety of structurally unrelated lesions from the genome, we will concentrate on NER in UV-irradiated mammalian cells since UV-induced pyrimidine-pyrimidone (6-4) photoproducts (6-4 PP) and cyclobutane pyrimidine dimers (CPD) (figure 1) are the lesions most intensively studied and as such paradigmatic for NER.

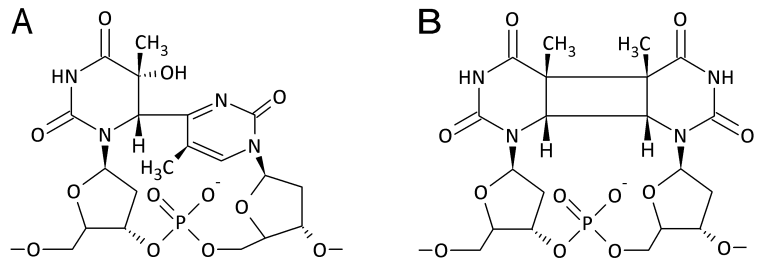

Figure 1: Structure of UV induced DNA photolesions. (A) pyrimidine-pyrimidone (6-4) photoproduct (6-4PP), (B) cis-syn cyclobutane thymine (pyrimidine) dimmer (CPD)

2.1 GLOBAL GENOME REPAIR (GG-NER)

Cells of all XP patients (except XP variant) were found to be defective in global genome repair of UV-induced photolesions. The identification of the different XP complementation groups led to the isolation of the XP genes and encoded proteins and allowed reconstitution of the process *in vitro* using purified proteins and naked DNA harboring a specific lesion. The first steps in NER, i.e. DNA lesion recognition and dual incision, require all XP factors (XPC, XPA, XPG, ERCC1-XPF) together with other factors (RPA, TFIIH). In addition, the *in vitro* reaction requires RF-C, PCNA, DNA polymerase ε and DNA ligase I for repair synthesis (Aboussekhra et al., 1995). This scheme represents the proteins to perform NER *in vitro*; additional factors are required for in vivo NER on chromatinized DNA templates.

2.1.1 DNA lesion recognition in GG-NER

Although XPA was originally proposed to be the principal damage recognition protein, it is now well established that GG-NER is initiated by the XPC protein which forms a trimeric complex with hHR23B (the human homologue of Rad23) and CEN2 (Masutani et al., 1994;Volker et al., 2001;Sugasawa et al., 1998;Araki et al., 2001). *In vivo* the recruitment of NER proteins to UV damage is abolished in XPC deficient cells, indicating that assembly of the NER complex is strictly XPC dependent. Mobility studies on GFP-tagged XPC suggest that the majority of XPC-hHR23B molecules (>90%) transiently interact non-specifically with genomic DNA (Hoogstraten et al., 2003;Politi et al., 2005;Hoogstraten et al., 2003). In fact, the general affinity of the complex for DNA and its specific affinity for photolesions such as CPD and 6-4PP are relatively low *in vivo* (Moser et al., 2005). The capacity of XPC-hHR23B to recognize a broad spectrum of structurally unrelated lesions might be understood from the observation that XPC binds to the accessible non-damaged DNA strand opposite to a DNA injury (Sugasawa and Hanaoka, 2007;Min and Pavletich, 2007).

Although the XPC-hHR23B complex acts as the principle initiator of NER, its action is preceded by the heterodimeric UV-DDB complex consisting of the p48 and p127 proteins, products of the DDB2 and DDB1 genes respectively (Keeney et al., 1993). In fact, repair of CPDs requires functional UV-DDB (Tang et al., 2000) and, in addition, UV-DDB significantly stimulates the repair of 6-4 PPs particularly at low UV doses (Hwang et al., 1999;Moser

et al., 2005). Microinjection of purified UV-DDB was originally found to restore the repair defect of XP-E cells as measured by unscheduled DNA synthesis. Subsequently it was found that the XP group E phenotype is caused by mutations in the DDB2 gene, encoding the p48 protein (XPE). The general affinity of UV-DDB for DNA is much higher (100–1000-fold) than that of XPC-hHR23B, while the specific affinity for 6-4PP is comparable (Batty et al., 2000). DDB2 is part of a functional CUL4A-based E3 ubiquitin ligase through its interaction with DDB1 (Groisman et al., 2003) and also binds to UV lesions as an active E3 ubiquitin ligase independent of XPC. UV irradiation activates the E3 ubiquitin ligase activity of the DDB2 complex by the binding of the ubiquitin-like protein Nedd 8 to the Cullin 4A. Several substrates for ubiquitylation were identified, including DDB2 itself, XPC and histones H2A, H3 and H4 (Kapetanaki et al., 2006;Sugasawa et al., 2005;Wang et al., 2006). The current view is that ubiquitylation (at least partly) facilitates NER: ubiquitylation of XPC enhances its affinity for DNA (both damaged and non-damaged DNA) whereas ubiquitylation of histones facilitates the access of repair proteins to DNA damage in chromatin by weakening the histone-DNA association. Interestingly and less well understood, ubiquitylated DDB2 is quickly targeted for degradation after UV (Sugasawa et al., 2005;Rapic-Otrin et al., 2002) even in the presence of large numbers of unrepaired photolesions.

As a general mechanism it was proposed (Moser *et al.*, 2005) that UV-DDB forms a stable complex when bound to DNA damage such as UV-induced 6-4PP, allowing subsequent repair proteins, starting with XPC-hHR23B, to accumulate and to verify the lesion, ultimately resulting in efficient repair. The fraction of 6-4PP that can be bound by UV-DDB is limited due to the low cellular quantity and fast UV dependent degradation of DDB2. In cells lacking UV-DDB a slow XPC-hHR23B dependent pathway is capable of repairing 6-4PP whereas repair of CPD is virtually absent.

2.1.2 Assembly of the preincision complex

Upon the recognition of lesions by a concerted action of UV-DDB and XPC-hHR23B, the latter recruits the multiprotein transcription factor TFIIH via direct protein-protein interactions (figure 2). The TFIIH complex is composed of a seven-subunit core containing two XP factors (XPB, XPD, TTD, p34, p44, p52, p62) and a three-subunit kinase complex (Cdk7, cyclin H and MAT1) termed the CAK unit. The complex exhibits dual functions i.e. it plays a role in RNAPI and RNAPII driven transcription as well as in NER. The XPB subunit of TFIIH is an ATP-dependent helicase that mediates unwinding of promoter DNA in a 3'-5' orientation during transcription initiation, whereas the XPD subunit of TFIIH is a 5'-3'ATP dependent helicase. Interestingly, the unwinding step of the damaged DNA during NER requires only the XPD helicase activity, whereas the ATPase activity of XPB is dispensable for NER (Coin et al., 2007). A two-step mechanism underlies the opening of the damaged DNA to allow assembly of the NER preincision complex: TFIIH mediates the initial opening after which RPA, XPA and XPG bind to obtain full opening of approximately 30 nucleotides around the lesion (Evans et al., 1997). XPA stimulates the ATPase activity of TFIIH whereas RPA and XPG stabilize the repair intermediate and contribute to full opening around the lesion. Since TFIIH functions in both transcription initiation and NER, it has been proposed that the recruitment of TFIIH to UV damage abolishes transcription initiation in UV-

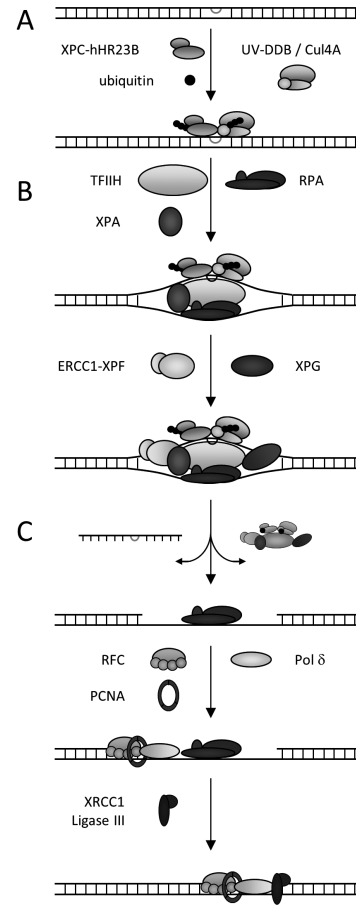

Figure 2: Model for global genome NER. (A) DNA damage recognition by UV-DDB and XPC-hHR23B. Ubiquitylation of damaged bound XPC and DDB2 is mediated via DDB1/Cul4A. (B) Assembly of the preincision complex. TFIIH is recruited to the lesion by the XPC-hHR23B complex, opening up the DNA though its helicase activity. The association of RPA further stimulates the unwinding. XPA binding contributes to damage verification and recruits the ERCC1-XPF complex. The ERCC1-XPF and XPG endonucleases incise the damaged DNA strand both 5' and 3' of the lesion. In addition its incision activity XPG also serves to stabilize the open DNA bubble structure. (C) Gap filling and ligation. Following dual incision the single stranded DNA patch is filled by the concerted action of RFC, PCNA and DNA polymerase δ, whereas XRCC1/Ligase III performs the final DNA ligation step. Note that in cycling cells DNA polymerase ε and DNA Ligase I also contribute to repair.

irradiated cells by a trans mechanism (Mone et al., 2001;Mullenders, 1998). However, inhibition of transcription by UV irradiation only occurs by direct interference of damage with the transcription machinery (Mone *et al.*, 2001) and does not otherwise affect the engagement of TFIIH in transcription (Hoogstraten et al., 2002).

Replication protein A (RPA) consists of three subunits and is an abundant single-stranded DNA-binding protein that binds optimally to approximately 30 nucleotides (de Laat et al., 1998). During the formation of the preincision complex RPA associates with the undamaged DNA strand partially unwound by TFIIH (~8-10 nucleotides) and subsequently extends it association to a 30-nucleotide region. This action leads to a separation of the DNA strands around the lesion. Importantly, RPA has been shown to interact with several core NER proteins including XPA, XPG and ERCC1-XPF. In living cells RPA can assemble into the pre-incision complex (consisting of XPC, TFIIH and XPG) in the absence of XPA. This complex, however, is insufficient to stimulate the 3' incision by XPG and incapable to recruit the 5' XRCC1-XPF endonuclease; the latter event requires recruitment of XPA in order to assemble the complete pre-incision complex (Rademakers et al., 2003). XPA is essential

for GG-NER and it is likely that RPA is required to recruit the XPA protein although direct *in vivo* evidence is lacking. The multiple protein interactions of XPA i.e. the association with RPA, and XRCC1-XPF, were demonstrated by the finding that the N-terminus of XPA binds to RPA and ERCC1, whereas the C-terminus interacts with TFIIH (Park et al., 1995) consistent with a central role for XPA in the formation of the NER pre-incision complex. Most notably, XPA deficient cells completely lack incision activity, indicating that XPA plays an important role in the coordination of dual incision. The observation that XPA binds preferentially to bent or kinked DNA duplexes (Camenisch et al., 2006;Camenisch et al., 2007) sheds light on its function in NER and links initial damage recognition by UV-DDB and XPC-hR23B to XPA recruitment. Both XPC and DDB2 introduce kinks in the DNA upon binding and hence might stimulate binding of XPA (Janicijevic et al., 2003). The binding of XPA most likely contributes to DNA damage verification in the pre-incision complex: the interaction between RPA bound to the undamaged strand and XPA with the kinked DNA duplex, provide the molecular tools that allow identification of the DNA lesion in the pre-incision complex.

RPA plays a key role at the interface of the pre-and post incision step of NER as the protein precipitates in chromatin immunoprecipitation (ChIP) reactions with antibodies raised against pre-incision and post-incision proteins (Moser et al., 2007). Analysis of the assembly and disassembly of repair proteins on immobilized damaged-DNA templates *in vitro* revealed that RPA remains bound after dual incision and initiates the assembly of DNA synthesis factors such as PCNA (Riedl et al., 2003).

2.1.3 Dual incision step

The two structure specific endonucleases XPG and ERCC1-XPF are involved in dual incision 3' and 5' of the lesion respectively. In the presence of both proteins, both 5' and 3' uncoupled incisions have been observed indicating that both incisions are made simultaneously (Moggs et al., 1996). The XPG protein specifically incises DNA at the side of the junction between single-stranded DNA and double stranded DNA (O'Donovan et al., 1994) approximately 2-8 nucleotides from the 3' side of the lesion. The protein interacts with RPA and TFIIH and the recruitment of XPG to the preincision complex was shown to depend on functional TFIIH. However, the presence of XPG in the pre-incision complex was shown to be required for stabilizing the open DNA bubble structure containing the DNA lesion, allowing binding and 5' incision by XRCC1-XPF (Wakasugi et al., 1997). Hence, XPG also has a structural role in NER and this goes along with the recent finding that XPG may act as a major stabilizing factor by associating with TFIIH (Ito et al., 2007), although dynamic measurements support separate moieties rather than a joined complex *in vivo* (Zotter et al., 2006). In cells of XPG patients with a combined XP and CS phenotype, XPG fails to associate with TFIIH and as a consequence the CAK subunit dissociates from core TFIIH. Deletion mutant analysis of XPG revealed that the so-called spacer region within the protein (which is not required for endonuclease activity) contributes to the substrate specificity of XPG and is required for the interaction with TFIIH and for NER activity *in vitro* and *in vivo* (Dunand-Sauthier et al., 2005).

The 5' junction between single-stranded and double-stranded DNA is cleaved by the heterodimeric endonuclease ERCC1-XPF approximately 15-24 nucleotides away from the 5' side of the lesion (Matsunaga et al., 1995). The two proteins cannot be isolated as separate entities indicating that complex formation underlies the stability of the dimeric endonuclease (Sijbers et al., 1996). Both *in vivo* and *in vitro* it has been shown that the interaction of ERCC1-XPF with XPA is essential for NER and that XPA recruits ERCC1-XPF to the pre-incision complex (Volker *et al.*, 2001). The incision activity of ERCC1-XPF is stimulated by direct interactions with RPA in model substrates (de Laat et al., 1998). Mutations in XPF are associated with mild XP; however, a unique XP-F patient with a severe phenotype was recently described displaying signs of accelerated aging (Niedernhofer et al., 2006). Moreover, mutations in ERCC1 have so far only been reported for one patient with severe clinical features but only a mild repair defect at the cellular level (Jaspers et al., 2007). These latter findings suggest additional functions for ERCC1 and XPF. Indeed, ERCC1-XPF is involved in several other processes such as homologous recombination, repair of interstrand cross-links and telomere maintenance.

2.1.4 The post-incision step in NER

Dual incision and removal of the lesion containing single stranded DNA fragment is followed by gap filling and ligation, generally termed repair synthesis. The transition between dual incision and repair synthesis needs to be coordinated to omit activation of the DNA damage signaling and to prevent recombination, the formation of deletions etc. Conceivably the incision reactions might not occur simultaneously and might be initiated by ERCC1-XPF to start DNA synthesis before XPG cutting takes place (Gillet and Scharer, 2006). An alternative mechanism to prevent undesired processing is that one key factor is partner in the pre-and post-incision stages of NER and remains bound to the DNA. The two stages of NER can be separated *in vitro* (Riedl *et al.*, 2003) and pre-and post- incision complexes have been isolated from living cells (Moser *et al.*, 2007). These analyses revealed RPA as common factor in the reaction and showed that RPA remains associated with the DNA upon dual incision. In addition to RPA, repair synthesis requires RF-C, PCNA, DNA polymerases ε and δ as well as Ligase I *in vitro* (Aboussekhra et al., 1995;Shivji et al., 1992;Shivji et al., 1995); the recruitment of the post-incision factors is entirely depending on dual incision. PCNA is a homotrimeric sliding clamp that encircles the DNA and acts as a template to allocate DNA polymerases ε and δ to the DNA (Maga and Hubscher, 2003). Loading of PCNA on the DNA requires the clamp loader RF-C and ATP. Recent *in vivo* experiments showed that predominantly DNA polymerase δ is recruited to repair patches upon UV irradiation in replicating and quiescent cells and that the role of DNA polymerase ε is restricted to S-phase cells (Moser *et al.*, 2007). Moreover, the surprising finding was recently made that under certain conditions (G_0 cells, DNA synthesis inhibitors) the translesion synthesis DNA polymerase κ may also play a role in repair synthesis during NER (Ogi and Lehmann, 2006), emphasizing the need to confirm the roles of these late factors in NER *in vivo*.

The NER reaction is completed by ligation of the 5' end of the newly synthesized DNA to the original sequence. Although Ligase I is sufficient for sealing nicks during *in vitro*

repair synthesis, XRCC1-LigIIIα appears to be indispensable for ligation of NER-induced breaks. Two distinct complexes were identified that differentially carry out gap filling in NER (Moser *et al.*, 2007). XRCC1-LigIIIα and DNA polymerase δ co-localize and interact with NER components in a UV- and incision-dependent manner throughout the cell cycle. In contrast, DNA Ligase I and DNA polymerase ε are recruited to UV-damage sites only in proliferating cells. These findings indicate that cells have differential requirements for ligases and polymerases in repair synthesis depending on the cell cycle.

Finally, the progression of NER seems to be controlled and requires the completion of the post-incision step in NER. Inhibition of DNA polymerases δ and ε in non-dividing normal human cells by the DNA polymerase inhibitors HU/AraC leads to accumulation of DNA strand breaks, DNA damage signaling (H2AX signaling) but also to strong retardation of repair of UV induced photolesions such as 6-4PP (Moser *et al.*, 2007). Obviously, efficient gap filling by DNA synthesis and ligation of the repair patch is required to drive NER to completeness and implicates either the existence of efficient cellular control mechanisms or factors that limit the number of (pre-) incision events.

2.1.5 Damage signaling in GG-NER

It has been long acknowledged that exposure of cells to UV light not only activates NER, but also modulates other DNA damage responses impacting cell cycle progression and apoptosis. The exact mechanisms underlying the decision in cell fate have long remained obscure. However, recent works have begun to uncover the molecular mechanisms determining cell fate following UV exposure and demonstrate links between NER and other pathways in the DNA damage response. One of the most prominent players in the UV-induced DNA damage response would be the ataxia telangiectasia mutated and Rad3-related (ATR) protein. ATR is a member of the phosphoinositol-3-kinase like kinase family that also includes the ataxia telangiectasia mutated (ATM) protein. It has now become clear that both proteins act as one of the earliest components in the damage response, their main function being the phosphorylation various proteins to effectively propagate the damage signaling. While ATM and ATR share many substrates for phosphorylation, the activating structures for these kinases themselves differ. ATM is activated by double stranded DNA breaks (Savitsky et al., 1995), whereas it is RPA bound to single stranded DNA what activates the ATR kinase at stalled replication forks (Zou and Elledge, 2003). Although it was initially believed that the capacity to activate ATR was restricted to cells in S phase, it was later demonstrated that H2AX is phosphorylated in an ATR dependent manner following UV exposure of non-replicating cells (O'Driscoll et al., 2003). The origin of this signaling lies in the formation of single stranded DNA patches following the excision of the damage containing oligo by GG-NER (Marini et al., 2006;Marti et al., 2006;Matsumoto et al., 2007;O'Driscoll et al., 2003). Such RPA containing ssDNA patches would resemble the structures formed after replication fork stalling and hence allow ATR signaling via a common mechanism. This allows not only the phosphorylation of the many substrates of this kinase, but also serves as a prerequisite for ubiquitylation of histone H2A (Bergink et al., 2006).

Normally the activation of ATR is associated with cell cycle checkpoint arrest and NER dependent activation of ATR indeed is able to induce cell cycle arrest outside the S phase (Stiff et al., 2008). Whether other processes are affected by this signaling is currently unknown. However, one possibility would be that ATR activation could regulate the levels of checkpoint protein p53. As a transcriptional regulator p53 mediates the expression of genes involved in DNA repair, cell cycle arrest and apoptosis. The fact that both DDB2 and XPC expression are regulated in a p53 dependent manner allows for the possibility that ATR activation could enhance the NER capacity following damage induction. Although the existence of such a regulatory mechanism remains to be demonstrated, support comes from the observation that cells lacking functional p53 have a deficiency in GG-NER (Ford and Hanawalt, 1995). Recent experiments indicate that ATR is indeed important for efficient repair of photolesions as ATR deficient cells are profoundly defective in GG-NER but, surprisingly, only during S-phase (Auclair et al., 2008). The mechanism underlying this cell cycle specific regulation of repair remains to be clarified. Although GG-NER mediated signaling is now well established, the first demonstration that UV exposure induced a checkpoint response (Yamaizumi and Sugano, 1994) was in TC-NER deficient cells. Here checkpoint activation does not depend on processing of UV lesions by NER, but rather it is the absence of repair that results in enhanced checkpoint activation. DNA lesions that block RNA polymerase II, such as UV lesions, cause a dramatic increase in the levels of both normal and phosphorylated p53 when cells are deficient in TC-NER. Despite the fact that p53 induction has long been associated with stalled transcription, the molecular mechanisms that underlie it remain enigmatic. The identification of ATR as the kinase that, in conjunction with RPA, phosphorylates p53 has begun to shed some light on this matter (Derheimer et al., 2007). However, this discovery itself raises a question about the mechanism of ATR activation at stalled RNA polymerases. The archetypical activating structure for ATR is believed to be a single stranded DNA gap and activation of the kinase depends on additional proteins (e.g. TopBP1, Rad9) that are independently recruited to such substrates (Delacroix et al., 2007;Kumagai et al., 2006). It is questionable whether a stalled RNA polymerase confers a structure that resembles gapped DNA, and as such it would be of interest to investigate the participation of other factors normally associated with ATR signaling in the context of RNA polymerase II mediated signaling.

2.1.6 Chromatin structure and NER

In general, the condensed structure of chromatin poses problems to DNA metabolizing processes; notably, NER in a chromatin context is severely inhibited compared to naked DNA (Hara et al., 2000). To overcome this barrier, different mechanisms have evolved to remodel chromatin enhancing the accessibility of damaged DNA for repair proteins. In addition, following removal of the lesion and completing of the post incision stage of NER, cells need to restore the original chromatin structure to maintain the epigenetic information (Green and Almouzni, 2002). Finally, there is clear evidence that repair efficiencies differ greatly in various chromatin environments but the underlying mechanism is not well understood (Mullenders et al., 1991). Two major mechanisms may alter chromatin structure: posttranslational modification of histone tails and ATP dependent chromatin remodelling.

As mentioned in section 1.1, the role of UV-DDB in NER has revealed unexpected complexities as this complex associates with proteins that are involved in chromatin remodeling (acetylation) and ubiquitylation (Groisman et al., 2003;Datta et al., 2001); the latter activity is related to the participation of DDB1 and DDB2 in a large complex making up a ubiquitin ligase together with Cul4A and Roc1. The ligase activity of this complex is regulated by the COP9 signalosome (CSN). The ubiquitin ligase activity is stimulated by UV (at least with respect to GG-NER) leading to poly-ubiquitylation and subsequent degradation of DDB2 itself; importantly, ubiquitylation of XPC does not serve as a signal for degradation, but merely stimulates the activity of XPC–HR23B by an unknown mechanism. It is conceivably that the ubiquitylation of histones and DDB2 may lead to increased accessibility of the site of damage by removal and/or loosening of DNA–histone contacts and the displacement of UV-DDB from the lesion.

One of the important changes after UV irradiation is the appearance of hyperacetylated histones, most notably shown by the inhibition of histone deacetylases (HDAC) that trigger genome-wide histone hyperacetylation at both histone H3 and H4 upon UV irradiation. Recently, histone acetyl transferases (HAT) such as the HAT p300 (Fousteri et al., 2006) and Gcn5 (Yu et al., 2005) have been suggested to play a role in increasing the accessibility of chromatin to NER proteins. A role for p300 in NER is suggested by interactions of p300 with the repair factors UV-DDB (Rapic-Otrin *et al.*, 2002) and PCNA (Hasan et al., 2001), stimulation of repair by p300 *in vitro* (Frit et al., 2002) and enhancement of NER by the histone deacetylase inhibitor sodium butyrate (Ramanathan and Smerdon, 1989). Genetic approaches (Smerdon et al., 1982;Mullenders et al., 1986) revealed that histone acetylation is not only important for GG-NER but also for TC-NER, although transcriptionally active genes themselves are enriched for acetylated histones.

In vitro NER assays using chromatin substrates with defined lesions, generally reveal that repair is slow in the nucleosomal DNA with no movement or disruption of nucleosomes (Gaillard et al., 2003). Repair measurement of a defined DNA lesion (i.e. 6-4PP) located in a dinucleosome chromatin template demonstrated that ATP-dependent remodeling might enhance the pre-and postincision steps of NER as dual incision is facilitated by ACF, an ATP-dependent chromatin remodeling factor (Ura et al., 2001). The ACF protein moves nucleosomes rather than displacing them. Also incubation with the nucleosome remodeling complex SWI/SNF and ATP altered the conformation of nucleosomal DNA and promoted more homogeneous repair by nucleosome sliding, thereby increasing accessibility to DNA (Gaillard *et al.*, 2003;Hara and Sancar, 2003). *In vivo* data in yeast suggest that SWI/SNF has a significant role in modulating the accessibility of UV induced photolesions for the NER repair machinery thereby enhancing repair (Yu *et al.*, 2005). Interestingly, the SWI/SNF complex and the abovementioned Gcn5 histone acetyl transferase facilitate chromatin modifications independent of functional NER, indicating that chromatin remodeling precedes NER. In spite of this, and unexpectedly, the homologues of XPC-HR23B in yeast (Rad4-Rad23) directly interact with the SWI/SNF remodeling complex via two subunits and this interaction was shown to be enhanced following UV irradiation (Gong et al., 2006). Taken together the limited data available to date, suggest important roles for histone modifying enzymes such as HATs and ATP-dependent chromatin remodelers,

yet mechanistic understanding of their impact on NER awaits further experimentation particularly to clarify their roles in mammalian NER.

Several studies have provided evidence for the involvement of the acidic HMG proteins that destabilize higher order chromatin structures, in the response to bulky DNA lesions. High mobility group protein B1 (HMGB1) binds to and bends damaged DNA and recent evidence demonstrates that mouse cells lacking HMGB1 are hypersensitive to the toxic effects of UVC radiation and may display reduced NER (Lange et al., 2008). HMGN1 was demonstrated to be recruited to TCR complexes (Fousteri *et al.*, 2006) and is exclusively involved in TC-NER as HMGN1-deficient mouse cells showed decreased rates of CPDs removal in actively transcribed genes (Birger et al., 2003). HMGN1 proteins directly compete for DNA binding sites with histone H1, elevate the level of histone H3 acetylation (Lim et al., 2005) and modulate the level of histone H3 phosphorylation (Lim et al., 2004). It is feasible that the loss of H1 in concert with histone modifications might enhance the DNA damage response following UV irradiation, but surprisingly this only affects TC-NER.

The current models of NER propose that chromatin structure is transiently disrupted during the various stages of repair to facilitate access of the repair machinery to DNA lesions and to carry out the subsequent steps. As a final step it is then necessary to restore the preexisting chromatin structure. A central question is whether chromatin restoration involves recycling of parental histones or new histone incorporation. The chromatin assembly factor (CAF-1), a key factor involved in histone deposition, plays a role in the restoration of chromatin following gap filling and ligation. In living cells this protein is recruited to sites of UV-induced DNA damage in a NER-dependent manner (Green and Almouzni, 2002); a process that is possibly mediated by PCNA (Gerard et al., 2006). The role of CAF-1 as chromatin assembly factor was further highlighted by the observation that histone H3.1 was assembled *de novo* at repair sites, reflecting a chromatin restoration step following NER (Polo et al., 2006). Hence, chromatin restoration after DNA damage is more than recycling of histones and may represent an imprint for newly repaired chromatin.

Taken together, it appears that repair proteins, DNA and histone binding proteins and chromatin modifiers play a key role in modulating the accessibility of nucleosomal DNA to the repair machinery as well as in the restoration of the chromatin state following repair. However, it is also evident that we are only beginning to understand the modifications that are required to allow NER in different chromatin environments.

2.2 TRANSCRIPTION COUPLED REPAIR

As pointed out, stalled transcription elongation by a DNA lesion is counteracted by the activation of a specialized NER subpathway named transcription coupled repair (TC-NER). A hallmark of TC-NER is the accelerated repair of DNA lesions (most notably demonstrated for UV-induced CPD) in the transcribed strand of active genes and the inability of TC-NER deficient cells to resume DNA damage-inhibited DNA and RNA synthesis (van Oosterwijk et al., 1996;Mayne and Lehmann, 1982;van Oosterwijk et al., 1996). Obviously, the elongating RNA polymerase II (RNAPIIo) when stalled at a lesion efficiently triggers the recruitment of TC-NER specific factors and NER proteins. Once the lesion has been recognized, all

subsequent steps leading to assembly of a functional NER complex require the same NER core factors as described for GG-NER (figure 3). TC-NER is a strongly conserved repair pathway identified in a variety of organisms including bacteria, yeast and mammals. In UV-irradiated E. coli cells, a 130 kDa protein encoded by the mfd gene (termed TRCF: transcription-repair coupling factor) was found to be essential for TC-NER (Selby et al., 1991). This protein releases the RNA polymerase and transcript from the DNA in an ATP dependent manner and also facilitates repair of DNA damage by attracting NER factors, in particular UvrA. Also in mammalian cells specific factors for TC-NER have been identified. Measurements of UV–photolesions in transcriptionally active genes of cells derived from various UV sensitive patients identified impaired TC-NER in cells from individuals suffering from Cockayne syndrome (CS). CS is a rare disorder that is associated with a wide variety of clinical symptoms including dwarfism, mental retardation, cataract and eye abnormalities as well as photosensitivity, but no enhanced susceptibility to cancer. As a consequence, these patients die at an early age and CS has been classified as a premature aging syndrome. Complementation studies have identified two CS complementation groups, CS-A and CS-B. A third group encompasses patients with mutations in XPB, XPD or XPG genes exhibiting both XP and CS symptoms. The CSB gene encodes a 168 kDa protein that contains helicase domains (strong homology to similar domains in SNF2-like proteins) and that displays DNA-dependent ATPase and DNA binding activity, but no helicase activity. Also, the bacterial and yeast counterparts of CSB, i.e. Mfd and Rad26 respectively, are DNA dependent ATPases. In addition, CSB has nucleosome remodelling activity and binds to core histone proteins *in vitro* (Citterio et al., 2000) and transcriptome analysis of CS-B cells revealed deregulation of gene expression similar to that caused by agents that disrupt chromatin structure (Newman et al., 2006).

The CSA protein contains WD-40 repeats (a motif involved in protein-protein interactions) and is part of an E3-ubiquitin ligase (E3-ub ligase) complex consisting of DDB1, Cullin 4A and ROC1/Rbx1 proteins (Groisman *et al.*, 2003). In response to UV the COP9 signalosome (CSN) was found to associate with the CSA complex resulting in the inactivation of the ubiquitin ligase activity of the CSA complex in TC-NER.

XAB2 is an XPA binding protein and an essential factor in TCR, but so far mutations in XAB2 have not been associated with UV sensitive patients. The protein is involved in pre-mRNA splicing and transcription, interacts with chromatin bound stalled RNAPIIo complex in a UV- and CS-dependent manner and might function as a scaffold for protein complex formation in TC-NER (Kuraoka et al., 2008). Finally, deficiency in HMGN1 (a nucleosome binding protein) leads to UV-B sensitivity in HMGN1 knock out mice and impairs TC-NER in UV-C irradiated mouse embryonic fibroblasts. Interestingly, HMGN1 interacts with UV-stalled RNAPIIo and this interaction depends on CS proteins (Fousteri *et al.*, 2006).

2.2.1 Molecular models for TC-NER

The additional involvement of RNAPII in TC-NER replaces the requirement for XPC-HR23B and UV-DDB to identify DNA lesions, as is the case in GG-NER. Instead the system utilises a factor that is capable to couple blockage of transcription by DNA damage to

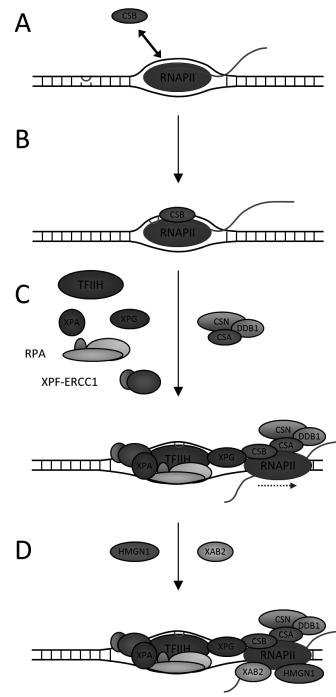

Figure 3: Model for transcription coupled NER. (A) During transcription CSB dynamically interacts with elongating RNAPII. (B) Stalling of RNAPII on DNA lesions stabilizes the interaction of CSB with the polymerase. (C) The stalled RNAPII/CSB complex allows for the recruitment of the core NER factors as well as the CSA/DDB1/CSN ubiquitin ligase complex. Conformational changes to the stalled RNAPII complex imposed by TFIIH and XPG would allow access to the damaged DNA strand. (D) The association of CSA with the stalled polymerase enables the recruitment of additional repair factors like HMGN1 and XAB2.

efficient DNA damage recognition and repair. The transcription-repair coupling factor in mammalian cells appears to be CSB: a DNA dependent ATPase that interacts with RNAPII even in undamaged cells (van Gool et al., 1997). Mu and Sancar (Mu and Sancar, 1997) showed that purified human excision repair factors and a DNA substrate analogous to a transcription bubble terminating at a CPD, are capable to excise the lesion independent of XPC. Hence the transcription bubble may substitute for XPC function, which in GG-NER causes the two damaged base pairs to flip out of the double helix.

Persistent blockage of transcription activates a stress response leading to stabilization of p53 and specific modifications of p53 at Ser 15 providing a strong signal for apoptosis in cultured cells and in the epidermis of mice (Ljungman et al., 1999;van Oosten et al., 2000). To relieve the strong apoptotic signal the cell has to remove the transcription blockage; however, the stalled RNAPII is likely to shield the DNA lesion and prevents access to the NER machinery. Two scenarios exist to cope with this problem. One potential mechanism would be that the RNAPII is displaced from the DNA or removed by ubiquitylation and subsequent degradation by the proteosome thereby making the lesion available for the NER machinery. This mechanism has been described for bacterial TC-NER as Mfd releases RNAP and recruits repair proteins (Selby and Sancar, 1994). In mammals such a scenario would require the recruitment of NER proteins by the action of CS proteins.

Another possible mechanism is that TC-NER occurs without displacement/removal of RNAPIIo but requires conformational changes of RNAPII to allow access to the DNA lesion and resume transcription. Particularly the XPG endonuclease in concert with the

basal transcription factor TFIIH have been implicated in an ATP dependent remodelling of the arrested RNAPII, allowing incision 3' of the lesion without the need for CSB (Sarker et al., 2005). Although *in vitro* experiments indicate a prominent role of XPG in the early stages of TC-NER, recruitment of XPG to stalled RNAPII in intact cells requires functional CSB (Fousteri *et al.*, 2006). Upon binding to stalled RNAPIIo, CSB functions as a coupling factor that mediates the recruitment of subsequent NER repair factors TFIIH, XPG, RPA and ERCC1-XPF. Indeed, live cell imaging revealed that GFP-tagged CSB interacts with the transcription machinery in the presence of DNA damage. Recruitment of CSA is CSB dependent and required for binding of both HMGN1 and XAB2 but is dispensable for the recruitment of pre-incision NER proteins. The emerging picture of TC-NER is rather complex and not well understood at the molecular level. Most strikingly, repair of transcription blocking lesions in mammalian cells occurs without displacement of the stalled RNAPIIo and requires at least two essential assembly factors with differential modes of action: CSB as a repair–transcription coupling factor to attract the core NER pre-incision factors and CSA to recruit chromatin remodelers. However, the precise role of CSB ATP-ase activity and the CSA associated the E3-ubiquitin ligase complex in TC-NER are not known.

2.3 NER DEFICIENCIES AND CANCER

As pointed out, inherited defects in the NER pathway are manifested in at least three different diseases: XP, CS and the photosensitive form of trichothiodystrophy (TTD). Of these, only patients with XP are prone to sunlight-induced skin cancer, although patients with CS and the photosensitive form of trichothiodystrophy (TTD) are clearly UV-sensitive. For most cancers the causative agent is unknown but skin cancer is a notorious exception. In fact, XP is a paradigm for a causal link between defective DNA repair and exposure to an exogenous (environmental) component i.e. sunlight, as XP patients have a >1000-fold increased risk to develop skin tumors primarily at sun-exposed sites of their body. Mutation analysis of TTD revealed a complicated genotype as patients have been identified with mutations in the XPB, XPD and TTDA genes, all components of the TFIIH complex. Since TFIIH functions both in DNA repair and transcription it is assumed that photosensitive TTD patients have a defect in both processes; these patients are characterized by sulphur-deficient brittle hair and nails, ichthyosis, neurological/developmental abnormalities and short life span. Finally, patients exist that belong to the XP-B, XP-D or XP-G complementation group that display severe features of CS (early death and neurological/developmental abnormalities) and XP (skin lesions and skin cancer).

As mentioned above, the most overt phenotype of XP patients is their enhanced susceptibility to develop skin cancer including basal cell carcinomas (BCCs) and squamous cell carcinomas (SCCs) but also melanomas. Increased cancer susceptibility is not only seen at the sun-exposed parts of the body but is also evidenced by a low incidence of internal tumors. Since epidemiological data on the relationship between skin cancers and ambient solar UV radiation are very restricted, animal models i.e. (transgenic) mice, have been used to study the process of UV carcinogenesis in depth and to gain quantitative data on tumor development and dose, time and wavelength of the UV radiation and genetic

make-up. Transgenic hairless mice (to facilitate UVB irradiation and the identification of tumors) mimicking the human XP phenotype have been extremely useful in studying the role of (exogenously-induced) DNA damage in mutagenesis, carcinogenesis and aging. The protective role of GG-NER and TC-NER against the acute (i.e. erythema, apoptosis, cell cycle arrest) and long term (i.e. skin cancer, aging) effects of genotoxic (UV-B light, bulky chemicals) exposure has been dissected in mouse models with defined mutations in NER genes, i.e. XPE (DDB2), XPA (defective in GG-NER and TC-NER), XPC (defective in GG-NER) or CSB (defective in TC-NER) deficient mice. DDB2$^{-/-}$ mice are deficient in GG-NER of CPD, but otherwise TC-NER proficient. XPA$^{-/-}$ and CSB$^{-/-}$ mice appeared to be 10-fold more sensitive to the acute toxic effects of UV-B light (erythema/edema of the skin) and to the polycyclic aromatic hydrocarbon DMBA (lethality) compared to normal, XPC$^{-/-}$ or DDB2$^{-/-}$ mice (Wijnhoven et al., 2001;Berg et al., 1998). The difference in UV-B sensitivity relates to enhanced apoptosis and severe cell cycle arrest of epidermal keratinocytes in XPA$^{-/-}$ and CSB$^{-/-}$ mice (van Oosten *et al.*, 2000;Stout et al., 2005). These results highlight TC-NER as a profound survival pathway and identify TC-NER as the principal defense mechanism towards the deleterious effects of transcription blocking DNA lesions by counteracting apoptosis and cell cycle arrest. However, this increased survival occurs at expense of increased mutagenesis manifested by the fast appearance of epidermal patches expressing mutant p53 in UV-B irradiated XPC$^{-/-}$ mice (Rebel et al., 2005) but also by increased spontaneous mutagenesis in lymphocytes (Wijnhoven *et al.*, 2001). Mutation spectrum analysis showed that almost all UV-B light induced mutations in rodent and human were at dipyrimidine positions with C→T transition mutations being the most prominent. The latter is caused by three factors. Firstly, DNA polymerase η preferentially incorporates adenine residues opposite to non-instructional lesions. Secondly, 5-methylcytosines within CPD lesions display accelerated deamination rates, resulting in base changes to uracil. Moreover, CPDs are formed preferentially at dipyrimidines containing 5-methylcytosine when cells are irradiated with UV-B or sunlight. Finally, CC→TT double transitions are caused in vivo exclusively by UV-induced pre-mutagenic lesions in XPA and XPC deficient mice and human XPC patients (Spatz et al., 2001). Also in tumors isolated from UV-B irradiated mice (with high frequencies of p53 mutations) defective GG-NER and TC-NER resulted in increased mutations in p53 through UV-targeted dipyrimidine sites but strikingly, only XPA$^{-/-}$ and CSB$^{-/-}$ mice developed benign papillomas before squamous cell carcinomas (SCC). These papillomas carried mutations in the 12th Hras codon with a dipyrimidine site in the transcribed strand; such mutations were not observed in the UV-induced SCCs. Evidently, proficient TC-NER prevents Hras mutagenesis and therefore prevents the development of papillomas.

Taken together, GG-NER and TC-NER protect against UV-B induced skin cancer in mice. Although the mouse cancer data reveals remarkable similarities with skin cancer susceptibility in human, striking differences exist as well. Most notably, the XPA$^{-/-}$ mice, in contrast to XP patients, do not develop melanoma whereas CSB$^{-/-}$ mice, but not CSB patients, are skin cancer prone. The latter is related to the poorly expressed GG-NER system in rodents. Unlike human cells, rodent epidermal cells express DDB2 at a low level. Mice ectopically expressing DDB2 display delayed onset of squamous cell carcinoma following

chronic UV-B light exposure and at the cellular level enhanced repair of UV-photolesions (Alekseev et al., 2005;Pines et al., 2008) whereas DDB2$^{-/-}$ mice were hypersensitive to UV-induced skin carcinogenesis. Ectopic expression of DDB2 in CSB$^{-/-}$ mice counteracts the cancer proness of UVB exposed CSB$^{-/-}$ mice indicating that GG-NER serves as a back-up system for TC-NER deficiency (Pines et al., in preparation).

2.4 PERSPECTIVES

Molecular, cellular and animal studies over the last three decades have greatly improved our understanding of the interplay between cellular processes (DNA damage, NER and transcription) and human disease. However, much is to be learned about the exact functions of key players in NER and the mechanisms by which eukaryotic cells sense DNA damage in their genome and which signals activate and regulate NER. The mammalian genome is protected against genotoxic insults by a network of DNA damage response (DDR) mechanisms initiated by sensing of DNA damage or damage-induced chromatin alterations through specific sensors. The next stage in the process is to transmit the signal to transducers that are able to pass the signal to effectors that control various protective pathways i.e. different DNA repair pathways, cell cycle checkpoints, apoptosis, transcription and chromatin remodeling. Hence, full understanding of mammalian NER not only requires insights into the mechanisms of NER but also the DNA damage signaling cascade.

Faithful DNA damage processing in various chromatin environments requires process control at each individual step including regulation of the expression of NER factors, regulation of NER protein activity by post-translational modifications, remodeling of chromatin at sites of DNA damage, monitoring progress and completeness of repair and checking integrity of chromatin after damage removal. Presently, little is known about these regulatory processes and how NER is connected with DNA damage signaling pathways i.e. specific sensors of DNA damage (such as UV-induced photolesions) and transducers able to pass the signal to downstream effectors i.e. transcription, chromatin remodeling and protein modification. Which are the factors that control initiation, progression and completion of the NER process? Which factors enable GG-NER activity in different chromatin environments such as heterochromatic and euchromatic regions? The ultimate goal is to use this information to further improve the mathematical modeling of NER. The current model based on in vivo kinetic data (Politi *et al.*, 2005) unveils that a sequential assembly mechanism appears remarkably advantageous in terms of repair efficiency and suggests that random assembly and preassembly are kinetically unfavorable.

Multiple gene products are implicated in TC-NER but we lack knowledge of the signals that regulate TC-NER and we do not know the precise function of key components in TC-NER. Most notably, it is not clear why chromatin remodeling would be required for TC-NER in addition to the structural changes that are needed to allow transcription of actively transcribed chromatin-embedded DNA substrates. Currently it is not well understood which factors or processes are required to resume transcription although it is clear that besides TC-NER other mechanisms play a role (Rockx et al., 2000). Of particular interest to resolve is the fate of stalled RNAPII when TC-NER fails to operate and to find

out which types of oxidative DNA damage (induced by metabolic processes) can inhibit transcription *in vivo*. A stalled RNAPII transcription machinery senses DNA damage and leads to a strong signal for apoptosis. Moreover, there is increasing evidence that during S-phase collisions of replication forks with transcription complexes stalled at DNA lesions, are a very mutagenic event (Hendriks et al., 2008). Hence, it is of pivotal importance to dissect the contributions of impaired TC-NER and transcription defects in the aetiology of the progeroid, neurodevelopmental disorder of CS.

Knowledge of the NER pathway and repair proteins has lead to the identification of inherited polymorphisms of NER genes (SNPs). These SNPs may contribute to variations in DNA repair capacity and genetic susceptibility to cancer. Numerous published data provide emerging evidence that polymorphisms in NER genes may contribute to the genetic susceptibility to cancers in man. However, many of the studies are of limited value because of the limited size of the study populations. It is obvious that large and well-designed population-based studies are warranted to identify NER genes as biomarkers to screen high-risk populations for early detection of cancer. Knowledge of the NER pathway and repair proteins can also be applied as basis for enzyme therapy to counteract sunlight induced skin cancer. The bacterial DNA repair enzyme T4 endonuclease V packaged in an engineered delivery vehicle was shown to be capable of reversing the defective repair in xeroderma pigmentosum cells (Yarosh, 2002). Moreover, expression of the CPD-photolyase in mouse epidermis is an effective tool to combat UV-B induced non-melanoma skin cancer (Jans et al., 2005). These findings directly proof that enhancement of repair activity can be used as a therapeutic tool to protect against UVB induced skin cancer although NER proteins have not been applied so far.

ACKNOWLEDGEMENTS

This work was supported by grants from ZonMw (912-03-012 and 917-46-364) and from EU (MRTN-Ct-2003-503618).

REFERENCE LIST

1. Aboussekhra, A., M. Biggerstaff, M. K. Shivji, J. A. Vilpo, V. Moncollin, V. N. Podust, M. Protic, U. Hubscher, J. M. Egly, and R. D. Wood. 1995. Mammalian DNA nucleotide excision repair reconstituted with purified protein components. *Cell* **80**: 859-868.
2. Alekseev, S., H. Kool, H. Rebel, M. Fousteri, J. Moser, C. Backendorf, F. R. de Gruijl, H. Vrieling, and L. H. Mullenders. 2005. Enhanced DDB2 expression protects mice from carcinogenic effects of chronic UV-B irradiation. *Cancer Res.* **65**: 10298-10306.
3. Araki, M., C. Masutani, M. Takemura, A. Uchida, K. Sugasawa, J. Kondoh, Y. Ohkuma, and F. Hanaoka. 2001. Centrosome protein centrin 2/caltractin 1 is part of the xeroderma pigmentosum group C complex that initiates global genome nucleotide excision repair. *J. Biol. Chem.* **276**: 18665-18672.
4. Auclair, Y., R. Rouget, e. B. Affar, and E. A. Drobetsky. 2008. ATR kinase is required for global genomic nucleotide excision repair exclusively during S phase in human cells. *Proc. Natl. Acad. Sci. U. S. A* **105**: 17896-17901.
5. Batty, D., V. Rapic'-Otrin, A. S. Levine, and R. D. Wood. 2000. Stable binding of human XPC complex to irradiated DNA confers strong discrimination for damaged sites. *J. Mol. Biol.* **300**: 275-290.
6. Berg, R. J., H. J. Ruven, A. T. Sands, F. R. de Gruijl, and L. H. Mullenders. 1998. Defective global genome repair in XPC mice is associated with skin cancer susceptibility but not with sensitivity to UVB induced erythema and edema. *J. Invest Dermatol.* **110**: 405-409.
7. Bergink, S., F. A. Salomons, D. Hoogstraten, T. A. Groothuis, H. de Waard, J. Wu, L. Yuan, E. Citterio, A. B. Houtsmuller, J. Neefjes, J. H. Hoeijmakers, W. Vermeulen, and N. P. Dantuma. 2006. DNA damage triggers nucleotide excision repair-dependent monoubiquitylation of histone H2A. *Genes Dev.* **20**: 1343-1352.
8. Birger, Y., K. L. West, Y. V. Postnikov, J. H. Lim, T. Furusawa, J. P. Wagner, C. S. Laufer, K. H. Kraemer, and M. Bustin. 2003. Chromosomal protein HMGN1 enhances the rate of DNA repair in chromatin. *EMBO J.* **22**: 1665-1675.
9. Camenisch, U., R. Dip, S. B. Schumacher, B. Schuler, and H. Naegeli. 2006. Recognition of helical kinks by xeroderma pigmentosum group A protein triggers DNA excision repair. *Nat. Struct. Mol. Biol.* **13**: 278-284.
10. Camenisch, U., R. Dip, M. Vitanescu, and H. Naegeli. 2007. Xeroderma pigmentosum complementation group A protein is driven to nucleotide excision repair sites by the electrostatic potential of distorted DNA. *DNA Repair (Amst)* **6**: 1819-1828.
11. Citterio, E., d. B. van, V, G. Schnitzler, R. Kanaar, E. Bonte, R. E. Kingston, J. H. Hoeijmakers, and W. Vermeulen. 2000. ATP-dependent chromatin remodeling by the Cockayne syndrome B DNA repair-transcription-coupling factor. *Mol. Cell Biol.* **20**: 7643-7653.
12. Coin, F., V. Oksenych, and J. M. Egly. 2007. Distinct roles for the XPB/p52 and XPD/p44 subcomplexes of TFIIH in damaged DNA opening during nucleotide excision repair. *Mol. Cell* **26**: 245-256.
13. Datta, A., S. Bagchi, A. Nag, P. Shiyanov, G. R. Adami, T. Yoon, and P. Raychaudhuri. 2001. The p48 subunit of the damaged-DNA binding protein DDB associates with the CBP/p300 family of histone acetyltransferase. *Mutat. Res.* **486**: 89-97.
14. de Laat, W. L., E. Appeldoorn, K. Sugasawa, E. Weterings, N. G. Jaspers, and J. H. Hoeijmakers. 1998. DNA-binding polarity of human replication protein A positions nucleases in nucleotide excision repair. *Genes Dev.* **12**: 2598-2609.
15. Delacroix, S., J. M. Wagner, M. Kobayashi, K. Yamamoto, and L. M. Karnitz. 2007. The Rad9-Hus1-Rad1 (9-1-1) clamp activates checkpoint signaling via TopBP1. *Genes Dev.* **21**: 1472-1477.
16. Derheimer, F. A., H. M. O'Hagan, H. M. Krueger, S. Hanasoge, M. T. Paulsen, and M. Ljungman. 2007. RPA and ATR link transcriptional stress to p53. *Proc. Natl. Acad. Sci. U. S. A* **104**: 12778-12783.
17. Dunand-Sauthier, I., M. Hohl, F. Thorel, P. Jaquier-Gubler, S. G. Clarkson, and O. D. Scharer. 2005. The spacer region of XPG mediates recruitment to nucleotide excision repair complexes and determines substrate specificity. *J. Biol. Chem.* **280**: 7030-7037.

18. Evans, E., J. Fellows, A. Coffer, and R. D. Wood. 1997. Open complex formation around a lesion during nucleotide excision repair provides a structure for cleavage by human XPG protein. *EMBO J.* **16**: 625-638.
19. Ford, J. M. and P. C. Hanawalt. 1995. Li-Fraumeni syndrome fibroblasts homozygous for p53 mutations are deficient in global DNA repair but exhibit normal transcription-coupled repair and enhanced UV resistance. *Proc. Natl. Acad. Sci. U. S. A* **92**: 8876-8880.
20. Fousteri, M., W. Vermeulen, A. A. van Zeeland, and L. H. Mullenders. 2006. Cockayne syndrome A and B proteins differentially regulate recruitment of chromatin remodeling and repair factors to stalled RNA polymerase II in vivo. *Mol. Cell* **23**: 471-482.
21. Frit, P., K. Kwon, F. Coin, J. Auriol, S. Dubaele, B. Salles, and J. M. Egly. 2002. Transcriptional activators stimulate DNA repair. *Mol. Cell* **10**: 1391-1401.
22. Gaillard, H., D. J. Fitzgerald, C. L. Smith, C. L. Peterson, T. J. Richmond, and F. Thoma. 2003. Chromatin remodeling activities act on UV-damaged nucleosomes and modulate DNA damage accessibility to photolyase. *J. Biol. Chem.* **278**: 17655-17663.
23. Gerard, A., S. Koundrioukoff, V. Ramillon, J. C. Sergere, N. Mailand, J. P. Quivy, and G. Almouzni. 2006. The replication kinase Cdc7-Dbf4 promotes the interaction of the p150 subunit of chromatin assembly factor 1 with proliferating cell nuclear antigen. *EMBO Rep.* **7**: 817-823.
24. Gillet, L. C. and O. D. Scharer. 2006. Molecular mechanisms of mammalian global genome nucleotide excision repair. *Chem. Rev.* **106**: 253-276.
25. Gong, F., D. Fahy, and M. J. Smerdon. 2006. Rad4-Rad23 interaction with SWI/SNF links ATP-dependent chromatin remodeling with nucleotide excision repair. *Nat. Struct. Mol. Biol.* **13**: 902-907.
26. Green, C. M. and G. Almouzni. 2002. When repair meets chromatin. First in series on chromatin dynamics. *EMBO Rep.* **3**: 28-33.
27. Groisman, R., J. Polanowska, I. Kuraoka, J. Sawada, M. Saijo, R. Drapkin, A. F. Kisselev, K. Tanaka, and Y. Nakatani. 2003. The ubiquitin ligase activity in the DDB2 and CSA complexes is differentially regulated by the COP9 signalosome in response to DNA damage. *Cell* **113**: 357-367.
28. Hara, R., J. Mo, and A. Sancar. 2000. DNA damage in the nucleosome core is refractory to repair by human excision nuclease. *Mol. Cell Biol.* **20**: 9173-9181.
29. Hara, R. and A. Sancar. 2003. Effect of damage type on stimulation of human excision nuclease by SWI/SNF chromatin remodeling factor. *Mol. Cell Biol.* **23**: 4121-4125.
30. Hasan, S., P. O. Hassa, R. Imhof, and M. O. Hottiger. 2001. Transcription coactivator p300 binds PCNA and may have a role in DNA repair synthesis. *Nature* **410**: 387-391.
31. Hendriks, G., F. Calleja, H. Vrieling, L. H. Mullenders, J. G. Jansen, and N. de Wind. 2008. Gene transcription increases DNA damage-induced mutagenesis in mammalian stem cells. *DNA Repair (Amst)* **7**: 1330-1339.
32. Hoogstraten, D., A. L. Nigg, H. Heath, L. H. Mullenders, R. van Driel, J. H. Hoeijmakers, W. Vermeulen, and A. B. Houtsmuller. 2002. Rapid switching of TFIIH between RNA polymerase I and II transcription and DNA repair in vivo. *Mol. Cell* **10**: 1163-1174.
33. Hoogstraten, D., A. L. Nigg, W. A. van Cappellen, J. H. Hoeijmakers, A. B. Houtsmuller, and W. Vermeulen. 2003. DNA-damage sensing in living cells by xeroderma pigmentosum group C.
34. Hwang, B. J., J. M. Ford, P. C. Hanawalt, and G. Chu. 1999. Expression of the p48 xeroderma pigmentosum gene is p53-dependent and is involved in global genomic repair. *Proc. Natl. Acad. Sci. U. S. A* **96**: 424-428.
35. Ito, S., I. Kuraoka, P. Chymkowitch, E. Compe, A. Takedachi, C. Ishigami, F. Coin, J. M. Egly, and K. Tanaka. 2007. XPG stabilizes TFIIH, allowing transactivation of nuclear receptors: implications for Cockayne syndrome in XP-G/CS patients. *Mol. Cell* **26**: 231-243.
36. Janicijevic, A., K. Sugasawa, Y. Shimizu, F. Hanaoka, N. Wijgers, M. Djurica, J. H. Hoeijmakers, and C. Wyman. 2003. DNA bending by the human damage recognition complex XPC-HR23B. *DNA Repair (Amst)* **2**: 325-336.
37. Jans, J., W. Schul, Y. G. Sert, Y. Rijksen, H. Rebel, A. P. Eker, S. Nakajima, H. van Steeg, F. R. de Gruijl, A. Yasui, J. H. Hoeijmakers, and G. T. van der Horst. 2005. Powerful skin cancer protection by a CPD-photolyase transgene. *Curr. Biol.* **15**: 105-115.
38. Jaspers, N. G., A. Raams, M. C. Silengo, N. Wijgers, L. J. Niedernhofer, A. R. Robinson,

G. Giglia-Mari, D. Hoogstraten, W. J. Kleijer, J. H. Hoeijmakers, and W. Vermeulen. 2007. First reported patient with human ERCC1 deficiency has cerebro-oculo-facio-skeletal syndrome with a mild defect in nucleotide excision repair and severe developmental failure. *Am. J. Hum. Genet.* **80**: 457-466.

39. Kapetanaki, M. G., J. Guerrero-Santoro, D. C. Bisi, C. L. Hsieh, V. Rapic-Otrin, and A. S. Levine. 2006. The DDB1-CUL4ADDB2 ubiquitin ligase is deficient in xeroderma pigmentosum group E and targets histone H2A at UV-damaged DNA sites. *Proc. Natl. Acad. Sci. U. S. A* **103**: 2588-2593.
40. Keeney, S., G. J. Chang, and S. Linn. 1993. Characterization of a human DNA damage binding protein implicated in xeroderma pigmentosum E. *J. Biol. Chem.* **268**: 21293-21300.
41. Kumagai, A., J. Lee, H. Y. Yoo, and W. G. Dunphy. 2006. TopBP1 activates the ATR-ATRIP complex. *Cell* **124**: 943-955.
42. Kuraoka, I., S. Ito, T. Wada, M. Hayashida, L. Lee, M. Saijo, Y. Nakatsu, M. Matsumoto, T. Matsunaga, H. Handa, J. Qin, Y. Nakatani, and K. Tanaka. 2008. Isolation of XAB2 complex involved in pre-mRNA splicing, transcription, and transcription-coupled repair. *J. Biol. Chem.* **283**: 940-950.
43. Lange, S. S., D. L. Mitchell, and K. M. Vasquez. 2008. High mobility group protein B1 enhances DNA repair and chromatin modification after DNA damage. *Proc. Natl. Acad. Sci. U. S. A* **105**: 10320-10325.
44. Lim, J. H., F. Catez, Y. Birger, K. L. West, M. Prymakowska-Bosak, Y. V. Postnikov, and M. Bustin. 2004. Chromosomal protein HMGN1 modulates histone H3 phosphorylation. *Mol. Cell* **15**: 573-584.
45. Lim, J. H., K. L. West, Y. Rubinstein, M. Bergel, Y. V. Postnikov, and M. Bustin. 2005. Chromosomal protein HMGN1 enhances the acetylation of lysine 14 in histone H3. *EMBO J.* **24**: 3038-3048.
46. Ljungman, M., F. Zhang, F. Chen, A. J. Rainbow, and B. C. McKay. 1999. Inhibition of RNA polymerase II as a trigger for the p53 response. *Oncogene* **18**: 583-592.
47. Maga, G. and U. Hubscher. 2003. Proliferating cell nuclear antigen (PCNA): a dancer with many partners. *J. Cell Sci.* **116**: 3051-3060.
48. Marini, F., T. Nardo, M. Giannattasio, M. Minuzzo, M. Stefanini, P. Plevani, and M. M. Falconi. 2006. DNA nucleotide excision repair-dependent signaling to checkpoint activation. *Proc. Natl. Acad. Sci. U. S. A* **103**: 17325-17330.
49. Marti, T. M., E. Hefner, L. Feeney, V. Natale, and J. E. Cleaver. 2006. H2AX phosphorylation within the G1 phase after UV irradiation depends on nucleotide excision repair and not DNA double-strand breaks. *Proc. Natl. Acad. Sci. U. S. A* **103**: 9891-9896.
50. Masutani, C., K. Sugasawa, J. Yanagisawa, T. Sonoyama, M. Ui, T. Enomoto, K. Takio, K. Tanaka, P. J. van der Spek, D. Bootsma, and . 1994. Purification and cloning of a nucleotide excision repair complex involving the xeroderma pigmentosum group C protein and a human homologue of yeast RAD23. *EMBO J.* **13**: 1831-1843.
51. Matsumoto, M., K. Yaginuma, A. Igarashi, M. Imura, M. Hasegawa, K. Iwabuchi, T. Date, T. Mori, K. Ishizaki, K. Yamashita, M. Inobe, and T. Matsunaga. 2007. Perturbed gap-filling synthesis in nucleotide excision repair causes histone H2AX phosphorylation in human quiescent cells. *J. Cell Sci.* **120**: 1104-1112.
52. Matsunaga, T., D. Mu, C. H. Park, J. T. Reardon, and A. Sancar. 1995. Human DNA repair excision nuclease. Analysis of the roles of the subunits involved in dual incisions by using anti-XPG and anti-ERCC1 antibodies. *J. Biol. Chem.* **270**: 20862-20869.
53. Mayne, L. V. and A. R. Lehmann. 1982. Failure of RNA synthesis to recover after UV irradiation: an early defect in cells from individuals with Cockayne's syndrome and xeroderma pigmentosum. *Cancer Res.* **42**: 1473-1478.
54. Min, J. H. and N. P. Pavletich. 2007. Recognition of DNA damage by the Rad4 nucleotide excision repair protein. *Nature* **449**: 570-575.
55. Moggs, J. G., K. J. Yarema, J. M. Essigmann, and R. D. Wood. 1996. Analysis of incision sites produced by human cell extracts and purified proteins during nucleotide excision repair of a 1, 3-intrastrand d(GpTpG)-cisplatin adduct. *J. Biol. Chem.* **271**: 7177-7186.
56. Mone, M. J., M. Volker, O. Nikaido, L. H. Mullenders, A. A. van Zeeland, P. J. Verschure, E. M. Manders, and R. van Driel. 2001. Local UV-induced DNA damage in cell nuclei results in local transcription inhibition. *EMBO Rep.* **2**: 1013-1017.

57. Moser, J., H. Kool, I. Giakzidis, K. Caldecott, L. H. Mullenders, and M. I. Fousteri. 2007. Sealing of chromosomal DNA nicks during nucleotide excision repair requires XRCC1 and DNA ligase III alpha in a cell-cycle-specific manner. *Mol. Cell* **27**: 311-323.

58. Moser, J., M. Volker, H. Kool, S. Alekseev, H. Vrieling, A. Yasui, A. A. van Zeeland, and L. H. Mullenders. 2005. The UV-damaged DNA binding protein mediates efficient targeting of the nucleotide excision repair complex to UV-induced photo lesions. *DNA Repair (Amst)* **4**: 571-582.

59. Mu, D. and A. Sancar. 1997. Model for XPC-independent transcription-coupled repair of pyrimidine dimers in humans. *J. Biol. Chem.* **272**: 7570-7573.

60. Mullenders, L. H. 1998. Transcription response and nucleotide excision repair. *Mutat. Res.* **409**: 59-64.

61. Mullenders, L. H., A. C. van Kesteren, C. J. Bussmann, A. A. van Zeeland, and A. T. Natarajan. 1986. Distribution of u. v. -induced repair events in higher-order chromatin loops in human and hamster fibroblasts. *Carcinogenesis* **7**: 995-1002.

62. Mullenders, L. H., H. Vrieling, J. Venema, and A. A. van Zeeland. 1991. Hierarchies of DNA repair in mammalian cells: biological consequences. *Mutat. Res.* **250**: 223-228.

63. Newman, J. C., A. D. Bailey, and A. M. Weiner. 2006. Cockayne syndrome group B protein (CSB) plays a general role in chromatin maintenance and remodeling. *Proc. Natl. Acad. Sci. U. S. A* **103**: 9613-9618.

64. Niedernhofer, L. J., G. A. Garinis, A. Raams, A. S. Lalai, A. R. Robinson, E. Appeldoorn, H. Odijk, R. Oostendorp, A. Ahmad, W. van Leeuwen, A. F. Theil, W. Vermeulen, G. T. van der Horst, P. Meinecke, W. J. Kleijer, J. Vijg, N. G. Jaspers, and J. H. Hoeijmakers. 2006. A new progeroid syndrome reveals that genotoxic stress suppresses the somatotroph axis. *Nature* **444**: 1038-1043.

65. O'Donovan, A., A. A. Davies, J. G. Moggs, S. C. West, and R. D. Wood. 1994. XPG endonuclease makes the 3' incision in human DNA nucleotide excision repair. *Nature* **371**: 432-435.

66. O'Driscoll, M., V. L. Ruiz-Perez, C. G. Woods, P. A. Jeggo, and J. A. Goodship. 2003. A splicing mutation affecting expression of ataxia-telangiectasia and Rad3-related protein (ATR) results in Seckel syndrome. *Nat. Genet.* **33**: 497-501.

67. Ogi, T. and A. R. Lehmann. 2006. The Y-family DNA polymerase kappa (pol kappa) functions in mammalian nucleotide-excision repair. *Nat. Cell Biol.* **8**: 640-642.

68. Park, C. H., D. Mu, J. T. Reardon, and A. Sancar. 1995. The general transcription-repair factor TFIIH is recruited to the excision repair complex by the XPA protein independent of the TFIIE transcription factor. *J. Biol. Chem.* **270**: 4896-4902.

69. Pines, A., C. Backendorf, S. Alekseev, J. G. Jansen, F. R. de Gruijl, H. Vrieling, and L. H. Mullenders. 2008. Differential activity of UV-DDB in mouse keratinocytes and fibroblasts: Impact on DNA repair and UV-induced skin cancer. *DNA Repair (Amst)*.

70. Politi, A., M. J. Mone, A. B. Houtsmuller, D. Hoogstraten, W. Vermeulen, R. Heinrich, and R. van Driel. 2005. Mathematical modeling of nucleotide excision repair reveals efficiency of sequential assembly strategies. *Mol. Cell* **19**: 679-690.

71. Polo, S. E., D. Roche, and G. Almouzni. 2006. New histone incorporation marks sites of UV repair in human cells. *Cell* **127**: 481-493.

72. Rademakers, S., M. Volker, D. Hoogstraten, A. L. Nigg, M. J. Mone, A. A. van Zeeland, J. H. Hoeijmakers, A. B. Houtsmuller, and W. Vermeulen. 2003. Xeroderma pigmentosum group A protein loads as a separate factor onto DNA lesions. *Mol. Cell Biol.* **23**: 5755-5767.

73. Ramanathan, B. and M. J. Smerdon. 1989. Enhanced DNA repair synthesis in hyperacetylated nucleosomes. *J. Biol. Chem.* **264**: 11026-11034.

74. Rapic-Otrin, V., M. P. McLenigan, D. C. Bisi, M. Gonzalez, and A. S. Levine. 2002. Sequential binding of UV DNA damage binding factor and degradation of the p48 subunit as early events after UV irradiation. *Nucleic Acids Res.* **30**: 2588-2598.

75. Rebel, H., N. Kram, A. Westerman, S. Banus, H. J. van Kranen, and F. R. de Gruijl. 2005. Relationship between UV-induced mutant p53 patches and skin tumours, analysed by mutation spectra and by induction kinetics in various DNA-repair-deficient mice. *Carcinogenesis* **26**: 2123-2130.

76. Riedl, T., F. Hanaoka, and J. M. Egly. 2003. The comings and goings of nucleotide excision

repair factors on damaged DNA. *EMBO J.* **22**: 5293-5303.

77. Rockx, D. A., R. Mason, A. van Hoffen, M. C. Barton, E. Citterio, D. B. Bregman, A. A. van Zeeland, H. Vrieling, and L. H. Mullenders. 2000. UV-induced inhibition of transcription involves repression of transcription initiation and phosphorylation of RNA polymerase II. *Proc. Natl. Acad. Sci. U. S. A* **97**: 10503-10508.
78. Sarker, A. H., S. E. Tsutakawa, S. Kostek, C. Ng, D. S. Shin, M. Peris, E. Campeau, J. A. Tainer, E. Nogales, and P. K. Cooper. 2005. Recognition of RNA polymerase II and transcription bubbles by XPG, CSB, and TFIIH: insights for transcription-coupled repair and Cockayne Syndrome. *Mol. Cell* **20**: 187-198.
79. Savitsky, K., A. Bar-Shira, S. Gilad, G. Rotman, Y. Ziv, L. Vanagaite, D. A. Tagle, S. Smith, T. Uziel, S. Sfez, M. Ashkenazi, I. Pecker, M. Frydman, R. Harnik, S. R. Patanjali, A. Simmons, G. A. Clines, A. Sartiel, R. A. Gatti, L. Chessa, O. Sanal, M. F. Lavin, N. G. Jaspers, A. M. Taylor, C. F. Arlett, T. Miki, S. M. Weissman, M. Lovett, F. S. Collins, and Y. Shiloh. 1995. A single ataxia telangiectasia gene with a product similar to PI-3 kinase. *Science* **268**: 1749-1753.
80. Selby, C. P. and A. Sancar. 1994. Mechanisms of transcription-repair coupling and mutation frequency decline. *Microbiol. Rev.* **58**: 317-329.
81. Selby, C. P., E. M. Witkin, and A. Sancar. 1991. Escherichia coli mfd mutant deficient in "mutation frequency decline" lacks strand-specific repair: in vitro complementation with purified coupling factor. *Proc. Natl. Acad. Sci. U. S. A* **88**: 11574-11578.
82. Shivji, K. K., M. K. Kenny, and R. D. Wood. 1992. Proliferating cell nuclear antigen is required for DNA excision repair. *Cell* **69**: 367-374.
83. Shivji, M. K., V. N. Podust, U. Hubscher, and R. D. Wood. 1995. Nucleotide excision repair DNA synthesis by DNA polymerase epsilon in the presence of PCNA, RFC, and RPA. *Biochemistry* **34**: 5011-5017.
84. Sijbers, A. M., W. L. de Laat, R. R. Ariza, M. Biggerstaff, Y. F. Wei, J. G. Moggs, K. C. Carter, B. K. Shell, E. Evans, M. C. de Jong, S. Rademakers, J. de Rooij, N. G. Jaspers, J. H. Hoeijmakers, and R. D. Wood. 1996. Xeroderma pigmentosum group F caused by a defect in a structure-specific DNA repair endonuclease. *Cell* **86**: 811-822.
85. Smerdon, M. J., S. Y. Lan, R. E. Calza, and R. Reeves. 1982. Sodium butyrate stimulates DNA repair in UV-irradiated normal and xeroderma pigmentosum human fibroblasts. *J. Biol. Chem.* **257**: 13441-13447.
86. Spatz, A., G. Giglia-Mari, S. Benhamou, and A. Sarasin. 2001. Association between DNA repair-deficiency and high level of p53 mutations in melanoma of Xeroderma pigmentosum. *Cancer Res.* **61**: 2480-2486.
87. Stiff, T., K. Cerosaletti, P. Concannon, M. O'Driscoll, and P. A. Jeggo. 2008. Replication independent ATR signalling leads to G2/M arrest requiring Nbs1, 53BP1 and MDC1. *Hum. Mol. Genet.* **17**: 3247-3253.
88. Stout, G. J., M. Oosten, F. Z. Acherrat, J. Wit, W. P. Vermeij, L. H. Mullenders, F. R. Gruijl, and C. Backendorf. 2005. Selective DNA damage responses in murine Xpa-/-, Xpc-/- and Csb-/- keratinocyte cultures. *DNA Repair (Amst)* **4**: 1337-1344.
89. Sugasawa, K. and F. Hanaoka. 2007. Sensing of DNA damage by XPC/Rad4: one protein for many lesions. *Nat. Struct. Mol. Biol.* **14**: 887-888.
90. Sugasawa, K., J. M. Ng, C. Masutani, S. Iwai, P. J. van der Spek, A. P. Eker, F. Hanaoka, D. Bootsma, and J. H. Hoeijmakers. 1998. Xeroderma pigmentosum group C protein complex is the initiator of global genome nucleotide excision repair. *Mol. Cell* **2**: 223-232.
91. Sugasawa, K., Y. Okuda, M. Saijo, R. Nishi, N. Matsuda, G. Chu, T. Mori, S. Iwai, K. Tanaka, K. Tanaka, and F. Hanaoka. 2005. UV-induced ubiquitylation of XPC protein mediated by UV-DDB-ubiquitin ligase complex. *Cell* **121**: 387-400.
92. Tang, J. Y., B. J. Hwang, J. M. Ford, P. C. Hanawalt, and G. Chu. 2000. Xeroderma pigmentosum p48 gene enhances global genomic repair and suppresses UV-induced mutagenesis. *Mol. Cell* **5**: 737-744.
93. Ura, K., M. Araki, H. Saeki, C. Masutani, T. Ito, S. Iwai, T. Mizukoshi, Y. Kaneda, and F. Hanaoka. 2001. ATP-dependent chromatin remodeling facilitates nucleotide excision repair of UV-induced DNA lesions in synthetic dinucleosomes. *EMBO J.* **20**: 2004-2014.
94. van Gool, A. J., E. Citterio, S. Rademakers, R. van Os, W. Vermeulen, A. Constantinou, J. M. Egly, D. Bootsma, and J. H. Hoeijmakers. 1997. The Cockayne syndrome B protein, involved

in transcription-coupled DNA repair, resides in an RNA polymerase II-containing complex. *EMBO J.* **16**: 5955-5965.

95. van Oosten, M., H. Rebel, E. C. Friedberg, H. van Steeg, G. T. van der Horst, H. J. van Kranen, A. Westerman, A. A. van Zeeland, L. H. Mullenders, and F. R. de Gruijl. 2000. Differential role of transcription-coupled repair in UVB-induced G2 arrest and apoptosis in mouse epidermis. *Proc. Natl. Acad. Sci. U. S. A* **97**: 11268-11273.
96. van Oosterwijk, M. F., A. Versteeg, R. Filon, A. A. van Zeeland, and L. H. Mullenders. 1996. The sensitivity of Cockayne's syndrome cells to DNA-damaging agents is not due to defective transcription-coupled repair of active genes. *Mol. Cell Biol.* **16**: 4436-4444.
97. Volker, M., M. J. Mone, P. Karmakar, A. van Hoffen, W. Schul, W. Vermeulen, J. H. Hoeijmakers, R. van Driel, A. A. van Zeeland, and L. H. Mullenders. 2001. Sequential assembly of the nucleotide excision repair factors in vivo. *Mol. Cell* **8**: 213-224.
98. Wakasugi, M., J. T. Reardon, and A. Sancar. 1997. The non-catalytic function of XPG protein during dual incision in human nucleotide excision repair. *J. Biol. Chem.* **272**: 16030-16034.
99. Wang, H., L. Zhai, J. Xu, H. Y. Joo, S. Jackson, H. Erdjument-Bromage, P. Tempst, Y. Xiong, and Y. Zhang. 2006. Histone H3 and H4 ubiquitylation by the CUL4-DDB-ROC1 ubiquitin ligase facilitates cellular response to DNA damage. *Mol. Cell* **22**: 383-394.
100. Wijnhoven, S. W., H. J. Kool, L. H. Mullenders, R. Slater, A. A. van Zeeland, and H. Vrieling. 2001. DMBA-induced toxic and mutagenic responses vary dramatically between NER-deficient Xpa, Xpc and Csb mice. *Carcinogenesis* **22**: 1099-1106.
101. Yamaizumi, M. and T. Sugano. 1994. U. v. -induced nuclear accumulation of p53 is evoked through DNA damage of actively transcribed genes independent of the cell cycle. *Oncogene* **9**: 2775-2784.
102. Yarosh, D. B. 2002. Enhanced DNA repair of cyclobutane pyrimidine dimers changes the biological response to UV-B radiation. *Mutat. Res.* **509**: 221-226.
103. Yu, Y., Y. Teng, H. Liu, S. H. Reed, and R. Waters. 2005. UV irradiation stimulates histone acetylation and chromatin remodeling at a repressed yeast locus. *Proc. Natl. Acad. Sci. U. S. A* **102**: 8650-8655.
104. Zotter, A., M. S. Luijsterburg, D. O. Warmerdam, S. Ibrahim, A. Nigg, W. A. van Cappellen, J. H. Hoeijmakers, R. van Driel, W. Vermeulen, and A. B. Houtsmuller. 2006. Recruitment of the nucleotide excision repair endonuclease XPG to sites of UV-induced dna damage depends on functional TFIIH. *Mol. Cell Biol.* **26**: 8868-8879.
105. Zou, L. and S. J. Elledge. 2003. Sensing DNA damage through ATRIP recognition of RPA-ssDNA complexes. *Science* **300**: 1542-1548.

3

PARP1 promotes nucleotide excision repair through DDB2 stabilization and recruitment of ALC1

Alex Pines*, Mischa G. Vrouwe*, Jurgen A. Marteijn, Dimitris Typas, Martijn S. Luijsterburg, Medine Cansoy, Paul Hensbergen, André Deelder, Anton de Groot, Syota Matsumoto, Kaoru Sugasawa, Nicolas Thoma, Wim Vermeulen, Harry Vrieling, and Leon Mullenders

* These authors contributed equally to this work

Journal of Cell Biology. In press.

ABSTRACT

The WD40-repeat protein DDB2 is essential for efficient recognition and subsequent removal of ultraviolet (UV)-induced DNA lesions by nucleotide excision repair (NER). However, how DDB2 promotes NER in chromatin is poorly understood. Here, we identify poly(ADP-ribose) polymerase 1 (PARP1) as a novel DDB2-associated factor. We demonstrate that DDB2 facilitated poly(ADP-ribosyl)ation of UV-damaged chromatin through the activity of PARP1 resulting in the recruitment of the chromatin remodeling enzyme ALC1. Depletion of ALC1 rendered cells sensitive to UV and impaired repair of UV-induced DNA lesions. Additionally, DDB2 itself was targeted by poly(ADP-ribosyl)ation, resulting in increased protein stability and a prolonged chromatin retention time. Our *in vitro* and *in vivo* data support a model in which poly(ADP-ribosyl)ation of DDB2 suppresses DDB2 ubiquitylation and outline a molecular mechanism for PARP1-mediated regulation of NER through DDB2 stabilization and recruitment of the chromatin remodeler ALC1.

INTRODUCTION

Nucleotide excision repair (NER) is a multistep process that mediates the removal of structurally and chemically diverse DNA lesions including ultraviolet (UV) light-induced cyclobutane pyrimidine dimers (CPD) and 6-4 pyrimidine pyrimidone photoproducts (6-4PP). The importance of NER in protecting organisms against solar UV-induced DNA damage is underscored by the hereditary disease xeroderma pigmentosum (XP), which is clinically characterized by hypersensitivity to sunlight and predisposition to skin cancer (Cleaver et al., 2009). XP has been linked to defects in seven proteins (XP-A through XP-G) which, with the exception of XPC and XPE (hereafter named DDB2), function in the core NER reaction. The proteins encoded by the XPC and XPE genes are involved in the global genome NER sub-pathway (GG-NER), but are dispensable for transcription-coupled NER (TC-NER) (Cleaver et al., 2009).

Reconstitution of the NER reaction with purified proteins has defined the minimal set of proteins required for GG-NER *in vitro* (Aboussekhra et al., 1995). The initial step of DNA damage recognition depends on the XPC-Rad23 complex and subsequently results in local DNA unwinding and damage verification by the basal transcription factor TFIIH, the single-stranded DNA-binding complex RPA and XPA. Dual incision of the damaged DNA strand is carried out by the 5'and 3' structure-specific endonucleases XPF-ERCC1 and XPG, respectively, followed by gap filling and DNA ligation (Aboussekhra et al., 1995).

DNA damage recognition by XPC involves the detection of unpaired bases (Min and Pavletich, 2007;Clement et al., 2010), which renders lesion recognition of minor helix-distorting lesions such as CPD very inefficient (Sugasawa et al., 2001). In addition to XPC, efficient repair of CPDs therefore requires the heterodimeric UV-DDB protein complex consisting of the DDB1 and DDB2 subunits (Fitch et al., 2003;Moser et al., 2005). The crystal structure of UV-DDB bound to a 6-4PP-containing DNA duplex revealed the direct and exclusive binding of DDB2 to the photodimer (Scrima et al., 2008). XP-E cells lacking functional DDB2 are deficient in repair of CPD but competent in repair of 6-4PP albeit at reduced rates (Hwang et al., 1999;Moser et al., 2005). This partial requirement for UV-DDB in GG-NER is reflected in the relative mild sensitivity of XP-E cells to UV-induced cell death (Tang and Chu, 2002). Although UV-DDB deficiency impairs repair of photolesions *in vivo*, it is dispensable for NER *in vitro* (Aboussekhra et al., 1995;Mu et al., 1995;Rapic, V et al., 1998) suggesting that UV-DDB is important for the repair of DNA lesions in a chromatin context.

The UV-DDB complex interacts with several factors known to modulate chromatin structure such as histone acetyltransferase p300, the STAGA complex (Datta et al., 2001;Rapic-Otrin et al., 2002;Martinez et al., 2001) and the Cullin-RING ubiquitin ligase (CRL4) complex CUL4A-RBX1 (Shiyanov et al., 1999;Groisman et al., 2003). The CRL4-DDB2 complex ubiquitylates DDB2 and XPC in response to UV irradiation, which facilitates efficient recognition of photolesions by XPC (Sugasawa et al., 2005). Moreover, the CRL4 complex also ubiquitylates histones H2A, H3 and H4 (Kapetanaki et al., 2006) of which H3 and H4 ubiquitylation affects nucleosome stability (Wang et al., 2006).

Despite these studies, the molecular mechanisms through which UV-DDB facilitates recognition of DNA damage in chromatin remain poorly understood. Here we purified DDB2

and associated factors from human cells and identified poly(ADP-ribose) polymerase 1 (PARP1) as a novel component of the UV-DDB complex. We provide evidence for a central role of DDB2-associated PARP1 in mediating poly(ADP-ribose) (PAR) synthesis and recruitment of the SWI/SNF chromatin remodeler ALC1 to UV-damaged DNA. Moreover, we show that poly(ADP-ribos)ylation of DDB2 itself regulates the stability as well as the chromatin retention time of DDB2. Interfering with either PARP1 or ALC1 function impairs CPD repair and renders cells highly sensitive to UV irradiation. Together, these findings outline a novel molecular mechanism for the DDB2-mediated and PARP1-executed regulation of NER.

RESULTS

PARP1 is a component of the UV-DDB complex

To identify novel factors involved in the DNA damage recognition step of GG-NER we isolated DDB2-associated protein complexes by chromatin immunoprecipitation (figure 1A-B) and analysed purified proteins by mass spectrometry (MS). MRC5 cells expressing FLAG-tagged DDB2 were either mock-treated or irradiated with UV-C light (20 J/m^2) and incubated for five minutes prior to chromatin isolation and immunoprecipitation using FLAG antibody. MS analysis identified several proteins known to interact with DDB2, including DDB1, CUL4A, CUL4B, and components of the COP9 signalosome (supplementary table 1) showing that native DDB2 is indeed isolated from cells using this approach. Interestingly, multiple DDB2 peptides were identified by MS with protein weights exceeding 50 kDa in UV-irradiated cells but not in mock treated cells (figure 1A), suggesting the presence of UV-specific posttranslational modifications of DDB2. In addition to these known factors, we also identified poly (ADP-ribose) polymerase 1 (PARP1) as a novel DDB2-associated factor. We confirmed the interaction between endogenous DDB2 and endogenous PARP1 by reciprocal immunoprecipitation experiments (figure 1C) using chromatin prepared from UV-irradiated or mock-treated normal human fibroblasts (NHF). These results show that UV irradiation stimulates the interaction between the UV-DDB complex and PARP1 on chromatin. Moreover, an interaction between recombinant UV-DDB and recombinant PARP1 could indeed be detected *in vitro* supporting a direct interaction between these factors (supplementary figure 1A-B). To test which subunit of the UV-DDB complex interacts with PARP1, we purified GFP-DDB1 or GFP-DDB2 under denaturing conditions from cells. The results revealed that both DDB1 and DDB2 interact with PARP1 (figure 1D). Consistent with this notion, we found that GFP-DDB2^{D307Y}, which is unable to form a complex with DDB1 (Luijsterburg et al., 2012), also binds PARP1, indicating that DDB2-PARP1 interaction does not require DDB1. To corroborate these findings, we isolated GFP-DDB1 or GFP-DDB2 from polyacrylamide gels and found both extracted proteins to interact with PARP1 *in vitro* (supplementary figure 1C). Finally, far-western blotting also revealed that both DDB1 and DDB2 avidly bind to PARP1 (supplementary figure 1B). Together, our findings reveal a novel and direct interaction between the UV-DDB complex and PARP1, which prompted us to assess the involvement of PARP1 in modifying DDB2 and regulating NER.

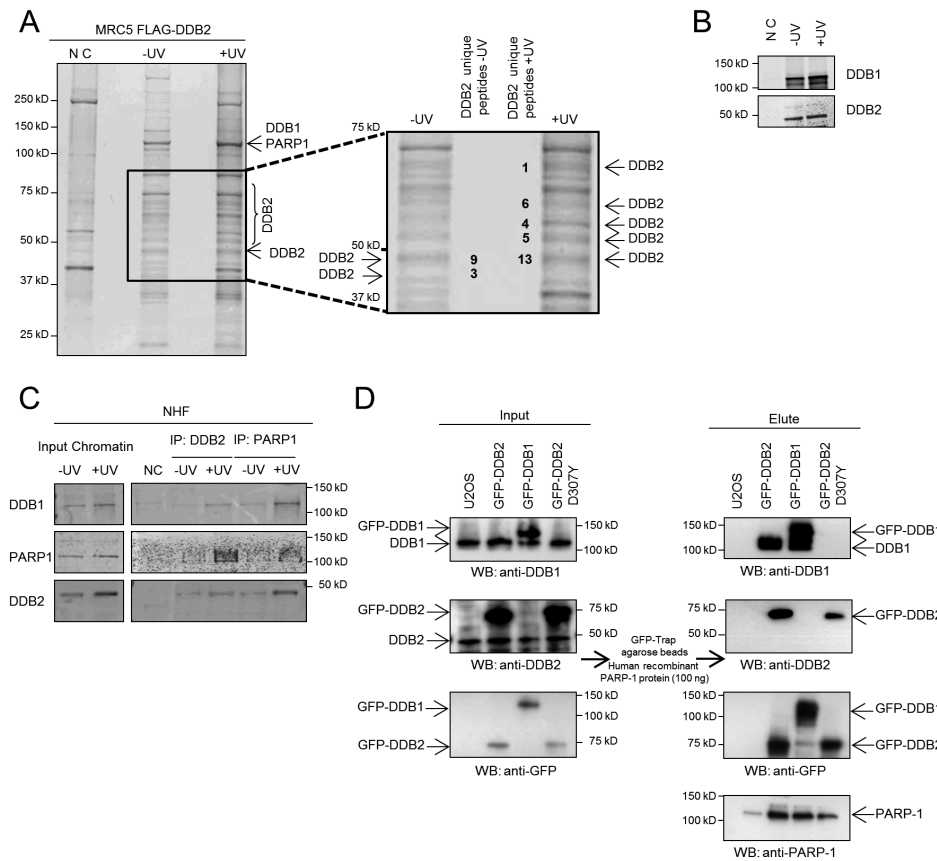

Figure1. **(A)** SDS-PAGE electrophoresis and Coomassie staining of FLAG-DDB2 immunoprecipitates obtained from FLAG-DDB2 expressing MRC5 cells mock treated or irradiated with 20 J/m^2 UV-C. Negative control (NC) indicates the elute obtained from agarose beads incubated with MRC5 FLAG-DDB2 chromatin. The arrows in the zoom-in window indicate the position of the gel where DDB2 and the respective unique-peptides detected by MS (A unique peptide is defined as a peptide, irrespective of its length, that exists only in one protein of a proteome of interest). **(B)** Western blot of FLAG-DDB2 immunoprecipitates. Cells were mock treated or irradiated with 20 J/m^2 UV-C and immunoblotted with DDB1 and DDB2 specific antibodies. Negative control (NC) indicates the elute obtained from agarose beads incubated with chromatin from MRC5 FLAG-DDB2 cells. **(C)** Western blot of DDB2 and PARP1 immunoprecipitates from NHF cells mock treated or irradiated with 20 J/m^2 UV-C followed by 5 minutes incubation and immunoblotted against DDB1, DDB2 or PARP1. **(D)** *GFP-DDB2-PARP-1 binding assay*. U2OS cells transfected with the indicated GFP constructs were lysed in denaturing buffer and subjected to immunoprecipitation with GFP-TRAP beads and then incubated with 100 ng purified recombinant PARP-1. The beads were then processed for immunoblotting.

Poly(ADP-ribose) chains are synthesized at UV-induced DNA lesions

We first assessed whether poly(ADP-ribose) (PAR) chains are synthesized in chromatin containing UV-induced DNA lesions. To this end, we locally irradiated G0/G1 synchronized telomerase-immortalized human fibroblasts with UV-C light (254 nm) through a polycarbonate mask (Mone et al., 2001). Staining with specific antibodies revealed the presence of PAR chains at sites of DNA damage marked by the recruitment of the p89 subunit of TFIIH or replication factor PCNA known to be involved in NER (figure 2A-B). Moreover, PAR staining in Ki67-negative cells confirmed that PAR synthesis occurred at DNA lesions in non-proliferating cells underlining the replication-independent nature of these events (figure 2C). Finally, chemical inhibition of PARP1 impaired the formation of PAR chains at damaged sites (figure 2D) indicating that the activity of PARP1 is responsible for PAR synthesis at sites of local UV damage.

PARG and DNA synthesis inhibition modulate UV-dependent PARylation

We noted during our experiments that the synthesis of PAR chains at DNA lesions was only detectable in a subset of cells (figure 2A-B). To gain insight into this phenomenon, we locally UV irradiated human fibroblasts with different doses (30 or 100 J/m^2) and subsequently monitored the formation of PAR chains 30 minutes after irradiation (figure 2E). The percentage of cells with PAR chains at sites of local damage significantly increased between 30 J/m^2 and 100 J/m^2, but did not exceed 50% of the cells (figure 2E-F). It is known that the transient and highly dynamic nature of PAR chains is due to the rapid reversal of this modification by the activity of the poly (ADP-ribose) glycohydrolase (PARG) (Slade et al., 2011). To increase the steady-state level of UV-induced PAR chains, we lowered the levels of PARG by siRNAs. Indeed, depletion of PARG resulted in a significantly elevated percentage of cells that displayed PAR chains at DNA lesions, which was roughly 60% at 30 J/m^2 and 75% at 100 J/m^2 (figure 2E-F). These findings show that UV-induced PAR chains are formed in the majority of cells, but are rapidly reversed by the activity of PARG. We then hypothesized that single-stranded DNA gaps transiently generated during NER, might elicit the synthesis of PAR chains. In support of this we found that inhibition of DNA synthesis and ligation by hydroxyurea (HU) and cytosine-β-arabinofuranoside (AraC), known to result in the formation of persistent single-stranded DNA gaps (Overmeer et al., 2011), resulted in robust PAR synthesis in all UV-irradiated cells (figure 2E-F).

DDB2 mediates PARylation during the pre-incision stage of NER

To evaluate whether UV-induced PAR synthesis was exclusively dependent on the presence of a single-stranded DNA repair intermediate, we examined PARylation in XP-A cells that are unable to perform incision and hence do not accumulate ssDNA (Friedberg, 2001) (figure 3C). Indeed, PAR synthesis could not be detected in XP-A cells even following treatment with HU and AraC (figure 3A-B), consistent with a role of dual incision in triggering these events. Strikingly, however, the formation of PAR chains was still detected in XP-A cells upon the depletion of PARG (figure 3A-B), suggesting that PAR chain formation is not solely dependent on the formation of ssDNA. Given our finding that UV-DDB interacts with PARP1, we addressed whether DDB2 contributes to PAR synthesis at sites of DNA damage.

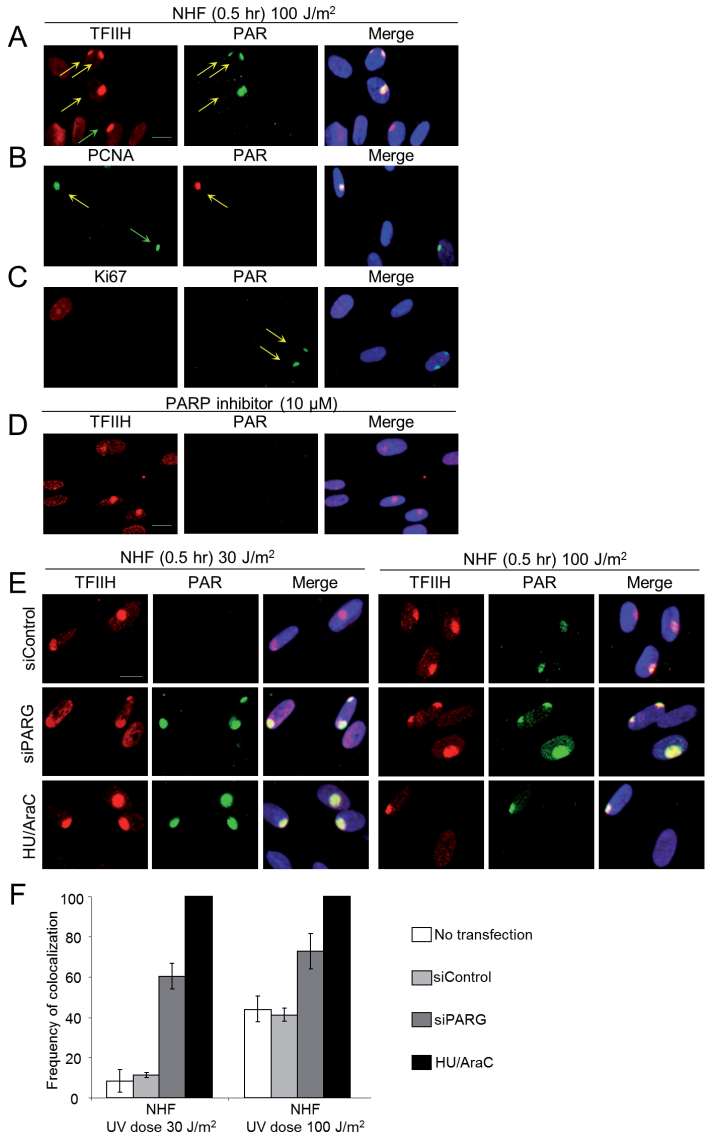

Figure2. **(A-B-C-D)** NHF cells were locally UV irradiated (100 J/m2), fixed after the indicated time and stained with an antibody-recognizing PAR, TFIIH, PCNA or Ki67. PAR colocalizes with the damage markers TFIIH and PCNA **(A-B)** including non-cycling cells (Ki67 negative staining) (**C**). Treatment with a specific PARPi (10μM) resulted in a complete loss of PAR signal **(D)**. Arrows indicate local damage sites. Scale bar represent 20μm. **(E)** NHF cells were transfected with indicated siRNA or treated with HU/AraC. 48 hours after transfection the cells were locally UV exposed (30 or 100 J/m^2), fixed after the indicated time and stained with an antibody recognizing PAR or TFIIH. Scale bar represent 20μm. **(F)** The percentage of colocalization of PAR with TFIIH in NHF cells is plotted for the different siRNA transfections and HU/AraC treatment. The results are from three independent experiments in which about 100 cells per condition were analysed; Error bars indicate standard deviation. The data shown are from a single representative experiment out of three repeats.

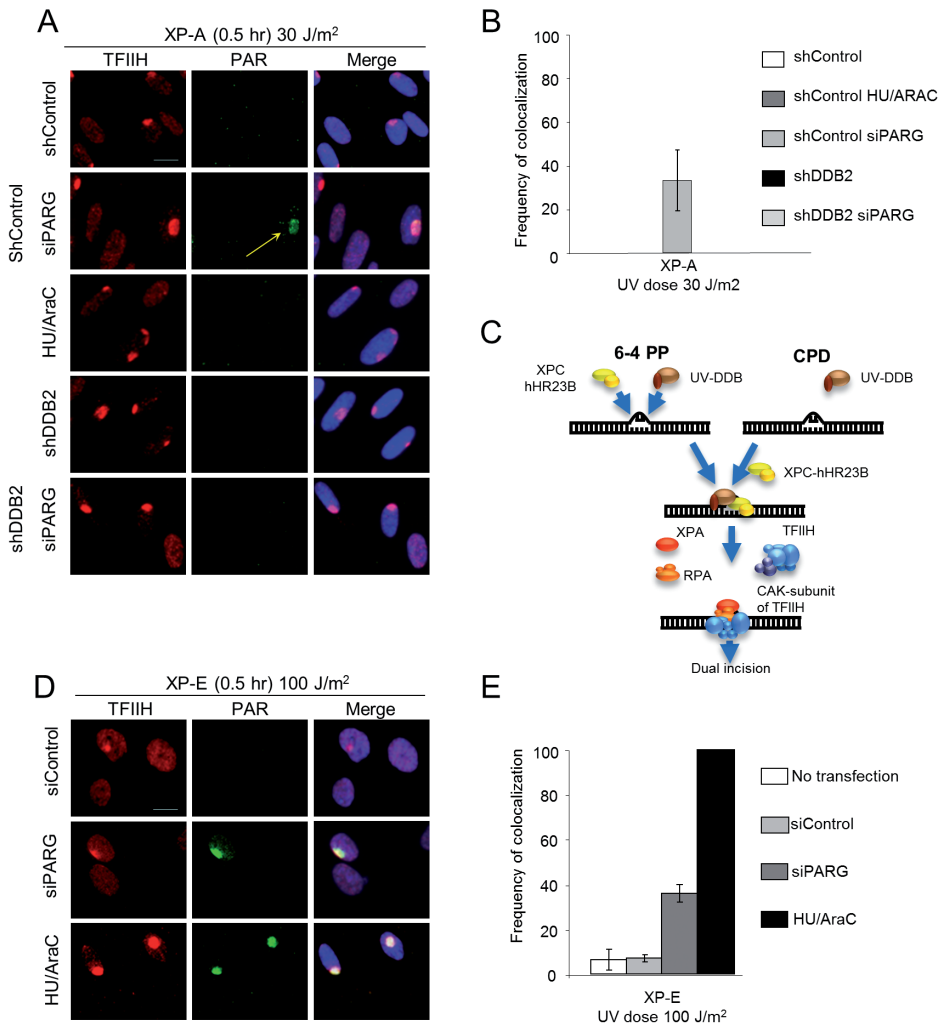

Figure3. **(A)** XP-A cells expressing sh-Control or shDDB2 were transfected with indicated siRNA or treated with HU/AraC. 48 hours after transfection the cells were locally exposed to 30 J/m^2, fixed after the indicated time and stained with an antibody recognizing PAR or TFIIH. Scale bar represent 20μm. **(B)** The percentage of colocalization of PAR with TFIIH in XP-A cells expressing sh-Control or shDDB2 is plotted for the different siRNA transfections and HU/AraC treatment. The results are from three independent experiments in which about 100 cells per condition were analysed; Error bars indicate standard deviation. **(C)** Scheme of the early stage of Nucleotide Excision Repair **(D)** XP-E cells were transfected with indicated siRNA or treated with HU/AraC. The cells were locally UV exposed with 100 J/m2, fixed after the indicated time and stained with an antibody-recognizing PAR or TFIIH. Scale bar represent 20μm. **(E)** The percentage of colocalization of PAR with TFIIH in XP-E cells is plotted for the different siRNA transfections and HU/AraC treatment. Error bars indicate standard deviation. The data shown are from a single representative experiment out of three repeats.

At later time-points after UV irradiation (30 minutes after 100 J/m^2), when stretches of ssDNA have been generated, we detected an substantial difference in PAR synthesis between normal human cells and DDB2-deficient XP-E cells as only 10% of the XP-E cells displayed clear PARylation at damaged sites when compared to normal cells (figures 3D-E). However, similar to repair-proficient cells we found inhibition of PAR turnover by PARG depletion to increase the percentage of PAR-positive cells to about 40%, while inhibition of DNA synthesis resulted in PAR synthesis at all locally damaged sites (figure 3D-E). These findings are consistent with the notion that XP-E cells are impaired in dual incision due to deficient repair of CPD and underscore the role of ssDNA formation in UV-induced PAR synthesis. During the time period of 30 minutes after UV-irradiation, a substantial part of repair represents removal of 6-4PP being repaired much more rapidly than CPD. XPE cells display efficient repair of 6-4PP under the conditions described in figure 3 (Moser et al., 2005;Nishi et al., 2009) and all these repair events (in the presence of HU/AraC) provoke PAR synthesis although the absolute number of events is lower than in NHF.

We then took advantage of the finding that DDB2 is very rapidly recruited to UV-induced DNA lesions (Luijsterburg et al., 2007) compared to the assembly rates of the pre-incision factors and especially those of the post-incision factors (Luijsterburg et al., 2010). We therefore examined PAR synthesis very shortly after UV exposure when DDB2 readily accumulates, but PCNA recruitment cannot yet be detected (Luijsterburg et al., 2010). At five minutes after UV irradiation (30 or 100 J/m^2), we could not detect PAR synthesis in normal human, XP-A or XP-E fibroblasts, not even when DNA synthesis was inhibited by HU/AraC treatment (figure 4). Strikingly, whereas the stabilization of PAR chains by PARG depletion (supplementary figure 3E) resulted in clearly detectable PARylation at UV-damaged regions in wild-type and XP-A fibroblasts (figure 4A-C-D-E), PAR synthesis at these early time-points was completely abolished in XP-E cells even at 100 J/m^2 (figure 4B-D). Taken together, our results suggest that two temporally distinct waves of PARylation take place at sites of UV-induced DNA damage. The early (pre-incision) wave of PAR synthesis is fully dependent on functional DDB2 whereas the late (post-incision) wave of PAR formation requires the generation of single-stranded DNA gaps resulting from dual incision. In concordance, we found that PAR synthesis was completely abolished in DDB2 depleted XP-A cells even when PARG was depleted (figures 3A-B and 4C-E, supplementary figure 3C).

PARylation regulates DDB2 release from UV-induced DNA lesions

To gain insight into the role of PARylation in NER complex formation, we investigated the assembly kinetics of GFP-tagged DDB2 at UV-C laser-induced DNA lesions. The kinetics of GFP-DDB2 accumulation were not affected by PARPi or depletion of PARG (supplementary figure 2A-B) indicating that the recruitment of DDB2 is not regulated by PAR chains. We subsequently applied fluorescence loss in photobleaching (FLIP) to measure the dissociation rate of DDB2 from UV-damaged DNA. Although the dissociation of DDB2 ($t_{1/2}$ = 19 seconds) was not affected by PARPi, we measured a prolonged chromatin retention time ($t_{1/2}$ = 27 seconds) upon knock-down of PARG (figure 5A) suggesting that PAR synthesis positively affects the retention of DDB2 on UV-damaged chromatin. Likewise, the immobilization of GFP-DDB2 following global UV irradiation, as measured by fluorescence

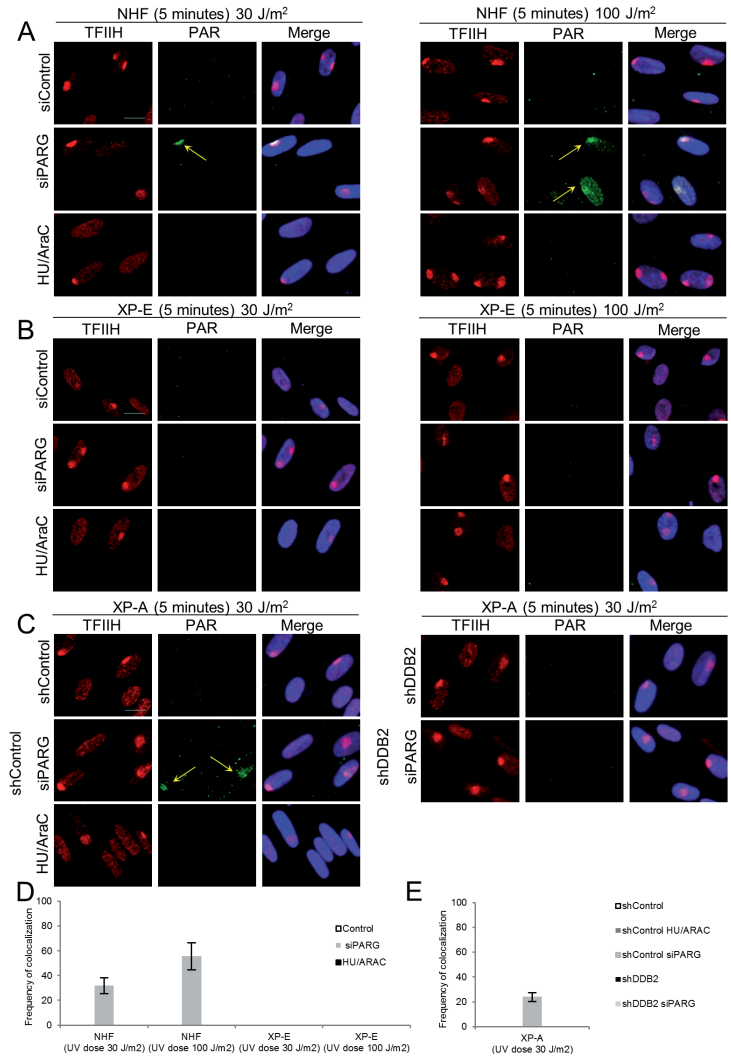

Figure4. **(A-B)** NHF**(A)** and XP-E**(B)** cells were transfected with indicated siRNA or treated with HU/AraC. 48 hours after transfection the cells were locally UV exposed with 30 or 100 J/m^2, fixed after the indicated time and stained with an antibody recognizing PAR or TFIIH. Scale bar represent 20µm. **(C)** XP-A cells expressing shControl or shDDB2 were transfected with indicated siRNA or treated with HU/AraC. 48 hours after transfection the cells were locally UV exposed to 30 J/m^2, fixed after the indicated time and stained with an antibody-recognizing PAR or TFIIH. Scale bar represent 20µm. **(D)** The percentage of colocalization of PAR with TFIIH in NHF and XPE cells is plotted for the different siRNA transfections and HU/AraC treatment. The results are from three independent experiments in which about 100 cells per condition were analysed; Error bars indicate standard deviation. **(E)** The percentage of colocalization of PAR with TFIIH in XP-A cells expressing sh-Control or shDDB2 is plotted for the different siRNA transfections and HU/AraC treatment. The results are from three independent experiments in which about 100 cells per condition were analysed; Error bars indicate standard deviation. The data shown are from a single representative experiment out of three repeats.

recovery after photo-bleaching (FRAP), was significantly reduced following treatment with PARP inhibitors (figure 5B), suggesting that PAR synthesis positively affects the retention of DDB2 on UV-damaged chromatin. Consistent with these findings, western blot analysis revealed that the UV-induced degradation of DDB2 was significantly retarded by PARG depletion (figure 5C) when cells were exposed to a UV dose (100J/m^2) comparable with the UV-laser treatment (figure 5A). Inhibition of PARP activity resulted in accelerated degradation of DDB2 following UV irradiation most clearly seen at 30 J/m^2. This result indicates that PARylation of DDB2 affects its UV-induced degradation presumably by affecting ubiquitylation. To address how PARylation modulates the chromatin binding and stability of DDB2, we biochemically examined whether UV-DDB is modified by PARP1. *In vitro* PARylation experiments using purified components revealed that both DDB2 and DDB1 are directly modified by PARP1 (figure 6A, and supplementary figure 2C). Conversely, human DDB2 lacking its first 40 N-terminal amino acids including 7 lysines ,(Fischer et al., 2011) failed to undergo PARylation (figure 6A). This finding was further substantiated by the lack of *in vitro* PARylation of the zebrafish orthologue of DDB2 (drDDB2) lacking the first 93 N-terminal residues (Scrima et al., 2008) showing that the N-terminus of DDB2 is targeted for PARylation. Both Cul4A or Rbx1 were not modified by PARP1 (figure 6A) suggesting that DDB1 and DDB2 are specific targets of PARP1. To assess PARylation of DDB2 *in vivo*, we expressed double-tagged DDB2 in human cells followed by its isolation using two consecutive purifications under denaturing conditions in order to disrupt protein-protein interactions while preserving post-translational modifications (Figure 6B). Using this purification approach we detected robust PARylation of DDB2 in response to UV irradiation, while PARylation was virtually absent in mock-treated cells showing that DDB2 is modified in a DNA damage-specific manner. Strikingly, inhibition of PARP activity, which resulted in suppressed DDB2 PARylation, was accompanied by increased level and altered spectrum of ubiquitylation of DDB2 (figure 6B). However, it is obvious that lysine residues on the N-terminus of DBB2 are the major target of ubiquitylation (Fischer et al., 2011) and these might have more impact on DDB2 degradation than modification of lysine residues toward the C-terminus when PARP activity is inhibited. These findings identify DDB2 as a novel target for PARP1-mediated PARylation and suggest that poly(ADP-ribosyl)ation of DDB2 directly suppresses DDB2 auto-ubiquitylation providing a molecular explanation for the PAR-dependent stabilization of DDB2 in response to UV irradiation.

DDB2-dependent and -independent recruitment of the chromatin remodeling enzyme ALC1 to UV-induced photolesions

Recent studies uncovered that PAR chains mediate the recruitment of PAR-binding proteins to single-stranded and double-stranded DNA breaks (Timinszky et al., 2009;Gottschalk et al., 2009;Ahel et al., 2009). In particular, the macrodomain-containing chromatin remodeling enzyme ALC1 promotes PAR-dependent nucleosome remodeling *in vitro* and is recruited to sites of DNA breaks, which prompted us to test whether ALC1 is involved in the repair of UV-induced DNA lesions. Staining with a specific antibody revealed that endogenous ALC1 was readily recruited to UV-induced DNA lesions shortly after UV exposure (figure 7A). Live cell imaging of GFP-tagged ALC1-expressing cells confirmed the rapid, but transient

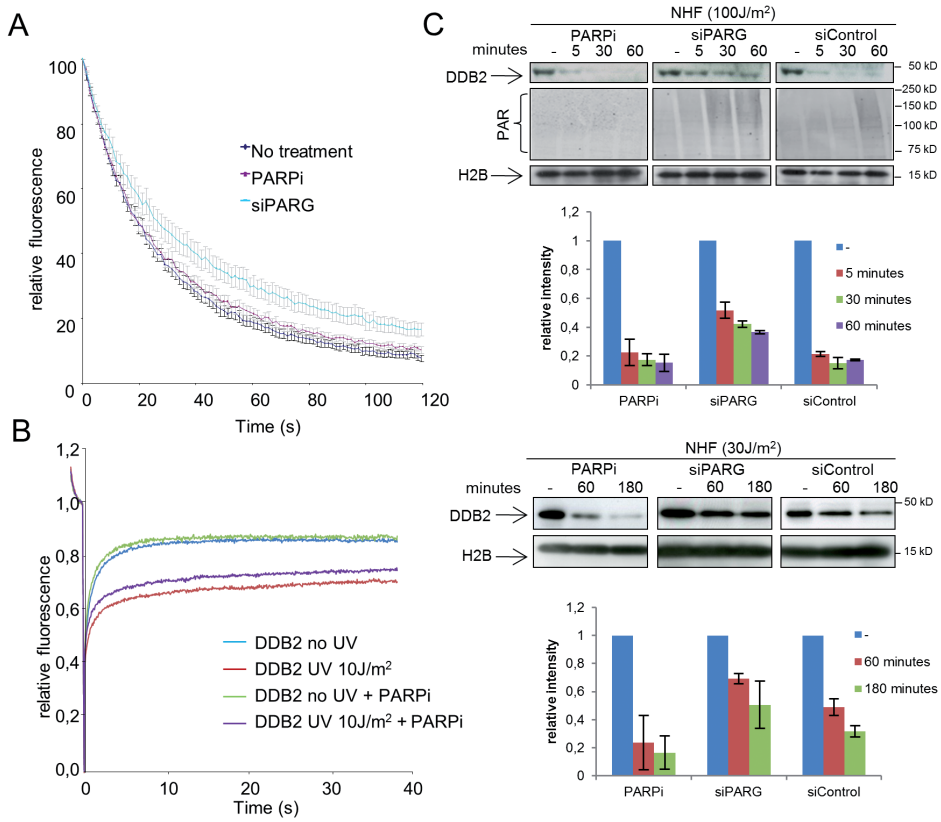

Figure 5. (A) NHF cells stably expressing GFP-DDB2 were transfected with the indicated siRNA or treated with PARPi (10μM). 48 hours after transfection cells were UV irradiated using a UV-C (266 nm) laser. To determine the dissociation kinetics of DDB2 from UV-damaged DNA, the undamaged nucleus was continuously bleached and the fluorescence decrease in the local damage was monitored. Relative fluorescence was normalized at 100% (before bleach at maximum level of accumulation). The half-time ($t_{1/2}$) of a FLIP curve corresponds to the residence time of a protein molecule in the locally damaged area. Error bars indicate SEM. **(B)** VH10-tert cells stably expressing GFP-DDB2 were incubated in CO2-independent microscopy medium supplemented with 1‰ DMSO (mock treatment) or 10 μM PARP inhibitor dissolved in DMSO three hours prior to FRAP analysis. Cells were mock-treated or globally UV-C irradiated (10 J.m-2) and transferred to the microscope chamber in microscopy medium. Cells were incubated on the microscope chamber at 37° for 10 minutes to allow repair proteins to accumulate at UV-induced DNA lesions after which the mobility of GFP-tagged NER factors was analyzed by strip-FRAP. The data were normalized to pre-bleach intensity (set to 1) and bleach depth (set to 0). Three independent experiments were performed for each condition. **(C)** Western blot of normal fibroblasts transfected with the indicated siRNA or treated with PARPi (10μM). Whole cell extracts of non-irradiated and UV-irradiated cells (30-100 J/m²) after the indicated time were probed with antibodies against DDB2, PAR or H2B.

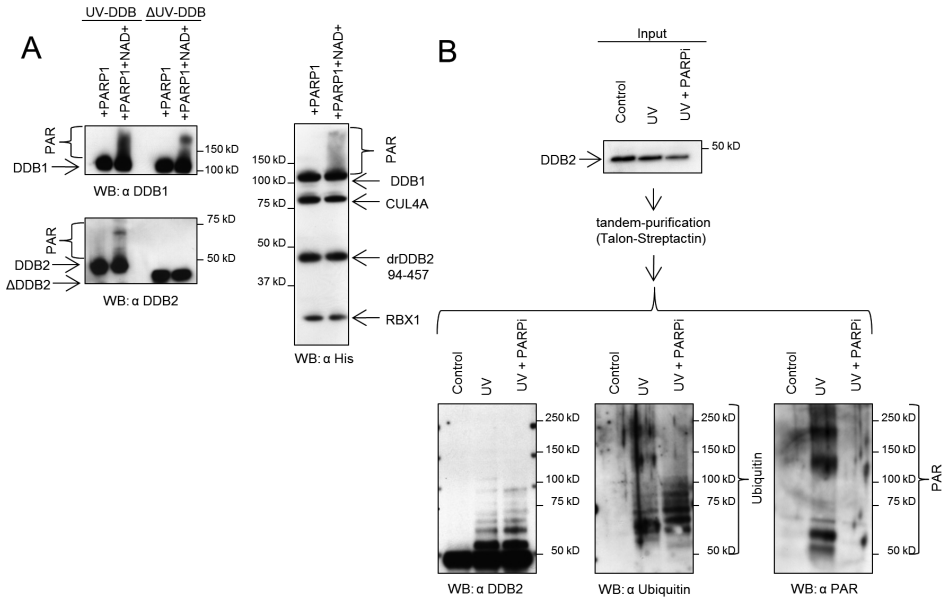

Figure 6. (A) The N-terminus of DDB2 is targeted for PARylation. *In vitro* PARylation experiments using purified components reveal that both DDB2 and DDB1 are directly modified by PARP1. Human DDB2 lacking its first 40 N-terminal amino acids including 7 lysines (δUVDDB), failed to undergo PARylation. The zebrafish orthologue of DDB2 (drDDB) lacking the first 93 N-terminal residues is also not PARylated *in vitro*. **(B)** 6His StrepII-tag DDB2 isolation using tandem purifications under denaturing conditions. NHF cells stably expressing 6His StrepII-tag DDB2 were irradiated with UV-C light (100 J/m2) in presence or in absence of PARPi (10μM) or mock-irradiated and incubated for 30 minutes. The final Strep-Tactin column purifications were separated on SDS-PAGE gels, and proteins were visualized with antibodies against DDB2, PAR or Ubiquitin.

recruitment of ALC1 to sites of UV-C laser-induced DNA damage (figure 7B). GFP-ALC1 was rapidly recruited to UV-induced DNA lesions in wild-type (supplementary figure 3B) and XP-A cells (figure 7B) shortly after exposure to the UV-C laser and could be completely suppressed by addition of the PARPi (supplementary figure 3A). Strikingly, knockdown of DDB2 significantly reduced the recruitment of GFP-ALC1 in XPA-deficient cells (figure 7B) as well as in repair-proficient cells at early time-points after UV irradiation (supplementary figure 3B), suggesting an important role for DDB2 in the recruitment of chromatin remodeler ALC1 through PARP1-mediated PAR synthesis. Consistent with our findings that two mechanistically distinct PARylation waves exist in response to UV irradiation, we found that single-stranded DNA gaps also triggered robust GFP-ALC1 recruitment at later time-points after UV irradiation in normal human as well as in XP-E cells (supplementary figure 4) whereas recruitment of ALC1 was absent in dual incision-defective XP-A cells not even in the presence of HU/AraC (supplementary figure 4). In contrast the stabilization of PAR chains by PARG depletion (supplementary figure 4) resulted in clearly detectable GFP-ALC1 recruitment at UV-damaged regions in XP-A fibroblasts. In summary, our results

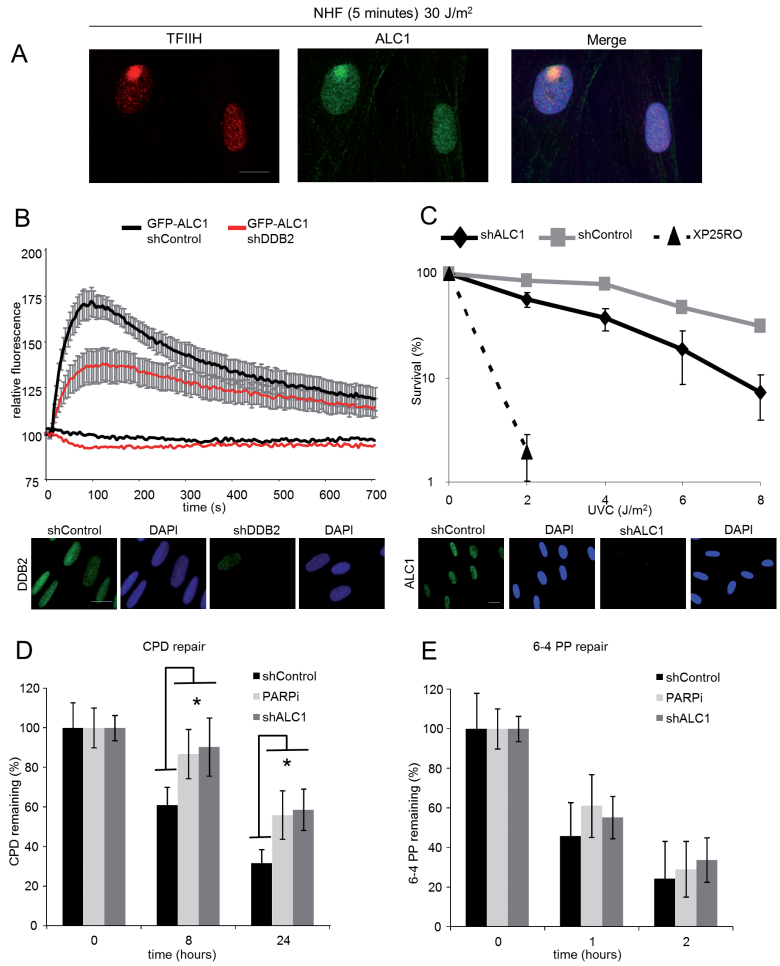

Figure 7. (A) NHF cells were locally UV irradiated (100 J/m²), fixed after the indicated time and stained with an antibody recognizing ALC1 or TFIIH. ALC1 colocalizes with the damage marker TFIIH. Scale bars represent 20µm. **(B)** XP-A cells stably expressing GFP-ALC1 were infected with the indicated short hairpin RNA. The cells were UV damaged using UV-C (266 nm) laser irradiation. GFP fluorescence intensities at the site of UV damage were measured by real time imaging until they reached a maximum. Assembly kinetic curves were derived from at least six cells for each protein. Error bars indicate SEM. Scale bar represent 20µm. **(C)** Clonal survival of UV-irradiated NHF cells expressing shControl or shALC1 and XPA cells. The percentage of surviving cells is plotted against the applied UV-C dose (J/m²). The results are from three independent experiments; Error bars indicate standard deviation. Scale bar represent 20µm. **(D)** NHF cells expressing shControl or shALC1 RNAi or treated with PARPi (10µM) were irradiated with 10 J/m² UV-C, fixed immediately, at 8 or 24 hours after UV treatment and stained with anti-CPD antibody. (asterisk indicates $p<0.05$, ANOVA) **(E)** NHF cells expressing shControl or shALC1 or treated with PARPi (10µM) were irradiated with 10 J/m2 UV-C, fixed immediately, at 1 or 2 hours after UV treatment and stained with an anti-6-4PP antibody. The total fluorescence intensity of the nucleus was quantified and divided by the surface area, resulting in a specific fluorescence intensity expressed in arbitrary units. Values are the result of three independent experiments (100 cells per time point).

reveal that the chromatin remodeling enzyme ALC1 is recruited to PAR chains synthesized during repair by NER through distinct molecular mechanisms.

PARP1 inhibition and ALC1 depletion impair CPD repair and render cells sensitive to UV irradiation

Having established that ALC1 is recruited to sites of local damage, we subsequently addressed the biological impact of this finding. To this end, we generated a cell line stably expressing a shRNA targeting endogenous ALC1. Knock-down of ALC1 rendered cells sensitive to UV irradiation compared to control cells (figure 7C), indicating that ALC1 protects cells against UV-induced cytotoxicity. Likewise, chemical inhibition of PARP also rendered cells UV sensitive (supplementary figure 3D), underscoring an important role for PAR synthesis in NER. Finally, we directly measured the repair of UV-induced DNA lesions following a UV dose of 10 J/m^2 by immunostaining using antibodies against 6-4 PPs or CPDs. While the repair of 6-4 PP was not significantly affected, we measured a significant reduction in CPD repair upon ALC1 depletion or chemical inhibition of PARP1 (figure 7D-E). Corroborating these findings, an ELISA-based assay confirmed that knock-down of ALC1 conferred a significant reduction in CPD repair (supplementary figure 5). These findings reveal an unanticipated role of PAR synthesis and ALC1 in efficient repair of CPDs by human NER.

DISCUSSION

Despite detailed insights into the NER reaction and the core proteins involved (Gillet and Scharer, 2006;Sugasawa, 2010), the regulatory pathways that govern NER activity in living cells are still poorly understood. Among others, these pathways involve the post-translational modifications of NER proteins and the activity of chromatin remodelling enzymes to optimize repair of DNA damage embedded in chromatin. DDB2 is the first NER factor to be recruited to UV-induced DNA lesions (Luijsterburg et al., 2007) and it regulates NER by direct DNA lesion recognition (Scrima et al., 2008) and modulation of chromatin structure (Palomera-Sanchez and Zurita, 2011). We identified PARP1 as a novel DDB2-associated factor in UV–irradiated cells The fact that the interaction between these factors occurred in non-diving UV-irradiated human fibroblasts excludes the possibility that involvement of PARP1 in NER is merely related to the stalling of replication forks (Bryant et al., 2009). Although we found PARP1 as a novel DDB2-associated factor, *in vitro* assays with purified proteins revealed that PARP binds to both DDB1 and DDB2 but with higher presence for DDB2.

We found robust synthesis of PAR chains in nuclear regions containing UV-induced DNA lesions that was completely suppressed by chemical PARP inhibition. These findings directly link PARP1 to the repair of photolesions and fit with previous observations that UV irradiation triggers both stimulation of poly(ADP-ribose) synthesis (Cleaver et al., 1983) and association of PARP1 with UV-photolesions in chromatin (Vodenicharov et al., 2005). Although these findings clearly implicate PARP1 activity in response to UV irradiation, we and others (Bryant et al., 2009;Schultz et al., 2003) failed to detect the recruitment of endogenous PARP1 to UV-induced DNA lesions or UV-induced stalled replication forks,

which is possibly due to transient nature of its interaction or the abundance of PARP1 in the nucleus (Krishnakumar and Kraus, 2010).

Our study identified two distinct molecular mechanisms that orchestrate the synthesis of PAR chains at UV-induced DNA damage. Firstly, we show that persistent single-stranded DNA gaps generated by inhibition of repair synthesis, elicit DDB2-independent PARylation at NER sites. However, a possible role of PARylation in regulation of post-incision repair has not yet dissected although recruitment of post-incision factor XRCC1, disassembly kinetics of NER complexes (Moser et al., 2007) or sealing of UV–induced single-stranded DNA gaps was not impaired by PARP inhibition (Cleaver et al., 1983). Secondly and more importantly, we show that DDB2 regulates fast and transient PARylation at sites of UV-induced DNA damage during the pre-incision stage of NER. One target of PARylation is DDB2 itself as shown by PARylated DDB2 purified from UV-irradiated cells. It is likely that this modification underlies among others the UV-specific occurrence of DDB2 peptides of larger than 50 KDa molecular weight in immunoprecipitates of chromatin bound DDB2. The initial DDB2-mediated wave of PAR synthesis does not require incision and is regulated by the activity of PARG. Indeed, there is increasing evidence that DNA breaks are not an absolute requirement for PARP1 activation (Krishnakumar and Kraus, 2010). Several alternative mechanisms to activate PARP1 in the absence of DNA breaks have been proposed, including interaction with other proteins (Cohen-Armon et al., 2007), or post-translational modifications such as phosphorylation, acetylation (Hassa et al., 2003;Rajamohan et al., 2009), SUMOylation and ubiquitylation (Martin et al., 2009;Messner et al., 2009). In this light, it is feasible that the DDB2-associated E3 ubiquitin ligase activity (Shiyanov et al., 1999;Groisman et al., 2003) might activate PARP1. At the same time, it is possible that PARP1 activation is modulated by DDB2-mediated acetylation through its interaction with histone acetyltransferases p300 and the STAGA complex (Datta et al., 2001;Rapic-Otrin et al., 2002;Martinez et al., 2001).

Molecular mechanisms for DDB2-mediated and PARP1-executed regulation of NER

Our data provide mechanistic insights into how DDB2 promotes NER in chromatin through two novel mechanisms. On one hand, DDB2 is directly targeted by poly(ADP-ribosyl)ation and ubiquitylation (Fischer et al., 2011) in response to UV irradiation. As PARylation (Messner et al., 2010) and ubiquitylation are targeted to lysine and both modifications appear to occur in the same N-terminal region of DDB2, competition between PARylation and ubiquitylation of target lysine residues might constitute an important mechanism of DDB2 mediated regulation of NER. The *in vivo* data supports a competition model in which the poly(ADP-ribosyl)ation of DDB2 results in increased protein stability and a prolonged chromatin retention time on the UV lesion. At the same time poly(ADP-ribosyl)ation of DDB2 suppresses its UV-induced ubiquitylation and consequently leads to reduced degradation of DDB2. Together our data disclose a mechanism by which two opposing modifications regulate the steady-state levels and retention time of DDB2 at sites of UV-photolesions.

On the other hand, DDB2-dependent PARylation events also stimulate the pre-incision step of NER. We show that DDB2-dependent PARylation through PARP1 at UV-induced DNA lesions targets chromatin remodeler ALC1 to these sites. ALC1 belongs to the Swi2/Snf2

ATPase superfamily and through its macrodomain, interacts transiently with chromatin that is modified by PARP1. We propose that these protein modifications serve to locally modulate chromatin structure through PARP1-stimulated nucleosome sliding to promote NER (Gottschalk et al., 2009;Ahel et al., 2009). Consistent with this scenario, we show that loss of ALC1 or chemical inhibition of PARP1 resulted in defects in the repair of CPDs concomitantly with increased sensitivity to UV exposure, underscoring the importance of the DDB2-PARP1-ALC1 pathway in promoting NER. We noted that the defects in CPD repair due to loss of ALC1 or PARP1 activity are less pronounced than repair defects caused by loss of DDB2 (Pines et al., 2009), suggesting that the essential role of DDB2 in CPD repair is not solely due to its recruitment of PARP1-mediated activities, but also involves other functions of DDB2 such as its ubiquitin ligase activity. Interestingly, XPC contains a putative PAR binding sequence (Gagne et al., 2008), suggesting that UV-DDB dependent PAR may promote the accessibility of UV lesions through remodeling of the chromatin structure as well as providing an enhancer signal for the recruitment of preincision NER proteins.

A model of DDB2 and PARP1 dependent regulation of NER

The high affinity of DDB2 for DNA and its preference for UV-damaged DNA makes UV-DDB the most important DNA damage recognition factor for 6-4PP and CPD (Wittschieben et al., 2005). UV-DDB is the first NER factor to be recruited to UV damage (Luijsterburg et al., 2007;Nishi et al., 2009) as part of the Cullin-RING ubiquitin ligase (CRL4) complex CUL4A-RBX1 (Figure7). As shown for 6-4 PP (Scrima et al., 2008), the CUL4A-RBX1 complex binds to photolesions by the WD40 domain of DDB2 and in concert with PARP1 tightly regulates steady-state levels and retention time of DDB2 by opposing modifications (PARylation and ubiquitylation) of the same N-terminal region of DDB2. The enhanced extension time of PARylated DDB2 on UV-damage might be particularly important for CPD photolesions that induce much less disruption of base pairing interactions than 6-4PP (Kim and Choi, 1995) and fully depend on functional DDB2 for their repair. Purified (nonPARylated) DDB2 recognizes CPD and 6-4PP with a 5 and 80 fold higher affinity respectively than nondamaged DNA (Wittschieben et al., 2005); this affinity of DDB2 for CPD might too low for productive repair i.e. recruitment of XPC. We speculate that extended binding of PARylated DDB2 to CPD will provoke the induction of chromatin modifications at the site of DNA damage to allow productive interaction and ubiquitylation of XPC and UV-DDB required for NER (Sugasawa et al., 2005). Underscoring the importance of PAR synthesis in the assembly of the pre-incision NER complex, we found that PARP inhibition leads to reduced recruitment of the pre-incision factor XPC as shown in our recent work (Luijsterburg et al., 2012) whereas depletion of PARG stimulates binding of XPC (Luijsterburg et al., 2012) and TFIIH (data no shown). Whether UV-DDB activates PARP1 through its E3 ubiquitin ligase activity or whether PARP1 activation occurs in parallel with or precedes ubiquitylation is not clear. PARP1 mediated increase of retention time of DDB2 at UV damage and DDB2 protection by suppressing its ubiquitylation-dependent degradation argue for PARylation as the initiating event. Moreover, PARP1 might create accessibility for recruitment of NER factors by its ability to disrupt chromatin structure by PARylation of histones and destabilizing nucleosomes (Krishnakumar and Kraus, 2010). Additionally

PARylation of chromatin effectuates recruitment of NER promoting factors such as the Swi2/Snf2 chromatin remodeler ALC1 to UV damaged DNA to locally modulate chromatin structure through nucleosome sliding (Figure 8) thereby stimulating the recruitment of XPC to assemble a functional repair complex. Our study also identified DDB2-independent PARylation and recruitment of ALC1 at NER sites that is trigged by transient single-stranded DNA gaps generated by the dual incision step of NER (figure 8); this process of PARylation is amplified by inhibition of DNA repair synthesis. The role of PARylation and ALC1 in regulation of post-incision step of NER remains to be resolved.

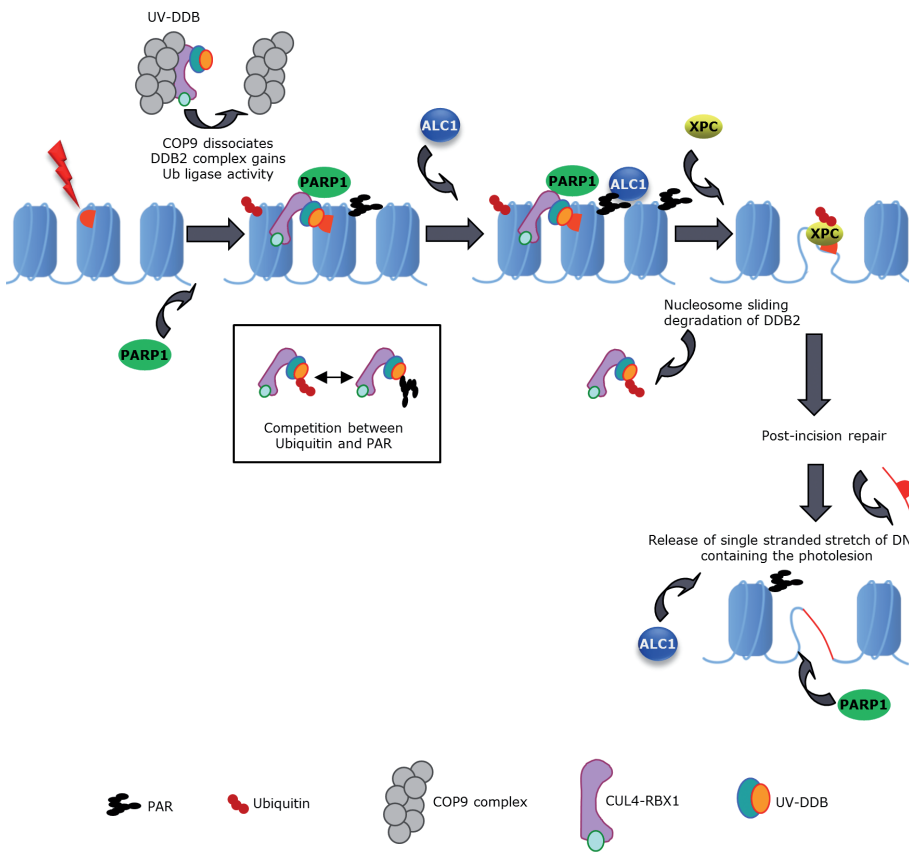

Figure 8: Model of DDB2 and PARP 1 dependent regulation of NER. UV-DDB is the first NER factor to be recruited to UV damage as part of the Cullin-RING ubiquitin ligase (CRL4) complex CUL4A-RBX1. This complex binds to UV damage and both DDB1 and DDB2 might be involved in binding of PARP1. In concert with PARP1, the CUL4A-RBX1 complex tightly regulates steady-state levels and retention time of DDB2 by opposing modifications (PARylation and ubiquitylation) of the same N-terminal region of DDB2. Additionally, PARP1-dependent PARylation of chromatin also effectuates recruitment of the Swi2/Snf2 chromatin remodeler ALC1 to UV damaged DNA in order to locally modulate chromatin structure through nucleosome sliding thereby stimulating the recruitment of XPC. The second distinct waves of PARylation and ALC1 recruitment requires the generation of single-stranded DNA gaps resulting from dual incision.

EXPERIMENTAL PROCEDURES

Cell culture and UV-C irradiation

The following cell lines were used for this study: VH10 hTert (normal human fibroblast, NHF), XP25RO hTert (XP-A), GM01389 hTert (XP-E), U2OS and MRC5 fibroblast. Cells were grown in DMEM supplemented with 10% fetal calf serum, penicillin and streptomycin. Two days prior to experiments medium was changed to DMEM supplemented with 0.2% serum fetal calf serum, penicillin and streptomycin. UV-radiation of cells was carried out using a 254 nm UV-C source. Local irradiation was performed using 5 μm filters as described previously (Volker et al., 2001). UV lamp–induced damage was inflicted using a 254 nm UV source (TUV PL-S 9W; Philips). For induction of global UV damage, cells were rinsed with PBS and irradiated with 8 or 16 J/m2. For induction of local UV damage, cells were UV irradiated through a polycarbonate mask (Millipore) with pores of 8 μm and subsequently irradiated with 30, or 100 J/m2.The AZ12640831-009 PARPi was used at a final concentration of 10 μM and was a gift from AstraZeneca. Cells were pretreated 30 minutes before irradiation.

Generation of cell lines

ALC1 and DDB2 cDNA were cloned into vector pENTR4-GFP-C1 (E.Campeau; addgene: w392-1) and were subsequently recombined into pLenti6.3 V5-DEST (Invitrogen) using gateway recombination. VH10 hTert or XP25RO hTert fibroblasts were transduced with pLenti6.3 GFP-ALC1 or pLenti6.3 GFP-DDB2 lentiviral particles and cultured with 5 μg/ml blasticidin (Invivogen) to select for integrands.

For DDB2 isolation a 6 His and strepII-tag were fused to the N-terminus of DDB2. A synthetic oligo coding for 6His StrepII-tag was inserted into pENTR4 (invitrogen) and DDB2 cDNA was subsequently cloned in. Lentiviral particles were generated after recombination of this vector to pLenti6.3 V5-DEST and used for transducing VH10 hTert cells.

NHF and XP-A fibroblasts stably expressing short hairpin RNA (shRNA) were generated by lentiviral transduction of control, ALC1 or DDB2 targeting constructs followed by 1 μg/ml puromycin selection. The following shRNA vectors were used: TRCN0000013471 (ALC1); TRCN0000083995 (DDB2) and SHC002 (non-targeting control) from the RNAi Consortium (Sigma-Aldrich).

RNA interference

Short interfering RNA (siRNA) duplexes used were as follows: smartpool siRNA targeting the PARG transcript and smartpool non-targeting siRNA (Dharmacon). Cells were transfected using Hiperfect (Qiagen) according to the manufacturer's protocol. For PARG knockdown two sequential transfections were performed. Immunostaining and western-blot experiments were performed 48 hours after the final transfection.

Complex isolation

Isolation of DDB2complex was performed according to published procedures with some modifications (Groisman et al., 2003). Briefly, cells were irradiated with UV-C at 20 J/m^2, and incubated for 5 minutes. To prepare nuclear extracts, cells were suspended in hypotonic buffer (10 mM Tris-HCl pH 7.3, 10 mM KCl, 1.5 mM MgCl2, 10

mM β-mercaptoethanol, and 0.2 mM PMSF) and disrupted by Dounce homogenization. Nuclei were collected by centrifugation at 2000g for 15 min at 4°C and resuspended in extraction buffer (15 mM Tris-HCl pH 7.3, 1 mM EDTA, 0.21 M NaCl, 1 mM MgCl2, 10% glycerol, 10 mM β-mercaptoethanol, and 0.2 mM PMSF). After incubating on ice for 30 minutes, the samples were centrifuged at 20,000g for 30 min at 4°C, and the supernatant was used as the nuclear extract fraction. The nuclear pellet fraction was washed and resuspended in the micrococcal nuclease buffer (20 mM Tris-HCl pH 7.5, 100 mM KCl, 2 mM MgCl2, 1 mM CaCl2, 0.3 M sucrose, 0.1% Triton X-100, and complete protease inhibitor cocktail (Roche). Micrococcal nuclease was added at 3 U/ml and the samples incubated for 10 min at room temperature, whereupon the reaction was terminated by adding 5mM EGTA and 5mM EDTA. The samples were centrifuged at 2000g for 5 min at 4°C, and the supernatant was used as the solubilized chromatin fraction. The UV-DDB complex was immunoprecipitated from solubilized chromatin prepared from MRC5 cells expressing FLAG-DDB2 by incubating with M2 anti-FLAG agarose ovwernight with rotation. After an extensive wash with wash buffer (0.1 M KCl, 20 mM Tris-HCl pH 8.0, 5 mM MgCl2, 10% glycerol, 1 mM PMSF, 0.1% Tween 20, 10 mM β-mercaptoethanol), the bound proteins were eluted from M2 agarose by incubation for 30 min with FLAG peptide (0.2 mg/ml in PBS). The elution procedure was repeated three times.

In-gel tryptic digestion

Immunoprecipitates were separated on SDS-PAGE gels, and proteins were visualized with Coomassie (SimplyBlue, Invitrogen). Gel lanes were sliced into 25–30 bands, cut into small pieces and washed with 25 mM NH4HCO3 followed by two rounds of dehydration with 100% acetonitrile for 10 min. For reduction and alkylation, gel particles were first incubated with 10 mM dithiothreitol for 30 minutes at 56°C. Following dehydration with acetonitrile, gel plugs were subsequently incubated in 55 mM iodoacetamide for 20 minutes at room temperature. After two rounds of washing with 25 mM NH4HCO3 and dehydration with 100% acetonitrile, the gel particles were completely dried in a centrifugal vacuum concentrator (Eppendorf, Hamburg, Germany). Dried gel particles were re-swollen for 15 min. on ice by addition of 15 µl of a trypsin solution (12.5 ng/µl in 25 mM NH4HCO3, Sequencing grade modified trypsin, Promega, Madison, WI). Following this, 20 µl of 25 mM NH4HCO3 was added and samples were kept on ice for an additional 30 min. Tryptic digestion was subsequently performed overnight at 37 °C. Following tryptic digestion, the overlaying digestion-solution was collected. Two additional rounds of extraction with 20 µl 0.1% TFA were used to extract peptides from the gel plugs and all extracts were pooled.

Nano LC ESI MS/MS

Nanoflow LC was performed on an Ultimate LC system (Dionex, Sunnyvale, CA). A volume of 10 µL of sample was injected onto a C18 PepMapTM 0.3 mm×5 mm trapping column (Dionex) and washed with 100% A (2% acetonitrile in 0.1% formic acid in MQ water, v/v) at 20 µL/min for 15 min. Following valve switching, peptides were separated on a C18 PepMap 75 µm×150 mm column (Dionex) at a constant flow of 200 nL/min. The peptide elution gradient was from 10 to 60% B (95% acetonitrile in 0.1% formic acid in MQ water v/v) over

50 min. The nanoflow LC system was coupled to an HCTultra IonTrap (Bruker Daltonics, Bremen, Germany) using a nano-electrospray ionisation source. The spray voltage was set at 1.2 kV and the temperature of the heated capillary was set to 165 °C. Eluting peptides were analyzed using the data dependent MS/MS mode over a 300–1500 m/z range. The five most abundant ions in an MS spectrum were selected for MS/MS analysis by collision-induced dissociation using helium as the collision gas.

Mass spectrometry data analysis

Peak lists were generated using DataAnalysis 4.0 software (Bruker Daltonics) and exported as Mascot Generic (MGF) files. These files were searched against the human IPI database using the Mascot (version 2.2.1) search algorithm (Matrix Science, London, UK) An MS tolerance of 0.6 Da (with # 13C = 1) and a MS/MS tolerance of 0.5 Da was used. Trypsin was designated as the enzyme and up to one missed cleavage site was allowed. Carbamidomethylcysteine was selected as a fixed modification and oxidation of methionine as a variable modification.

Immunofluorescent labelling (IF) and Western blotting (WB)

The cells were fixed with methanol/acetone (50%/50%) for 10 minutes at 4°C. After an extensive wash with PBS the cells were incubated for 60 minutes at room temperature with buffer contains 0.5% BSA and 0.05% Tween-20 in PBS. Antibody incubations were performed at room temperature and cells were counterstained with DAPI. Images were captured with a Zeiss Axioplan2 microscope equipped with a Zeiss Axiocam MRm camera using either a Plan-NEOFLUAR 40×/1.30 or 63×/1.25 objective. Fluorescence intensity of randomly captured images was quantified using Zeiss Axiovision software. For total extract the cells were lysed directly in Laemli-SDS-sample buffer. Western blot analysis was performed as described previously (Fousteri et al., 2006) and protein bands were visualised via chemiluminescence (ECL-Plus, Amersham Biosciences) using Horseradish Peroxidase (HP)-conjugated secondary antibodies or via Odyssey Infrared Imaging System (LI-COR) using secondary antibodies labeled with IR fluorophores (LI-COR). The following antibodies were used: mouse α-DDB2 at 1:500 (IF)- 1:1000 (WB) (MyBioSource); mouse α-Parp1 at 1:1000 (WB) (Abnova); mouse α-Poly (ADP-Ribose) at 1:100 (IF and WB) (Abcam); mouse α-ALC1 at 1:500 (IF)- 1:1000 (WB) (Abcam); mouse α-GFP at 1:5000 (WB) (Roche); goat α-DDB1 at 1:1000 (WB) (Abcam); goat α-DDB2 at 1:1000 (WB) (Santa-Cruz); rabbit α-Poly (ADP-Ribose) at 1:100 (IF and WB) (BD pharmingen); rabbit α-H2B at 1:5000 (WB) (Santa-Cruz); rabbit α-PARG at 1:1000 (C-term) (WB) (Origene);mouse α-6-4PP and α-CPD at 1:1000 (IF) (CosmoBio) Alexafluor 488 and 555 conjugated antibodies were purchased from Invitrogen.

Live cell confocal laser-scanning microscopy

Confocal laser-scanning microscopy images were obtained using a confocal microscope (LSM 510 META) with a 63× oil Plan Apochromat 1.4 NA oil immersion lens (Carl Zeiss, Inc.) equipped with a cell culture microscopy stage. GFP fluorescence imaging was recorded after excitation with a 488-nm argon laser and a 515–540-nm band-pass

filter. Fluorescence loss in photobleaching (FLIP) was performed as described previously (Houtsmuller and Vermeulen, 2001;Zotter et al., 2006). Kinetics of GFP-tagged ALC1, and DDB2 accumulation were performed using a UV-C (266 nm) laser irradiation as described previously (Dinant et al., 2007). Briefly, VH10-tert cells stably expressing GFP-DDB2 and GFP-ALC1 were incubated in CO2-independent microscopy medium (137 mM NaCl, 5.4 mM KCl, 1,8 mM CaCl2, 0.8 mM MgSO4, 20 mM D-glucose, 20 mM HEPES and 10% FCS) and 2 mW pulsed (7.8 kHz) diode pumped solid state laser emitting at 266 nm (Rapp OptoElectronic, Hamburg GmbH) was used for local UV-C irradiation. To determine the dissociation kinetics of DDB2 from UV-damaged DNA, the undamaged nucleus was continuously bleached and the fluorescence decrease in the local damage was monitored. Relative fluorescence was normalized at 100% (before bleach at maximum level of accumulation). The half-time ($t_{1/2}$) of a FLIP curve corresponds to the residence time of a protein molecule in the locally damaged area. Images obtained with the confocal microscope were analyzed using AIM software (Zeiss). Fluorescence levels were determined for the specified region where damage was induced in addition to the complete nucleus. From these datapoints the relative amount of protein in the damaged area was determined in time.

Fluorescence recovery after photobleaching (FRAP)

VH10-tert cells stably expressing GFP-DDB2 were incubated in CO2-independent microscopy medium (137 mM NaCl, 5.4 mM KCl, 1,8 mM CaCl2, 0.8 mM MgSO4, 20 mM D-glucose, 20 mM HEPES and 10% FCS) supplemented with 1‰ DMSO (mock treatment) or 10 μM PARP inhibitor dissolved in DMSO three hours prior to FRAP analysis. Cells were subsequently rinsed with PBS, mock-treated or globally UV-C irradiated (10 J.m-2) and transferred to the microscope chamber in microscopy medium (supplemented with DMSO or PARP inhibitor). Cells were incubated on the microscope chamber at 37° for 10 minutes to allow repair proteins to accumulate at UV-induced DNA lesions after which the mobility of GFP-tagged NER factors was analyzed by strip-FRAP. Briefly, FRAP analysis was performed by bleaching (5 iterations) a narrow strip (512 x 40 pixels at zoom 8) spanning the nucleus with maximal 488 nm laser intensity (AOTF 100%). The re-equilibration of bleached and non-bleached molecules was monitored in a region of 512 x 50 pixels (zoom 8) with low laser intensity (0.5% for GFP-DDB2) for at least 700 images with a 38 ms time-interval between images. The data were normalized to pre-bleach intensity (set to 1) and bleach depth (set to 0). Three independent experiments were performed for each condition.

UV survival

Cellular survival of VH10 hTert shControl, VH10 hTert shALC1, and XP-A cells was determined using a colony assay. Cells were plated in 10-cm and after 16 hours cells were exposed to UV-C (254 nm; TUV lamp; Phillips) and left to grow for 14 days, fixed, and stained with methylene blue. Colonies were counted to assess the colony-forming ability.

In vitro polyADP-ribosylation assay

The assay was performed according to published procedures (Deng et al., 2005) using recombinant proteins purified as described in Fischer et al. (Fischer et al., 2011).

DDB2 purification

VH10 hTert cells stably expressing 6His StrepII-tag DDB2 were irradiated with UV-C light (100 J/m2) or mock-irradiated and incubated for 30 minutes. Cells were collected and lysed in lysis buffer (8 M urea, 2 M NaCl, 25 mM Tris pH 8, 1 mM MgCl2, 0.2 % Triton). The lysates were diluted ≥ 7 times, after which 25 benzonase units were added per ml. After incubating at room temperature for 30 minutes samples were centrifuged at 16,000g for 10 minutes. TALON beads (Clontech) were added to the supernatants and incubated for 4 hr at room temperature. After an extensive wash with wash buffer (8 M urea, 25 mM Tris pH 8, 1 mM MgCl2, 20mM imidazole), the 6His StrepII-tag DDB2 was eluted by overnight incubation with the elution buffer (8 M urea, 25 mM Tris pH 8, 500 mM imidazole, 1 % SDS). The elutes were concentrated by Vivaspin centrifugal concentrators (Sartorius) and diluted in Strep-Tactin buffer (100 mM Tris pH 8, 1 mM EDTA, 150 mM NaCl). A second purification step was performed using Strep-Tactin spin columns according to the manufacturer's protocol (IBA). Elutes were separated on SDS-PAGE gels, and proteins were visualized by Western-blot.

GFP-DDB2-PARP-1 binding assay.

U2OS cells transfected with GFP constructs for 24 hours were lysed in denaturing buffer (20 mM Tris, pH 7.5; 50 mM NaCl; 0.5% NP-40; 1% Sodium Deoxycholate; 1% SDS; 1 mM EDTA, Benzonase final conc. 0,25U/µl) containing protease inhibitor cocktails (Roche) and subjected to immunoprecipitation with GFP-TRAP beads (Chromotek) for 1 hours at RT. The beads were then washed extensively in a buffer (20 mM Tris, pH 7.5; 50 mM NaCl; 0.5% NP-40; 0.5% Sodium Deoxycholate; 0.5% SDS; 1 mM EDTA) that disrupts protein-protein interactions, followed by two washes in EBC buffer (50 mM Tris, pH 7.5; 150 mM NaCl; 0.5% NP-40; 1 mM EDTA), and incubated with 100 ng purified, recombinant PARP-1 (Sigma) for 2 hours at RT. The beads were then washed thoroughly in EBC buffer and processed for immunoblotting.

In vitro co-immunoprecipitation

UV-DDB, δUV-DDB (DDB2 lacking its first 40 N-terminal amino acids), GFP and PARP-1 recombinant protein were used to test direct interaction in vitro. The reaction volume was adjusted to 400 µL in EBC buffer (50 mM Tris, pH 7.5; 150 mM NaCl; 0.5% NP-40; 1 mM EDTA), and 0,5 µg of anti-PARP-1 antibody was added. The mixture was incubated and rotated at 4°C for 3 hours. The antigen-antibody complex was captured by incubation with 15 µl of protein A-agarose beads (GE Healthcare) for 2 hr in cold room. The beads were washed extensively in EBC buffer,and resuspended in 20 µL of Laemili sample buffer and processed for immunoblotting.

Farwestern analysis

100 ng of UV-DDB and 1000 ng of GFP recombinat proteins were separated by SDS-PAGE and transferred to a PVDF membrane. The proteins on the membrane were denaturated for 10 min with a 6 M guanidine hydrochloride (GuHCl) solution in HBB buffer (10 mM HEPES, pH 7.5, 60 mM KCl, 1 mM EDTA and 1 mM DTT). Proteins were then renaturated in the same HBB buffer with progressively decreasing GuHCl concentration. The membrane was rinsed extensively in HBB and blocked for 1 hour in blocking solution. Following the

membrane was incubated with PARP-1 recombinant protein (10 µg/ml) in HBB for 16 h. Unbound proteins were removed with extensive washes for 30 min in the same buffer. The PARP-1 binding was visualised by Western-blot.

CPD/6-4 PP ELISA

Cells were plated in 96 well plates, irradiated with 10 J/m^2 UV and incubated for various periods to allow cells to repair DNA photolesions. The cells were fixed with methanol/acetone (50%/50%) for 10 minutes. After an extensive wash with PBS the cells were incubated for 3 minutes at room temperature with 10 mM NaOH. The cells were rinsed extensively in PBS and incubated for 60 minutes at room temperature with buffer contains 0.5% BSA and 0.05% Tween-20 in PBS. The plates were sequentially incubated with TDM-2 or 64M-2 antibodies specific for CDP or 6-4PP, respectively, and secondary antibody conjugated with horseradish peroxidase (HRP). After washings, substrate solution Turbo TMB-ELISA (Pierce) was added to the plates and incubated for 15-30 min. Absorbance at 490 nm was measured using a microplate reader after the addition of 2 M H_2SO_4.

Online supplemental material

Table1 shows the proteins identified in Flag immunoprecipitates material from FLAG-DDB2 expressing MRC5 cells mock treated or irradiated with UV-C. Fig. S1 shows direct interaction in vitro between DDB2 and PARP-1. Fig. S2 shows that the kinetics of GFP-DDB2 accumulation were not affected by PARPi or depletion of PARG. Fig. S3 shows transient recruitment of GFP-ALC1 to sites of UV-C laser-induced DNA damage. Fig. S4 demonstrates that single-stranded DNA gaps also triggered robust GFP-ALC1 recruitment at later time-points after UV irradiation in normal human as well as in XP-E cells, whereas recruitment of ALC1 was absent in dual incision-defective XP-A cells Fig. S5 shows a significant reduction in CPD repair upon ALC1 depletion or chemical inhibition of PARP1.

ACKNOWLEDGEMENTS

We thank Dr. A.G. Ladurner for providing ALC1 cDNA (European Molecular Biology Laboratory (EMBL), Heidelberg, Germany) and Ms Irina Dragan for excellent technical assistance. This work was funded by the Dutch Organization for Scientific Research (NWO): Veni Grant 917-96-120 (J.A.M.), Veni Grant (M.S.L.), ZonMW Grant 40-00812-98-08031 and an EMBO and FEBS long-term fellowship (M.S.L.), and the Netherlands Genomics Initiative/Netherlands Organisation for Scientific Research (NWO): nr 050-060-510.

REFERENCE LIST

1. Aboussekhra,A., M.Biggerstaff, M.K.Shivji, J.A.Vilpo, V.Moncollin, V.N.Podust, M.Protic, U.Hubscher, J.M.Egly, and R.D.Wood. 1995. Mammalian DNA nucleotide excision repair reconstituted with purified protein components. *Cell* **80**: 859-868.
2. Ahel,D., Z.Horejsi, N.Wiechens, S.E.Polo, E.Garcia-Wilson, I.Ahel, H.Flynn, M.Skehel, S.C.West, S.P.Jackson, T.Owen-Hughes, and S.J.Boulton. 2009. Poly(ADP-ribose)-dependent regulation of DNA repair by the chromatin remodeling enzyme ALC1. *Science* **325**: 1240-1243.
3. Bryant,H.E., E.Petermann, N.Schultz, A.S.Jemth, O.Loseva, N.Issaeva, F.Johansson, S.Fernandez, P.McGlynn, and T.Helleday. 2009. PARP is activated at stalled forks to mediate Mre11-dependent replication restart and recombination. *EMBO J.* **28**: 2601-2615.
4. Cleaver,J.E., W.J.Bodell, W.F.Morgan, and B.Zelle. 1983. Differences in the regulation by poly(ADP-ribose) of repair of DNA damage from alkylating agents and ultraviolet light according to cell type. *J. Biol. Chem.* **258**: 9059-9068.
5. Cleaver,J.E., E.T.Lam, and I.Revet. 2009. Disorders of nucleotide excision repair: the genetic and molecular basis of heterogeneity. *Nat. Rev. Genet.* **10**: 756-768.
6. Clement,F.C., U.Camenisch, J.Fei, N.Kaczmarek, N.Mathieu, and H.Naegeli. 2010. Dynamic two-stage mechanism of versatile DNA damage recognition by xeroderma pigmentosum group C protein. *Mutat. Res.* **685**: 21-28.
7. Cohen-Armon,M., L.Visochek, D.Rozensal, A.Kalal, I.Geistrikh, R.Klein, S.Bendetz-Nezer, Z.Yao, and R.Seger. 2007. DNA-independent PARP-1 activation by phosphorylated ERK2 increases Elk1 activity: a link to histone acetylation. *Mol. Cell* **25**: 297-308.
8. Datta,A., S.Bagchi, A.Nag, P.Shiyanov, G.R.Adami, T.Yoon, and P.Raychaudhuri. 2001. The p48 subunit of the damaged-DNA binding protein DDB associates with the CBP/p300 family of histone acetyltransferase. *Mutat. Res.* **486**: 89-97.
9. Deng,Z., C.Atanasiu, K.Zhao, R.Marmorstein, J.I.Sbodio, N.W.Chi, and P.M.Lieberman. 2005. Inhibition of Epstein-Barr virus OriP function by tankyrase, a telomere-associated poly-ADP ribose polymerase that binds and modifies EBNA1. *J. Virol.* **79**: 4640-4650.
10. Dinant,C., J.M.de, J.Essers, W.A.van Cappellen, R.Kanaar, A.B.Houtsmuller, and W.Vermeulen. 2007. Activation of multiple DNA repair pathways by sub-nuclear damage induction methods. *J. Cell Sci.* **120**: 2731-2740.
11. Fischer,E.S., A.Scrima, K.Bohm, S.Matsumoto, G.M.Lingaraju, M.Faty, T.Yasuda, S.Cavadini, M.Wakasugi, F.Hanaoka, S.Iwai, H.Gut, K.Sugasawa, and N.H.Thoma. 2011. The Molecular Basis of CRL4(DDB2/CSA) Ubiquitin Ligase Architecture, Targeting, and Activation. *Cell* **147**: 1024-1039.
12. Fitch,M.E., S.Nakajima, A.Yasui, and J.M.Ford. 2003. In vivo recruitment of XPC to UV-induced cyclobutane pyrimidine dimers by the DDB2 gene product. *J. Biol. Chem.* **278**: 46906-46910.
13. Fousteri,M., W.Vermeulen, A.A.van Zeeland, and L.H.Mullenders. 2006. Cockayne syndrome A and B proteins differentially regulate recruitment of chromatin remodeling and repair factors to stalled RNA polymerase II in vivo. *Mol. Cell* **23**: 471-482.
14. Friedberg,E.C. 2001. How nucleotide excision repair protects against cancer. *Nat. Rev. Cancer* **1**: 22-33.
15. Gagne,J.P., M.Isabelle, K.S.Lo, S.Bourassa, M.J.Hendzel, V.L.Dawson, T.M.Dawson, and G.G.Poirier. 2008. Proteome-wide identification of poly(ADP-ribose) binding proteins and poly(ADP-ribose)-associated protein complexes. *Nucleic Acids Res.* **36**: 6959-6976.
16. Gillet,L.C. and O.D.Scharer. 2006. Molecular mechanisms of mammalian global genome nucleotide excision repair. *Chem. Rev.* **106**: 253-276.
17. Gottschalk,A.J., G.Timinszky, S.E.Kong, J.Jin, Y.Cai, S.K.Swanson, M.P.Washburn, L.Florens, A.G.Ladurner, J.W.Conaway, and R.C.Conaway. 2009. Poly(ADP-ribosyl)ation directs recruitment and activation of an ATP-dependent chromatin remodeler. *Proc. Natl. Acad. Sci. U. S. A* **106**: 13770-13774.
18. Groisman,R., J.Polanowska, I.Kuraoka, J.Sawada, M.Saijo, R.Drapkin, A.F.Kisselev, K.Tanaka, and Y.Nakatani. 2003. The ubiquitin ligase activity in the DDB2 and CSA complexes is differentially regulated by the COP9 signalosome in response to DNA damage. *Cell* **113**: 357-367.
19. Hassa,P.O., C.Buerki, C.Lombardi, R.Imhof, and M.O.Hottiger. 2003. Transcriptional coactivation of nuclear factor-kappaB-

dependent gene expression by p300 is regulated by poly[ADP]-ribose polymerase-1. *J. Biol. Chem.* **278**: 45145-45153.

20. Houtsmuller,A.B. and W.Vermeulen. 2001. Macromolecular dynamics in living cell nuclei revealed by fluorescence redistribution after photobleaching. *Histochem. Cell Biol.* **115**: 13-21.
21. Hwang,B.J., J.M.Ford, P.C.Hanawalt, and G.Chu. 1999. Expression of the p48 xeroderma pigmentosum gene is p53-dependent and is involved in global genomic repair. *Proc. Natl. Acad. Sci. U. S. A* **96**: 424-428.
22. Kapetanaki,M.G., J.Guerrero-Santoro, D.C.Bisi, C.L.Hsieh, V.Rapic-Otrin, and A.S.Levine. 2006. The DDB1-CUL4ADDB2 ubiquitin ligase is deficient in xeroderma pigmentosum group E and targets histone H2A at UV-damaged DNA sites. *Proc. Natl. Acad. Sci. U. S. A* **103**: 2588-2593.
23. Kim,J.K. and B.S.Choi. 1995. The solution structure of DNA duplex-decamer containing the (6-4) photoproduct of thymidylyl(3'-->5') thymidine by NMR and relaxation matrix refinement. *Eur. J. Biochem.* **228**: 849-854.
24. Krishnakumar,R. and W.L.Kraus. 2010. The PARP side of the nucleus: molecular actions, physiological outcomes, and clinical targets. *Mol. Cell* **39**: 8-24.
25. Luijsterburg,M.S., J.Goedhart, J.Moser, H.Kool, B.Geverts, A.B.Houtsmuller, L.H.Mullenders, W.Vermeulen, and R.van Driel. 2007. Dynamic in vivo interaction of DDB2 E3 ubiquitin ligase with UV-damaged DNA is independent of damage-recognition protein XPC. *J. Cell Sci.* **120**: 2706-2716.
26. Luijsterburg,M.S., M.Lindh, K.Acs, M.G.Vrouwe, A.Pines, A.H.van, L.H.Mullenders, and N.P.Dantuma. 2012. DDB2 promotes chromatin decondensation at UV-induced DNA damage. *J. Cell Biol.* **197**: 267-281.
27. Luijsterburg,M.S., B.G.von, A.M.Gourdin, A.Z.Politi, M.J.Mone, D.O.Warmerdam, J.Goedhart, W.Vermeulen, D.R.van, and T.Hofer. 2010. Stochastic and reversible assembly of a multiprotein DNA repair complex ensures accurate target site recognition and efficient repair. *J. Cell Biol.* **189**: 445-463.
28. Martin,N., K.Schwamborn, V.Schreiber, A.Werner, C.Guillier, X.D.Zhang, O.Bischof, J.S.Seeler, and A.Dejean. 2009. PARP-1 transcriptional activity is regulated by sumoylation upon heat shock. *EMBO J.* **28**: 3534-3548.
29. Martinez,E., V.B.Palhan, A.Tjernberg, E.S.Lymar, A.M.Gamper, T.K.Kundu, B.T.Chait, and R.G.Roeder. 2001. Human STAGA complex is a chromatin-acetylating transcription coactivator that interacts with pre-mRNA splicing and DNA damage-binding factors in vivo. *Mol. Cell Biol.* **21**: 6782-6795.
30. Messner,S., M.Altmeyer, H.Zhao, A.Pozivil, B.Roschitzki, P.Gehrig, D.Rutishauser, D.Huang, A.Caflisch, and M.O.Hottiger. 2010. PARP1 ADP-ribosylates lysine residues of the core histone tails. *Nucleic Acids Res.* **38**: 6350-6362.
31. Messner,S., D.Schuermann, M.Altmeyer, I.Kassner, D.Schmidt, P.Schar, S.Muller, and M.O.Hottiger. 2009. Sumoylation of poly(ADP-ribose) polymerase 1 inhibits its acetylation and restrains transcriptional coactivator function. *FASEB J.* **23**: 3978-3989.
32. Min,J.H. and N.P.Pavletich. 2007. Recognition of DNA damage by the Rad4 nucleotide excision repair protein. *Nature* **449**: 570-575.
33. Mone,M.J., M.Volker, O.Nikaido, L.H.Mullenders, A.A.van Zeeland, P.J.Verschure, E.M.Manders, and R.van Driel. 2001. Local UV-induced DNA damage in cell nuclei results in local transcription inhibition. *EMBO Rep.* **2**: 1013-1017.
34. Moser,J., H.Kool, I.Giakzidis, K.Caldecott, L.H.Mullenders, and M.I.Fousteri. 2007. Sealing of chromosomal DNA nicks during nucleotide excision repair requires XRCC1 and DNA ligase III alpha in a cell-cycle-specific manner. *Mol. Cell* **27**: 311-323.
35. Moser,J., M.Volker, H.Kool, S.Alekseev, H.Vrieling, A.Yasui, A.A.van Zeeland, and L.H.Mullenders. 2005. The UV-damaged DNA binding protein mediates efficient targeting of the nucleotide excision repair complex to UV-induced photo lesions. *DNA Repair (Amst)* **4**: 571-582.
36. Mu,D., C.H.Park, T.Matsunaga, D.S.Hsu, J.T.Reardon, and A.Sancar. 1995. Reconstitution of human DNA repair excision nuclease in a highly defined system. *J. Biol. Chem.* **270**: 2415-2418.
37. Nishi,R., S.Alekseev, C.Dinant, D.Hoogstraten, A.B.Houtsmuller, J.H.Hoeijmakers, W.Vermeulen, F.Hanaoka, and K.Sugasawa. 2009. UV-DDB-dependent regulation of nucleotide excision repair kinetics in living cells. *DNA Repair (Amst)* **8**: 767-776.
38. Overmeer,R.M., J.Moser, M.Volker, H.Kool, A.E.Tomkinson, A.A.van Zeeland, L.H.Mullenders, and M.Fousteri. 2011. Replication protein A safeguards genome integrity by controlling NER incision events. *J. Cell Biol.* **192**: 401-415.

39. Palomera-Sanchez,Z. and M.Zurita. 2011. Open, repair and close again: chromatin dynamics and the response to UV-induced DNA damage. *DNA Repair (Amst)* **10**: 119-125.
40. Pines,A., C.Backendorf, S.Alekseev, J.G.Jansen, F.R.de Gruijl, H.Vrieling, and L.H.Mullenders. 2009. Differential activity of UV-DDB in mouse keratinocytes and fibroblasts: impact on DNA repair and UV-induced skin cancer. *DNA Repair (Amst)* **8**: 153-161.
41. Rajamohan,S.B., V.B.Pillai, M.Gupta, N.R.Sundaresan, K.G.Birukov, S.Samant, M.O.Hottiger, and M.P.Gupta. 2009. SIRT1 promotes cell survival under stress by deacetylation-dependent deactivation of poly(ADP-ribose) polymerase 1. *Mol. Cell Biol.* **29**: 4116-4129.
42. Rapic,O., V, I.Kuraoka, T.Nardo, M.McLenigan, A.P.Eker, M.Stefanini, A.S.Levine, and R.D.Wood. 1998. Relationship of the xeroderma pigmentosum group E DNA repair defect to the chromatin and DNA binding proteins UV-DDB and replication protein A. *Mol. Cell Biol.* **18**: 3182-3190.
43. Rapic-Otrin,V., M.P.McLenigan, D.C.Bisi, M.Gonzalez, and A.S.Levine. 2002. Sequential binding of UV DNA damage binding factor and degradation of the p48 subunit as early events after UV irradiation. *Nucleic Acids Res.* **30**: 2588-2598.
44. Schultz,N., E.Lopez, N.Saleh-Gohari, and T.Helleday. 2003. Poly(ADP-ribose) polymerase (PARP-1) has a controlling role in homologous recombination. *Nucleic Acids Res.* **31**: 4959-4964.
45. Scrima,A., R.Konickova, B.K.Czyzewski, Y.Kawasaki, P.D.Jeffrey, R.Groisman, Y.Nakatani, S.Iwai, N.P.Pavletich, and N.H.Thoma. 2008. Structural basis of UV DNA-damage recognition by the DDB1-DDB2 complex. *Cell* **135**: 1213-1223.
46. Shiyanov,P., A.Nag, and P.Raychaudhuri. 1999. Cullin 4A associates with the UV-damaged DNA-binding protein DDB. *J. Biol. Chem.* **274**: 35309-35312.
47. Slade,D., M.S.Dunstan, E.Barkauskaite, R.Weston, P.Lafite, N.Dixon, M.Ahel, D.Leys, and I.Ahel. 2011. The structure and catalytic mechanism of a poly(ADP-ribose) glycohydrolase. *Nature* **477**: 616-620.
48. Sugasawa,K. 2010. Regulation of damage recognition in mammalian global genomic nucleotide excision repair. *Mutat. Res.* **685**: 29-37.
49. Sugasawa,K., T.Okamoto, Y.Shimizu, C.Masutani, S.Iwai, and F.Hanaoka. 2001. A multistep damage recognition mechanism for global genomic nucleotide excision repair. *Genes Dev.* **15**: 507-521.
50. Sugasawa,K., Y.Okuda, M.Saijo, R.Nishi, N.Matsuda, G.Chu, T.Mori, S.Iwai, K.Tanaka, K.Tanaka, and F.Hanaoka. 2005. UV-induced ubiquitylation of XPC protein mediated by UV-DDB-ubiquitin ligase complex. *Cell* **121**: 387-400.
51. Tang,J. and G.Chu. 2002. Xeroderma pigmentosum complementation group E and UV-damaged DNA-binding protein. *DNA Repair (Amst)* **1**: 601-616.
52. Timinszky,G., S.Till, P.O.Hassa, M.Hothorn, G.Kustatscher, B.Nijmeijer, J.Colombelli, M.Altmeyer, E.H.Stelzer, K.Scheffzek, M.O.Hottiger, and A.G.Ladurner. 2009. A macrodomain-containing histone rearranges chromatin upon sensing PARP1 activation. *Nat. Struct. Mol. Biol.* **16**: 923-929.
53. Vodenicharov,M.D., M.M.Ghodgaonkar, S.S.Halappanavar, R.G.Shah, and G.M.Shah. 2005. Mechanism of early biphasic activation of poly(ADP-ribose) polymerase-1 in response to ultraviolet B radiation. *J. Cell Sci.* **118**: 589-599.
54. Volker,M., M.J.Mone, P.Karmakar, A.van Hoffen, W.Schul, W.Vermeulen, J.H.Hoeijmakers, R.van Driel, A.A.van Zeeland, and L.H.Mullenders. 2001. Sequential assembly of the nucleotide excision repair factors in vivo. *Mol. Cell* **8**: 213-224.
55. Wang,H., L.Zhai, J.Xu, H.Y.Joo, S.Jackson, H.Erdjument-Bromage, P.Tempst, Y.Xiong, and Y.Zhang. 2006. Histone H3 and H4 ubiquitylation by the CUL4-DDB-ROC1 ubiquitin ligase facilitates cellular response to DNA damage. *Mol. Cell* **22**: 383-394.
56. Wittschieben,B.O., S.Iwai, and R.D.Wood. 2005. DDB1-DDB2 (xeroderma pigmentosum group E) protein complex recognizes a cyclobutane pyrimidine dimer, mismatches, apurinic/apyrimidinic sites, and compound lesions in DNA. *J. Biol. Chem.* **280**: 39982-39989.
57. Zotter,A., M.S.Luijsterburg, D.O.Warmerdam, S.Ibrahim, A.Nigg, W.A.van Cappellen, J.H.Hoeijmakers, D.R.van, W.Vermeulen, and A.B.Houtsmuller. 2006. Recruitment of the nucleotide excision repair endonuclease XPG to sites of UV-induced dna damage depends on functional TFIIH. *Mol. Cell Biol.* **26**: 8868-8879.

Table 1. Proteins identified in Flag immunoprecipitates material from FLAG-DDB2 expressing MRC5 cells mock treated or irradiated with 20 J/m^2 UV-C. A unique peptide is defined as a peptide, irrespective of its length, that exists only in one protein of a proteome of interest.

-UV			+UV		
Protein	**Protein Score**	**Unique peptides**	**Protein**	**Protein Score**	**Unique peptides**
DDB2	274	9	DDB2	305	13
DDB1	462	24	DDB1	263	16
PARP1	172	6	CUL4B	221	9
CUL4B	65	4	PARP1	126	6
GPS1	65	1	COPS4	103	3
CUL4A	44	1	CUL4A	83	1
			GPS1	65	1
			COPS7A	64	1

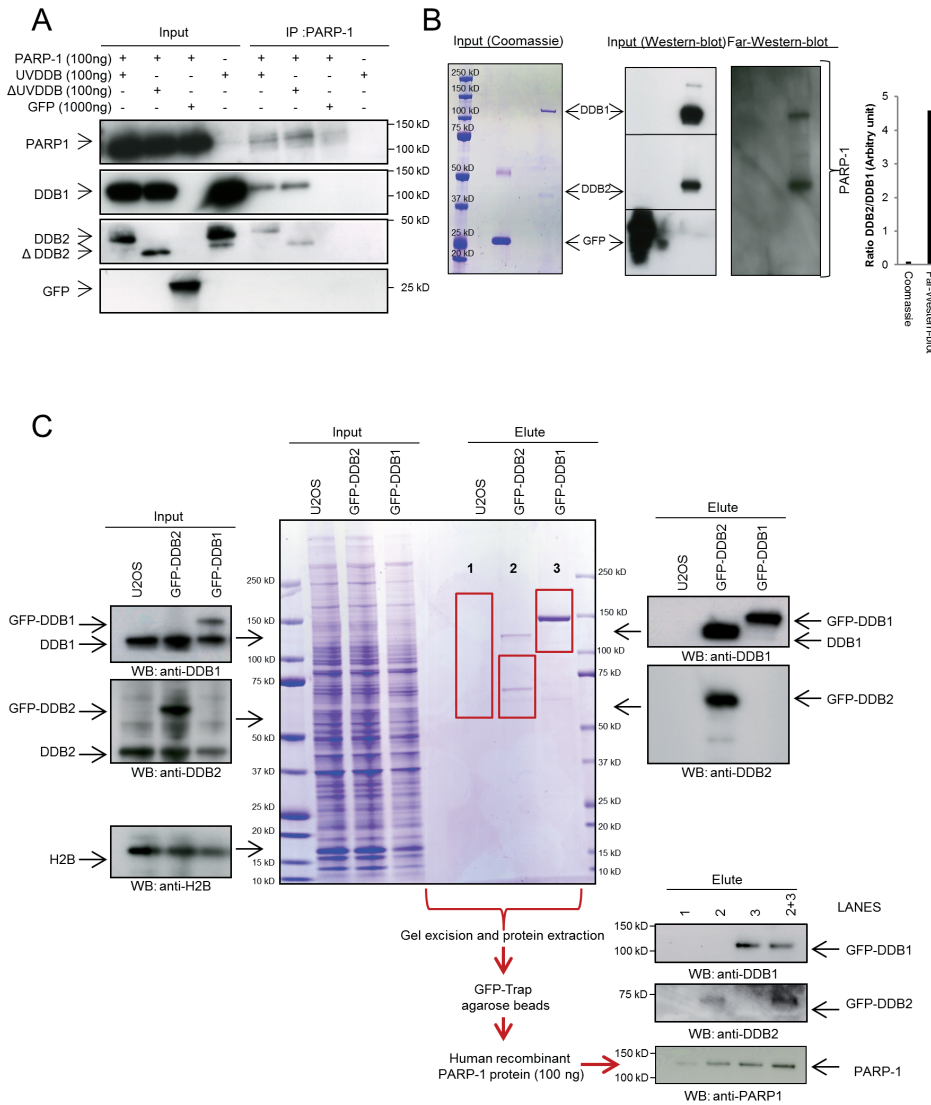

Figure 1S. **(A)** In vitro co-immunoprecipitation. UVDDB, ▪UVDDB (DDB2 lacking its first 40 N-terminal amino acids) and PARP-1 recombinant proteins were used to test direct interaction *in vitro*. GFP recombinant protein was used as negative control. **(B)** Far-western assay. UVDDB recombinant proteins were separated by SDS-PAGE, transferred to a membrane and incubated with PARP-1 recombinant protein (10 µg/ml). The PARP-1 binding was visualised by Western-blot. GFP recombinant protein was used as negative control. **(C)** GFP-DDB2-PARP-1 binding assay. U2OS cells transfected with the indicated GFP constructs were lysed in denaturing buffer and subjected to immunoprecipitation with GFP-TRAP beads. The elute was separated by SDS-PAGE and GFP-DDB1 or GFP-DDB2 were isolated from polyacrylamide gels (red square). The proteins were subjected to immunoprecipitation with GFP-TRAP beads and incubated with 100 ng purified recombinant PARP-1. The beads were processed for immunoblotting.

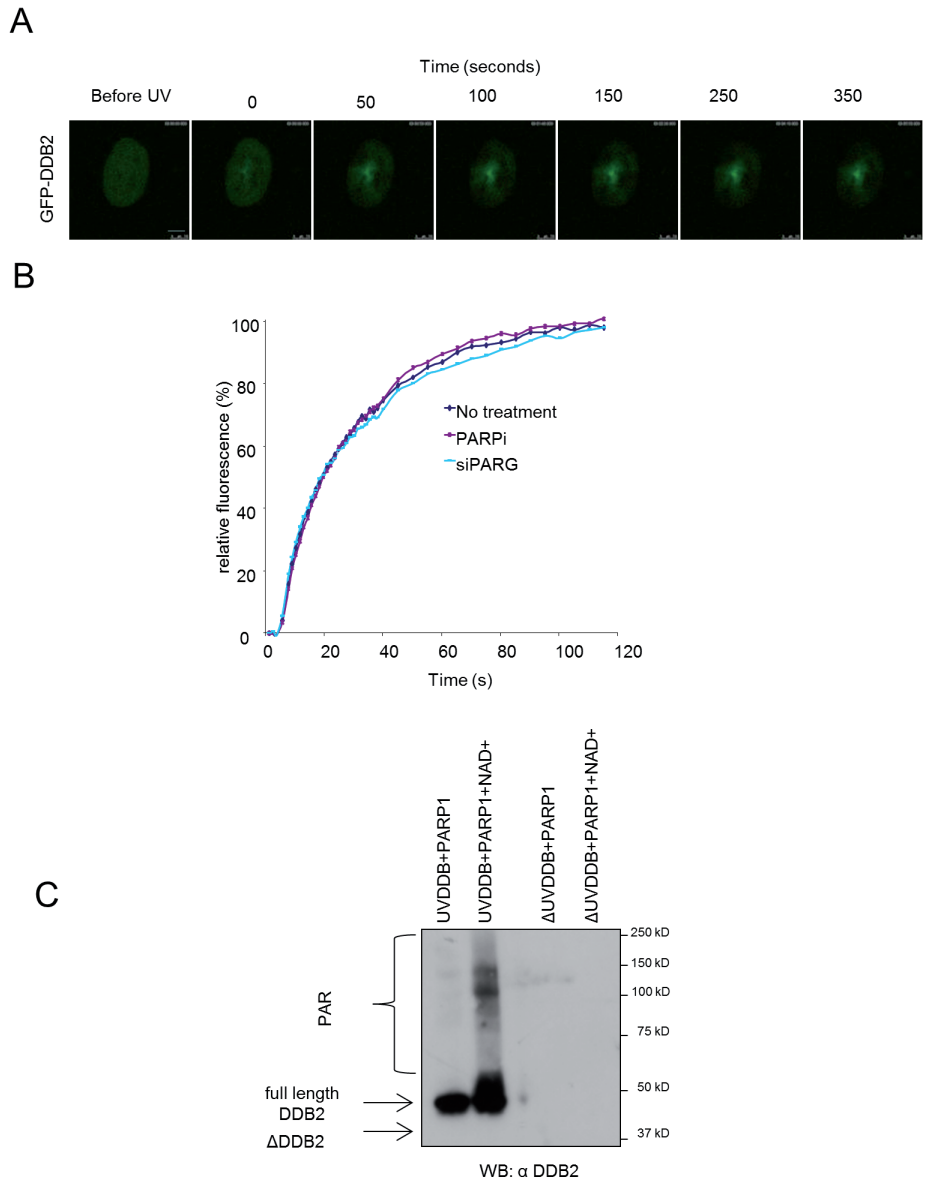

Figure 2S. **(A)** Real-time recruitment of GFP-DDB2 in NHF at the site of DNA damage using UV-C (266 nm) laser irradiation. Scale bar represent 7,5μm. **(B)** NHF cells stably expressing the GFP-DDB2 were transfected with the indicated siRNA or treated with PARPi (10μM). 48 hours after transfection the cells were UV damaged using UV-C (266 nm) laser irradiation. GFP fluorescence intensities at the site of UV damage were measured by real time imaging until they reached a maximum. Assembly kinetic curves were derived from at least six cells for each protein. Relative fluorescence was normalized at 0 (before damage) and 100% (maximum level of accumulation). Error bars indicate SEM. **(C)** *In vitro* PARylation experiments using purified components. Antibody against the N-terminal of DDB2 revealed that DDB2 is directly modified by PARP1. DDB2 lacking its first 40 N-terminal amino acids (δUV-DDB) was not detectable.

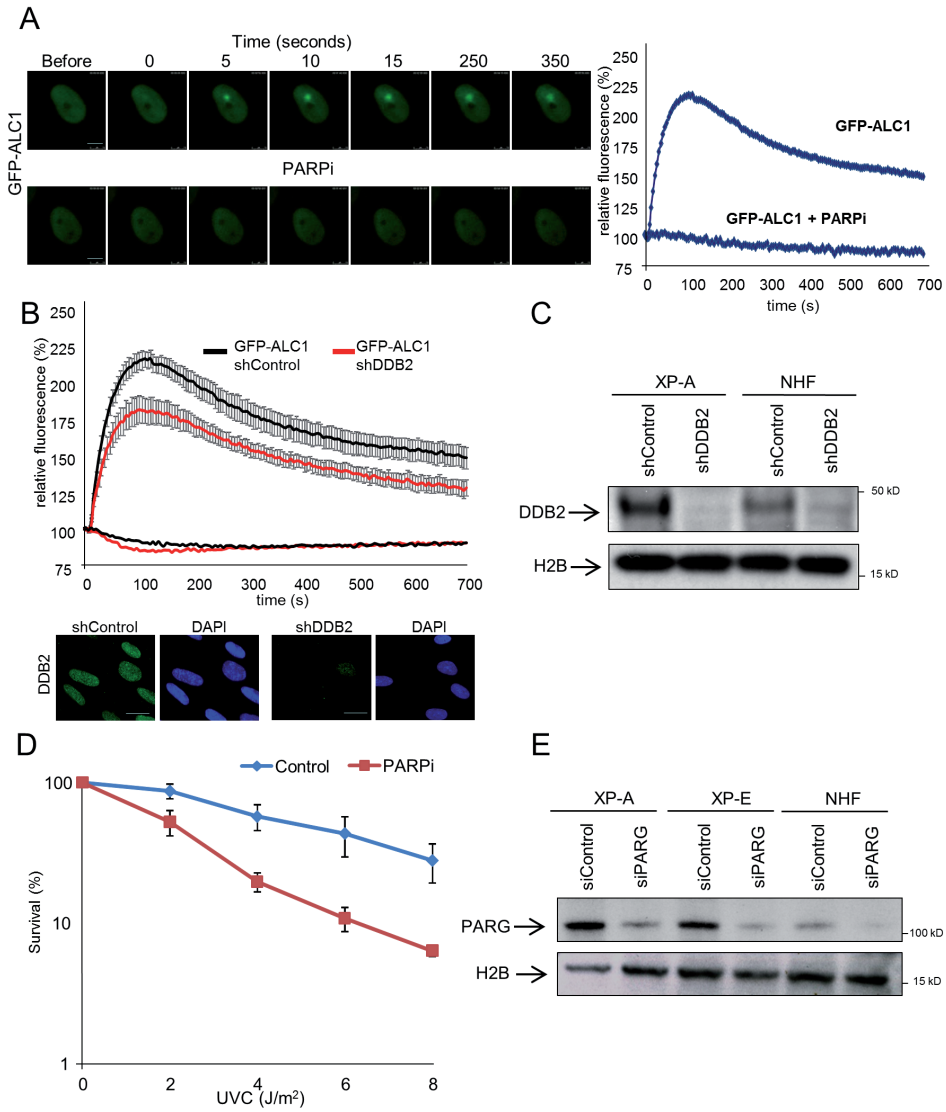

Figure 3S. **(A)** Real-time recruitment of GFP-ALC1 in NHF in presence or absence of PARPi (10μM) at the site of DNA damage using UV-C (266 nm) laser irradiation. Scale bar represent 7,5μm. **(B)** NHF cells stably expressing GFP-ALC1 were infected with the indicated short hairpin RNA. The cells were UV damaged using UV-C (266 nm) laser irradiation. GFP fluorescence intensities at the site of UV damage were measured by real time imaging until they reached a maximum. Assembly kinetic curves were derived from at least six cells for each protein. Error bars indicate SEM. Scale bar represent 20μm. **(C)** Anti-DDB2 and histone H2B western blots of total lysates from NHF and XP-A cells expressing shRNAs targeting DDB2 or a non-targeting shControl (mock). **(D)** Clonal survival of UV-irradiated NHF cells in presence or absence of PARPi (1μM). The percentage of surviving cells is plotted against the applied UV-C dose (J/m2). The results are from three independent experiments; Error bars indicate standard deviation. **(E)** Anti-PARG and histone H2B western blots of total lysates from XP-A, XP-E and NHF transfected with siRNA targeting PARG or a non-targeting siControl (mock).

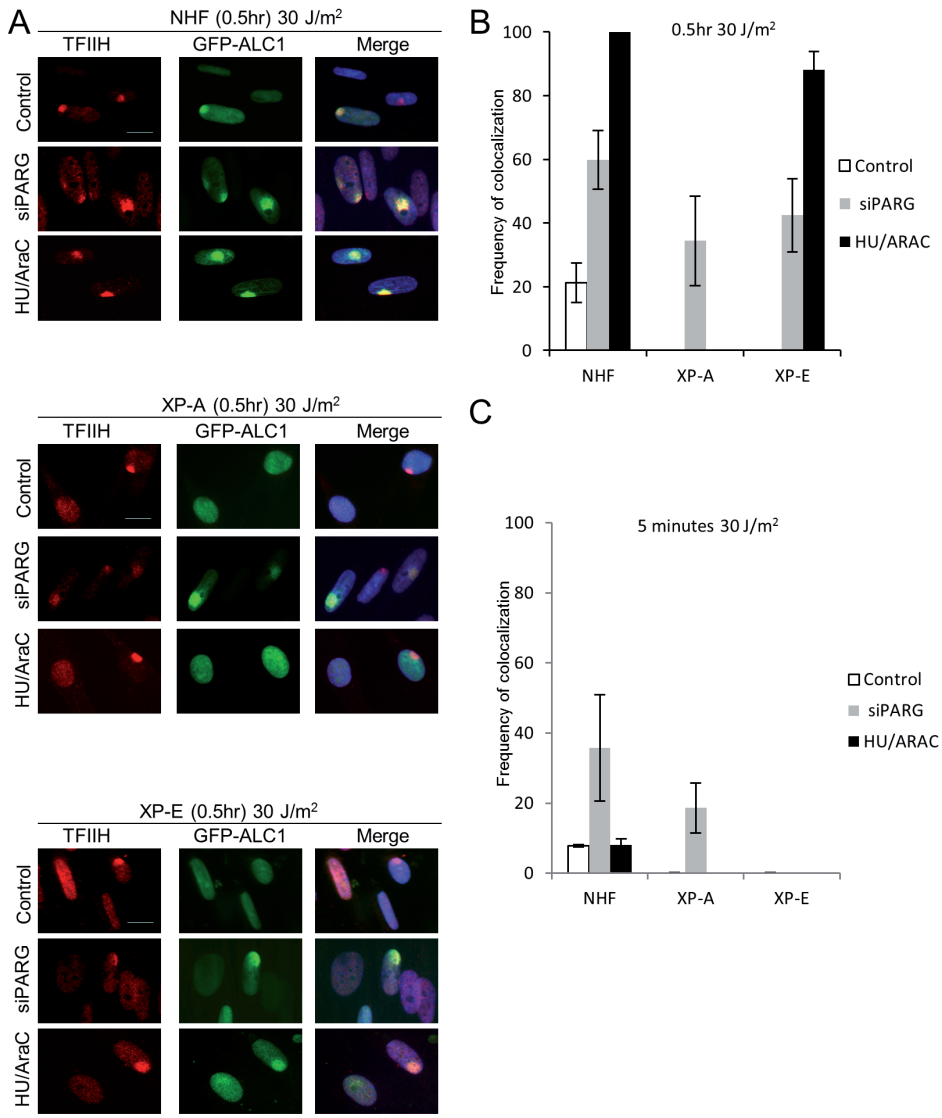

Figure 4S. **(A)** NHF, XP-E and XP-A cells stably expressing GFP-ALC1 transfected with indicated siRNA or treated with HU/AraC were locally UV exposed to 30 J/m^2, fixed after the indicated time and stained with an antibody recognizing TFIIH. Scale bars represent 20µm. **(B)** The percentage of colocalization of GFP-ALC1 with TFIIH in NHF, XP-A and XP-E cells after 0,5 hours UV local damage is plotted for the different siRNA transfections and HU/AraC treatment. The results are from three independent experiments in which about 100 cells per condition were analysed; Error bars indicate standard deviation. **(C)** The percentage of colocalization of GFP-ALC1 with TFIIH in NHF, XP-A and XP-E cells after 5 minutes UV local damage is plotted for the different siRNA transfections and HU/AraC treatment. The results are from three independent experiments in which about 100 cells per condition were analysed; Error bars indicate standard deviation. The data shown are from a single representative experiment out of three repeats.

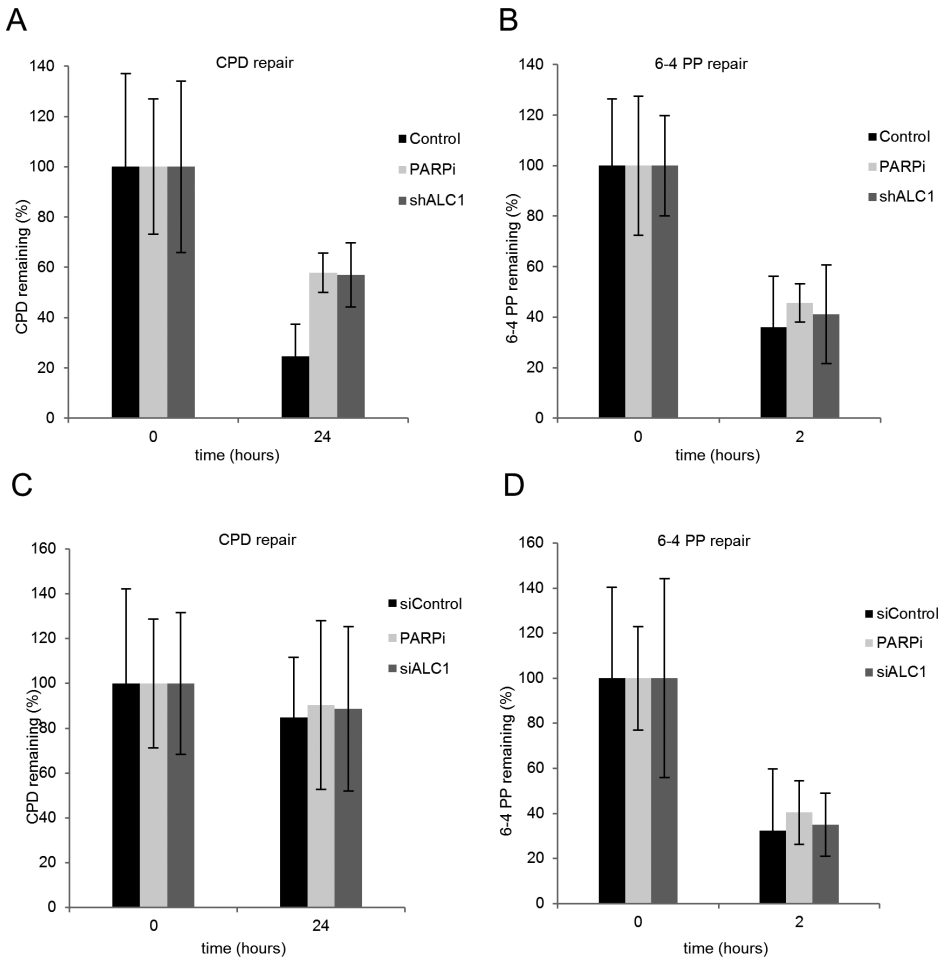

Figure 5S. (A-B) NHF cells expressing shControl or shALC1 or treated with PARPi (10μM) were irradiated with 10 J/m^2 UV-C; CPDs and 6-4 PPs were detected immediately and 24 or 2 hours respectively after UV treatment by ELISA assay. Error bars indicate standard deviation. **(C-D)** XPE cells siRNA transfected or treated with PARPi (10μM) were irradiated with 10 J/m^2 UV-C; CPDs and 6-4 PPs were detected immediately and 24 or 2 hours respectively after UV treatment by ELISA assay. Error bars indicate standard deviation. The results are from three independent experiments.

4

UV-induced DNA lesions elicit ATR-dependent signaling in non-cycling cells through NER-dependent and NER-independent pathways

Mischa G. Vrouwe, Alex Pines, Rene M. Overmeer, Katsuhiro Hanada and Leon H.F. Mullenders

Journal of Cell Science. Feb 1; 144(Pt3):435-46. 2011

ABSTRACT

Activation of signaling pathways by UV light is a key event in the DNA damage response and initiated by different cellular processes. Here we show that non-cycling nucleotide excision repair (NER) proficient cells initiate a rapid but transient activation of the damage response proteins p53 and H2AX; in contrast, repair deficient cells display delayed but persistent signaling and additionally inhibition of cell cycle progression upon release from G_0 phase. In the absence of repair, UV-induced checkpoint activation coincides with the formation of single strand DNA breaks by the action of endonuclease Ape1. Although temporally distinct, activation of checkpoint proteins in NER proficient and deficient cells depends on a common pathway involving the ATR kinase. These data reveal that damage signaling in non-dividing cells proceeds via NER dependent and independent UV photolesion processing through generation of DNA strand breaks ultimately preventing the transition from G_1 to S phase.

INTRODUCTION

Bulky DNA helix distorting lesions such as UV-induced cyclobutane pyrimidine dimers (CPD) or 6-4 photoproducts (6-4PP), will interfere with replication and transcription resulting in cell death and enhanced mutagenesis (Latonen and Laiho, 2005;Lehmann, 2000). The mammalian genome is protected against genotoxic insults by a network of DNA damage response (DDR) mechanisms initiated by sensing of DNA damage or chromatin alterations through specific sensors. The next stage in the process is to transmit the signal to transducers that are able to pass the signal to effectors that control various protective pathways i.e. DNA repair, cell cycle checkpoints, apoptosis, transcription and chromatin remodelling. To date, nucleotide excision repair (NER) pathway is the only known pathway capable of removing CPD and 6-4PP lesions from DNA in human cells. NER consists of the global genome repair pathway (GG-NER) and the transcription coupled repair pathway (TC-NER) that remove lesions throughout the genome or specifically from the transcribed strand of actively transcribed DNA respectively. Defects in GG-NER are associated with the genetic disorder xeroderma pigmentosum (XP), for which 7 disease causing genes have been identified (XP-A through XP-G). Defects in TC-NER are associated with Cockayne syndrome (CS), a disorder that is clinically distinct from XP (de Boer and Hoeijmakers, 2000).

Activation of the cell cycle checkpoints by signal transduction cascades depends on members of the phosphoinositol-3-kinase-like kinase family such as the ATM and ATR proteins. Once activated, these kinases phosphorylate downstream targets that are part of the DDR like p53 and histone H2AX. In addition, ATR and RNF-8 dependent ubiquitylation of histone H2A is an integral part of the UV-induced DDR (Bergink et al., 2006;Marteijn et al., 2009). Impaired initiation of signaling, as is the case for ATM and ATR-Seckel cells defective in ATM and ATR signaling respectively, results in impaired DNA damage induced checkpoint activation (Shiloh, 2003;Alderton et al., 2004). Although both kinases appear to have many downstream targets in common, they are activated by different events. Whereas ATM becomes activated upon the formation of DNA double strand breaks (DSBs), ATR signals after replication fork stalling. This latter signaling is thought to be mediated via the single stranded DNA binding protein complex RPA and the subsequent recruitment of ATR to these sites via its binding partner ATRIP. Although activation of the ATR pathway upon UV exposure was initially shown to occur in S phase cells, later experiments indicated this pathway also to be activated in non-dividing human fibroblasts in response to UV (O'Driscoll et al., 2003). In the G_0/G_1 phase of the cell cycle UV-induced checkpoint activation has been reported to depend on active NER (Marini et al., 2006;Marti et al., 2006;Hanasoge and Ljungman, 2007). One of the essential components in the NER pathway is the RPA complex (Araujo et al., 2000). It has been proposed that during NER RPA containing single stranded DNA gaps are formed which are substrates for the ATR/ATRIP complex thereby initiating the damage signaling (Matsumoto et al., 2007).

Recent experiments have implicated ATR in the DDR following transcription blockage through exposure to UV or transcription blocking chemicals (Jiang and Sancar, 2006;Derheimer et al., 2007). When exposed to UV, serine 15 phosphorylated p53 accumulates in normal cells and this is much more pronounced in cells that lack TC-NER

such as CS-B and XP-A cells (Ljungman et al., 2001). The ability of XPA deficient cells to promote this damage response demonstrates that this response is independent of NER induced incisions. It is conceivable that stalled RNA polymerase complexes could adopt a chromatin configuration facilitating RPA mediated activation of the ATR kinase. Indeed, alterations in the structure of chromatin have previously been proposed to initiate checkpoint signaling (Bakkenist and Kastan, 2003). However, whether UV-induced chromatin alterations can directly activate the DDR without prior processing of the UV-lesion, has not been fully resolved. Most experimental data indicate that initial lesion recognition or processing by either transcription, replication or NER is required in order to trigger checkpoint signaling by UV-light. Nevertheless, assembly of checkpoint damage sensors at non-processed UV damage sites has also been reported (Jiang and Sancar, 2006). Furthermore, experiments using Saccharomyces cerevisiae indicated that UV induced checkpoint activation can occur independent of replication or NER (Zhang et al., 2003;Giannattasio et al., 2004) initiated by breakage of DNA strands possibly due to spontaneous decay of damaged DNA (Giannattasio et al., 2004). Also, non-dividing NER deficient XP-A cells have been shown to accumulate PCNA foci late after UV irradiation by an unknown mechanism (Miura et al., 1992).

Here we investigate the DDR in non-dividing cells after UV exposure. We show that repair proficient and repair deficient cells display a distinct, but temporally different damage response after UV-C irradiation. In both normal and GG-NER deficient cells this response depends on the ATR kinase and results in activation of the G_1 checkpoint. In the absence of repair, the UV-induced checkpoint activation coincides temporally with the formation of single strand breaks as well as damage specific recruitment of the chromatin binding factors PCNA, γH2AX and TopBP1. We demonstrate that this process depends, at least in part, on the activity of Ape1. Our data supports a model of checkpoint activation in the absence of repair as a consequence of NER independent UV lesion processing that ultimately prevents the transition from G_1 to S phase.

RESULTS

Enhanced UV-induced damage signaling in quiescent fibroblasts deficient in GG-NER and TC-NER

To examine how UV-induced DNA lesions activate the DNA damage response (DDR) in non-dividing cells, we measured p53 and serine 15 phosphorylated p53 levels in normal, CSB and XPC deficient human fibroblasts following treatment with UV-C light. We checked the non-dividing state of the primary human fibroblasts after reaching confluence by BrdU or EdU labeling: the frequency of positive cells amounted less than 4% depending on the cell strain used. Two hours after exposure to 8 J/m^2 of UV, repair proficient normal human fibroblasts (NHF) displayed an induction of phosphorylated p53 (Fig. 1A), but at later time points the levels of p53 phosphorylation were reduced. In contrast, exposure of CSB deficient cells lacking functional TC-NER resulted in both phosphorylation and accumulation of p53 that was most pronounced between 8 and 72 hours after UV exposure (Fig. 1A). These data are consistent with previous reports demonstrating that both active GG-NER and persistent

transcription blockage by UV activate p53 (Ljungman et al., 2001;Yamaizumi and Sugano, 1994;Marini et al., 2006). To determine if UV lesions activate the DDR independently of GG-NER or UV-induced transcription blockage, we examined GG-NER deficient XP-C fibroblasts that repair transcribed DNA and can overcome RNA polymerase stalling. In XP-C cells the amount of phosphorylated p53 was marginally enhanced 2 hours after UV exposure, but steadily increased up to 72 hours (Fig. 1A). The increase in phosphorylation went together with an increase in the total level of p53 as well as induced expression of the G_1/S checkpoint regulator protein p21. Prolonged activation of this checkpoint cascade was also observed in XP-A cells lacking both GG-NER and TC-NER (Fig. 1A). Although both XP-A and CS-B cells efficiently accumulated p53 and p21, a reduction in protein levels was observed at 72 hours post UV. This reduction coincided with increased cell death as shown by activated caspase 3 (Fig. 1A) which is a consequence of their deficiency in TC-NER (Andera and Wasylyk, 1997;Ljungman and Zhang, 1996). No decrease in viability was observed in either normal or XP-C cells. Despite the absence of GG-NER in XP-C cells, the repair of transcribed DNA in these cells is as efficient as in normal cells (Venema et al., 1991). These results therefore suggest that non-repaired UV lesions provoke a checkpoint response independent of both NER and DNA replication.

XP-C cells are arrested in G_1 after UV

We hypothesized that the constitutive phosphorylation of p53 and the upregulation of p21 in XP-C cells after UV would impact the G_1 to S phase transition when cells are stimulated to divide. In contrast, the transient upregulation of p53 and p21 in normal repair proficient cells is expected to only temporarily delay cell cycle progression. To test this hypothesis, normal and XP-C cells were arrested in the G_0/G_1 stage of the cell cycle by serum starvation and subsequently stimulated to enter S phase by reintroducing serum. Next, we analyzed the cell cycle distribution in normal and XP-C cells after different recovery periods following UV irradiation or mock treatment (Fig. 1B). Mock treated normal and XP-C cells enter S phase 15 hours after release from the low serum block. When cells were UV-irradiated at the G_1/S transition, both normal and XP-C cell populations showed a significant fraction of cells progressing into S phase despite the presence of UV-photolesions (Fig. 1C and supplementary figure S6). UV irradiation of normal human cells just prior to serum block removal, resulted in a reduced progression into S phase when compared to cells exposed just before S phase entry. This was unexpected, as normal cells will repair a large fraction of the UV-photolesions during the intervening 15 hours. The reduced S phase entry therefore most likely reflects the transient upregulation of checkpoint proteins in normal cells. Extended incubation of normal human cells in G_0 after UV exposure reduces the level of phosphorylated p53 and p21 and lead to unperturbed entry of normal cells into S phase (Fig. 1C). XP-C cells, however, were strongly arrested in G_1, when irradiated just prior to serum block removal, with only few cells reaching S phase. Moreover, the impaired S phase entry could not be alleviated by allowing the cells more time to recover after UV exposure (Fig. 1C), demonstrating that S phase entry of XP-C cells was persistently restricted following UV exposure. This cell cycle block coincided with the extended induction of the checkpoint proteins p53 and p21 in XP-C cells as shown in Fig 1A.

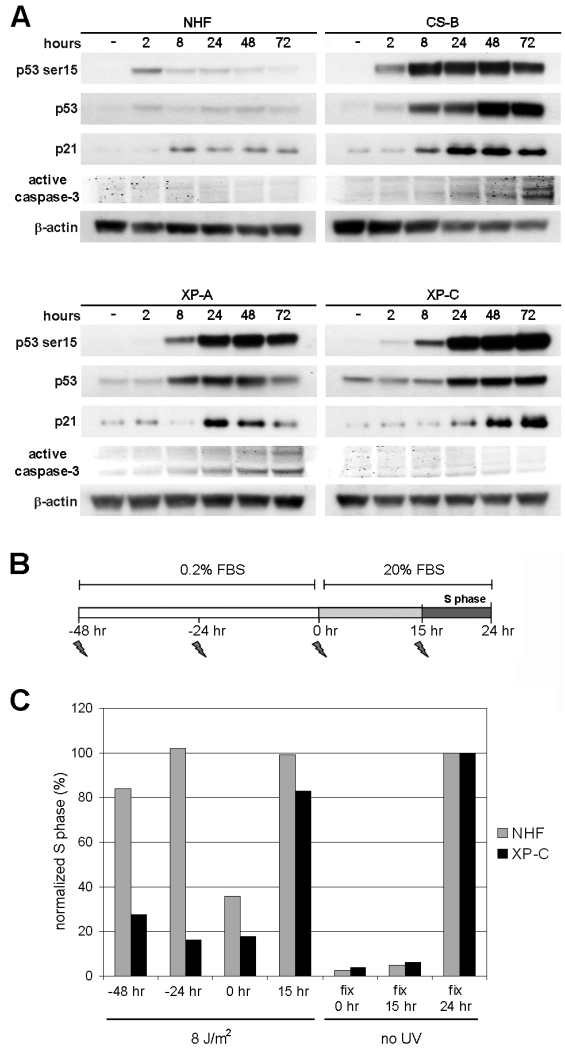

Figure 1: The p53 signaling pathway is activated in confluent fibroblasts deficient in GG-NER, TC-NER or both subpathways. (A) Confluent normal human fibroblasts (NHF), CS-B, XP-A and XP-C fibroblasts were exposed to 8 J/m^2 UV-C and analyzed 2, 8, 24, 48 and 72 hours later with the indicated antibodies. The lane denoted with minus (-) sign indicates unexposed sample. **(B)** Schematic overview of the experiment design for flow cytometry. Confluent NHF and XP-C cells were maintained in G_0 by low serum (0.2% FBS). At various times samples were irradiated with 8 J/m^2, as indicated by lightning bolts. At time 0 hr medium containing 20% FBS and EdU was added to all samples with the exception of the G_0 control. At times 0 hr and 15 hr mock irradiated samples (fix 0 hr, fix 15 hr) were fixed to validate the absence of S phase cells. All UV exposed samples, as well as an unexposed control (fix 24 hr) were collected at time 24 hr. **(C)** XP-C cells are blocked in G_1 after UV exposure. Bar graph indicating the progression from G_0/G_1 to S phase relative to the unexposed control NHF and XP-C cells (fix 24 hr) as determined by EdU incorporation. Values were normalized by setting the S phase population in unexposed cells to 100%. The percentage of S phase cells (not normalized) in unexposed NHF and XP-C samples (fix 24 hr) was 67% and 34% respectively.

Persistent phosphorylation of histone H2AX in UV-irradiated GG-NER deficient cells

Activation of the cell cycle checkpoints by signal transduction cascades depends on members of the phosphoinositol-3-kinase-like kinase family such as the ATM and ATR proteins. Once activated, these kinases phosphorylate downstream targets that are part of the DDR like p53 and histone H2AX. In repair proficient human cells histone H2AX is phosphorylated following the formation of DSBs and during apoptosis, but also after UV exposure of both dividing and stationary cells (Marti et al., 2006;Ward and Chen, 2001). We locally UV-irradiated quiescent repair proficient and deficient fibroblasts to examine phosphorylation of H2AX. Shortly after local UV irradiation repair proficient human cells displayed H2AX phosphorylation (γH2AX) at the UV spots, but this phosphorylation disappeared in time (Fig. 2A) most likely due to excision of UV photoproducts. This rapid phosphorylation was absent in XPA and XPC deficient cells, however, γH2AX became clearly visible in local UV-spots at later time points (24 and 48 hours). At these late time points the frequency of colocalization of UV spots (CPD) with γH2AX (Fig. 2B) in XP-A and XP-C cells was 98% or more. Similar results (Fig. 2C) were obtained with NER deficient primary mouse dermal fibroblasts derived from *XPA*$^{-/-}$ knock out mice (Nakane et al., 1995;de Vries et al., 1995) although the γH2AX signal was lower at 1.5 hours after UV relative to human cells, possibly due to low DDB2 expression in mouse cells (Pines et al., 2009). Together these data provide evidence for the existence of an additional DNA damage signaling route independent of stalled replication forks or active NER (Marini et al., 2006;Marti et al., 2006;Ward and Chen, 2001).

To check whether delayed phosphorylation of H2AX is a general feature of cells lacking functional NER proteins, we quantified the amount of immunostained γH2AX. In normal human cells H2AX became phosphorylated within 90 minutes following UV exposure (8 J/m^2) and returned to control level within 24 hours (Fig. 2D and supplementary fig. S1). Similar to normal cells, XP-E cells (proficient for TC-NER but defective in GG-NER of CPD) (Hwang et al., 1999) and CS-B cells are capable of forming γH2AX within 90 minutes after UV (Fig. 2D), most likely reflecting their ability to efficiently remove 6-4PP. In contrast, both XP-A and XP-C cells failed to display γH2AX during the first 90 minutes post UV; instead, a strong γH2AX signal appeared in both cell strains 24 and 48 hours after UV exposure. In XP-C cells the amount of γH2AX continued to increase up to 48 hours, although at 24 hours the level of γH2AX was lower when compared to XP-A cells.

Interestingly, despite having defects in NER, neither XP-E nor CS-B cells displayed persistent H2AX phosphorylation even though the absence of a functional TC-NER pathway in CS-B cells resulted in robust activation of checkpoint proteins (Fig. 1A), (Ljungman et al., 2001). The delayed formation of γH2AX in XP-A and XP-C cells is therefore more likely a consequence of impaired GG-NER. Corroborating this, we also observed γH2AX 24 hours after UV in XP-F and XP-G cells, both of which have a defect in the GG-NER pathway (Supplementary Fig. S1).

The ATR-TopBP1 pathway is activated in both normal and GG-NER deficient cells

H2AX is a known phosphorylation target of the ATM, ATR and DNA-PK$_{cs}$ kinases. Using immunofluorescence we quantified γH2AX in normal, AT (deficient in ATM) and ATR-Seckel (deficient in ATR) cells following UV exposure. Whereas quiescent AT cells phosphorylated H2AX

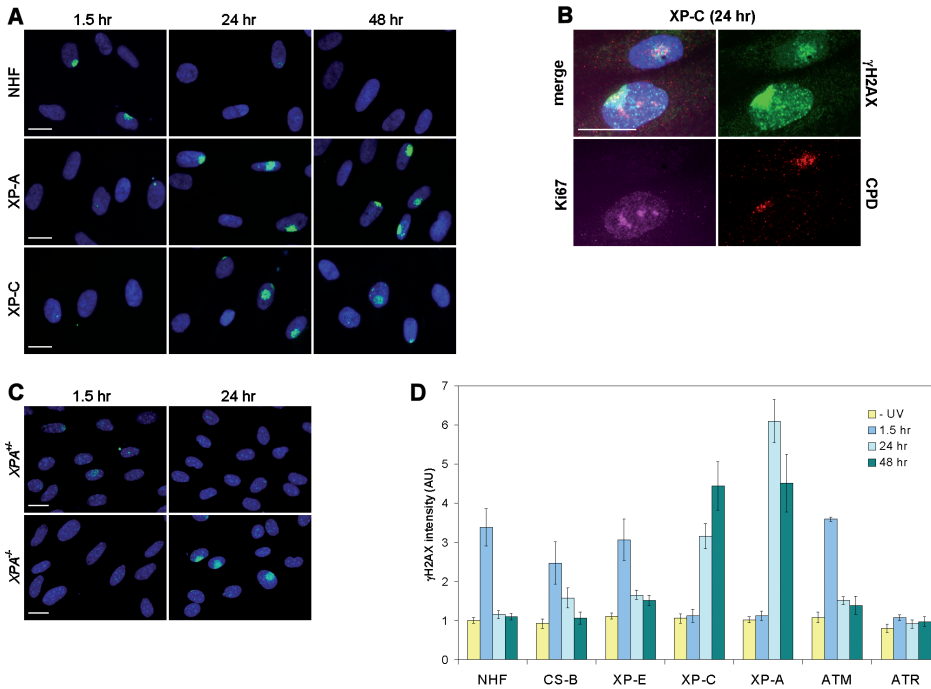

Figure 2: Histone H2AX is persistently phosphorylated in GG-NER deficient cells. (A) Confluent NHF, XP-A and XP-C fibroblasts were locally exposed to 20 J/m^2 UV-C and immunostained for γH2AX at the indicated times. **(B)** Local irradiated XP-C cells (20 J/m^2) showing co localization of γH2AX with CPD. Ki67 negative staining shows γH2AX formed in non cycling cells. **(C)** Confluent mouse *XPA*$^{+/-}$ and *XPA*$^{-/-}$ dermal fibroblasts locally exposed to 20 J/m^2 UV-C and immunostained for γH2AX at indicated times. **(D)** Confluent fibroblasts were globally irradiated with 8 J/m^2 UV-C and immunostained for γH2AX and ki67. The γH2AX signal intensity was determined for ki67 negative cells. Histograms are means of at least three independent experiments. Error bars indicate SEM.

as efficiently as normal cells upon UV, γH2AX formation was severely impaired in ATR-Seckel cells (Fig. 2D) in agreement with previous reports (Matsumoto et al., 2007;O'Driscoll et al., 2003). Next we identified the kinase responsible for delayed UV-dependent phosphorylation of H2AX in GG-NER deficient cells. Treatment of XP-C cells with the ATM kinase specific inhibitor KU55933 did not impair UV-mediated phosphorylation of H2AX (Supplementary Fig. S1). As ATR is activated after UV in NER proficient cells we tested if a similar, albeit delayed, activation occurs in NER deficient cells. siRNA mediated knockdown of ATR in normal human cells (Supplementary Fig. S1) resulted in a reduction of H2AX phosphorylation similarly to ATR-Seckel cells (Fig. 3A). Depletion of ATR in XP-C cells also resulted in a profound reduction in γH2AX levels 24 hours following UV exposure, establishing a role for ATR kinase in delayed DNA damage signaling. This conclusion is further corroborated by siRNA mediated depletion of TopBP1 (Supplementary Fig. S1), an ATR interacting protein and crucial activator of the ATR kinase during replication stress (Kumagai et al., 2006;Delacroix et al., 2007). Following

exposure to UV-light, both normal and XP-C cells treated with TopBP1 siRNA failed to phosphorylate H2AX, whereas control siRNA did not affect γH2AX formation (Fig. 3A). These data indicate that NER dependent repair of UV lesions as well as persistent non-repaired UV lesions initiate checkpoint signaling by an ATR and TopBP1 dependent pathway.

Using immunofluorescence we were unsuccessful to visualize the recruitment of ATR or its binding partner ATRIP to sites of local UV damage in either normal or XP-C cells. Possibly, low levels of target protein or insufficient affinity of antibodies prevented the detection of minor changes in protein distribution. Despite the inability to detect ATR and ATRIP, we did observe a UV dependent colocalization of TopBP1 with γH2AX in normal human cells one hour after local UV exposure (Fig. 3B). At this time point neither TopBP1 nor γH2AX spots were visible in XP-C cells. In contrast, γH2AX and TopBP1 co-localized in UV spots in XP-C cells 24 hours after treatment.

The binding of ATR and ATRIP to DNA is mediated by the single stranded DNA binding protein complex RPA (Zou and Elledge, 2003). Apart from its function in ATR checkpoint activation, RPA is a core component of NER. In both normal and XPA deficient cells RPA localized at local UV-damage within 30 minutes after irradiation, whereas no such localization was found in XP-C cells (Rademakers et al., 2003) (Fig. 3C). XP-A and XP-C cells differ in the compositions of preincision NER complexes. Whereas XP-A cells are capable to assemble an abortive preincision complex including RPA (Volker et al., 2001;Rademakers et al., 2003), XP-C cells only recruit DDB2 (Wakasugi et al., 2002). However, RPA was recruited to local UV spots in XP-C cells 24 hours after UV demonstrating a central role for RPA in UV damage signaling in both normal and GG-NER deficient cells. In spite of this, reduction of ATR activity has no impact on NER, as removal of 6-4PP lesions in ATR-Seckel cells was as efficient as in normal cells (Supplementary Fig. S2).

GG-NER deficient cells accumulate DNA breaks

The UV-dependent checkpoint response in GG-NER cells implicates a direct activation by UV lesions in chromatin, or activation as a consequence UV lesion processing. Because DNA damage mediated H2AX phosphorylation is generally associated with chromatin containing either single strand gaps or DSBs, we examined the presence of UV induced DNA breaks by the alkaline comet assay. In NER proficient cells increased DNA tailing was detected one hour after exposure to UV, indicating the presence of DNA breaks (Fig. 4A). No increased tailmoments were observed in either XP-A or XP-C cells, indicating that the breaks in normal cells represent incisions by NER. As expected, only relatively few breaks were detected in normal cells 24 hours after 8 J/m^2 of UV, when repair of UV-photolesions is almost complete. In contrast, both XP-A and XP-C cells accumulated DNA breaks 24 hours post treatment. As the alkaline comet assay detects both single as well as double stand DNA breaks, pulsed field gel electrophoresis was performed to specifically detect DSBs in UV-irradiated cells. However, this analysis revealed no clear differences between normal and XP-C cells (Supplementary Fig. S3). We note here that, due to the limited sensitivity of the assay low frequencies of DSBs will not be detected.

Upon exposure to ionizing radiation (IR) γH2AX is known to form nuclear foci that are thought to represent sites of DSBs. Comparison of the nuclear distribution of γH2AX in

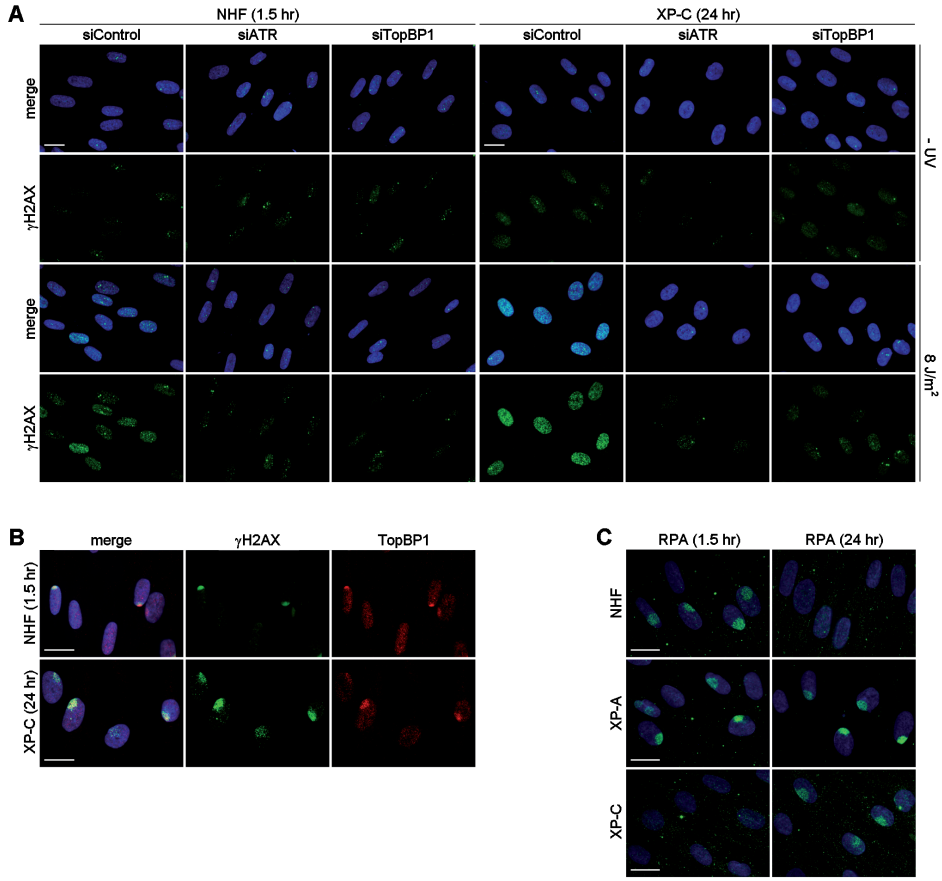

Figure 3: The ATR-TopBP1 pathway is activated in both normal and GG-NER deficient cells. (A) γH2AX formation in cells treated with control, ATR or TopBP1 siRNA and either non-exposed or irradiated with 8 J/m² UV-C. NHF and XP-C cells were immunostained 1.5 and 24 hours after exposure respectively **(B)** Immunolocalization of γH2AX and TopBP1 after local irradiation with 20 J/m². NHF and XP-C cells were stained 1.5 and 24 hours after treatment. **(C)** Immunolocalization of RPA after local exposure to 20 J/m² UV-C.

IR and UV treated normal and XP-C cells revealed a clear difference. Whereas one Gy of IR induced few but distinct large nuclear foci, UV exposure resulted in a more granular appearance of γH2AX consisting of many small and less intense nuclear foci when compared to IR induced foci (Fig. 4B). We observed no difference in morphology between γH2AX nuclear staining in normal cells 1.5 hour after UV exposure and XP-C cells 24 hours after UV exposure, consistent with the UV induced activation of the ATR/TopBP1 pathway in both normal and XP-C cells. Together these data show that upon UV exposure DNA breaks are generated in cells deficient in GG-NER. Furthermore, the comet assay, the dependence on ATR as well as the morphological appearance of the γH2AX foci all suggest that the majority of these DNA breaks are single stranded.

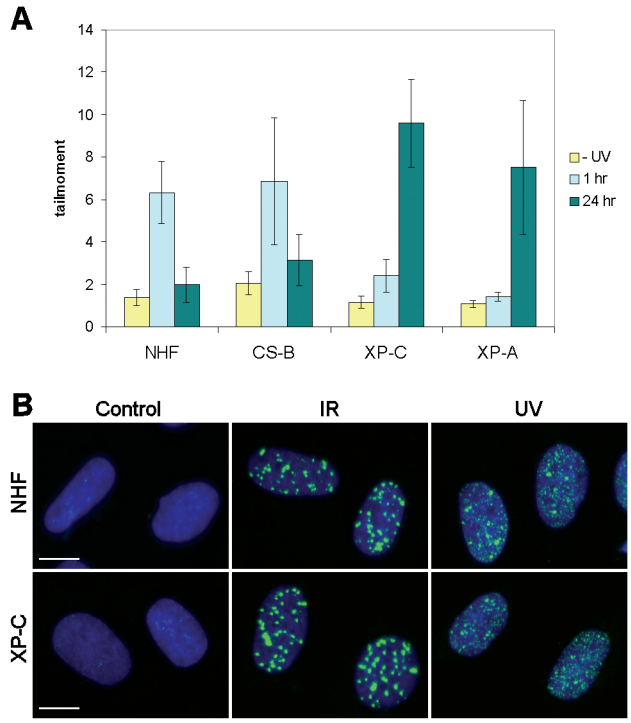

Figure 4: GG-NER deficient cells accumulate DNA breaks. (A) Stand-break induction after exposure to 8 J/m^2 UV-C measured by alkaline comet assay. Breaks were quantified as comet tailmoments. Histograms are the means of at least three independent experiments ± SEM **(B)** γH2AX formation after 1 Gy IR (0.5 hour) and UV. NHF and XP-C cells were irradiated with 8 J/m^2 UV-C and stained 1.5 hour and 24 hours later respectively.

DNA synthesis factors are recruited to UV damage in GG-NER deficient cells

To gain further insight into the mechanism leading to DNA break formation in XP-C cells we investigated the recruitment of various repair proteins to sites of UV damage. Upon replication fork stalling the DNA repair proteins RAD51, BRCA1 and FANCD2 form nuclear foci (Tibbetts et al., 2000;Pichierri and Rosselli, 2004), but non of these proteins were recruited to local UV-spots in non-dividing normal or XPC deficient cells (Supplementary Fig. 4). However, chromatin bound PCNA was recruited early after UV irradiation in normal human cells whereas PCNA binding in XP-A and XP-C cells was delayed (Fig. 5A).

PCNA is involved in NER by facilitating the loading of DNA polymerases on chromatin (Shivji et al., 1992). Indeed, concomitant with PCNA we found DNA polymerase δ (pol δ) to be recruited to local UV-spots in both normal and repair deficient cells (Fig. 5A). Unexpectedly, western blot analysis for PCNA in UV-exposed chromatin fractions revealed high molecular weight PCNA (Fig. 5B) co-migrating with ubiquitinated PCNA from UV-exposed cycling cells (Kannouche et al., 2004;Ogi et al., 2010). In S phase cells PCNA ubiquitination activates translesion synthesis (TLS) (Hoege et al., 2002). Also in quiescent repair deficient cells

we found a pronounced accumulation of the TLS polymerase η (pol η) at local UV-spots late after exposure (Fig. 5C). We note here that also in normal cells some pol η and PCNA localized at damaged DNA 24 hours after UV, particularly at high UV doses (Fig. 5C). Although we were unable to detect DNA synthesis 24 hours after UV using BrdU, consistent with previous findings (Miura et al., 1992), a low level of incorporation was detected by EdU labeling in line with the recruitment of pol δ and pol η in XP-A cells (supplementary Fig. S6).

DNA break induction in UV-irradiated XPC cells is mediated by Ape1

We focused on Ape1 as a possible candidate to incise UV irradiated chromatin of NER deficient cells. Although Ape1 is the major endonuclease in base excision repair (BER), it has also been implicated in repair of oxidatively damaged bases and exocyclic bulky DNA lesions by a process termed nucleotide incision repair (NIR) (Daviet et al., 2007;Ischenko and Saparbaev, 2002). Moreover, the observation that $XPC^{-/-}$ mice with one functional Ape1 allele displayed an increased predisposition to UVB-induced skin cancer (Cheo et al., 2000) points to a role of Ape1 in UV lesion processing. We used siRNA to deplete Ape1 to assess a potential role in the generation of DNA breaks in NER deficient cells. A limited depletion of Ape1, in the order of 50%, resulted in markedly lower levels of γH2AX and chromatin associated PCNA in UV-irradiated XP-C cells (Fig. 6A). Single cell analysis confirmed that cells expressing low amounts of Ape1 have reduced levels of γH2AX (Supplementary Fig. S5) and alkaline comets revealed significantly fewer breaks in Ape1 depleted cells when compared to non-depleted cells (Fig. 6B). To establish a direct activity of Ape1 on UV damaged DNA we performed an in vitro endonuclease activity assay using purified Ape1 protein. As shown in Fig. 6C, Ape1 incised an oligonucleotide containing a single 6-4PP albeit with low efficiency, whereas an identical non-damaged oligonucleotide remained uncut. The incised fragment was identical in size as the UVDE cut 6-4PP oligonucleotide, indicating that Ape1 incises, primarily, directly 5' of the lesion. Cutting of a single CPD containing oligo was very much reduced when compared to an oligo harboring a 6-4PP (Fig. 6C). These results are consistent with the finding that in vivo photoreactivation of CPD had no effect on γH2AX formation whereas photoreactivation of 6-4PP strongly reduced the γH2AX formation (Fig. 6D). Together these data demonstrate the ability of Ape1 to incise UV damaged DNA in vivo particularly at 6-4PP.

DISCUSSION

Persistent UV damage triggers the DDR in non-dividing mammalian cells

UV light provokes an ATR kinase mediated damage response initiated by stalled replication and transcription as well as repair. Although transcription arrest and GG-NER have been identified as events that elicit phosphorylation of p53 (Ljungman et al., 2001;Marini et al., 2006), these studies only addressed early events following damage induction (i.e. up to 8 hours). In this study we examined the damage response for more extended time periods. We show that also a deficiency in GG-NER is sufficient to activate the DDR in UV-irradiated non-dividing XP-C and XP-A cells. Checkpoint proteins p53 and p21 continued to accumulate in time in TC-NER proficient XP-C cells without apparent cell death consistent with other findings (McKay et al., 2000). We propose that in the absence of stalled replication and transcription, non-repaired

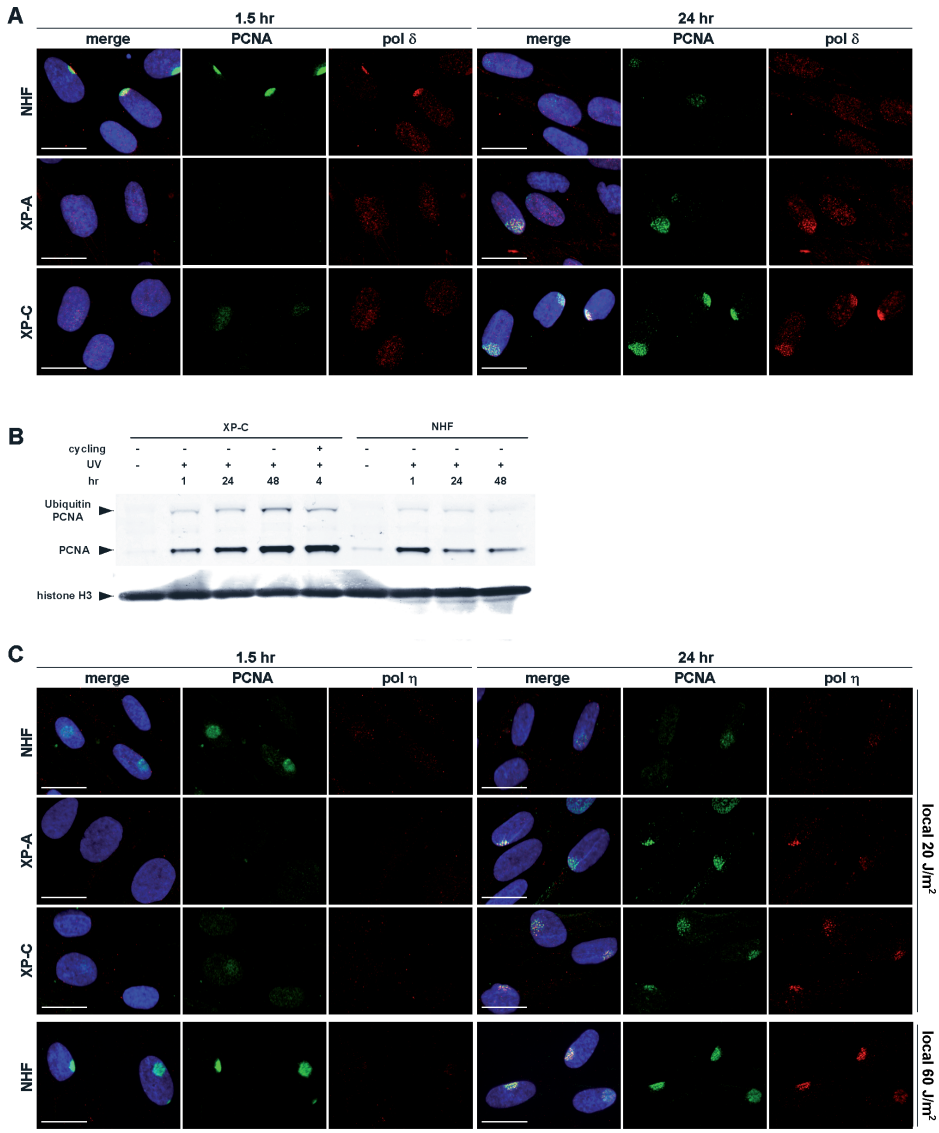

Figure 5: DNA synthesis factors are recruited to UV damage in GG-NER deficient cells. **(A)** UV dependent localization of Triton X-100 insoluble PCNA and pol δ in NHF, XP-A and XP-C cells after local exposure to 20 J/m^2 UV-C. **(B)** PCNA western blot of NHF and XP-C chromatin fractions either mock treated or exposed to 8 J/m^2 UV-C. **(C)** UV dependent localization of Triton X-100 insoluble PCNA and pol η in NHF, XP-A and XP-C cells after local exposure to 20 J/m^2 or 60 J/ m^2 UV-C.

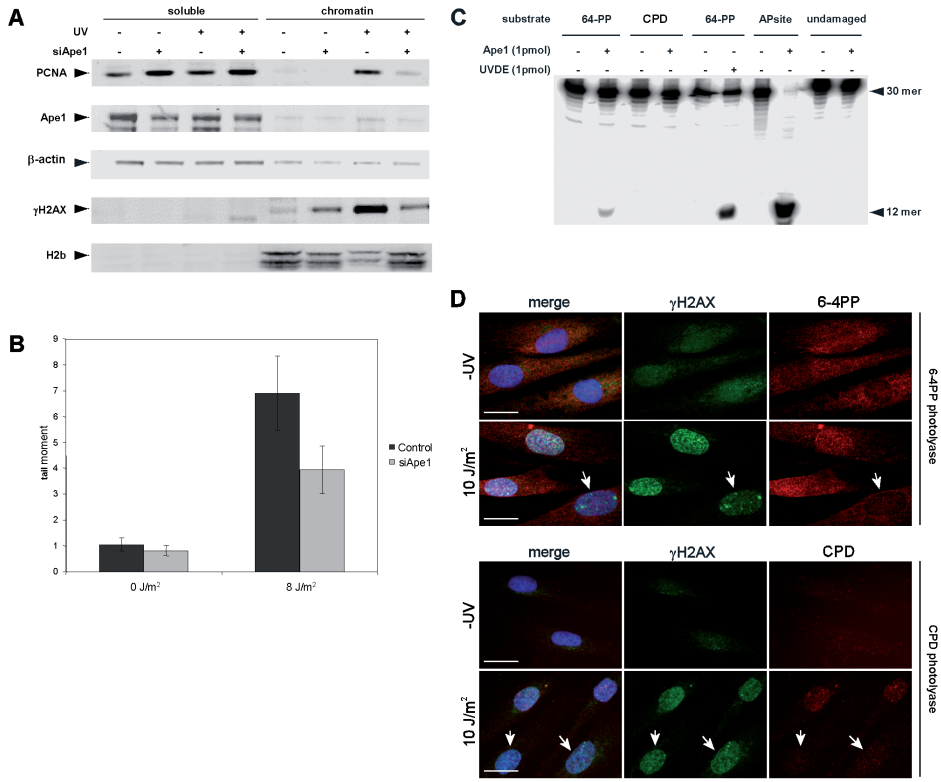

Figure 6: DNA break induction in UV-irradiated XP-C cells is mediated by Ape1. **(A)** Western blot of XP-C cells following treatment with Ape1 siRNA. Soluble and chromatin fractions were obtained 24 hours after either mock treatment or exposure to 8 J/m^2 UV-C. **(B)** DNA break induction in XP-C cells either mock treated or treated with Ape1 siRNA. Alkaline comets were measured 48 hours after exposure to UV-C and are the average of four independent experiments. Statistical analysis using Student's t-Test shows P<0.046 for UV exposed cells (P<0.05 was considered significant). Error bars indicate SEM. **(C)** Endonuclease activity assay on 30 mer oligonucleotides either undamaged or with a defined 6-4PP or AP site. Samples were either mock treated or incubated with purified Ape1 or UVDE. **(D)** Confluent XP-C cells were infected with lentivirus expressing either 6-4PP photolyase (top panel) or CPD photolyase (bottom panel). Cells were irradiated with 10 J/m^2 and photoreactivated for 1 hour. 48 hours after UV cells were fixed and stained either for γH2AX and 6-4PP (top panel) or γH2AX and CPD (bottom panel). Arrows indicate cells that photoreactivated UV lesions. Approximately 10 cells were examined for both photolyases.

UV photolesions elicit an ATR dependent damage signaling response ultimately preventing G_0/G_1 cells to enter S phase upon proliferation stimulus. It is very unlikely that the dominant mechanism to activate ATR in nondividing XP-A and XP-C cells is the direct recognition of UV lesions by checkpoint proteins. Based on in vitro experiments Choi et al (Choi et al., 2007) suggested that ATR in the presence of TopBP1 is capable to phosphorylate Chk1 in the presence of DNA containing bulky base lesions such as the UV mimicking lesion N-acetoxy-acetylaminofluorene adduct. Two observations strongly argue against this mechanism:

firstly, the absence of TopBP1 localization at UV damaged DNA at early times in vivo and secondly, the slow kinetics of checkpoint activation in XP-C cells.

Single strand DNA gaps trigger the DDR

A likely explanation for the checkpoint activation is the accumulation of single strand DNA gaps in XP-C and XP-A cells despite their repair defect. Single stranded DNA coated with RPA is the archetype structure for activating the ATR kinase. RPA coated single stranded DNA gaps formed during NER provoke a signaling reaction as demonstrated by the rapid induction ATR mediated damage signaling in repair proficient cells (Matsumoto et al., 2007). Our data reveals that H2AX is also phosphorylated in GG-NER deficient human cells and in mouse *XPA*$^{-/-}$ knock out dermal fibroblasts; the latter exclude residual GG-NER to account for γH2AX formation. The ATR and TopBP1 dependent phosphorylation of H2AX in UV-irradiated cells is most likely mediated by single strand breaks given that single stranded DNA can induce H2AX phosphorylation at serine 139 (Matsumoto et al., 2007;Ward and Chen, 2001) and that kinetics of γH2AX formation mimic the slow induction of DNA strand breaks.

The role of RPA in recruiting the ATR/ATRIP signaling complex (Zou and Elledge, 2003) is exemplified by its late (24 hours) localization at UV damage in XP-C cells. Yet, binding of RPA to chromatin per se is not sufficient for ATR activation as XP-A cells very rapidly recruit RPA to UV photolesions as part of an abortive NER reaction (Rademakers et al., 2003) without instant formation of γH2AX. In XP-A cells γH2AX was only present after formation of DNA breaks (24 hours after UV), in line with reports showing that the ATR activator TopBP1 is loaded onto chromatin via the Rad9-Hus1-Rad1 (9-1-1) clamp (Delacroix et al., 2007) which in turn is loaded on recessed DNA ends (Ellison and Stillman, 2003;Zou et al., 2003;Bermudez et al., 2003;Majka and Burgers, 2003). Moreover, different compositions of abortive preincision NER complexes might affect this loading process indicated by different levels of γH2AX in XP-A and XP-C cells in spite of similar DNA break frequencies. In XP-A cells TFIIH, XPG and RPA are assembled in a preincision complex (Volker et al., 2001;Rademakers et al., 2003), whereas in XP-C cells only DDB2 is recruited (Wakasugi et al., 2002).We speculate that the preincision complex in XP-A cells facilitates a more open DNA structure that is more prone to induce late DNA damage signaling explaining the differences in H2AX phosphorylation between XPA and XPC cells at 24 hr.

In summary, DNA strand breaks activate the UV induced DDR and although we cannot exclude a role of DSBs, our data favor a key role for single stranded DNA gaps in the UV induced signaling in NER deficient cells. This conclusion is based on the presence of RPA and the ATR dependent signaling after UV, whereas the ATM kinase, activated upon DSBs, did not contribute to γH2AX formation.

Early and late UV-responses in CS-B cells are activated by different mechanisms.

Whereas the early UV response in CS-B cells is nearly indistinguishable from GG-NER proficient cells (i.e. γH2AX and SSBs were transiently detectable after UV exposure) we note that phosphorylation of p53 in CS-B cells persisted for up to 72 hours, whereas SSBs and γH2AX no longer exceeded the background level of non UV-irradiated cells. Hence, formation of ser15 phosphorylated p53 generally followed the kinetics of H2AX phosphorylation except

for CS-B cells. This is in spite of the fact that phosphorylation of p53 due to transcription stalling is mediated by ATR (Derheimer et al., 2007). The absence of breaks suggests that p53 phosphorylation is mediated by a different mechanism possibly independent of the 9-1-1 clamp and TopBP1 or, alternatively, phosphorylated p53 in CS-B cells might represent a stable form of p53, resistant to degradation and dephosphorylation during this time course.

Persistent 6-4PP provoke the formation of single strand gaps and trigger the DDR.

The kinetics of H2AX phosphorylation in XP-E cells lacking functional DDB2 (Hwang et al., 1999) mimicked the kinetics of repair proficient normal human cells despite their deficient CPD repair. Likewise, wildtype mouse dermal fibroblasts that lack significant repair of CPDs due to much reduced expression of DDB2 (Tan and Chu, 2002;Itoh et al., 2004;Pines et al., 2009) do not display late γH2AX phosphorylation, whereas $XPA^{-/-}$ mouse dermal fibroblasts displayed H2AX phosphorylation. Photoreactivation of 6-4PP in UV irradiated human XP-C cells abolished H2AX phosphorylation, whereas photoreactivation of CPD had no effect. We conclude, that the late appearance of γH2AX in NER deficient cells is primarily caused by non-repaired 6-4PP.

APE1 initiates a DDR in non-dividing repair deficient cells.

In vitro Ape1 is capable of incising 5' of a defined 6-4PP and to much lesser extent CPD suggesting that Ape1 might incise UV-irradiated chromosomal DNA in vivo and induce DNA breaks in repair deficient cells. Consistently, UV irradiation of Ape1 depleted XP-C cells lead to reduced levels of DNA breaks, γH2AX and chromatin associated PCNA through a mechanism divergent from oxidative DNA damage repair (Jiang et al., 2008;Vasko et al., 2005). Ape1 participates in base excision repair as the major endonuclease, cleaving 5' of abasic sites. Although this is considered to be its dominant function, Ape1 has also been implicated in the processing of oxidatively damaged bases by nucleotide incision repair (NIR), a process in which Ape1 removes aberrant nucleotides without prior removal of the damaged base (Daviet et al., 2007;Ischenko and Saparbaev, 2002). In addition, Ape1 mediated cleavage of exocyclic bulky adduct containing DNA has also been demonstrated (Hang et al., 1996). For both oxidative and exocyclic DNA lesions the endonucleolytic incision was immediately 5' of the lesion. We speculate that direct recognition of UV lesions (i.e. 6-4PP) by Ape1 leads to incision activity analogous to the Schizosaccharomyces pombe UV damage endonuclease (UVDE) (Takao et al., 1996). The UVDE protein efficiently incises UV photolesions directly 5' to the lesion, thereby facilitating repair. In addition UVDE incises abasic sites, dihydrouracil and mismatches (Goosen and Moolenaar, 2008) thus sharing the broad substrate specificity displayed by Ape1. Although these proteins are not structural homologues, the mechanism of lesion processing is similar: following the 5' incision, both Ape1 and UVDE require PCNA and the Fen1 5' to 3' exonuclease activity to subsequently remove the damaged nucleotide. Consistent with our results it has been shown that a single incision 5' to a UV lesion is sufficient for loading PCNA on DNA (Staresincic et al., 2009).

PCNA responds to UV damage in a NER and replication independent manner (Li et al., 1996;Miura et al., 1992), however, it is questionable whether this truly results in complete repair. Firstly, UV exposure of XPA deficient cells is accompanied by a very modest level of DNA synthesis only traceable by sensitive EdU labelling. Secondly, the increased levels of ubiquitinated PCNA

together with recruitment of the TLS polymerase η in UV-exposed repair deficient cells, resemble the response of S-phase cells to UV damage (Kannouche et al., 2004). Effective loading of pol η requires a stalled ubiquitinated PCNA clamp (Zhuang et al., 2008) providing a further indication that the incised DNA cannot be readily repaired. Furthermore, ubiquitination of PCNA depends on RPA coated single stranded DNA (Davies et al., 2008). The accumulation of RPA containing repair intermediates supports our hypothesis that UV lesion processing activates the ATR checkpoint kinase. Further repair would require the removal of damaged nucleotides, a process that, if analogous to NIR, would depend on the 5' to 3' exonuclease activity of Fen1. However, in contrast to single oxidized bases, this step would require the removal of two covalently linked bases in the case of 6-4PP. Whether Fen1 actually engages in the process of lesion removal and is capable to remove 6-4PP remains to be determined.

Together the data suggest that Ape1 initiates processing of UV lesions by creating single stranded DNA nicks that are converted into DNA gaps; these events are unlikely to result in repair of the lesions. As a consequence DNA damage signaling, as evidenced by phosphorylation of H2AX and p53, invokes a pronounced cell cycle arrest. This underlines the importance of NER in counteracting the effects of Ape1 mediated UV lesion processing as demonstrated in mouse cancer studies. $XPC^{-/-}$ mice with one functional Ape1 allele, display an increased predisposition to UVB-induced skin cancer when compared to $XPC^{-/-}$ mice (Cheo et al., 2000). However, the Ape1 haploinsufficiency with respect to skin cancer predisposition is only manifest in the absence of functional NER. We speculate that Ape1 haploinsufficiency in the absence of GG-NER reduces the cutting of persistent photolesions and thereby activation of cell cycle checkpoints allowing damaged cells to enter S phase and accumulate mutations.

We noticed that high dose UV exposure of repair proficient human cells (when NER saturates) induces similar effects as seen in repair deficient cells, i.e. delayed recruitment of PCNA, pol η and γH2AX, indicating that retarded or incomplete repair of UV photolesions in normal cells activates the DDR as well. Human skin epidermis from healthy individuals accumulates nondividing basal cells that contain high levels of unrepaired damage (Mitchell et al., 2001). The accumulation of DNA damage might be due to differences in the expression of repair genes in these epidermal cells. In addition it is known that nondividing mammalian cells including melanocytes and keratinocytes can be stimulated to divide by external stressors such as UV-light (Cohn et al., 1984) and 12-O-tetradecanoylphorbol-13-acetate (TPA) (Nijhof et al., 2007) in the presence of DNA damage. Therefore, this newly identified pathway might be relevant for the general population as well.

MATERIAL AND METHODS

Cell culture

Fibroblasts utilized in this study: VH10 hTert (control), CS1AN hTert (CS-B), XP21RO hTert (XP-C), XP25RO hTert (XP-A), AT4BI (AT), GM01389 (XP-E) and GM18366 (ATR-Seckel). Cells were grown in DMEM supplemented with 10% fetal calf serum, penicillin and streptomycin. Three days prior to experiments medium was changed to DMEM supplemented with 0.2% serum fetal calf serum, penicillin and streptomycin.

The KU55933 ATM inhibitor was used at a final concentration of 10 μM and was a gift from Kudos Pharmaceuticals. Cells were pretreated 30 minutes before irradiation.

For the expression of photolyase, lentiviral vectors were created by Gateway recombination of 6-4PP and CPD photolyase genes into the pLenti6.3/V5-DEST vector (invitrogen). Virus was made using the ViraPower HiPerform Lentiviral Expression System (Invitrogen). Confluent cells were infected and UV irradiated three days after infection. Directly after UV cells were exposed to photoreactivating light (425 nm) for one hour. 48 hours after UV exposure cells were fixed and immunostained.

RNA interference

Short interfering RNA (siRNA) duplexes used were as follows: 5'-AACGAGACUUCUGCGGAUUGC (ATR) (Wang and Qin, 2003), 5'-UACUCCAGUCGUACCAGACUU (Ape1), smartpool siRNA targeting the TopBP1 transcript and smartpool non-targeting siRNA (Dharmacon). Cells were transfected using Hiperfect (Qiagen) according to the manufacturer's protocol. For Ape1 knockdown two sequential transfections were performed. Immunostaining and comet assay experiments were performed 48 hours after the final transfection.

Immunofluorescence and western blotting

The following antibodies have been used: mouse α-PCNA (Abcam ab29 clone number PC10), rabbit α-polη (Abcam Ab17725), rabbit α-TopBP1;(Abcam ab2402) mouse α-γH2AX (Upstate 05-636 clone JBW301); rabbit α-H2B (Upstate 07-731) mouse α-p53 (Santa Cruz Biotechnology (DO-1): sc-126), rabbit α-p21 (Santa Cruz Biotechnology (C-19): sc-397), rabbit polδ (Santa Cruz Biotechnology (H-300): sc- 10784); rabbit α-p53 ser15 (Cell Signaling Technology #9284); rabbit α-Caspase-3 (Asp175) (5A1)(Cell Signaling Technology #9664); mouse α-RPA(Calbiochem NA19L), rabbit α-ATR (Oncogene research products PC538), mouse α-actin (Sigma A3853), rabbit α-Ape1 (Novus Biologicals NB100-101), rabbit α-Rad51 was a gift from Dr. R. Kanaar; mouse α-6-4PP was a gift from Dr. O. Nikaido, Alexafluor 488 and 555 conjugated antibodies used were purchased from Invitrogen. HRP conjugated antibodies were purchased from Dako.

For local UV irradiation, the cells on coverslips were covered with an isopore polycarbonate filter with pores of 8 μm diameter (Millipore, Badford, MA) during UV irradiation with the Philips TUV lamp (Volker et al., 2001). Subsequently, the filter was removed, the medium was added back to the cells and cells were returned to culture conditions.

For fluorescent labelling the cells were fixed either immediately in 3% formaldehyde in PBS followed by 10 min 0.5% Triton X-100 or after 10 min incubation with CSK buffer (100 mM NaCl, 300 mM sucrose, 10 mM PIPES pH 6.8, 3 mM $MgCl_2$, 0.5% Triton X-100) on ice. Antibody incubations were performed at room temperature and cells were counterstained with DAPI. Images were captured with a Zeiss Axioplan2 microscope equipped with a Zeiss Axiocam MRm camera using either a Plan-NEOFLUAR 40x/1.30 or 63x/1.25 objective. For quantification of fluorescent signals the camera exposure time was set based on the signal intensity in NHF 1.5 hr after UV; moreover, the exposure time remained constant for samples within an experiment. Fluorescence intensity of randomly captured images was quantified using Zeiss Axiovision software.

EdU labelling of cells was done by addition of 10 μM EdU to the culture medium. EdU was detected using Invitrogens EdU imaging kit following the manufacturer's protocol.

The chromatin fractions for western blot were prepared by incubating cells for 10 min in CSK buffer containing protease inhibitors on ice followed by centrifugation. The pellet was resuspended in CSK buffer and sonicated.

Comet assay

Alkaline comet assay was performed as described previously (Cramers et al., 2005) with the following modifications: electrophoresis was performed for 15 min at 1 V cm^{-1}; slides were stained with SYBR Green I (Invitrogen) and automated analysis was performed using a Zeiss Axio imager.M1 with Plan-APOCHROMAT 10x/0.45 objective and Metasystems CometScan software.

Flowcytometry analysis

EdU was added to the cells 24 hours before fixation except for the 'fix 15 hr' samples which were incubated with EdU for 15 hours. Cells were collected and stained for EdU and DNA using the Click-iT EdU flow cytometry assay kit from Invitrogen according to the manufacturer's protocol. Cells were analyzed using a BD LSR II flowcytometer (BD Biosciences) using FACSDiva 5.0 software. Results were analyzed with WinMDI 2.8 software. Experiments were done twice and also with single parameter (PI) flow cytometry.

Ape1 endonuclease activity assay

The Ape1 endonuclease activity was determined by an oligonucleotide cleavage assay as described previously (Yacoub et al., 1997). Reaction mixtures (20 μl) containing the recombinant protein Ape1 (1 pmol) (Pines et al., 2005) or UVDE (1 pmol) (Moser et al., 2005), 0.040 pmol of 5'-^{32}P end- labelled double-stranded oligonucleotide, 50 mM HEPES, 50 mM KCl, 10 mM $MgCl_2$, 1 mg/ml BSA and 0.05% Triton X-100 (pH 7.5) were incubated for 5 min at 30°C. The reaction was terminated by addition of 3 μl 0.33 M EDTA, 3.3% SDS and 2.4 μl glycogen (4 μg/μl) followed by ethanol precipitation. The incision products were separated on a 20% polyacrylamide gel containing 7 M urea.

The following DNA substrates were used: 5'-CTCGTCAGCATCTTCATCATACAGTCAGTG (undamaged), 5'-CTCGTCAGCATC**TT**CATCATACAGTCAGTG (6-4PP) and 5'-CTCGTCAGCATC**–**TCATCATACAGTCAGTG (AP site), where '**TT**' or '-' indicate the position of the 6-4PP and abasic site respectively.

SUPPLEMENTARY DATA

Supplementary data is available at Journal of Cell Science Online.

ACKNOWLEDGEMENTS

The authors would like to thank Dr. N. Goosen and R. Romeijn for technical assistance, Dr. S. Iwai for the oligonucleotide substrates and Dr H. van Dam for useful discussions. This work was supported by EU projects IP-DNA repair (contract 512113) and MRTN-CT-2003-503618; ZON-MW project 912-03-012; ALW-project 805.3.42-P and ESF project ALW-855.01.074.

REFERENCE LIST

1. Alderton,G.K., H.Joenje, R.Varon, A.D.Borglum, P.A.Jeggo, and M.O'Driscoll. 2004. Seckel syndrome exhibits cellular features demonstrating defects in the ATR-signalling pathway. *Hum. Mol. Genet.* **13**: 3127-3138.
2. Andera,L. and B.Wasylyk. 1997. Transcription abnormalities potentiate apoptosis of normal human fibroblasts. *Mol. Med.* **3**: 852-863.
3. Araujo,S.J., F.Tirode, F.Coin, H.Pospiech, J.E.Syvaoja, M.Stucki, U.Hubscher, J.M.Egly, and R.D.Wood. 2000. Nucleotide excision repair of DNA with recombinant human proteins: definition of the minimal set of factors, active forms of TFIIH, and modulation by CAK. *Genes Dev.* **14**: 349-359.
4. Bakkenist,C.J. and M.B.Kastan. 2003. DNA damage activates ATM through intermolecular autophosphorylation and dimer dissociation. *Nature* **421**: 499-506.
5. Bergink,S., F.A.Salomons, D.Hoogstraten, T.A.Groothuis, W.H.de, J.Wu, L.Yuan, E.Citterio, A.B.Houtsmuller, J.Neefjes, J.H.Hoeijmakers, W.Vermeulen, and N.P.Dantuma. 2006. DNA damage triggers nucleotide excision repair-dependent monoubiquitylation of histone H2A. *Genes Dev.* **20**: 1343-1352.
6. Bermudez,V.P., L.A.Lindsey-Boltz, A.J.Cesare, Y.Maniwa, J.D.Griffith, J.Hurwitz, and A.Sancar. 2003. Loading of the human 9-1-1 checkpoint complex onto DNA by the checkpoint clamp loader hRad17-replication factor C complex in vitro. *Proc. Natl. Acad. Sci. U. S. A* **100**: 1633-1638.
7. Cheo,D.L., L.B.Meira, D.K.Burns, A.M.Reis, T.Issac, and E.C.Friedberg. 2000. Ultraviolet B radiation-induced skin cancer in mice defective in the Xpc, Trp53, and Apex (HAP1) genes: genotype-specific effects on cancer predisposition and pathology of tumors. *Cancer Res.* **60**: 1580-1584.
8. Choi,J.H., L.A.Lindsey-Boltz, and A.Sancar. 2007. Reconstitution of a human ATR-mediated checkpoint response to damaged DNA. *Proc. Natl. Acad. Sci. U. S. A* **104**: 13301-13306.
9. Cohn,S.M., B.R.Krawisz, S.L.Dresler, and M.W.Lieberman. 1984. Induction of replicative DNA synthesis in quiescent human fibroblasts by DNA damaging agents. *Proc. Natl. Acad. Sci. U. S. A* **81**: 4828-4832.
10. Cramers,P., P.Atanasova, H.Vrolijk, F.Darroudi, A.A.van Zeeland, R.Huiskamp, L.H.Mullenders, and J.C.Kleinjans. 2005. Pre-exposure to low doses: modulation of X-ray-induced dna damage and repair? *Radiat. Res.* **164**: 383-390.
11. Davies,A.A., D.Huttner, Y.Daigaku, S.Chen, and H.D.Ulrich. 2008. Activation of ubiquitin-dependent DNA damage bypass is mediated by replication protein a. *Mol. Cell* **29**: 625-636.
12. Daviet,S., S.Couve-Privat, L.Gros, K.Shinozuka, H.Ide, M.Saparbaev, and A.A.Ishchenko. 2007. Major oxidative products of cytosine are substrates for the nucleotide incision repair pathway. *DNA Repair (Amst)* **6**: 8-18.
13. de Boer,J. and J.H.Hoeijmakers. 2000. Nucleotide excision repair and human syndromes. *Carcinogenesis* **21**: 453-460.
14. de Vries,A., C.T.van Oostrom, F.M.Hofhuis, P.M.Dortant, R.J.Berg, F.R.de Gruijl, P.W.Wester, C.F.van Kreijl, P.J.Capel, H.van Steeg, and . 1995. Increased susceptibility to ultraviolet-B and carcinogens of mice lacking the DNA excision repair gene XPA. *Nature* **377**: 169-173.
15. Delacroix,S., J.M.Wagner, M.Kobayashi, K.Yamamoto, and L.M.Karnitz. 2007. The Rad9-Hus1-Rad1 (9-1-1) clamp activates checkpoint signaling via TopBP1. *Genes Dev.* **21**: 1472-1477.
16. Derheimer,F.A., H.M.O'Hagan, H.M.Krueger, S.Hanasoge, M.T.Paulsen, and M.Ljungman. 2007. RPA and ATR link transcriptional stress to p53. *Proc. Natl. Acad. Sci. U. S. A* **104**: 12778-12783.
17. Ellison,V. and B.Stillman. 2003. Biochemical characterization of DNA damage checkpoint complexes: clamp loader and clamp complexes with specificity for 5' recessed DNA. *PLoS. Biol.* **1**: E33.
18. Giannattasio,M., F.Lazzaro, W.Siede, E.Nunes, P.Plevani, and M.Muzi-Falconi. 2004. DNA decay and limited Rad53 activation after liquid holding of UV-treated nucleotide excision repair deficient S. cerevisiae cells. *DNA Repair (Amst)* **3**: 1591-1599.
19. Goosen,N. and G.F.Moolenaar. 2008. Repair of UV damage in bacteria. *DNA Repair (Amst)* **7**: 353-379.
20. Hanasoge,S. and M.Ljungman. 2007. H2AX phosphorylation after UV irradiation is triggered by DNA repair intermediates and is mediated by the ATR kinase. *Carcinogenesis* **28**: 2298-2304.

21. Hang,B., A.Chenna, H.Fraenkel-Conrat, and B.Singer. 1996. An unusual mechanism for the major human apurinic/apyrimidinic (AP) endonuclease involving 5' cleavage of DNA containing a benzene-derived exocyclic adduct in the absence of an AP site. *Proc. Natl. Acad. Sci. U. S. A* **93**: 13737-13741.
22. Hoege,C., B.Pfander, G.L.Moldovan, G.Pyrowolakis, and S.Jentsch. 2002. RAD6-dependent DNA repair is linked to modification of PCNA by ubiquitin and SUMO. *Nature* **419**: 135-141.
23. Hwang,B.J., J.M.Ford, P.C.Hanawalt, and G.Chu. 1999. Expression of the p48 xeroderma pigmentosum gene is p53-dependent and is involved in global genomic repair. *Proc. Natl. Acad. Sci. U. S. A* **96**: 424-428.
24. Ischenko,A.A. and M.K.Saparbaev. 2002. Alternative nucleotide incision repair pathway for oxidative DNA damage. *Nature* **415**: 183-187.
25. Itoh,T., D.Cado, R.Kamide, and S.Linn. 2004. DDB2 gene disruption leads to skin tumors and resistance to apoptosis after exposure to ultraviolet light but not a chemical carcinogen. *Proc. Natl. Acad. Sci. U. S. A* **101**: 2052-2057.
26. Jiang,G. and A.Sancar. 2006. Recruitment of DNA damage checkpoint proteins to damage in transcribed and nontranscribed sequences. *Mol. Cell Biol.* **26**: 39-49.
27. Jiang,Y., C.Guo, M.R.Vasko, and M.R.Kelley. 2008. Implications of apurinic/apyrimidinic endonuclease in reactive oxygen signaling response after cisplatin treatment of dorsal root ganglion neurons. *Cancer Res.* **68**: 6425-6434.
28. Kannouche,P.L., J.Wing, and A.R.Lehmann. 2004. Interaction of human DNA polymerase eta with monoubiquitinated PCNA: a possible mechanism for the polymerase switch in response to DNA damage. *Mol. Cell* **14**: 491-500.
29. Kumagai,A., J.Lee, H.Y.Yoo, and W.G.Dunphy. 2006. TopBP1 activates the ATR-ATRIP complex. *Cell* **124**: 943-955.
30. Latonen,L. and M.Laiho. 2005. Cellular UV damage responses--functions of tumor suppressor p53. *Biochim. Biophys. Acta* **1755**: 71-89.
31. Lehmann,A.R. 2000. Replication of UV-damaged DNA: new insights into links between DNA polymerases, mutagenesis and human disease. *Gene* **253**: 1-12.
32. Li,R., G.J.Hannon, D.Beach, and B.Stillman. 1996. Subcellular distribution of p21 and PCNA in normal and repair-deficient cells following DNA damage. *Curr. Biol.* **6**: 189-199.
33. Ljungman,M., H.M.O'Hagan, and M.T.Paulsen. 2001. Induction of ser15 and lys382 modifications of p53 by blockage of transcription elongation. *Oncogene* **20**: 5964-5971.
34. Ljungman,M. and F.Zhang. 1996. Blockage of RNA polymerase as a possible trigger for u.v. light-induced apoptosis. *Oncogene* **13**: 823-831.
35. Majka,J. and P.M.Burgers. 2003. Yeast Rad17/Mec3/Ddc1: a sliding clamp for the DNA damage checkpoint. *Proc. Natl. Acad. Sci. U. S. A* **100**: 2249-2254.
36. Marini,F., T.Nardo, M.Giannattasio, M.Minuzzo, M.Stefanini, P.Plevani, and M.M.Falconi. 2006. DNA nucleotide excision repair-dependent signaling to checkpoint activation. *Proc. Natl. Acad. Sci. U. S. A* **103**: 17325-17330.
37. Marteijn,J.A., S.Bekker-Jensen, N.Mailand, H.Lans, P.Schwertman, A.M.Gourdin, N.P.Dantuma, J.Lukas, and W.Vermeulen. 2009. Nucleotide excision repair-induced H2A ubiquitination is dependent on MDC1 and RNF8 and reveals a universal DNA damage response. *J. Cell Biol.* **186**: 835-847.
38. Marti,T.M., E.Hefner, L.Feeney, V.Natale, and J.E.Cleaver. 2006. H2AX phosphorylation within the G1 phase after UV irradiation depends on nucleotide excision repair and not DNA double-strand breaks. *Proc. Natl. Acad. Sci. U. S. A* **103**: 9891-9896.
39. Matsumoto,M., K.Yaginuma, A.Igarashi, M.Imura, M.Hasegawa, K.Iwabuchi, T.Date, T.Mori, K.Ishizaki, K.Yamashita, M.Inobe, and T.Matsunaga. 2007. Perturbed gap-filling synthesis in nucleotide excision repair causes histone H2AX phosphorylation in human quiescent cells. *J. Cell Sci.* **120**: 1104-1112.
40. McKay,B.C., F.Chen, C.R.Perumalswami, F.Zhang, and M.Ljungman. 2000. The tumor suppressor p53 can both stimulate and inhibit ultraviolet light-induced apoptosis. *Mol. Biol. Cell* **11**: 2543-2551.
41. Mitchell,D.L., B.Volkmer, E.W.Breitbart, M.Byrom, M.G.Lowery, and R.Greinert. 2001. Identification of a non-dividing subpopulation of mouse and human epidermal cells exhibiting high levels of persistent ultraviolet photodamage. *J. Invest Dermatol.* **117**: 590-595.

42. Miura,M., M.Domon, T.Sasaki, S.Kondo, and Y.Takasaki. 1992. Two types of proliferating cell nuclear antigen (PCNA) complex formation in quiescent normal and xeroderma pigmentosum group A fibroblasts following ultraviolet light (uv) irradiation. *Exp. Cell Res.* **201**: 541-544.

43. Moser,J., M.Volker, H.Kool, S.Alekseev, H.Vrieling, A.Yasui, A.A.van Zeeland, and L.H.Mullenders. 2005. The UV-damaged DNA binding protein mediates efficient targeting of the nucleotide excision repair complex to UV-induced photo lesions. *DNA Repair (Amst)* **4**: 571-582.

44. Nakane,H., S.Takeuchi, S.Yuba, M.Saijo, Y.Nakatsu, H.Murai, Y.Nakatsuru, T.Ishikawa, S.Hirota, Y.Kitamura, and . 1995. High incidence of ultraviolet-B-or chemical-carcinogen-induced skin tumours in mice lacking the xeroderma pigmentosum group A gene. *Nature* **377**: 165-168.

45. Nijhof,J.G., A.M.Mulder, E.N.Speksnijder, E.M.Hoogervorst, L.H.Mullenders, and F.R.de Gruijl. 2007. Growth stimulation of UV-induced DNA damage retaining epidermal basal cells gives rise to clusters of p53 overexpressing cells. *DNA Repair (Amst)* **6**: 1642-1650.

46. O'Driscoll,M., V.L.Ruiz-Perez, C.G.Woods, P.A.Jeggo, and J.A.Goodship. 2003. A splicing mutation affecting expression of ataxia-telangiectasia and Rad3-related protein (ATR) results in Seckel syndrome. *Nat. Genet.* **33**: 497-501.

47. Ogi,T., S.Limsirichaikul, R.M.Overmeer, M.Volker, K.Takenaka, R.Cloney, Y.Nakazawa, A.Niimi, Y.Miki, N.G.Jaspers, L.H.Mullenders, S.Yamashita, M.I.Fousteri, and A.R.Lehmann. 2010. Three DNA polymerases, recruited by different mechanisms, carry out NER repair synthesis in human cells. *Mol. Cell* **37**: 714-727.

48. Pichierri,P. and F.Rosselli. 2004. The DNA crosslink-induced S-phase checkpoint depends on ATR-CHK1 and ATR-NBS1-FANCD2 pathways. *EMBO J.* **23**: 1178-1187.

49. Pines,A., C.Backendorf, S.Alekseev, J.G.Jansen, F.R.de Gruijl, H.Vrieling, and L.H.Mullenders. 2009. Differential activity of UV-DDB in mouse keratinocytes and fibroblasts: impact on DNA repair and UV-induced skin cancer. *DNA Repair (Amst)* **8**: 153-161.

50. Pines,A., L.Perrone, N.Bivi, M.Romanello, G.Damante, M.Gulisano, M.R.Kelley, F.Quadrifoglio, and G.Tell. 2005. Activation of APE1/Ref-1 is dependent on reactive oxygen species generated after purinergic receptor stimulation by ATP. *Nucleic Acids Res.* **33**: 4379-4394.

51. Rademakers,S., M.Volker, D.Hoogstraten, A.L.Nigg, M.J.Mone, A.A.van Zeeland, J.H.Hoeijmakers, A.B.Houtsmuller, and W.Vermeulen. 2003. Xeroderma pigmentosum group A protein loads as a separate factor onto DNA lesions. *Mol. Cell Biol.* **23**: 5755-5767.

52. Shiloh,Y. 2003. ATM and related protein kinases: safeguarding genome integrity. *Nat. Rev. Cancer* **3**: 155-168.

53. Shivji,K.K., M.K.Kenny, and R.D.Wood. 1992. Proliferating cell nuclear antigen is required for DNA excision repair. *Cell* **69**: 367-374.

54. Staresincic,L., A.F.Fagbemi, J.H.Enzlin, A.M.Gourdin, N.Wijgers, I.Dunand-Sauthier, G.Giglia-Mari, S.G.Clarkson, W.Vermeulen, and O.D.Scharer. 2009. Coordination of dual incision and repair synthesis in human nucleotide excision repair. *EMBO J.* **28**: 1111-1120.

55. Takao,M., R.Yonemasu, K.Yamamoto, and A.Yasui. 1996. Characterization of a UV endonuclease gene from the fission yeast Schizosaccharomyces pombe and its bacterial homolog. *Nucleic Acids Res.* **24**: 1267-1271.

56. Tan,T. and G.Chu. 2002. p53 Binds and activates the xeroderma pigmentosum DDB2 gene in humans but not mice. *Mol. Cell Biol.* **22**: 3247-3254.

57. Tibbetts,R.S., D.Cortez, K.M.Brumbaugh, R.Scully, D.Livingston, S.J.Elledge, and R.T.Abraham. 2000. Functional interactions between BRCA1 and the checkpoint kinase ATR during genotoxic stress. *Genes Dev.* **14**: 2989-3002.

58. Vasko,M.R., C.Guo, and M.R.Kelley. 2005. The multifunctional DNA repair/redox enzyme Ape1/Ref-1 promotes survival of neurons after oxidative stress. *DNA Repair (Amst)* **4**: 367-379.

59. Venema,J., A.van Hoffen, V.Karcagi, A.T.Natarajan, A.A.van Zeeland, and L.H.Mullenders. 1991. Xeroderma pigmentosum complementation group C cells remove pyrimidine dimers selectively from the transcribed strand of active genes. *Mol. Cell Biol.* **11**: 4128-4134.

60. Volker,M., M.J.Mone, P.Karmakar, A.van Hoffen, W.Schul, W.Vermeulen, J.H.Hoeijmakers, R.van Driel, A.A.van Zeeland, and L.H.Mullenders. 2001.

Sequential assembly of the nucleotide excision repair factors in vivo. *Mol. Cell* **8**: 213-224.

61. Wakasugi,M., A.Kawashima, H.Morioka, S.Linn, A.Sancar, T.Mori, O.Nikaido, and T.Matsunaga. 2002. DDB accumulates at DNA damage sites immediately after UV irradiation and directly stimulates nucleotide excision repair. *J. Biol. Chem.* **277**: 1637-1640.
62. Wang,Y. and J.Qin. 2003. MSH2 and ATR form a signaling module and regulate two branches of the damage response to DNA methylation. *Proc. Natl. Acad. Sci. U. S. A* **100**: 15387-15392.
63. Ward,I.M. and J.Chen. 2001. Histone H2AX is phosphorylated in an ATR-dependent manner in response to replicational stress. *J. Biol. Chem.* **276**: 47759-47762.
64. Yacoub,A., M.R.Kelley, and W.A.Deutsch. 1997. The DNA repair activity of human redox/repair protein APE/Ref-1 is inactivated by phosphorylation. *Cancer Res.* **57**: 5457-5459.
65. Yamaizumi,M. and T.Sugano. 1994. U.v.-induced nuclear accumulation of p53 is evoked through DNA damage of actively transcribed genes independent of the cell cycle. *Oncogene* **9**: 2775-2784.
66. Zhang,H., J.Taylor, and W.Siede. 2003. Checkpoint arrest signaling in response to UV damage is independent of nucleotide excision repair in Saccharomyces cerevisiae. *J. Biol. Chem.* **278**: 9382-9387.
67. Zhuang,Z., R.E.Johnson, L.Haracska, L.Prakash, S.Prakash, and S.J.Benkovic. 2008. Regulation of polymerase exchange between Poleta and Poldelta by monoubiquitination of PCNA and the movement of DNA polymerase holoenzyme. *Proc. Natl. Acad. Sci. U. S. A* **105**: 5361-5366.
68. Zou,L. and S.J.Elledge. 2003. Sensing DNA damage through ATRIP recognition of RPA-ssDNA complexes. *Science* **300**: 1542-1548.
69. Zou,L., D.Liu, and S.J.Elledge. 2003. Replication protein A-mediated recruitment and activation of Rad17 complexes. *Proc. Natl. Acad. Sci. U. S. A* **100**: 13827-13832.

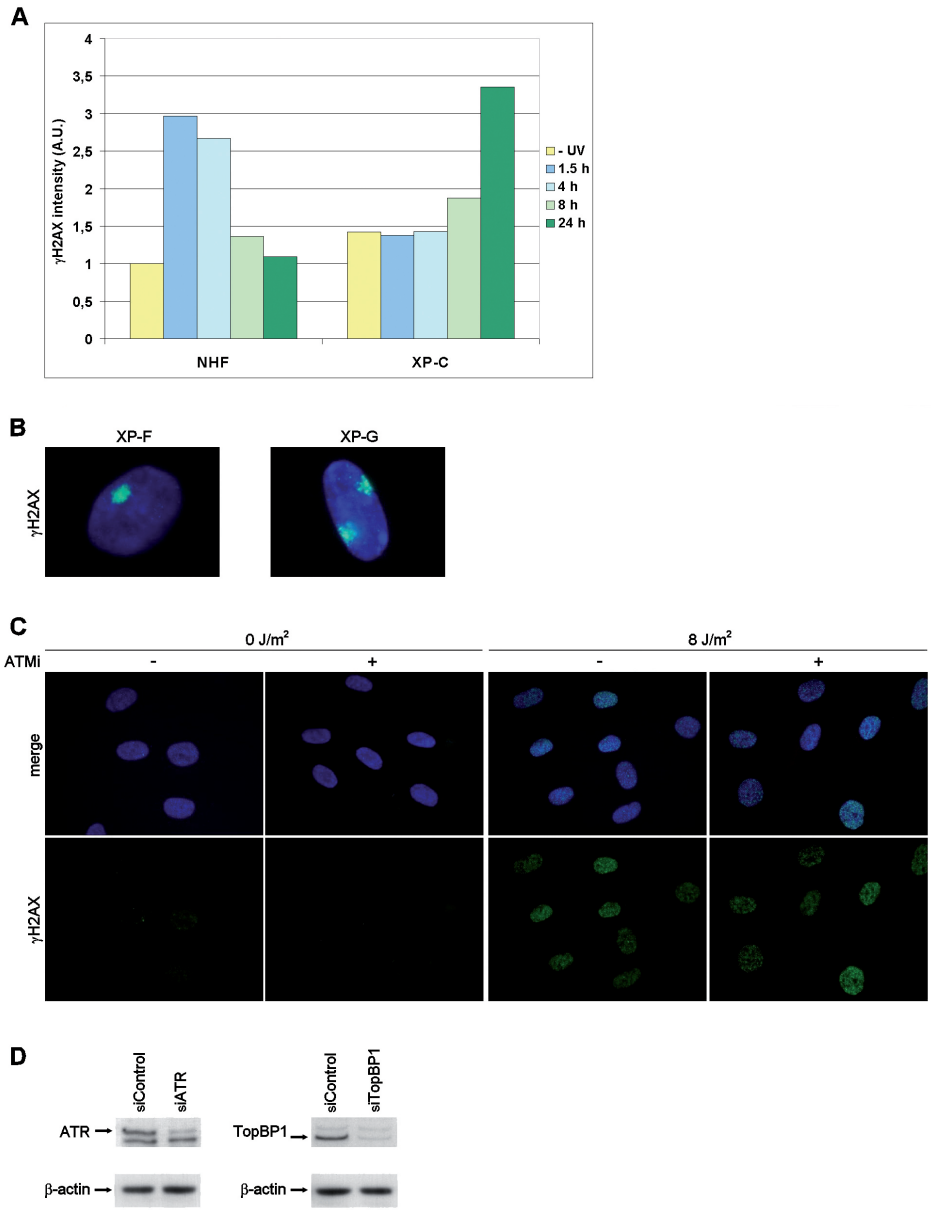

Figure S1. (A) Confluent normal and XP-C fibroblasts were globally irradiated with 8 J/m² UV-C and sampled 1.5 hrs, 4 hrs, 8 hrs and 24 hrs later. Cells were immunostained for γH2AX and ki67 and the γH2AX signal intensity was determined for ki67 negative cells. (B) γH2AX formation 24 hours after 30 J/m² local UV exposure in XP-F (XP24KY) and XP-G (XP2BI). (C) Inhibition of ATM by KU55933 in XP-C cells does not prevent γH2AX formation. ATM inhibitor or solvent was added 30 min before mock treatment or exposure to 8 J/m² UV. Cells were analyzed 16 hours after UV. (D) Western blot of XP-C cells showing siRNA-mediated knockdown of ATR and TopBP1. Knockdown levels were determined 48 hours after siRNA transfection.

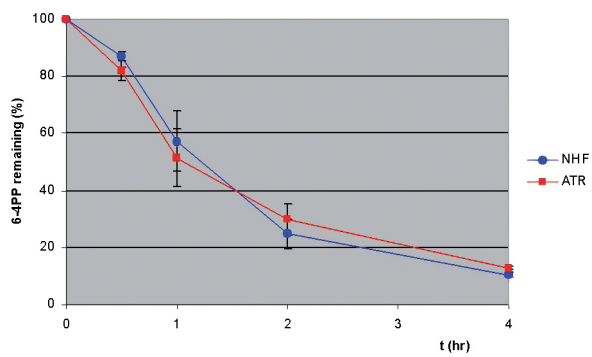

Figure S2: Impaired ATR signaling does not affect NER efficiency. Normal and ATR deficient fibroblasts were exposed to 15 J/m^2 UV-C. Cells were stained with a 6-4PP specific antibody and lesion removal was measured by quantitative immunofluorescence. Blue circles indicate normal cells; red squares indicate ATR deficient cells. Graphs represent the average of three independent experiments. Error bars represent SEM.

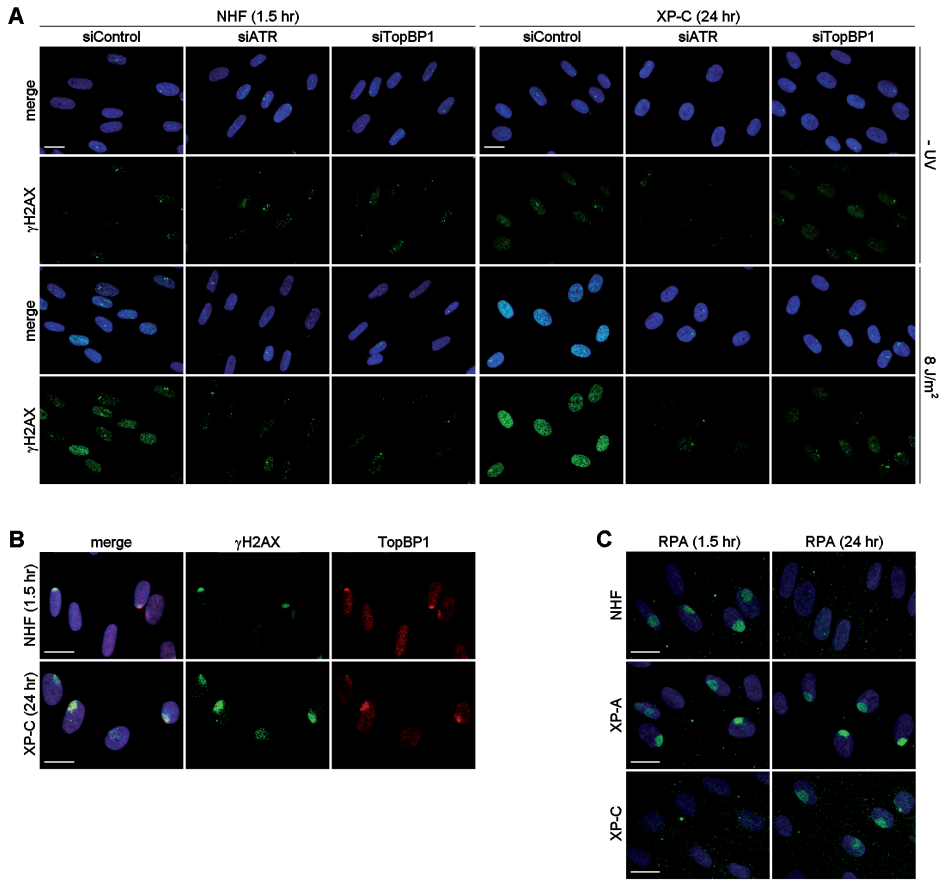

Figure S3: PFGE of normal and XP-C cells after exposure to 30 J/m² UV-C (right panel). Left panel shows X-ray treated XP-C cells as a reference. Under the electrophoresis conditions used high molecular weight genomic DNA remains in the well, while lower molecular weight DNA fragments (several Mbp to 500 kbp) are compacted into a single band (Hanada *et al.* (2007) Nat Struc Mol Biol 14:1096). The ratio of this low molecular weight (broken) DNA versus high molecular weight DNA was quantified with ethidium bromide staining using a Typhoon 9200 scanner.

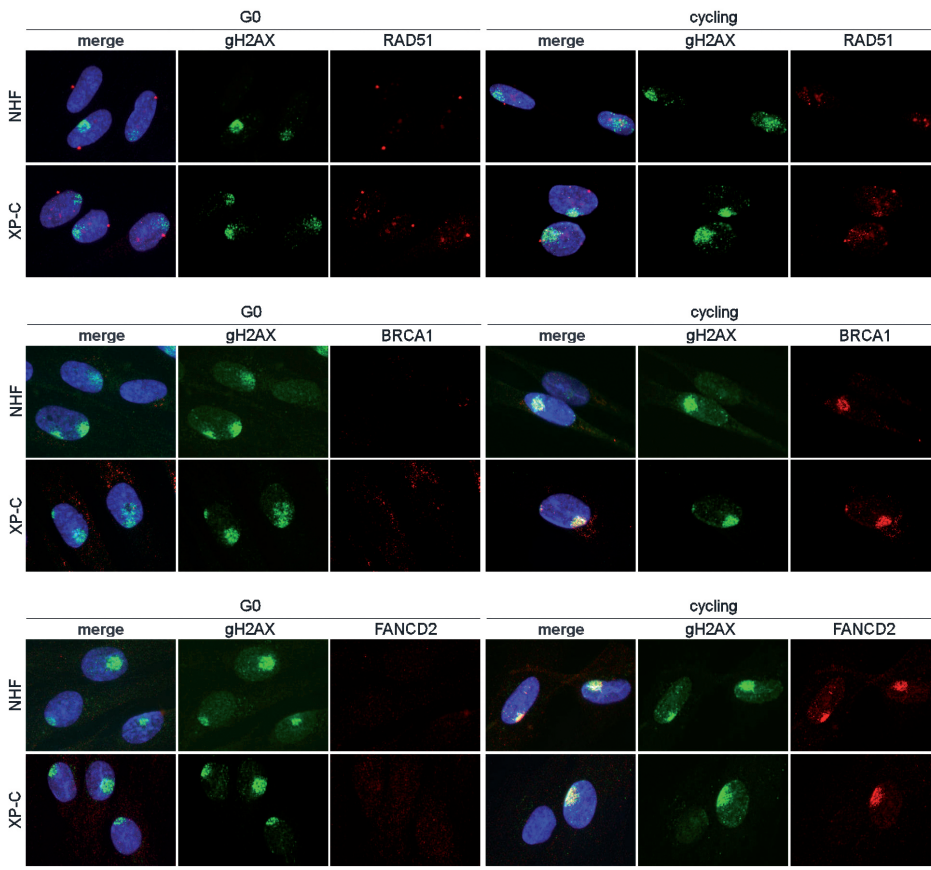

Figure S4: RAD51, BRCA1 and FANCD2 are not recruited to damaged DNA in G_0 cells. NHF and XP-C G_0 synchronized cells were locally irradiated with 20 J/m^2 and fixed 1.5 hour and 24 hours after UV respectively, non chromatin bound proteins were removed by incubation with CSK buffer. A cycling cell population was used as control and fixed 8 hours after UV. All cells were stained for γH2AX to mark the site of UV damage. Although the RAD51 staining showed some signal in non dividing cells this did not preferentially co localize with γH2AX. Also BRCA1 and FANCD2 did not co localize with γH2AX in G_0 cells.

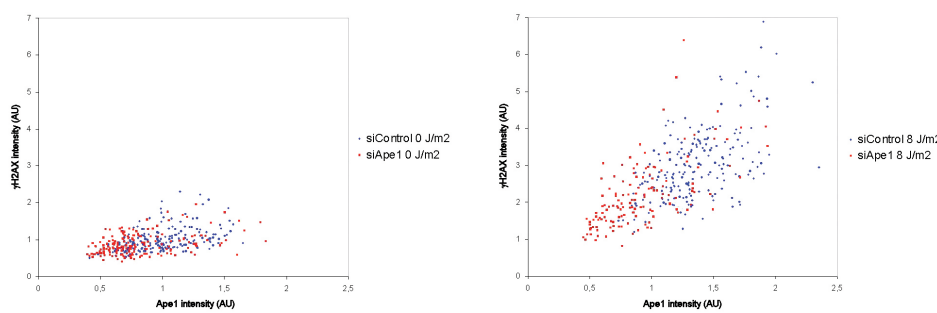

Figure S5: Ape1 depletion attenuates the formation of γH2AX after UV exposure. XP-C cells were either mock treated or treated with Ape1 siRNA prior to UV irradiation. 48 hours after 8 J/m^2 UV-C cells were stained for γH2AX and Ape1 and quantitative immunofluorescence was performed. Each dot represents a single cell measurement. Red squares indicate Ape1 siRNA treated cells; Blue circles indicate mock treated cells. Left plot represents non-exposed control; right plot represents UV exposed cells.

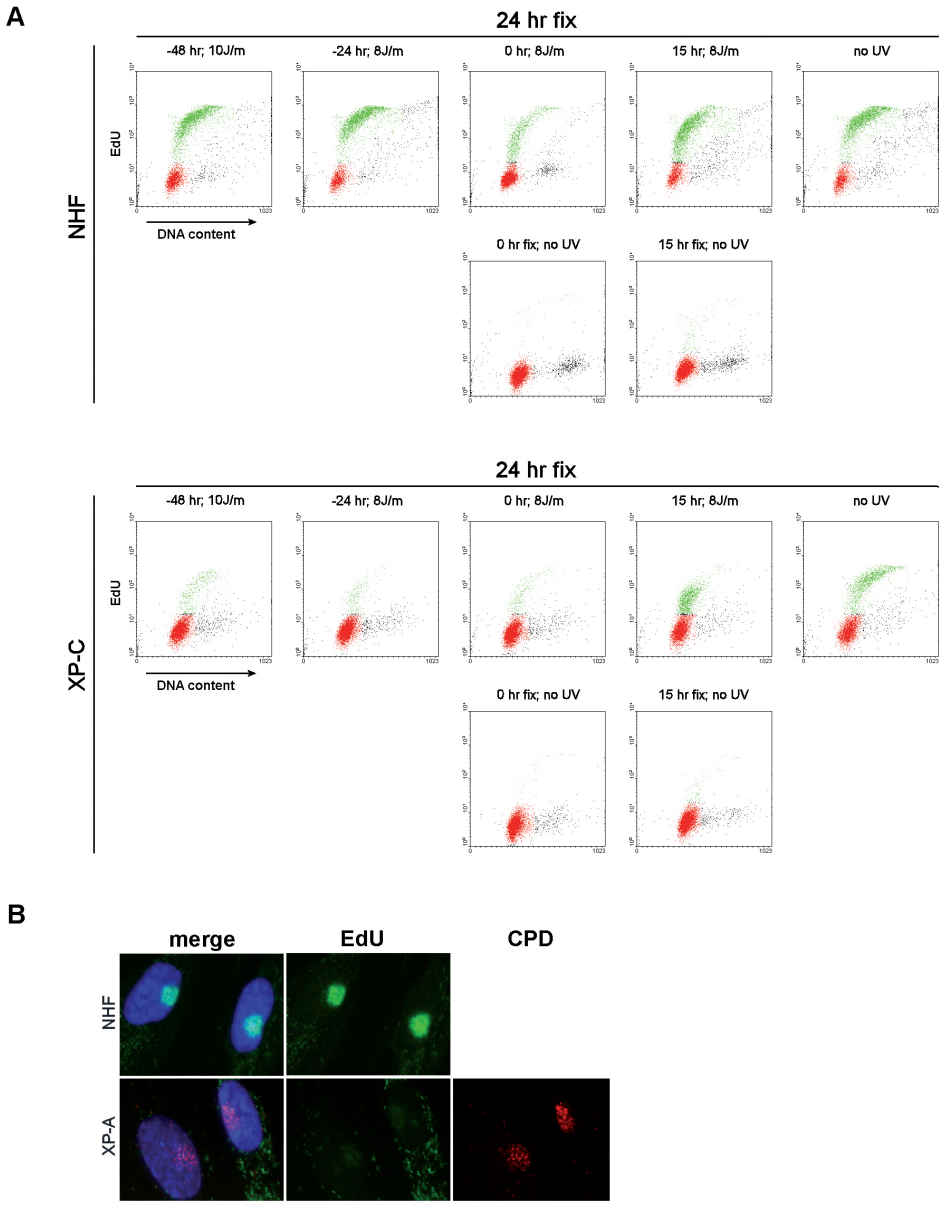

Figure S6. (A) Flowcytrometric distributions. Incorporated EdU label was detected with Alexa Fluor 488, DNA content was measured using the DNA stain 7-AAD. Red color indicates G0/G1 cells, whereas the green color indicates S phase cells. (B) Measurement of DNA repair synthesis using EdU incorporation. NHF and XP-A cells were locally irradiated with 20 J/m^2 UV and allowed to recover for 24 hours in the presence of 10 μM EdU. Cells were fixed and EdU was labeled with Alexa Fluor 488. Under these conditions DNA synthesis was readily detected in repair proficient cells. In XP-A cells we detected very low levels of EdU at UV irradiated sites (indicated by CPD staining).

5

Global phosphoproteome profiling reveals unanticipated networks responsive to cisplatin treatment of embryonic stem cells.

Alex Pines, Christian D. Kelstrup, Mischa G. Vrouwe[±], Jordi C. Puigvert[±], Dimitris Typas[±], Branislav Misovic, Anton de Groot, Louise von Stechow, Bob van de Water, Erik H.J. Danen, Harry Vrieling*, Leon H.F. Mullenders*, and Jesper V. Olsen[2]*

[±],* These authors contributed equally to this work

Molecular and Cellular Biology. Dec 31; 24:4964-77. 2011

ABSTRACT

Cellular responses to DNA damaging agents involve the activation of various DNA damage signaling and transduction pathways. Using quantitative and high-resolution tandem mass spectrometry we determined global changes in protein level and phosphorylation site profiles following treatment of SILAC labeled murine embryonic stem cells with the anticancer drug cisplatin. Network and pathway analyses indicated that processes related to the DNA damage response and cytoskeleton organization were significantly affected. Although the ATM and ATR consensus sequence (S/T-Q motif) was significantly over-represented among hyper-phosphorylated peptides, about half of the more than 2-fold up-regulated phosphorylation sites based on consensus sequence were not direct substrates of ATM and ATR. Eleven protein kinases mainly belonging to the MAPK family were identified to be regulated in their kinase domain activation loop. The biological importance of three of these kinases (CDK7, Plk1, and KPCD1) in the protection against cisplatin-induced cytotoxicity was demonstrated by siRNA mediated knockdown. Our results indicate that the cellular response to cisplatin involves a variety of kinases and phosphatases acting not only in the nucleus, but also regulating cytoplasmic targets resulting in extensive cytoskeletal rearrangements. Integration of transcriptomic and proteomic data revealed a poor correlation between changes in the relative level of transcripts and their corresponding proteins, but a large overlap in affected pathways at the level of mRNA, protein and phosphoprotein. This study provides an integrated view on pathways activated by genotoxic stress and deciphers kinases that play a pivotal role in regulating cellular processes other than the DNA damage response.

INTRODUCTION

Cancer chemotherapy drugs are designed to selectively kill cells that divide rapidly, being a main feature of most cancer cells. Cisplatin (cis-diamminedichloroplatinum (II) (CDDP) is among the most widely employed drugs in chemotherapy administered as curative treatment of several forms of cancer including ovarian, cervical, head and neck, esophagel, non-small-cell lung, and especially testicular cancer (Loehrer and Einhorn, 1984;Keys et al., 1999;Morris et al., 1999). Cisplatin binds to DNA and forms a spectrum of intra- and inter-strand DNA cross-links as well as mono adducts. These DNA adducts are thought to mediate their cytotoxic effects by interfering with transcription and replication, ultimately leading to the induction of apoptosis (Todd and Lippard, 2009). Cisplatin adducts distort the DNA duplex resulting in the exposure of the DNA minor groove to which several classes of proteins can bind, including high-mobility group (HMG) proteins and transcription factors that contribute to cisplatin induced toxicity (Wang and Lippard, 2005).

Repair of cisplatin-DNA adducts involves proteins from multiple DNA repair pathways, i.e., nucleotide excision repair (NER), homologous recombination, post-replication repair, and mismatch repair (MMR) (Wang and Lippard, 2005;Dronkert and Kanaar, 2001). NER is the major pathway responsible for the removal of cisplatin-DNA adducts *in vitro* and *in vivo* (Wang et al., 2003;Furuta et al., 2002) and hence, the marked sensitivity of testicular cancer to cisplatin has been correlated with low levels of NER proteins, i.e. XPA and ERCC1-XPF (Welsh et al., 2004). DNA damage caused by cisplatin activates several signal transduction pathways including MAPK, AKT, c-ABL, and ATM/ATR/DNA-PK dependent pathways regulating a variety of processes such as drug uptake, DNA damage signaling, cell cycle arrest, DNA repair, and cell death (Wang and Lippard, 2005).

Treatment of patients with cisplatin is compromised by the substantial risk of severe toxicity, i.e. anemia, nausea, and neurotoxicity (McWhinney et al., 2009). Tumors frequently become resistant to the drug (Oliver et al., 2010;Borst et al., 2008) and multiple resistance mechanisms have been identified, including an increased cellular efflux or a decreased cellular import of cisplatin (Safaei and Howell, 2005;Hall et al., 2008). Cisplatin resistance can also occur through enhanced DNA damage repair or increased tolerance to DNA damage (Borst et al., 2008).

Improvement of cancer therapy mediated by chemotherapeutic drug agents such as cisplatin requires better understanding of the cellular pathways underlying toxicity and drug resistance. Indeed, most of the recent advances in cancer treatment are based on drastic improvements in conceptual understanding of cellular networks. Cellular responses to DNA damage such as cisplatin-induced intra- and inter-strand DNA cross-links are controlled by a global signaling network called the DNA damage response (DDR) (Jackson and Bartek, 2009) and mediated by post-translational protein modifications (Choudhary and Mann, 2010). One of the most frequent modifications is the reversible and dynamic phosphorylation of proteins at specific serine, threonine, and tyrosine residues that control the activity of the majority of cellular processes. It has been estimated that almost 70% of all proteins in mammalian cells are phosphorylated at some point during their expression (Olsen et al., 2010). Key signalling molecules in DDR are the protein kinases

ATM (ataxia telangiectasia mutated) and ATR (ATM and Rad3-related) (Bartek and Lukas, 2007). Matsuoka and coworkers recently identified over 900 phosphorylation sites in about 700 proteins by phosphoproteome analysis of protein targeted by the ATM and ATR kinases after exposure to ionizing radiation (Matsuoka et al., 2007), however knowledge of the genome wide protein phosphorylation response to genotoxic insults is still limited. This study aimed to identify the molecular processes and cellular pathways that are affected after treatment with cisplatin one of the most commonly used chemotherapeutic drugs. To achieve these goals, we examined the cisplatin induced stress responses, changes in proteins level and global phosphorylation site profiles by quantitative phosphoproteomics. Besides activation of the DDR kinases ATM and ATR, we identified 11 other protein kinases with altered activities in response to cisplatin. We applied siRNA mediated knockdown to demonstrate that 3 kinases have important protective roles in the cellular response to cisplatin induced toxicity. Our dataset identified the cytoskeleton as a novel target of the cisplatin induced stress response. In addition, integration of transcriptome, proteome and phosphoproteome data disclosed a strong correlation in affected pathways at the levels of transcription and protein phosphorylation.

RESULTS

Cisplatin-induced stress responses

Murine embryonic stem (mES) cells were selected as the cellular model for this study since they have the unique combination of a virtually infinite lifespan with uncompromised DDR. mES cells manage to maintain their genomic integrity through robust defense mechanisms against DNA damage, including effective DNA repair and a hypersensitive apoptotic response (Tichy and Stambrook, 2008). These characteristics make mES suitable to study the molecular events that underlie the cellular responses related to cisplatin induced toxicity. To assess the kinetics of the cisplatin-induced stress response, we examined cell cycle progression, mitotic index and DNA strand breaks (by staining for γH2AX) in cisplatin exposed mES cells over time. Cell cycle analysis following DNA synthesis labeling by EdU showed that, in the absence of cisplatin, about 65% of the ES cells were in S phase (G1 ~15% and G2/M ~20%, supplementary figure 1A). After addition of cisplatin, we observed a time dependent inhibition of DNA synthesis: the incorporation of EdU was evident at 30 minutes, decreased after 2 hours, and was completely absent at 4 and 8 hours (figure 1A). Inhibition of DNA replication and transcription has been widely considered to be a key to the mechanism of cisplatin cytotoxicity (Todd and Lippard, 2009). No significant induction of apoptosis (estimated from the subG1 content) occurred during the treatment period (figure 1B) in agreement with previous results (Kruse et al., 2007). In the absence of cisplatin, about 5% of the cells were in mitosis as estimated by FACS analysis of serine 10 phosphorylation of histone H3; nocodazole treated cells arrested in G2 or M-phase were used as positive control (supplementary figure 1B). The maximal reduction in mitotic index was observed after 4 hours of cisplatin treatment and persisted through 8 hours (figure1C). Cisplatin mediated DNA damage signaling manifested by γH2AX phosphorylation increased

with time, reaching its maximal level at 4 hours post-treatment as evidenced by western blot and MS analysis (figure 1D). Together, these time course experiments indicated a complete inhibition of DNA synthesis, a significant reduction of mitotic index, and a strong induction of DNA damage signaling after 4 hours of cisplatin treatment.

Phosphoproteome analysis after cisplatin exposure

Stable isotope labeling by amino acids in cell culture technology (SILAC) (Ong et al., 2002) was applied to quantitatively and qualitatively analyze genome-wide protein phosphorylation events following exposure to cisplatin. mES were grown in media containing 'light' (control cells) or 'heavy' (treated cells) labeled forms of the amino acids arginine and lysine. Cells were exposed to 5 μM cisplatin for 4 hours, mixed with untreated cells, lysed and subsequently digested with trypsin. The 4 hours time point was selected based on the kinetics of cisplatin-induced stress responses (see figure 1). Phosphopeptides were selectively enriched by means of a two-step phosphopeptide enrichment procedure, i.e., SCX (strong cation exchange) chromatography followed by TiO_2 column separation and subjected to online nanoflow liquid chromatography tandem mass spectrometry (nano-LC-MS/MS) analysis (Macek et al., 2009). A total of 14 fractions were collected from SCX chromatography and after TiO_2 enrichment, each fraction was analyzed by high-resolution tandem mass spectrometry on an LTQ-Orbitrap Velos MS (Olsen et al., 2009) using Higher-energy Collisional Dissociation (HCD) (Olsen et al., 2007) for all MS/MS events (figure 1E). The tandem mass spectra were identified by Mascot (www.matrixscience.com) and SILAC phosphopeptide pairs were quantified using the MaxQuant software suite (Cox et al., 2009) and the final dataset showed 11,034 unique phosphopeptides (false discovery rate (FDR) of < 1%) originating from 3,395 proteins (supplementary table 1). Most phosphopeptides contained only a single phosphorylation site (figure 1F), but multiple phosphorylation sites were detected as well. Serine, threonine, and tyrosine phosphorylation sites comprised ~86.7%, ~13%, and ~0.3%, respectively (figure 1G).

The quantified phosphorylation site dataset revealed that approximately 4% of the phosphopeptides underwent a more than two-fold change in phosphorylation level after exposure to cisplatin, corresponding to 183 and 194 up- and down-regulated phosphopeptides, respectively. 324 phosphorylation sites were 1.5-2 fold up-regulated, while 725 phosphorylation sites were found to be 1.5-2 fold down-regulated (figure 2A and supplementary table1). Many of the top 50 up-regulated phosphopeptides stemmed from proteins that are known to play key roles in DNA repair, chromatin remodeling, cell-cycle checkpoints (G1/S and G2/M) and transcription (figure 2B). Typically, multiple individual phosphorylation sites were identified for each protein but, interestingly, 44 proteins (most of them related to DNA repair) were found to contain both up-regulated phosphorylation sites and down-regulated (dephosphorylated) sites (supplementary figure 2).

To examine general validity of our findings we performed an independent experiment in the same ES cell line employing an identical concentration of cisplatin and exposure time (4hrs), as well as identical protocols to purify phosphopeptides (supplementary figure 6A). The final dataset showed 11,966 unique phosphopeptides (supplementary table 6). The quantified phosphorylation site dataset revealed that 224 and 706 up- and

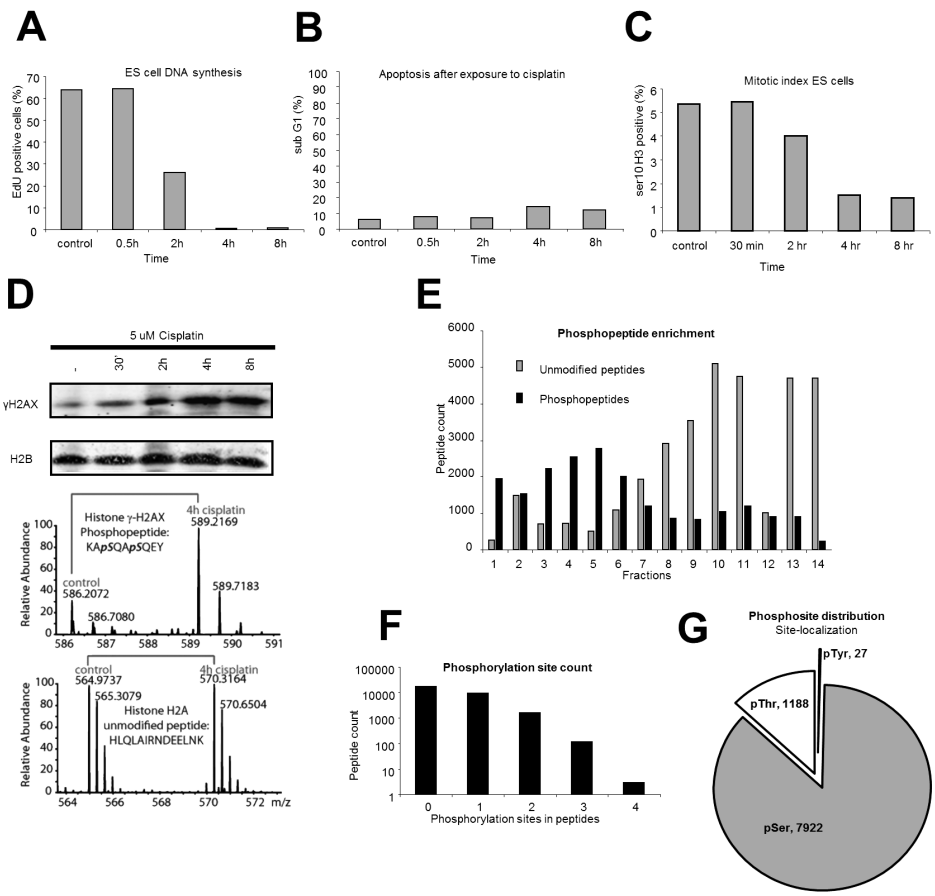

Figure 1. (A) mES cells were treated with 5 μM cisplatin for different times (as indicated) followed by EdU labeling for 45 minutes. Flow cytometric analysis evidenced a time-dependent inhibition of DNA synthesis. **(B)** mES cells were treated with 5 μM cisplatin and the subG1 cell content was determined by flow cytometric analysis at different time points (as indicated). **(C)** Mitotic index of mES cells treated with 5 μM cisplatin was determined at different time points (as indicated) by flow cytometric analysis **(D)** mES cells were treated with 5 μM cisplatin and analyzed 0.5, 2, 4 and 8 hours later with indicated antibodies. (-) untreated sample. SILAC mass spectrometry spectrum of γ-H2AX phosphopepdite and unmodified H2A peptide. **(E)** Number of phosphopeptides (black bars) and unmodified peptides (grey bars) identified by MS analysis. **(F)** Number of peptides containing 0, 1, 2, 3, and 4 phosphorylation sites. **(G)** Phosphorylation site distribution over serine, threonine, and tyrosine residues.

down-regulated phosphopeptides respectively, underwent more than two-fold change in phosphorylation level after exposure to cisplatin (supplementary figure 6C).

Cellular network analysis

Network and pathway analysis using MetaCore software indicated that processes related to DDR, i.e. cell cycle control, checkpoint activation, as well as apoptosis, were significantly overrepresented among proteins containing up-regulated phosphorylation sites (>1.5-fold and >2 fold) (figure 2C-E and supplementary figure 3). The central signal transducers in the early cellular response to cisplatin are the protein kinases ATM and ATR (figure 3A-B). On the other hand, the analysis of proteins containing down-regulated phosphorylation sites identified cytoskeleton and mitotic processes (>1.5-fold and >2 fold). Anaphase-promoting complex (APC), cell adhesion, Rho GTPases (RAC1, Cdc42), and mitosis initiation pathways were found significantly affected (figure 2D-F and supplementary figure 3). Together, the strong inhibition of replicative DNA synthesis, the formation of DNA strand breaks and the reduction of mitotic index fit well with the activation of DDR (i.e., cell cycle checkpoints, DNA repair, and apoptosis) and inactivation of processes related to mitosis. Analysis of phosphorylation levels revealed the same processes significantly affected by cisplatin, when thresholds were set at 1.5 or 2.0 fold changes. This finding indicates that fold changes of 1.5 of phospho-protein level is relevant threshold to identify proteins and processes related to the genotoxic stress induced by cisplatin.

Activation of ATM and ATR in response to cisplatin

In line with recent investigations (Matsuoka et al., 2007;Bennetzen et al., 2010;Stokes et al., 2007;Bensimon et al., 2010), we found that DNA damaging agents such as cisplatin provoke activation of ATM and ATR kinases as the substrate consensus sequence (SQ-TQ motif) of these kinases was significantly overrepresented (84 out of 183 peptide count) among the more than two-fold up-regulated phosphorylation sites (figure 3A). Interestingly, whereas the phosphorylation of S^{1987}, the important SQ motif in murine ATM required for its activation (Pellegrini et al., 2006), was found to be up-regulated, phosphorylation of SQ motifs in ATR was not detected. Notably, phosphorylation at S^{440} in ATR was found to be up-regulated, suggesting that the activity of this kinase may also be modulated by phosphorylation at a site different from the SQ motif. Direct targets of ATR and ATM included proteins involved in the initial enzymatic processing step of DNA damage such as DNA strand breaks (i.e., Nbs1, Rad50, and H2AX), signaling mediators (i.e., MDC1, 53BP1), repair factors (i.e., BRCA1, BARD1, FANCD2), and checkpoint activators (i.e., CHK1) (Bartek and Lukas, 2007). Interestingly, we identified multiple regulated phosphorylation sites on chromatin remodeling proteins (i.e., SMARCAD1, Chd1, Ino80, Rsf1, and HMGA1), E3 ubiquitin ligases (i.e., Np95, Ube3a, Huwe1, Rnf2, UBR7, Mdm2, TRIM33, and RNF19A), and a SUMO-protein ligase (i.e., RanBP2). Moreover, proteins known to bind cisplatin-DNA adducts such as the high-mobility group proteins HMGA1 and HMGA2 (Todd and Lippard, 2009), revealed altered phosphorylation site abundance after treatment. The phosphorylation of the acidic C-terminal tail of HMGA2 has been associated with reduced DNA binding activity (Sgarra et al., 2009). Phosphorylation sites S^{100}, S^{101}, and S^{104} on the

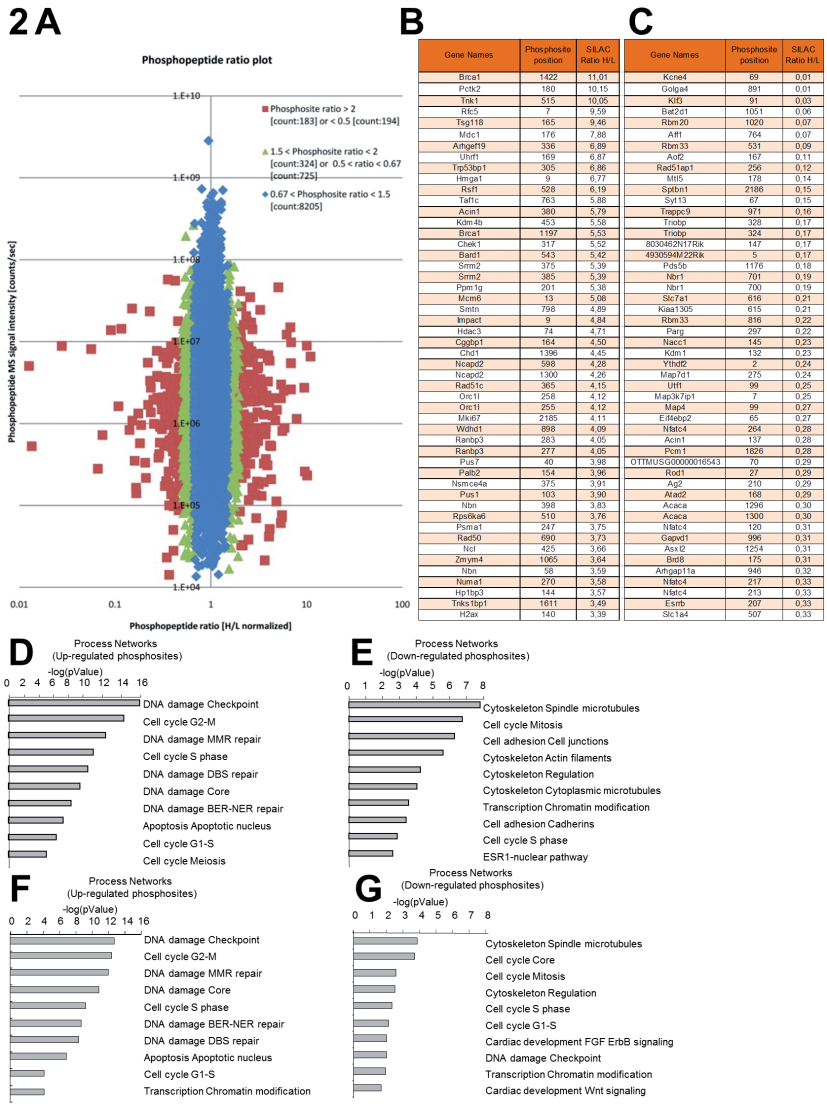

Gene Names	Phosphosite position	SILAC Ratio H/L
Brca1	1422	11,01
Pctk2	180	10,15
Trik1	515	10,05
Rfc5	7	9,59
Tsg118	165	9,46
Mdc1	176	7,88
Arhgef19	336	6,89
Uhrf1	169	6,87
Trp53bp1	305	6,86
Hmga1	9	6,77
Rsf1	528	6,19
Taf1c	763	5,88
Acin1	380	5,79
Kdm4b	453	5,58
Brca1	1197	5,53
Chek1	317	5,52
Baird1	543	5,42
Srrm2	375	5,39
Srrm2	385	5,39
Ppm1g	201	5,38
Mcm6	13	5,08
Smtn	798	4,89
Impact	9	4,84
Hdac3	74	4,71
Cggbp1	164	4,50
Chd1	1396	4,45
Ncapd2	598	4,28
Ncapd2	1300	4,26
Rad51c	365	4,15
Orc1l	258	4,12
Orc1l	255	4,12
Mki67	2185	4,11
Wdhd1	898	4,09
Ranbp3	283	4,05
Ranbp3	277	4,05
Pus7	40	3,98
Palb2	154	3,96
Nsmce4a	375	3,91
Pus1	103	3,90
Nbn	398	3,83
Rps6ka6	510	3,76
Psma1	247	3,75
Rad50	690	3,73
Ncl	425	3,66
Zmym4	1065	3,64
Nbn	58	3,59
Numa1	270	3,58
Hp1bp3	144	3,57
Tnks1bp1	1611	3,49
H2ax	140	3,39

Gene Names	Phosphosite position	SILAC Ratio H/L
Kcne4	69	0,01
Golga4	891	0,01
Kif3	91	0,03
Bat2d1	1051	0,06
Rbm20	1020	0,07
Aff1	764	0,07
Rbm33	531	0,09
Aof2	167	0,11
Rad51ap1	256	0,12
Mtl5	178	0,14
Sptbn1	2186	0,15
Syt13	67	0,15
Tnpp9	971	0,16
Triobp	328	0,17
Triobp	324	0,17
8030462N17Rik	147	0,17
4930594M22Rik	5	0,17
Pds5b	1176	0,18
Nbr1	701	0,19
Nbr1	700	0,19
Slc7a1	616	0,21
Kiaa1305	615	0,21
Rbm33	816	0,22
Parg	297	0,22
Nacc1	145	0,23
Kdm1	132	0,23
Ythdf2	2	0,24
Map7d1	275	0,24
Ulf1	99	0,25
Map3k7ip1	7	0,25
Map4	99	0,27
Eif4ebp2	65	0,27
Nfatc4	264	0,28
Acin1	137	0,28
Pcm1	1826	0,28
OTTMUSG00000016543	70	0,29
Rod1	27	0,29
Ag2	210	0,29
Afadl2	168	0,29
Acaca	1296	0,30
Acaca	1300	0,30
Nfatc4	120	0,31
Gapvd1	996	0,31
Asxl2	1254	0,31
Brd8	175	0,31
Arhgap11a	946	0,32
Nfatc4	217	0,33
Nfatc4	213	0,33
Esrrb	207	0,33
Slc1a4	507	0,33

Figure 2. (A) Phosphopeptide ratio plot. Red dots indicate phosphopeptides that were found more than 2-fold up- or down-regulated after cisplatin treatment; green dots indicate phosphopeptides that showed 1.5 to 2 fold up- and down-regulation after cisplatin treatment; blue dots indicate phosphopeptides that were not affected by cisplatin treatment. The y-axis represents signal intensity of the ions and it is related to the power (~amplitude squared) of the signal sine wave. **(B)** Top 50 up-regulated phosphopeptides. **(C)** Top 50 Down-regulated phosphopeptides. **(D)** MetaCore network analysis of proteins containing more than 1.5-fold up-regulated phosphorylation sites after cisplatin treatment. **(E)** MetaCore network analysis of proteins containing more than 1.5-fold down-regulated phosphorylation sites after cisplatin treatment. **(F)** MetaCore network analysis of proteins containing more than 2-fold up-regulated phosphorylation sites after cisplatin treatment. **(G)** MetaCore network analysis of proteins containing more than 2-fold down-regulated phosphorylation sites after cisplatin treatment.

acidic C-terminal tail and S^{44} outside that domain of HMGA2 were found down-regulated after cisplatin treatment, suggesting an increased DNA binding to cisplatin-modified DNA. In contrast, we observed an enhanced phosphorylation of the S^{102} and S^{103} sites on the acidic C-terminal tail of HMGA1 after cisplatin treatment and, moreover, the phospho-S^{9} (SQ motif) was present in the top ten cisplatin up-regulated phosphorylation sites.

Kinase domain loop phosphorylation sites changes by cisplatin stress response

Based on consensus sequence, about half of the more than two-fold up-regulated phosphorylation sites were no canonical substrates of ATM or ATR, revealing substantial involvement of other kinases in the genotoxic stress response. The activity of many kinases is modulated by phosphorylation of the kinase domain loop located between the conserved amino acid sequence motifs DFG and APE (Nolen et al., 2004). This domain plays a crucial role in substrate recognition. Phosphorylation of residues in this segment is frequently required for the correct alignment between the substrate and the catalytic site of the kinases (Johnson et al., 1996) and phosphorylation status of the activation loop can therefore be used as a proxy for kinase activity. Eleven kinases mainly belonging to the MAPK family were identified to be phosphorylated in the activation loop after cisplatin treatment (figure 4A). Plk1, a kinases that play essential roles in the regulation of mitosis by coordinating spindle assembly and dynamics was found to be specifically dephosphorylated in its activation loops after cisplatin treatment. We tested the biological relevance of 11 of the regulated kinases for cisplatin induced toxicity by siRNA mediated knockdown and demonstrated a novel protective role for 3 of them (CDK7, Plk1, and KPCD1) (figure 4B). In order to test the off-target effects, four individual siRNA were used to knockdown CDK7, Plk1, and KPCD1 respectively and the extent of knockdown was tested by western-blot (supplementary

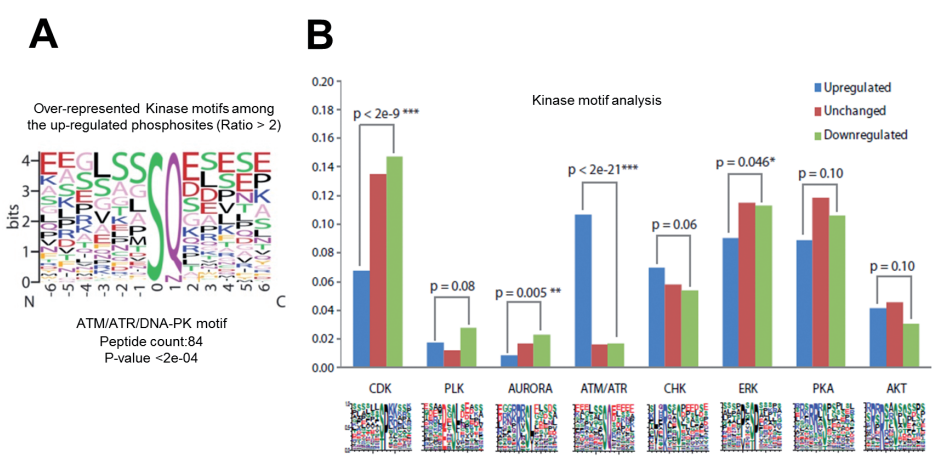

Figure 3. (A) Consensus sequence for ATM, ATR, and DNA-PK substrates among the more than 2-fold up-regulated phosphorylation sites. **(B)** Consensus sequence for different kinases among up-regulated, down-regulated, and unmodified phosphorylation sites.

figure 4). We note here, that a significant reduction in cell survival was detected for the Plk1 knockdown in the absence of cisplatin treatment, indicating a critical role of this kinase in normal cell growth (supplementary figure 4) (Tyagi et al., 2010).

Effects on mitosis

Analysis of kinase motifs among the phosphorylation sites showed a significant enrichment of CDK, ERK, and Aurora kinase substrates among the down-regulated phosphorylation sites

A

Phosphopeptide sequence	Kinase Domain Loop (DFG.....APE)	Ratio 4hrs CisPt
ETTSHNSLTTPCYTPYVAPEVLGPEK	>KinaseActivationLoop MAPK2_MOUSE	2.01
AYTHQVVTR	>KinaseActivationLoop CDK7_MOUSE	1.72
LQTICLSGTGMK	>KinaseActivationLoop M3K2_MOUSE	1.49
HTDDEMTGYVATR	>KinaseActivationLoop MK14_MOUSE	1.47
LDTFCGSPPYAAPELFQGK	>KinaseActivationLoop MARK1_MOUSE	1.41
ANSFVGTAQYVSPELLTEK	>KinaseActivationLoop PDPK1_MOUSE	0.73
SVVGTPAYLAPEVLR	>KinaseActivationLoop KPCD1_MOUSE	0.63
SVVGTPAYLAPEVLR	>KinaseActivationLoop KPCD3_MOUSE	0.63
GFSNSTER	>KinaseActivationLoop SG269_MOUSE	0.61
TLCGTPNYIAPEVLSK	>KinaseActivationLoop PLK1_MOUSE	0.60
EGLRPGDTTSTFCGTPNYIAPEILR	>KinaseActivationLoop KPCI_MOUSE	0.52

B

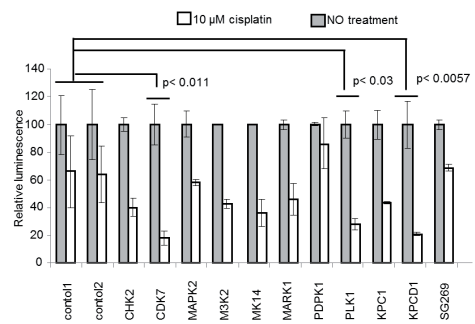

C

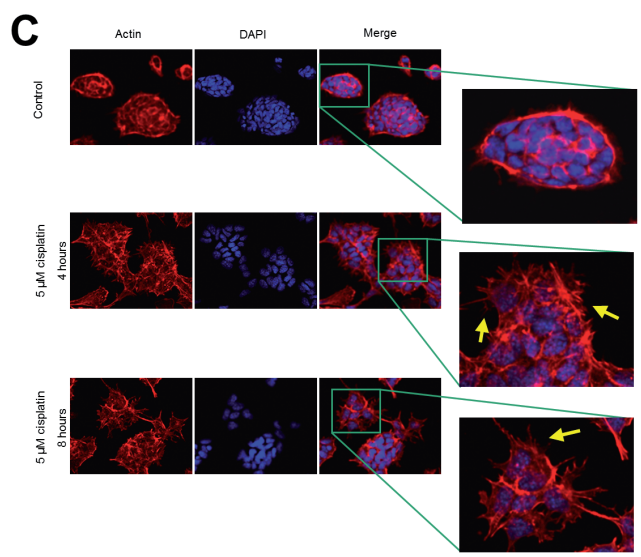

Figure 4. (A) Analysis of the kinase domain loop located between the conserved sequence DFG and APE. **(B)** The cellular sensitivity for cisplatin after siRNA knockdown was determined by an Adenosine TriPhosphate (ATP) monitoring system. Knock down of CDK7, PLK1, or KPCD1 kinases significantly reduced cell survival after cisplatin treatment (Student's *t* test). siGFP (control 1) and siLAMIN C/A (control 2) were used as negative controls (two independent experiments). **(C)** Effects of cisplatin on cytoskeleton structure. mES cells were exposed for 4 and 8 hours to cisplatin (5µM) treatment and stained with DY554-phalloidin and DAPI (nuclei). The arrows indicate microspikes.

(figure 3B). In response to persistent genotoxic stress, ATM and ATR and the subsequent Chk1/Chk2 signaling cascade prevent activation of Cdk1/CyclinB, thereby blocking entry into mitosis (Bartek and Lukas, 2007). The depletion of mitotic cells evidenced by FACS analysis (figure 1C) is consistent with the activity of these cell-cycle kinases as indicated by the phosphoproteomics dataset. Following DNA damage, two mitosis-specific kinases, Cdk1 and Plk1, are inactivated by inhibitory phosphorylation (T^{14} and Y^{15}) (O'Farrell, 2001) and dephosphorylation (T^{210}) (Tsvetkov and Stern, 2005) events, respectively. T^{14} and Y^{15} phosphorylation of Cdk1 and the dephosphorylation of the activation loop T^{210} of Plk1 were evident in our data (supplementary table 1). Several Plk1 targets involved in mitosis have been identified (Nigg, 2001), including FoxM1; this protein was found to be dephosphorylated after cisplatin treatment (supplementary table 1). The FoxM1 protein is an important transcription factor involved in the regulation of mitotic entry (Laoukili et al., 2005;Wang et al., 2005) and phosphorylation of FoxM1 by Plk1 and Cdk1 regulates the transcription network essential for mitotic progression (Fu et al., 2008). Remarkably, a wide range of proteins related to mitotic events were found to be dephosphorylated, i.e., KNSL1, nucleolin, histone H1, and the anaphase-promoting complex (APC). APC is a multisubunit protein complex with E3 ubiquitin ligase acitivity essential for the proteolysis process, a key mechanism that drives the events of mitosis. APC1, APC2, Cdc20, Cdh1, and Cdc23 subunits of anaphase-promoting complex were found down-phosphorylated and very likely this alteration may facilitate the binding of Emi1, an inhibitor of APC (Torres et al., 2010).

Effects on cytoskeleton

Cellular movement is orchestrated by microtubules and actin cytoskeleton and is controlled by the activity of Rho GTPases (Waterman-Storer and Salmon, 1999). Prominent Rho GTPase family members are Rac1 and Cdc42, which induce the formation of extensions (lamellipodia) and stimulate actin polymerization at the leading edge of the cell together with the formation of new adhesion sites to the matrix (Ridley, 2001). Cytoskeleton processes and, in particular, Rac-1 ($P<10e-5$) and Cdc42 ($P<10e-4$) pathways were found affected by genotoxic stress (supplementary figure 3). Proteins associated with RAC-1 and Cdc42 pathways i.e., ABR, ECT2, DBL, RacGAP1, p200RhoGAP, ARCGAP22, and ARHGAP12, were found to be dephosphorylated on proline-directed serine/threonine sites (potential CDK or MAPK substrates) or sites that are targeted by casein kinases (in an acidic amino acid context). To study the effect of cisplatin on cytoskeleton structure, we monitored the actin organization in mES cells after treatment (figure 4C). Cytoskeleton remodeling and specific microspike formation were clearly visible in cells treated with cisplatin, confirming the results of the pathway analysis obtained from the phosphoproteome.

Proteome and transcriptome

Non-phosphorylated peptides were analyzed to rule out that changes in overall protein levels might be responsible for the observed changes in phosphorylation site levels. Quantitative profiles were obtained for 4,349 proteins (figure 5A) out of a total of 5,917 proteins (supplementary table 2) based on the quantification of 16,305 non-phosphorylated but unique peptides (supplementary table 3). The abundance of most proteins that contained

up- or down-regulated phosphorylation sites did not change significantly during cisplatin treatment, indicating that the majority of observed phosphorylation changes was not due to alterations in protein quantity (figure 5C-D-E). Interestingly, cellular levels of 455 proteins were found to be altered when proteomics data analysis was performed with a statistical rigor of P<0.05. Network analysis identified cytoskeleton remodeling as one of the most prominent affected pathways. In particular, the NOTCH signaling pathway was statistically found to be significantly affected (supplementary figure 3). Metacore analysis shows an enrichment of p53 target genes ie 49 out of 455 proteins, double the expected frequency (P<10e-6), suggesting a p53-dependent response in line with previous studies (Kruse et al., 2007). We examined how the proteome correlates to the mES transcriptome previously generated under identical conditions of cell growth and cisplatin exposure (Kruse et al., 2007). Of a total of 3,616 Entrez gene ID shared among the gene expression and protein data sets, 386 proteins and 56 mRNAs transcripts were found to be significantly affected by cisplatin treatment (p<0.05), with surprisingly only 5 gene IDs being in common (supplementary table 5). A selected group of genes was examined by RT-PCR and western-blot analysis to quantify gene expression and protein levels in mES cells after cisplatin treatment. Indeed significant changes in protein levels were found for Cdh1, p53, Centrin2, Mark2 by immunoblotting whereas the corresponding mRNA transcripts were not affected after cisplatin (supplementary figure 5). Together, these data indicate that alterations in protein and transcript quantaties do not correlate well at the individual gene level after cisplatin treatment. In contrast, pathway analysis based on transcriptomics, proteomics and phosphoproteomics data revealed a large overlap in affected processes (figure 6). Cell cycle was the most prominent pathway affected at the transcriptome and phosphoproteome level whereas DNA repair pathways were only significantly affected at phosphoproteome level. In contrast, changes at the overall protein level primarily involved processes associated with cytoskeleton regulation.

DISCUSSION

Cisplatin is a widely used anticancer drug and, therefore, understanding of the molecular changes that underlie the biological consequences of treatment with this drug is of critical importance. Protein phosphorylation is one of the most prominent post-translational modifications that are triggered by cisplatin treatment and therefore, global phosphoproteome analysis is an excellently suited approach to identify molecular components and cellular pathways affected by cisplatin.

Inhibition of transcription and replication by cisplatin induced DNA lesions and subsequently the generation of DNA strand breaks activates the ATR and ATM kinases as well as p38MAPK/MK2 pathway (Bartek and Lukas, 2007;Reinhardt et al., 2007a;Reinhardt and Yaffe, 2009). Consistently, we found up-regulation of S^{1987} phosphorylation in ATM that is required for its activation (Pellegrini et al., 2006). Up-regulation of ATR phosphorylation was observed at S^{440}, a site that lacks the SQ motif and likely represents the site targeted by the NEK6 kinase. This kinase belongs to a large family of Ser/Thr kinases that have critical roles in coordinating microtubule dynamics during mitotic progression (Quarmby

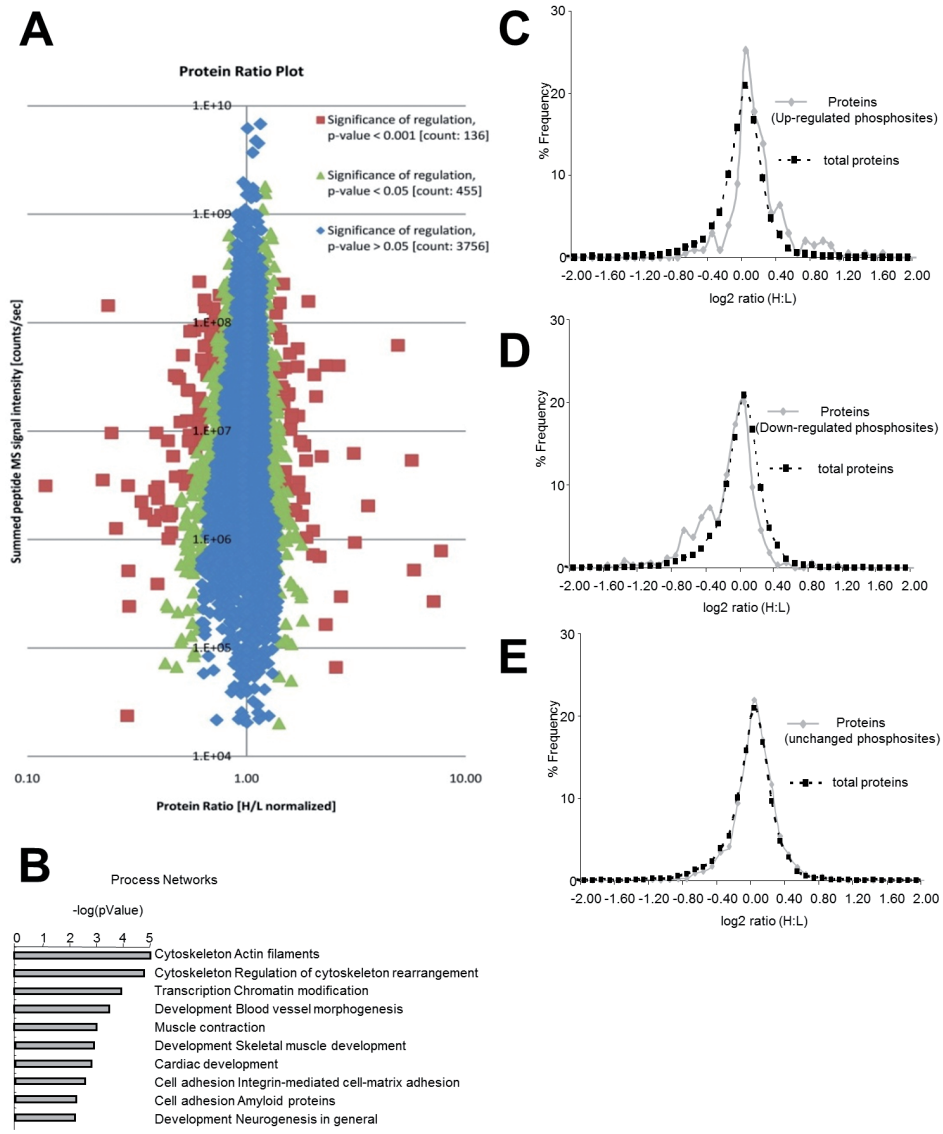

Figure 5. (A) Unmodified peptide ratio plot. Red dots, significantly (p<0.001) regulated peptides after cisplatin treatment; green dots, significantly (p<0.05) regulated peptides after cisplatin treatment; blue dots, unmodified peptides after cisplatin treatment. The y-axis represents signal intensity of the ions and it is related to the power (~amplitude squared) of the signal sine wave. **(B)** MetaCore networks analysis of significantly affected proteins (p<0.05) after cisplatin addition. **(C)** Abundance distributions of all proteins and proteins containing up-regulated phosphorylation sites (>1.5-fold) **(D)** Abundance distributions of all proteins and proteins containing down-regulated phosphorylation sites (>1.5-fold). **(E)** Abundance distributions of all proteins and proteins containing unmodified phosphorylation sites.

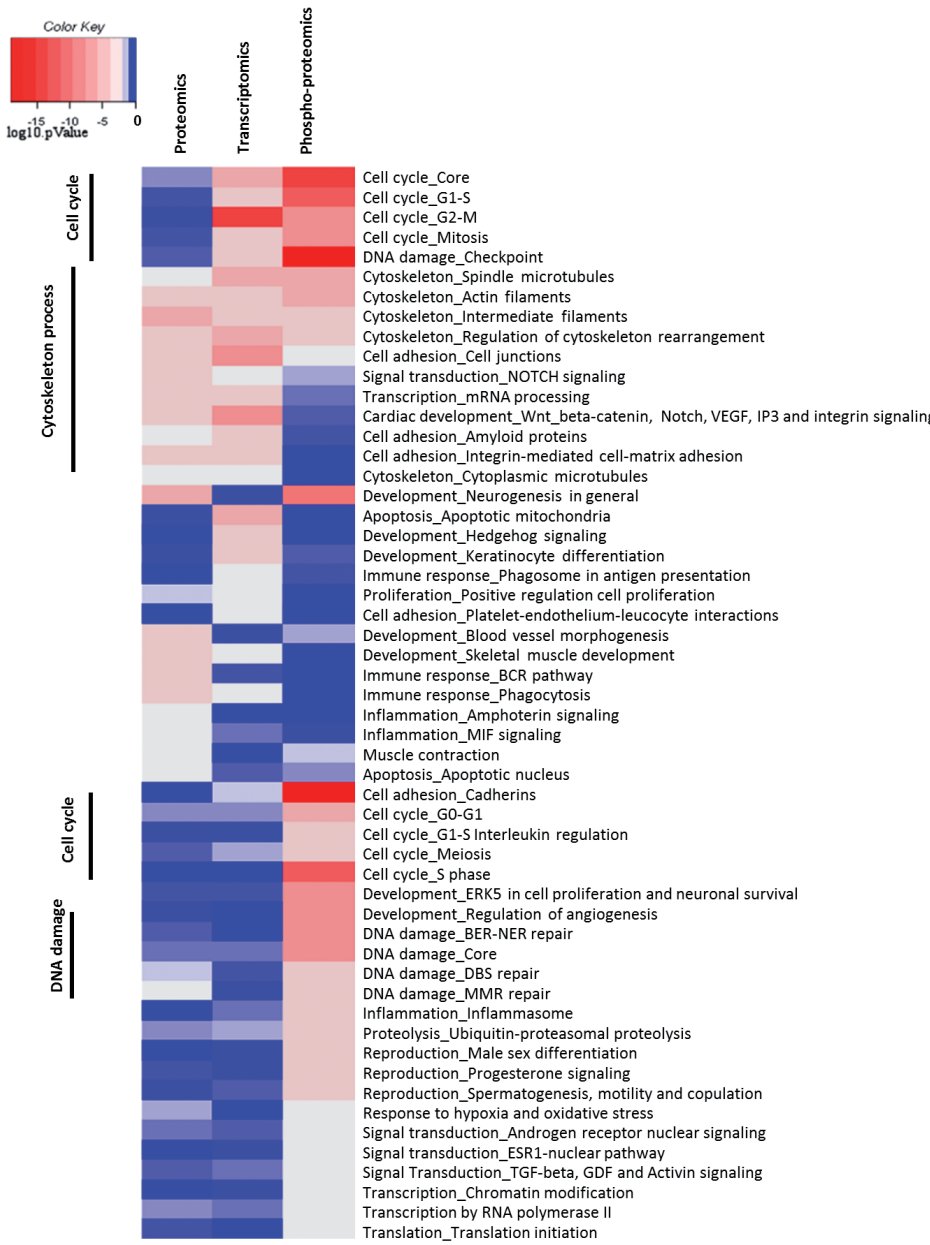

Figure 6: Comparison of significantly affected pathways (MetaCore network analysis) by cisplatin at the transcriptomic (mRNAs transcripts p<0.05), proteomic (proteins p<0,05) and phosphoproteomic level (phosphoprotein p<0,05).

and Mahjoub, 2005). This phosphorylation site has not been previously mapped and might represent a novel site involved in ATR activation. The top 50 up-regulated phosphorylation sites include a significant number of direct ATR and ATM targets related to DDR; most notably proteins involved in the processing step of double strand breaks (DSB), DNA damage signaling, stalled replication/transcription forks, checkpoint activation and chromatin remodeling proteins. In addition, E3 ubiquitin and SUMO-protein ligases were observed to be regulated by phosphorylation events highlighting the cross-talk between phosphorylation and other post-translational modifications in response to genotoxic stress (Bennetzen et al., 2010). In contrast to the large-scale proteomic analysis of SQ specific phosphorylation sites in response to DNA damage induced by IR and UV (Matsuoka et al., 2007;Stokes et al., 2007), our global phosphoproteomics strategy allowed identification of putative ATM/ATR dependent and independent phosphorylation events. Indeed, DNA repair proteins such as BRCA1, Rad50, p53BP1, FANCI, and BARD-1 were found to contain up-regulated phosphorylation sites unrelated to ATM and ATR activity. As these data are not based on direct experimental evidence, we cannot exclude that ATM/ATR may also phosphorylate at non-consensus sites. Moreover, 44 proteins (mostly involved in DNA repair and including BRCA1 and Ino80, supplementary figure 2) underwent differential phosphorylation of adjacent sites (2-5 amino acids). Differential phosphorylation might serve to create a molecular switching mechanism (Bennetzen et al., 2010) by a tightly controlled activity of several kinases and phosphatases. Different types of post-translational modifications controlled by such a mechanism might dynamically regulate the DDR for example the assembly and disassembly of factors at sites of damage (Bartek and Lukas, 2007).

Several of the HMG domain proteins recognize cisplatin adducts and display a selective affinity for clinically effective platinum drugs (Kartalou and Essigmann, 2001). HMGA proteins are expressed at a high levels during embryonic development, whereas they are barely detectable in differentiated or non-proliferating cells; noteworthy, these proteins are highly re-expressed following neoplastic transformation (Sgarra et al., 2004). HMGA1 and HMGA2 were found to be differentially phospho-regulated after cisplatin treatment. To our knowledge, these are the first *in vivo* data showing a discrepancy in phosphorylation state between HMGA1 and HMGA2 in response to genotoxic stress. The finding of differential phosphorylation profiles within the HMGA family after cisplatin treatment might offer potential targets for an improved cisplatin cancer therapy, considering that these proteins are overexpressed in cancers of different origins.

The outcome of an independent replicate experiment with same ES cells demonstrated the high reproducibility of the Cisplatin induced protein phosphorylation. The results also showed that ATM and ATR consensus sequences were significantly over-represented among hyper-phosphorylated peptides (supplementary figure 6D). The phosphopeptide ratio correlation between the two replicates is 0.61 (Pearson correlation coefficient, R, supplementary figure 6A) based on 7,275 unique phosphopeptide identified in both experiments (supplementary table7). These results are close to those achieved in a recent study using a similar experimental approach (Rigbolt et al., 2011). A much higher correlation (R=0.88) was found when the analysis was limited to putative ATM/ATR

substrate peptide ratios (supplementary figure 6A-B-E). Importantly, network analysis identified DDR and cytoskeleton regulation as affected cisplatin processes in both experiments. Together these results demonstrate the reproducibility and general validity of our findings (supplementary figure 6F-G).

Our results indicate that the cellular response to genotoxic stress involves a large variety of protein kinases and phosphatases. Indeed, 11 kinases were identified to be regulated at phosphorylation sites-in the activation loop after cisplatin treatment (figure 4A). Most of those regulated belong to the MAPK family, but kinases not related to the MAPK family i.e Plk1 essential in the regulation of mitosis, was found to be dephosphorylated as well. Mitogen-activated protein kinases (MAPKs) are critical components of the signaling network activated by genotoxic stress and critical in deciding cell fate in response to cisplatin (Brozovic and Osmak, 2007). Particularly, in the absence of p53, cells depend on p38MAPK/MK2 for cell-cycle arrest and survival after cisplatin (Reinhardt et al., 2007b). Here we show that the kinase domain of MK14 (p38α) is activated by specific phosphorylation of the activation loop TXY motif after cisplatin addition.

Knock-down of CDK7 significantly increased cell toxicity after cisplatin treatment. The cyclin-dependent protein kinase CDK7 forms a trimeric complex with cyclin H and MAT1 and is both a Cdk-activating kinase (CAK) (Drapkin et al., 1996;Reardon et al., 1996) and an essential component of the transcription factor TFIIH, involved in transcription initiation and nucleotide excision repair (Scrace et al., 2008). In addition, knock-down of Plk1, and KPCD1 also increased cisplatin mediated cytotoxicity (figure 4B). KPCD1 is a member of the protein kinase C (PKC) family involved in extracellular receptor-mediated signal transduction pathways (Johannes et al., 1994). The mitosis-specific kinase Plk1 has been shown to play an essential role in the regulation of mitotic progression, including mitotic entry, spindle formation, chromosome segregation and cytokinesis; moreover, it has been found to be over-expressed in different types of tumor (Takai et al., 2005). Inhibition of Plk1 is an efficient way to establish an irreversible G2 arrest after DNA damage induction in specific cancers with non-functional p53. In these cells typical G1 arrest is lost in response to DNA damage and cells display a stronger dependency on the G2 DNA damage checkpoint for protection against genotoxic insults (van Vugt et al., 2005) Our data suggest that the cellular response to inactivate PKL1 is directed towards prevention of mitotic entry in favor of apoptosis process (Macurek et al., 2008), that is in according to transcriptomics and phosphoproteomics analysis. Currently, several Plk inhibitors are in phase I or II clinical studies (Mross et al., 2008;Jimeno et al., 2010;Degenhardt and Lampkin, 2010), and in cancers with non-functional p53, Plk1 inhibition serves as a potent adjuvant therapy when combined with a DNA-damaging regimen such as cisplatin (Tyagi et al., 2010). Together, our results clearly indicate that dissection of the cellular responses induced by cisplatin using phosphoproteome analysis in concert with functional genomics allows unraveling of targets and pathways that enhance the cytotoxic effects of cisplatin.

Proteins that were identified to be differentially phosphorylated upon cisplatin treatment also belonged to biological processes and structures not classified as or related to core DDR processes. In fact, unanticipated processes associated with cytoskeleton events were

identified by network analysis of proteins containing down-regulated phosphorylation sites and, in particular, Rac-1 and Cdc42 pathways were found affected by cisplatin. The actin component of the cytoskeleton is dynamically implicated in a variety of cell functions, including regulation of cell shape, adhesion, and motility and recent studies underline mechanisms of cisplatin mediated inhibition on invasion and migration of human cancer cells (Ramer et al., 2007;Karam et al., 2010;Paduch et al., 2009). Cytoskeleton remodeling and specifically the induction of microspike formation was a clear effect of cisplatin treatment (figure 4C). These results are in line with reports on microspike formation related to Cdc42 (Umikawa et al., 1999). The regulation of phospho state of Rho GTPases (members of the Rac-1 and Cdc42 pathways) shown in this study, is consistent with the observed cisplatin mediated changes in cell morphology. Moreover, the link between cisplatin and Rac-1/ Cdc42 pathways is relevant in view of the fact that Cdc42 activity is associated with genome maintenance, cellular senescence regulation, and aging (Wang et al., 2007). Although classically regarded as a nuclear DNA damaging agent, recent studies support a more promiscuous mode of action for cisplatin (Mandic et al., 2003;Emert-Sedlak et al., 2005;Safaei et al., 2005;Zeidan et al., 2008). The current phosphoproteome analysis of kinases targets and their predicted activated substrates supports this finding by confirming previous data and providing evidence for the extra-nuclear targeting function that might play a role in cisplatin induced toxicity and in cell motility. A better understanding of the mechanisms of cisplatin action may provide novel therapeutic strategies that would block metastatic progression and reducing dissemination of tumor cells.

We tested the hypothesis whether changes in transcription profiling after cisplatin correlate with changes observed at the protein level. Consistent with previously published data (Olsen et al., 2010), we found no clear correlation between changes in the relative level of transcripts and corresponding proteins. This lack of correlation might be due to the fact that the cellular mechanisms involved in regulation of stability/degradation differ between mRNAs and their encoded proteins. This finding indicates that information derived from transcriptomic and proteomic analysis is different, but when merged generates a more comprehensive view of the signaling pathways affected by stressors. Interestingly, the phosphoproteomic analysis performed in our study led to the identification of most of the pathways that were affected at the transcriptome or proteome level. However, the impact of cisplatin on the DNA damage repair pathways was only manifested in the phosphoproteome analysis indicating that phosphorylation events are key to activate DNA repair pathways after genotoxic stress induced by cisplatin or in general to genotoxic agents that induce replication and transcription blocking lesions.

MATERIAL AND METHODS

Cell culture and cisplatin treatment

Cell culture and cisplatin treatment of wild type mES cells (B4418 and HM1 derived from C57/Bl6 and OLA/129 mouse genetic background, respectively) were essentially performed as previously described (Kruse et al., 2007). Sub-confluent cultures of mES

cells were exposed to cisplatin (5 μM), added directly to the culture medium. Cell cultures were incubated for different time periods after cisplatin administration (0.5, 2, 4, 8 h). The Thermo Scientific Pierce Mouse Embryonic Stem Cell Kit, containing media and reagents specifically designed for analysis of protein by mass spectrometry (Thermo Scientific), was used for SILAC experiments.

Phosphopeptides enrichment

Isolation and purification of phosphopeptides was performed according to already published procedures (Villen et al., 2007) with some modifications. Briefly, cells were lysed for 30 minutes in lysis buffer (8 M urea, 50 mM Tris pH 8.1, 75 mM NaCl, 1 mM MgCl2, 500 units benzonase and phosphatase inhibitors). Samples were centrifuged for 15 minutes at 13,000 rpm and protein concentration was established by Qubit Protein Assay (Invitrogen). 10 mg of proteins were first reduced with 2.5 mM DTT for 25 minutes at 60 °C and subsequently alkylated by incubation with 7 mM iodoacetamide for 15 minutes at room temperature, protected from light. The alkylation reaction was quenched by incubation with 2.5 mM DTT for 15 minutes at room temperature. Protein solution was diluted 8-fold with 25 mM Tris pH 8.1, 1 mM CaCl2 and incubated for 15 hr at 37 °C with 100 μg trypsin (Promega). On the following day, the digestion reaction was stopped by addition of TFA to 0.4 % final concentration and the precipitate was removed by centrifugation for 5 minutes at 3,200 rpm. The supernatant was loaded on a Sep-Pak Vac 1 ml C18 cartridge (Waters), desalted by washing with 0.1 % acetic acid and eluted with 0.1 % acetic acid, 30 % acetonitrile. Eluted peptides were lyophilized and fractionated at 1 ml/min on a 9.4x200mm 5 μm particle PolySULFOETHYL A SCX column (PolyLC) using a 70 minutes gradient from 0 to 75 mM KCl, 350 mM KCl for 38 minutes in 5 mM KH2PO4 pH 2.65, 30% acetonitrile. Eighteen fractions with 6 ml eluate were collected, desalted on Sep-Pak Vac 1 ml C18 cartridge and lyophilized as mentioned before. In the desalting step, the last eight fractions were reduced to four fractions by loading two fractions on one cartridge giving a total of 14 fractions. After lyophilization, peptides were dissolved in solution A (300 mg/ml lactic acid, 80 % acetonitrile, 0.1 % TFA) and loaded on a titanium tip column (TopTip 1 -100 μl, Glycen Corporation) prewashed with elution solution (15 mM NH4OH pH~10.5), equilibration solution (0.1 % TFA) and solution A. After sample loading, the tip column was washed with solution A and B (80 % acetonitrile (v/v), 0.1 % TFA (v/v)). After washing, phosphopeptides were eluted with elution buffer and collected in an equal volume of 2 % TFA. For desalting, phospeptides were loaded on a Stage Tip C18 column (PROXEON) prewashed with methanol, solution B and 0.1 % TFA. The phosphopeptide solution was loaded on a Stage Tip, washed with 0.1 % TFA and eluted with solution B. Liquid was removed by lyophilization and stored at -80 °C till MS analysis.

Mass spectrometric analysis.

LC-MS/MS

The dried phosphopeptide mixtures were acidified with 5% acetonitrile in 0.3% tri-fluoro acetic acid (TFA) to an end volume of 10 uL, transferred to a 96-well plate and analyzed by online nanoflow liquid chromatography tandem mass spectrometry (LC-MS/MS) as

described previously (Olsen et al., 2009) with a few modifications. Briefly, all nanoLC-MS/MS-experiments were performed on an EASY-nLC™ system (Proxeon Biosystems, Odense, Denmark) connected to the LTQ-Orbitrap Velos (Thermo Electron, Bremen, Germany) through a nanoelectrospray ion source.

5 uL of each phosphopeptide fraction was auto-sampled onto and directly separated in a 15 cm analytical column (75 µm inner diameter) in-house packed with 3µm C18 beads (Reprosil-AQ Pur, Dr. Maisch) with a 90 min gradient from 5% to 30% acetonitrile in 0.5% acetic acid at a flow rate of 250 nl/min. The effluent from the HPLC was directly electrosprayed into the mass spectrometer by a platinum-based liquid-junction.

The LTQ-Orbitrap Velos instrument was operated in data-dependent mode to automatically switch between full scan MS and MS/MS acquisition. Instrument control was through Tune 2.6.0 and Xcalibur 2.1 Survey full scan MS spectra (from m/z 300 – 2000) were analyzed in the orbitrap detector with resolution R=30K at m/z 400 (after accumulation to a 'target value' of 1e6 in the linear ion trap). The ten most intense peptide ions with charge states ≥ 2 were sequentially isolated to a target value of 5e4 and fragmented in octopole collision cell by Higher-energy Collisional Dissociation (HCD) with a normalized collision energy setting of 40%. The resulting fragments were detected in the Orbitrap system with resolution R=7,500. The ion selection threshold was 5,000 counts and the maximum allowed ion accumulation times were 500 ms for full scans and 250 ms for HCD.

Standard mass spectrometric conditions for all experiments were: spray voltage, 2.2 kV; no sheath and auxiliary gas flow; heated capillary temperature, 275ºC; predictive automatic gain control (pAGC) enabled, and an S-lens RF level of 65%. For all full scan measurements with the Orbitrap detector a lock-mass ion from ambient air (m/z 445.120024) was used as an internal calibrant as described (Olsen et al., 2005). A setting was also chosen where the additional SIM injection of the lock mass is deactivated, in order to save time.

Raw MS data analysis

Peptide identification and quantitation by MASCOT and MaxQuant.

Raw Orbitrap full-scan MS and ion trap MSA spectra were processed by MaxQuant as described (Cox et al., 2009;Cox and Mann, 2008). In brief, all identified SILAC doublets were quantified, accurate precursor masses determined based on intensity-weighing precursor masses over the entire LC elution profiles and MS/MS spectra were merged into peak-list files (*.msm). Peptides and proteins were identified by Mascot (Matrix Science, London, UK) via automated database matching of all tandem mass spectra against an in-house curated concatenated target/decoy database; a forward and reversed version of the mouse International Protein Index (IPI) sequence database (version 3.37; 102,934 forward and reversed protein sequences from EBI (http://www.ebi.ac.uk/IPI/)) supplemented with common contaminants such as human keratins, bovine serum proteins and porcine trypsin. Tandem mass spectra were initially matched with a mass tolerance of 7 ppm on precursor masses and 0.02 Da for HCD fragment ions. Scoring was performed in MaxQuant as described previously. We required strict trypsin enzyme specificity and allowed for up to two missed cleavage sites. Cysteine carbamidomethylation (Cys +57.021464 Da) was

searched as a fixed modification, whereas N-acetylation of proteins (N-term +42.010565 Da), N-pyroglutamine (-17.026549 Da), oxidized methionine (+15.994915 Da) and phosphorylation of serine, threonine and tyrosine (Ser/Thr/Tyr +79.966331 Da) were searched as variable modifications.

Peptide filtering and phosphorylation site localization

The resulting Mascot result files (*.dat) were loaded into the MaxQuant software suite for further processing. In MaxQuant we fixed the estimated false discovery rate (FDR) of all peptide and protein identifications at 1%, by automatically filtering on peptide length, mass error precision estimates and Mascot score of all forward and reversed peptide identifications. Finally, to pinpoint the actual phosphorylated amino acid residue (s) within all identified phospho-peptide sequences in an unbiased manner, MaxQuant calculated the localization probabilities of all putative serine, threonine and tyrosine phosphorylation sites using the PTM score algorithm as described (Olsen et al., 2006).

Phosphorylation Site Sequence Motifs Logo Plots

Only peptides with localization probabilities >0.75 were included in the downstream bioinformatic analysis (supplementary table 1S). To identify enriched sequence motifs in the phosphorylation site dataset we made use of the already published kinase motifs (www.phosida.com) and an algorithm that extracts overrepresented motifs in a more unbiased manner (Soufi et al., 2009). The algorithm was implemented in R (a programming language and software environment for statistical computing and graphics) using a Fisher's exact test to iteratively test for position specific over-representation of amino acid groups between two lists of prealigned sequences. The perl-package WebLogo was used internally in the algorithm to visualize the enriched sequence motifs as logo plots. Grouping of amino acids were done by the basis of related chemical properties (acidic, basic, aromatic, aliphatic, hydrophilic, amide, polar and cyclic) and alignment was done with a sequence window of +/- 6 amino acids surrounding the central phosphorylated serine, threonine or tyrosine residue. The iterative nature of the algorithm means it is successively reapplied on the result from an analysis – i.e. on both the subset of the lists which contains the most significantly overrepresented amino acid group and the subset that does not contain this amino acid group. All cisplatin regulated phosphorylation site sequences were compared to all unchanging sites and vice versa. We considered a motifs significant if it fulfilled our conservative cut-off of $P<0.001$ on the Bonferroni adjusted P-values.

Network and pathways analysis

Network and pathway analysis were performed using MetaCore software (http://www.genego.com/metacore.php). Proteins containing up-regulated phosphorylation sites (>1.5-fold and >2 fold) and down-regulated phosphorylation sites (>1.5-fold and >2 fold) were investigated. In most cases high-throughput experiments result in lists of genes or proteins of interest. The datasets usually contain anywhere between few dozens and few thousand genes/proteins. In MetaCore the significance is evaluated based on the size of the intersection between user's dataset and set of genes/proteins corresponding to a network

module/pathway in question, or rather the probability to randomly obtain intersection of certain size between user's set and a network/pathway follows hypergeometric distribution. The significance of the networks/pathways is evaluated for whether algorithm has succeeded in creating modules that have higher than random saturation with the genes of interest.

Networks are drawn from scratch by GeneGo annotators and manually curated and edited. There are about 110 cellular and molecular processes whose content is defined and annotated by GeneGo. Canonical pathway maps represent a set of about 650 signaling and metabolic maps covering human biology (signaling and metabolism) in a comprehensive way.

Western blot analysis

Total cell extracts were obtained by direct lysis of the cells in Laemmli-SDS-sample buffer. Western blot analysis was performed as described previously (Fousteri et al., 2006) and protein bands were analyzed and visualized with the Odyssey® Infrared Imaging System (LI-COR) using secondary antibodies labeled with visible fluorophores. Antibodies employed were: mouse α-γH2AX (Millipore), rabbit α-H2B (Santa-Cruz), mouse α-p53 (Santa Cruz Biotechnology DO-1), rabbit α-CDK7 (cell signaling), rabbit α-PLK1 (cell signaling), rabbit α-KPCD1 (cell signaling), rabbit α-centrin (cell signaling), rabbit α-E-cadherin (cell signaling) and rabbit α-mark2 (cell signaling).

Flowcytometry analysis

For cell cycle analysis, samples were either treated with 5 μM cisplatin for 0.5, 2, 4 or 8 hours or mock treated, after which EdU was added to a final concentration of 20 μM. Cells were collected 45 minutes after addition of EdU label and stained for EdU and DNA using the Click-iT EdU flow cytometry assay kit (Invitrogen) according to the manufacturer's protocol.

To determine the mitotic index, samples were either treated with 5 μM cisplatin for 0.5, 2, 4 or 8 hours, treated with 100 ng/ml nocodazole for 4 hours, or mock treated. Cells were collected and 10^6 cells were fixed with 70% ethanol. Cells were washed with PBS and incubated with Rb-α-Phospho (Ser10) Histone H3 antibody (Millipore). After washing, samples were incubated with Go-α-Rb Alexafluor 488 antibody (Invitrogen). After washing, cells were treated with RNase A (200 μg/ml) and stained with propidium iodide (Biorad). Cells were analyzed using a BD LSR II flowcytometer (BD Biosciences) and FACSDiva 5.0 software. Results were analyzed with WinMDI 2.8 software.

Immunofluorescence staining

Cells were fixed in 4% formaldehyde in CSK buffer (100 mM NaCl, 300 mM sucrose, 10mM PIPES pH 6.8, 3mM $MgCl_2$) and permeabilized by treatment with 0.5% Triton X-100 in PBS for 10 min. Actin was visualized by DY554-phalloidin (Sigma-Aldrich) and cells were counterstained with DAPI. Images were captured with a Zeiss Axioplan2 microscope equipped with a Zeiss Axiocam MRm camera using either a Plan-NEOFLUAR 40x/1.30 or 63x/1.25 objective.

siRNA transfection

HM1 mES cells were transfected with 50nM final concentration of siRNA (Dharmacon), targeting for CHK2, CDK7, MAPK2, M3K2, MK14, MARK1, PDPK1, PLK1, KPC1, KPCD1

and SG269, as well as siGFP (control 1) and siLAMIN A/C (control 2), which were used as negative controls. Transfection was performed using Dharmafect 1 (Dharmacon) according to the manufacturer's instructions. 10^3 HM1 mES cells were transfected for 16h in μClear® 96-well plates (Greiner), and the medium was refreshed every 24h for 48h.

Cell viability assay

At 64h post-siRNA transfection, HM1 mES cells were treated with either vehicle or 10μM of cisplatin (Ebewe Pharma) for 24h. ATP Lite ™ (Perkin Elmer) was then used according to the manufacturer's instructions for the assessment of cell viability. As an additional conformation that cisplatin was inducing apoptosis, the pan-caspase inhibitor benzyloxycarbonyl-Val-Ala-DL-Asp (OMe)-fluoromethylketone (zVAD-fmk) (Bachem, Bubendorf, Switzerland) was used to inhibit caspases and blocked cisplatin-induced apoptosis (supplementary figure 4A).

Gene expression analysis

The gene expression levels of Cdh1, p53, centrin2 and mark2 were quantified after exposure to 5μM cisplatin for 4 hours using quantitative reverse transcriptase PCR (qRT-PCR). The qRT-PCR was performed using the Applied 7900ht real-time PCR detection system (Applied Biosystems). In three independent experiments the RNA was isolated from mES and purified using an RNeasy-kit (Qiagen). qRT-PCR was performed using the FastStart Universal SYBR Green Master (Rox) (Roche) according to the manufacturer's instructions.

The following primers were used:

Cdh1 forward: atcctcgccctgctgatt and Cdh1 reverse: accaccgttctcctccgta.

- p53 forward: atgcccatgctacagaggag and p53 reverse: agactggccctttcttggtct.
- centrin2 forward: tgagactgggaaaatatcattcaa and centrin2 reverse: caccatctccatctcgatca
- mark2 forward: gaaagggacacggagcag and mark2 reverse: ccgcagcatgttggactt.
- mRNA expression values were normalized to the housekeeping genes: hypoxanthine-guanine phosphoribosyltransferase (HPRT).

SUPPLEMENTARY TABLES

Supplementary tables will be available at: http://mcb.asm.org/content/31/24/4964/suppl/DC1

Supplementary table 1 Phosphopeptides dataset

Supplementary table 2 Proteins dataset

Supplementary table 3 Peptides dataset

Supplementary table 4 phosphopeptide-data set merged with the protein-data set

Supplementary table 5 386 proteins and 56 mRNAs transcripts significantly affected by cisplatin treatment ($p<0.05$)

Supplementary table 6 Phosphopeptides dataset replicate experiment

Supplementary table 7 phosphopeptide-data set merged between the two replicate phosphopeptide experiments

REFERENCE LIST

1. Bartek,J. and J.Lukas. 2007. DNA damage checkpoints: from initiation to recovery or adaptation. *Curr. Opin. Cell Biol.* **19**: 238-245.
2. Bennetzen,M.V., D.H.Larsen, J.Bunkenborg, J.Bartek, J.Lukas, and J.S.Andersen. 2010. Site-specific phosphorylation dynamics of the nuclear proteome during the DNA damage response. *Mol. Cell Proteomics.* **9**: 1314-1323.
3. Bensimon,A., A.Schmidt, Y.Ziv, R.Elkon, S.Y.Wang, D.J.Chen, R.Aebersold, and Y.Shiloh. 2010. ATM-dependent and -independent dynamics of the nuclear phosphoproteome after DNA damage. *Sci. Signal.* **3**: rs3.
4. Borst,P., S.Rottenberg, and J.Jonkers. 2008. How do real tumors become resistant to cisplatin? *Cell Cycle* **7**: 1353-1359.
5. Brozovic,A. and M.Osmak. 2007. Activation of mitogen-activated protein kinases by cisplatin and their role in cisplatin-resistance. *Cancer Lett.* **251**: 1-16.
6. Choudhary,C. and M.Mann. 2010. Decoding signalling networks by mass spectrometry-based proteomics. *Nat. Rev. Mol. Cell Biol.* **11**: 427-439.
7. Cox,J. and M.Mann. 2008. MaxQuant enables high peptide identification rates, individualized p.p.b.-range mass accuracies and proteome-wide protein quantification. *Nat. Biotechnol.* **26**: 1367-1372.
8. Cox,J., I.Matic, M.Hilger, N.Nagaraj, M.Selbach, J.V.Olsen, and M.Mann. 2009. A practical guide to the MaxQuant computational platform for SILAC-based quantitative proteomics. *Nat. Protoc.* **4**: 698-705.
9. Degenhardt,Y. and T.Lampkin. 2010. Targeting Polo-like kinase in cancer therapy. *Clin. Cancer Res.* **16**: 384-389.
10. Drapkin,R., G.Le Roy, H.Cho, S.Akoulitchev, and D.Reinberg. 1996. Human cyclin-dependent kinase-activating kinase exists in three distinct complexes. *Proc. Natl. Acad. Sci. U. S. A* **93**: 6488-6493.
11. Dronkert,M.L. and R.Kanaar. 2001. Repair of DNA interstrand cross-links. *Mutat. Res.* **486**: 217-247.
12. Emert-Sedlak,L., S.Shangary, A.Rabinovitz, M.B.Miranda, S.M.Delach, and D.E.Johnson. 2005. Involvement of cathepsin D in chemotherapy-induced cytochrome c release, caspase activation, and cell death. *Mol. Cancer Ther.* **4**: 733-742.
13. Fousteri,M., W.Vermeulen, A.A.van Zeeland, and L.H.Mullenders. 2006. Cockayne syndrome A and B proteins differentially regulate recruitment of chromatin remodeling and repair factors to stalled RNA polymerase II in vivo. *Mol. Cell* **23**: 471-482.
14. Fu,Z., L.Malureanu, J.Huang, W.Wang, H.Li, J.M.van Deursen, D.J.Tindall, and J.Chen. 2008. Plk1-dependent phosphorylation of FoxM1 regulates a transcriptional programme required for mitotic progression. *Nat. Cell Biol.* **10**: 1076-1082.
15. Furuta,T., T.Ueda, G.Aune, A.Sarasin, K.H.Kraemer, and Y.Pommier. 2002. Transcription-coupled nucleotide excision repair as a determinant of cisplatin sensitivity of human cells. *Cancer Res.* **62**: 4899-4902.
16. Hall,M.D., M.Okabe, D.W.Shen, X.J.Liang, and M.M.Gottesman. 2008. The role of cellular accumulation in determining sensitivity to platinum-based chemotherapy. *Annu. Rev. Pharmacol. Toxicol.* **48**: 495-535.
17. Jackson,S.P. and J.Bartek. 2009. The DNA-damage response in human biology and disease. *Nature* **461**: 1071-1078.
18. Jimeno,A., B.Rubio-Viqueira, N.V.Rajeshkumar, A.Chan, A.Solomon, and M.Hidalgo. 2010. A fine-needle aspirate-based vulnerability assay identifies polo-like kinase 1 as a mediator of gemcitabine resistance in pancreatic cancer. *Mol. Cancer Ther.* **9**: 311-318.
19. Johannes,F.J., J.Prestle, S.Eis, P.Oberhagemann, and K.Pfizenmaier. 1994. PKCu is a novel, atypical member of the protein kinase C family. *J. Biol. Chem.* **269**: 6140-6148.
20. Johnson,L.N., M.E.Noble, and D.J.Owen. 1996. Active and inactive protein kinases: structural basis for regulation. *Cell* **85**: 149-158.
21. Karam,A.K., C.Santiskulvong, M.Fekete, S.Zabih, C.Eng, and O.Dorigo. 2010. Cisplatin and PI3kinase inhibition decrease invasion and migration of human ovarian carcinoma cells and regulate matrix-metalloproteinase expression. *Cytoskeleton (Hoboken.)* **67**: 535-544.
22. Kartalou,M. and J.M.Essigmann. 2001. Recognition of cisplatin adducts by cellular proteins. *Mutat. Res.* **478**: 1-21.
23. Keys,H.M., B.N.Bundy, F.B.Stehman, L.I.Muderspach, W.E.Chafe, C.L.Suggs, III,

J.L.Walker, and D.Gersell. 1999. Cisplatin, radiation, and adjuvant hysterectomy compared with radiation and adjuvant hysterectomy for bulky stage IB cervical carcinoma. *N. Engl. J. Med.* **340**: 1154-1161.

24. Kruse,J.J., J.P.Svensson, M.Huigsloot, M.Giphart-Gassler, W.G.Schoonen, J.E.Polman, H.G.Jean, W.B.van de, and H.Vrieling. 2007. A portrait of cisplatin-induced transcriptional changes in mouse embryonic stem cells reveals a dominant p53-like response. *Mutat. Res.* **617**: 58-70.
25. Laoukili,J., M.R.Kooistra, A.Bras, J.Kauw, R.M.Kerkhoven, A.Morrison, H.Clevers, and R.H.Medema. 2005. FoxM1 is required for execution of the mitotic programme and chromosome stability. *Nat. Cell Biol.* **7**: 126-136.
26. Loehrer,P.J. and L.H.Einhorn. 1984. Drugs five years later. Cisplatin. *Ann. Intern. Med.* **100**: 704-713.
27. Macek,B., M.Mann, and J.V.Olsen. 2009. Global and site-specific quantitative phosphoproteomics: principles and applications. *Annu. Rev. Pharmacol. Toxicol.* **49**: 199-221.
28. Macurek,L., A.Lindqvist, D.Lim, M.A.Lampson, R.Klompmaker, R.Freire, C.Clouin, S.S.Taylor, M.B.Yaffe, and R.H.Medema. 2008. Polo-like kinase-1 is activated by aurora A to promote checkpoint recovery. *Nature* **455**: 119-123.
29. Mandic,A., J.Hansson, S.Linder, and M.C.Shoshan. 2003. Cisplatin induces endoplasmic reticulum stress and nucleus-independent apoptotic signaling. *J. Biol. Chem.* **278**: 9100-9106.
30. Matsuoka,S., B.A.Ballif, A.Smogorzewska, E.R.McDonald, III, K.E.Hurov, J.Luo, C.E.Bakalarski, Z.Zhao, N.Solimini, Y.Lerenthal, Y.Shiloh, S.P.Gygi, and S.J.Elledge. 2007. ATM and ATR substrate analysis reveals extensive protein networks responsive to DNA damage. *Science* **316**: 1160-1166.
31. McWhinney,S.R., R.M.Goldberg, and H.L.McLeod. 2009. Platinum neurotoxicity pharmacogenetics. *Mol. Cancer Ther.* **8**: 10-16.
32. Morris,M., P.J.Eifel, J.Lu, P.W.Grigsby, C.Levenback, R.E.Stevens, M.Rotman, D.M.Gershenson, and D.G.Mutch. 1999. Pelvic radiation with concurrent chemotherapy compared with pelvic and para-aortic radiation for high-risk cervical cancer. *N. Engl. J. Med.* **340**: 1137-1143.
33. Mross,K., A.Frost, S.Steinbild, S.Hedbom, J.Rentschler, R.Kaiser, N.Rouyrre, D.Trommeshauser, C.E.Hoesl, and G.Munzert. 2008. Phase I dose escalation and pharmacokinetic study of BI 2536, a novel Polo-like kinase 1 inhibitor, in patients with advanced solid tumors. *J. Clin. Oncol.* **26**: 5511-5517.
34. Nigg,E.A. 2001. Mitotic kinases as regulators of cell division and its checkpoints. *Nat. Rev. Mol. Cell Biol.* **2**: 21-32.
35. Nolen,B., S.Taylor, and G.Ghosh. 2004. Regulation of protein kinases; controlling activity through activation segment conformation. *Mol. Cell* **15**: 661-675.
36. O'Farrell,P.H. 2001. Triggering the all-or-nothing switch into mitosis. *Trends Cell Biol.* **11**: 512-519.
37. Oliver,T.G., K.L.Mercer, L.C.Sayles, J.R.Burke, D.Mendus, K.S.Lovejoy, M.H.Cheng, A.Subramanian, D.Mu, S.Powers, D.Crowley, R.T.Bronson, C.A.Whittaker, A.Bhutkar, S.J.Lippard, T.Golub, J.Thomale, T.Jacks, and E.A.Sweet-Cordero. 2010. Chronic cisplatin treatment promotes enhanced damage repair and tumor progression in a mouse model of lung cancer. *Genes Dev.* **24**: 837-852.
38. Olsen,J.V., B.Blagoev, F.Gnad, B.Macek, C.Kumar, P.Mortensen, and M.Mann. 2006. Global, in vivo, and site-specific phosphorylation dynamics in signaling networks. *Cell* **127**: 635-648.
39. Olsen,J.V., L.M.de Godoy, G.Li, B.Macek, P.Mortensen, R.Pesch, A.Makarov, O.Lange, S.Horning, and M.Mann. 2005. Parts per million mass accuracy on an Orbitrap mass spectrometer via lock mass injection into a C-trap. *Mol. Cell Proteomics.* **4**: 2010-2021.
40. Olsen,J.V., B.Macek, O.Lange, A.Makarov, S.Horning, and M.Mann. 2007. Higher-energy C-trap dissociation for peptide modification analysis. *Nat. Methods* **4**: 709-712.
41. Olsen,J.V., J.C.Schwartz, J.Griep-Raming, M.L.Nielsen, E.Damoc, E.Denisov, O.Lange, P.Remes, D.Taylor, M.Splendore, E.R.Wouters, M.Senko, A.Makarov, M.Mann, and S.Horning. 2009. A dual pressure linear ion trap Orbitrap instrument with very high sequencing speed. *Mol. Cell Proteomics.* **8**: 2759-2769.
42. Olsen,J.V., M.Vermeulen, A.Santamaria, C.Kumar, M.L.Miller, L.J.Jensen, F.Gnad, J.Cox, T.S.Jensen, E.A.Nigg, S.Brunak, and M.Mann. 2010. Quantitative phosphoproteomics reveals widespread full phosphorylation site occupancy during mitosis. *Sci. Signal.* **3**: ra3.

43. Ong,S.E., B.Blagoev, I.Kratchmarova, D.B.Kristensen, H.Steen, A.Pandey, and M.Mann. 2002. Stable isotope labeling by amino acids in cell culture, SILAC, as a simple and accurate approach to expression proteomics. *Mol. Cell Proteomics.* **1**: 376-386.
44. Paduch,R., W.Rzeski, and J.Klatka. 2009. The effect of cisplatin on human larynx carcinoma cell motility. *Folia Histochem. Cytobiol.* **47**: 75-79.
45. Pellegrini,M., A.Celeste, S.Difilippantonio, R.Guo, W.Wang, L.Feigenbaum, and A.Nussenzweig. 2006. Autophosphorylation at serine 1987 is dispensable for murine Atm activation in vivo. *Nature* **443**: 222-225.
46. Quarmby,L.M. and M.R.Mahjoub. 2005. Caught Nek-ing: cilia and centrioles. *J. Cell Sci.* **118**: 5161-5169.
47. Ramer,R., K.Eichele, and B.Hinz. 2007. Upregulation of tissue inhibitor of matrix metalloproteinases-1 confers the anti-invasive action of cisplatin on human cancer cells. *Oncogene* **26**: 5822-5827.
48. Reardon,J.T., H.Ge, E.Gibbs, A.Sancar, J.Hurwitz, and Z.Q.Pan. 1996. Isolation and characterization of two human transcription factor IIH (TFIIH)-related complexes: ERCC2/CAK and TFIIH. *Proc. Natl. Acad. Sci. U. S. A* **93**: 6482-6487.
49. Reinhardt,H.C., A.S.Aslanian, J.A.Lees, and M.B.Yaffe. 2007a. p53-deficient cells rely on ATM- and ATR-mediated checkpoint signaling through the p38MAPK/MK2 pathway for survival after DNA damage. *Cancer Cell* **11**: 175-189.
50. Reinhardt,H.C., A.S.Aslanian, J.A.Lees, and M.B.Yaffe. 2007b. p53-deficient cells rely on ATM- and ATR-mediated checkpoint signaling through the p38MAPK/MK2 pathway for survival after DNA damage. *Cancer Cell* **11**: 175-189.
51. Reinhardt,H.C. and M.B.Yaffe. 2009. Kinases that control the cell cycle in response to DNA damage: Chk1, Chk2, and MK2. *Curr. Opin. Cell Biol.* **21**: 245-255.
52. Ridley,A.J. 2001. Rho GTPases and cell migration. *J. Cell Sci.* **114**: 2713-2722.
53. Rigbolt,K.T., T.A.Prokhorova, V.Akimov, J.Henningsen, P.T.Johansen, I.Kratchmarova, M.Kassem, M.Mann, J.V.Olsen, and B.Blagoev. 2011. System-wide temporal characterization of the proteome and phosphoproteome of human embryonic stem cell differentiation. *Sci. Signal.* **4**: rs3.
54. Safaei,R. and S.B.Howell. 2005. Copper transporters regulate the cellular pharmacology and sensitivity to Pt drugs. *Crit Rev. Oncol. Hematol.* **53**: 13-23.
55. Safaei,R., K.Katano, B.J.Larson, G.Samimi, A.K.Holzer, W.Naerdemann, M.Tomioka, M.Goodman, and S.B.Howell. 2005. Intracellular localization and trafficking of fluorescein-labeled cisplatin in human ovarian carcinoma cells. *Clin. Cancer Res.* **11**: 756-767.
56. Scrace,S.F., P.Kierstan, J.Borgognoni, L.Z.Wang, S.Denny, J.Wayne, C.Bentley, A.D.Cansfield, P.S.Jackson, A.M.Lockie, N.J.Curtin, D.R.Newell, D.S.Williamson, and J.D.Moore. 2008. Transient treatment with CDK inhibitors eliminates proliferative potential even when their abilities to evoke apoptosis and DNA damage are blocked. *Cell Cycle* **7**: 3898-3907.
57. Sgarra,R., E.Maurizio, S.Zammitti, S.A.Lo, V.Giancotti, and G.Manfioletti. 2009. Macroscopic differences in HMGA oncoproteins post-translational modifications: C-terminal phosphorylation of HMGA2 affects its DNA binding properties. *J. Proteome. Res.* **8**: 2978-2989.
58. Sgarra,R., A.Rustighi, M.A.Tessari, J.Di Bernardo, S.Altamura, A.Fusco, G.Manfioletti, and V.Giancotti. 2004. Nuclear phosphoproteins HMGA and their relationship with chromatin structure and cancer. *FEBS Lett.* **574**: 1-8.
59. Soufi,B., C.D.Kelstrup, G.Stoehr, F.Frohlich, T.C.Walther, and J.V.Olsen. 2009. Global analysis of the yeast osmotic stress response by quantitative proteomics. *Mol. Biosyst.* **5**: 1337-1346.
60. Stokes,M.P., J.Rush, J.MacNeill, J.M.Ren, K.Sprott, J.Nardone, V.Yang, S.A.Beausoleil, S.P.Gygi, M.Livingstone, H.Zhang, R.D.Polakiewicz, and M.J.Comb. 2007. Profiling of UV-induced ATM/ATR signaling pathways. *Proc. Natl. Acad. Sci. U. S. A* **104**: 19855-19860.
61. Takai,N., R.Hamanaka, J.Yoshimatsu, and I.Miyakawa. 2005. Polo-like kinases (Plks) and cancer. *Oncogene* **24**: 287-291.
62. Tichy,E.D. and P.J.Stambrook. 2008. DNA repair in murine embryonic stem cells and differentiated cells. *Exp. Cell Res.* **314**: 1929-1936.
63. Todd,R.C. and S.J.Lippard. 2009. Inhibition of transcription by platinum antitumor compounds. *Metallomics.* **1**: 280-291.

64. Torres,J.Z., K.H.Ban, and P.K.Jackson. 2010. A specific form of phospho protein phosphatase 2 regulates anaphase-promoting complex/cyclosome association with spindle poles. *Mol. Biol. Cell* **21**: 897-904.

65. Tsvetkov,L. and D.F.Stern. 2005. Phosphorylation of Plk1 at S137 and T210 is inhibited in response to DNA damage. *Cell Cycle* **4**: 166-171.

66. Tyagi,S., K.Bhui, R.Singh, M.Singh, S.Raisuddin, and Y.Shukla. 2010. Polo-like kinase1 (Plk1) knockdown enhances cisplatin chemosensitivity via up-regulation of p73alpha in p53 mutant human epidermoid squamous carcinoma cells. *Biochem. Pharmacol.* **80**: 1326-1334.

67. Umikawa,M., H.Obaishi, H.Nakanishi, K.Satoh-Horikawa, K.Takahashi, I.Hotta, Y.Matsuura, and Y.Takai. 1999. Association of frabin with the actin cytoskeleton is essential for microspike formation through activation of Cdc42 small G protein. *J. Biol. Chem.* **274**: 25197-25200.

68. van Vugt,M.A., A.Bras, and R.H.Medema. 2005. Restarting the cell cycle when the checkpoint comes to a halt. *Cancer Res.* **65**: 7037-7040.

69. Villen,J., S.A.Beausoleil, S.A.Gerber, and S.P.Gygi. 2007. Large-scale phosphorylation analysis of mouse liver. *Proc. Natl. Acad. Sci. U. S. A* **104**: 1488-1493.

70. Wang,D., R.Hara, G.Singh, A.Sancar, and S.J.Lippard. 2003. Nucleotide excision repair from site-specifically platinum-modified nucleosomes. *Biochemistry* **42**: 6747-6753.

71. Wang,D. and S.J.Lippard. 2005. Cellular processing of platinum anticancer drugs. *Nat. Rev. Drug Discov.* **4**: 307-320.

72. Wang,I.C., Y.J.Chen, D.Hughes, V.Petrovic, M.L.Major, H.J.Park, Y.Tan, T.Ackerson, and R.H.Costa. 2005. Forkhead box M1 regulates the transcriptional network of genes essential for mitotic progression and genes encoding the SCF (Skp2-Cks1) ubiquitin ligase. *Mol. Cell Biol.* **25**: 10875-10894.

73. Wang,L., L.Yang, M.Debidda, D.Witte, and Y.Zheng. 2007. Cdc42 GTPase-activating protein deficiency promotes genomic instability and premature aging-like phenotypes. *Proc. Natl. Acad. Sci. U. S. A* **104**: 1248-1253.

74. Waterman-Storer,C.M. and E.Salmon. 1999. Positive feedback interactions between microtubule and actin dynamics during cell motility. *Curr. Opin. Cell Biol.* **11**: 61-67.

75. Welsh,C., R.Day, C.McGurk, J.R.Masters, R.D.Wood, and B.Koberle. 2004. Reduced levels of XPA, ERCC1 and XPF DNA repair proteins in testis tumor cell lines. *Int. J. Cancer* **110**: 352-361.

76. Zeidan,Y.H., R.W.Jenkins, and Y.A.Hannun. 2008. Remodeling of cellular cytoskeleton by the acid sphingomyelinase/ceramide pathway. *J. Cell Biol.* **181**: 335-350.

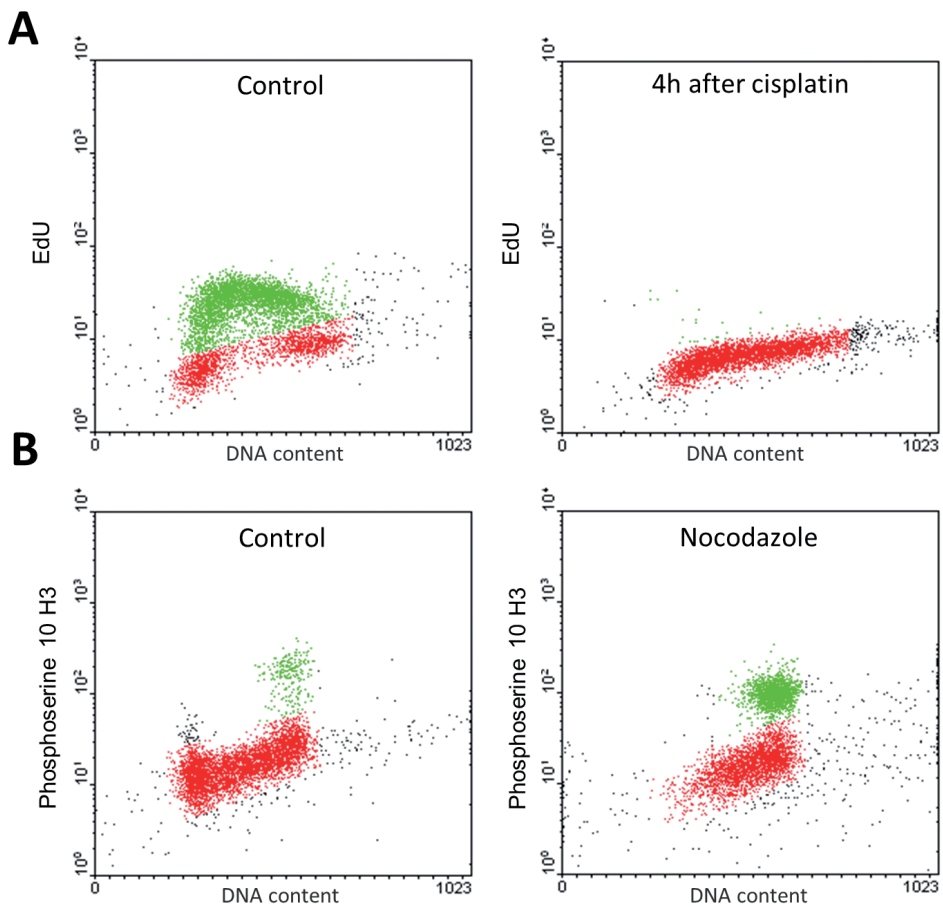

FigureS1. (A) FACS analysis of B4418 mES cells either mock or cisplatin (5 μM) treated for 4 hours and labeled by EdU for 45 minutes. Cells positive for EdU incorporation are indicated by green dots. The DNA content was analyzed by propidium iodide staining. **(B)** FACS analysis of mES cells either mock or Nocodazole treated for 2 hours. Cells positive for Phospho (Ser10) Histone H3 are indicated by green dots.

2 A

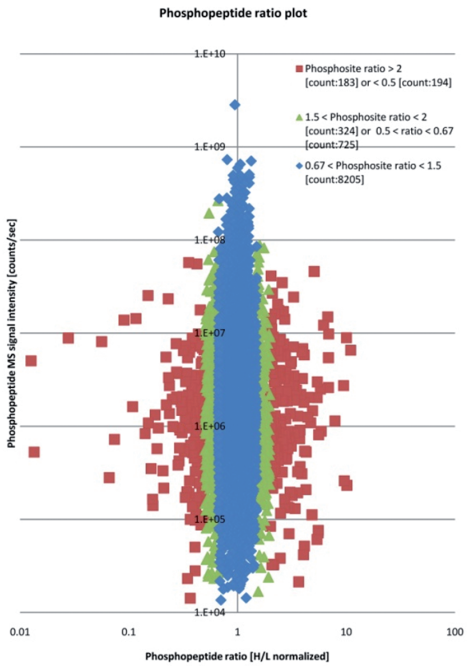

B

Gene Names	Phosphosite position	SILAC Ratio H/L
Brca1	1422	11,01
Pctk2	180	10,15
Tnk1	515	10,05
Rtc5	7	9,59
Tsg118	165	9,46
Mdc1	176	7,88
Arhgef19	336	6,89
Uhrf1	169	6,87
Trp53bp1	305	6,86
Hmga1	9	6,77
Rsf1	528	6,19
Taf1c	763	5,88
Acin1	380	5,79
Kdm4b	453	5,58
Brca1	1197	5,53
Chek1	317	5,52
Bard1	543	5,42
Srrm2	375	5,39
Srrm2	385	5,39
Ppm1g	201	5,38
Mcm6	13	5,08
Smtn	798	4,89
Impact	9	4,84
Hdac3	74	4,71
Cggbp1	164	4,50
Chd1	1396	4,45
Ncapd2	598	4,28
Ncapd2	1300	4,26
Rad51c	365	4,15
Orc1l	258	4,12
Orc1l	255	4,12
Mki67	2185	4,11
Wdhd1	898	4,09
Ranbp3	283	4,05
Ranbp3	277	4,05
Pus7	40	3,98
Palb2	154	3,96
Nsmce4a	375	3,91
Pus1	103	3,90
Nbn	398	3,83
Rps6ka6	510	3,76
Psma1	247	3,75
Rad50	690	3,73
Ncl	425	3,66
Zmym4	1065	3,64
Nbn	58	3,59
Numa1	270	3,58
Hp1bp3	144	3,57
Tnks1bp1	1611	3,49
H2ax	140	3,39

C

Gene Names	Phosphosite position	SILAC Ratio H/L
Kcne4	69	0,01
Golga4	891	0,01
Klf3	91	0,03
Bat2d1	1051	0,06
Rbm20	1020	0,07
Aff1	764	0,07
Rbm33	531	0,09
Aof2	167	0,11
Rad51ap1	256	0,12
Mtl5	178	0,14
Sptbn1	2186	0,15
Syt13	67	0,15
Trappc9	971	0,16
Triobp	328	0,17
Triobp	324	0,17
8030462N17Rik	147	0,17
4930594M22Rik	5	0,17
Pds5b	1176	0,18
Nbr1	701	0,19
Nbr1	700	0,19
Slc7a1	616	0,21
Kiaa1305	615	0,21
Rbm33	816	0,22
Parg	297	0,22
Nacc1	145	0,23
Kdm1	132	0,23
Ythdf2	2	0,24
Map7d1	275	0,24
Utf1	99	0,25
Map3k7ip1	7	0,25
Map4	99	0,27
Eif4ebp2	65	0,27
Nfatc4	264	0,28
Acin1	137	0,28
Pcm1	1826	0,28
OTTMUSG00000016543	70	0,29
Rod1	27	0,29
Ag2	210	0,29
Atad2	168	0,29
Acaca	1296	0,30
Acaca	1300	0,30
Nfatc4	120	0,31
Gapvd1	996	0,31
Asxl2	1254	0,31
Brd8	175	0,31
Arhgap11a	946	0,32
Nfatc4	217	0,33
Nfatc4	213	0,33
Esrrb	207	0,33
Slc1a4	507	0,33

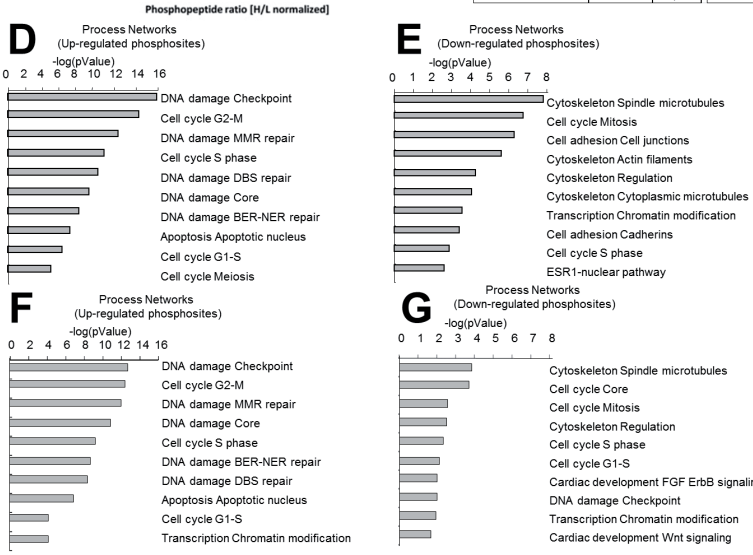

FigureS2. (A) Proteins containing both phosphorylated and dephosphorylated sites. **(B)** Process Networks analysis of proteins containing both phosphorylated and dephosphorylated sites (MetaCore software). **(C)** protein-protein interaction map.

A **Cell cycle and its regulation**

Pathways	up-regulated phospho-sites (>1.5-fold) pValue	up-regulated phospho-sites (>2-fold) pValue
1 DNA damage ATM/ATR regulation of G1/S checkpoint	$4.72\ 10^{-18}$	$2.989\ 10^{-11}$
2 DNA damage ATM / ATR regulation of G2 / M checkpoint	$1.63\ 10^{-12}$	$1.765\ 10^{-8}$

B **DNA-damage response**

Pathways	pValue	pValue
1 DNA damage Role of Brca1 and Brca2 in DNA repair	$1.49\ 10^{-18}$	$3.054\ 10^{-15}$
2 DNA damage Role of NFBD1 in DNA damage response	$1.84\ 10^{-14}$	$4.047\ 10^{-15}$
3 DNA damage DNA-damage-induced responses	$7.88\ 10^{-10}$	$1.661\ 10^{-9}$

C **Apoptosis**

Pathways	pValue	pValue
1 Apoptosis and survival DNA-damage-induced apoptosis	$1.23\ 10^{-13}$	$4.068\ 10^{-10}$
2 Apoptosis and survival p53-dependent apoptosis	$1.64\ 10^{-7}$	$4.352\ 10^{-5}$
3 Transcription P53 signaling pathway	$2.1\ 10^{-5}$	$2.976\ 10^{-2}$

D

Pathways	down-regulated phospho-sites (>1.5-fold) pValue	down-regulated phospho-sites (>2-fold) pValue
1 G-protein signaling regulation of RAC1 activity	$4.26\ 10^{-6}$	$1.376\ 10^{-2}$
2 Cell adhesion endothelial cell contacts by junctional mechanisms	$7.42\ 10^{-6}$	$1.22\ 10^{-1}$
3 Cell cycle role of APC in cell cycle regulation	$2.76\ 10^{-5}$	$5.18\ 10^{-4}$
4 Cell cycle initiation of mitosis	$9.32\ 10^{-5}$	$1.178\ 10^{-1}$
5 G-protein signaling regulation of CDC42 activity	$3.78\ 10^{-4}$	$5.678\ 10^{-4}$

E

Pathways	pValue
1 Development NOTCH signaling pathway	$7.1\ 10^{-5}$
2 Development NOTCH-induced EMT	$7.3\ 10^{-5}$

FigureS3: Topscores of most statistically relevant (lowest p value) pathways obtained from phosphopeptides up-regulated more than 1.5 and 2-fold after cisplatin treatment. **(A)** Cell cycle and its regulation. **(B)** DNA-damage response. **(C)** Apoptosis. **(D)** Topscores of, most statistically relevant (lowest p value), pathways obtained from phosphopeptides down-regulated more than 1.5 and 2-fold after cisplatin treatment. **(E)** Most statistically relevant pathways among of proteins with altered expression ($p<0.05$) after cisplatin treatment.

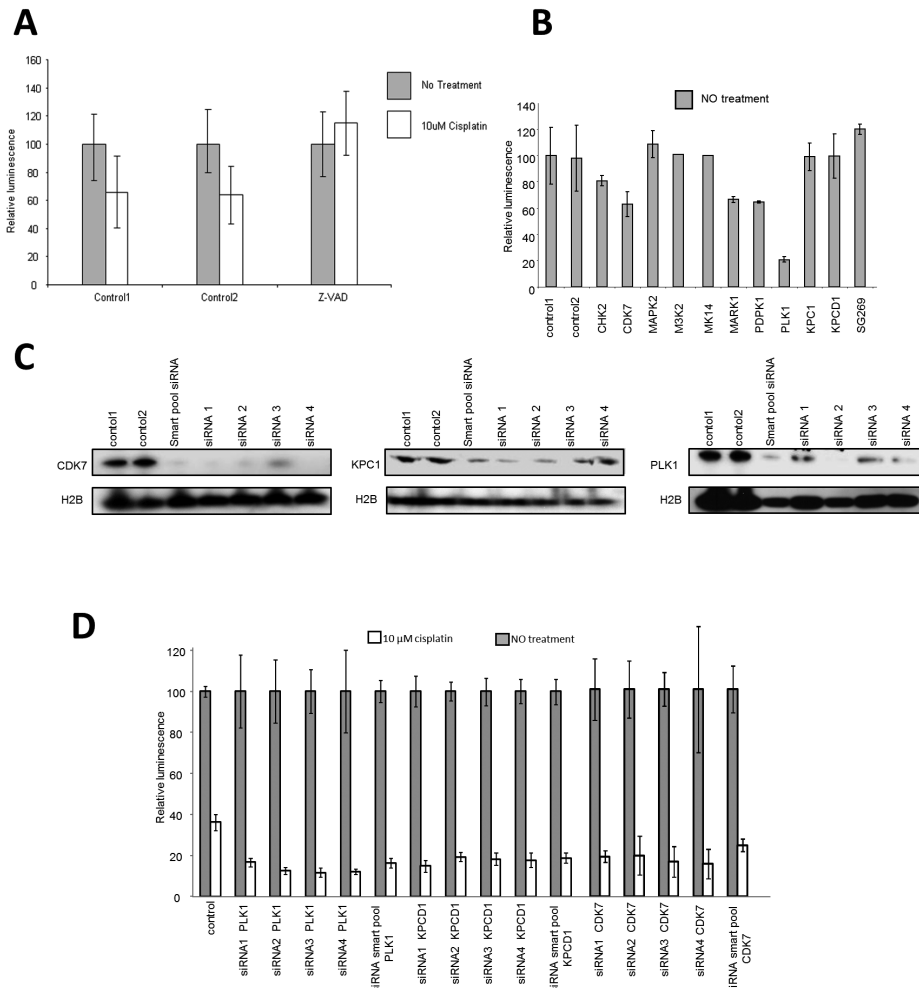

FigureS4. (A) Cell viability in presence of cisplatin. siGFP (control 1) and siLAMIN C/A (control 2) were used as negative controls. Cell viability could be restored by addition of the pan-caspase inhibitor (Z-VAD). **(B)** Cell viability in absence of cisplatin was investigated after siRNA knockdown. Luminescence is relative to control 1. **(C)** The protein level of CDK7, PLK1, and KPCD1 kinases was determined by western-blot to test the protein knockdown for four independent siRNAs. **(D)** Four independent siRNAs for CDK7, PLK1, and KPCD1 kinases were used to test the cellular sensitivity for cisplatin by an Adenosine TriPhosphate (ATP) monitoring system. siGFP (control) was used as negative controls (two independent experiments).

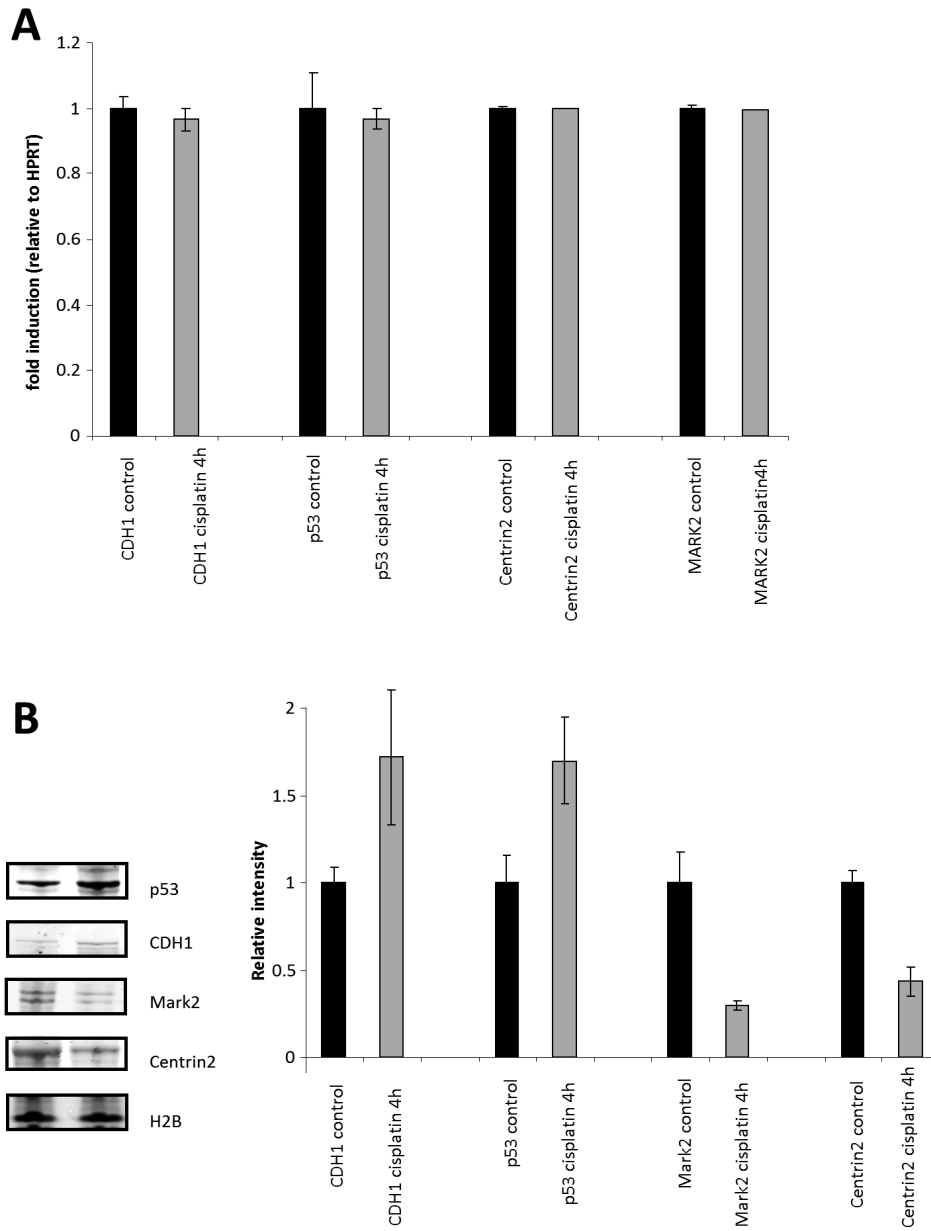

FigureS5. (A) Relative gene expression levels of Cdh1, p53, centrin2 and Mark2 measured by quantitative RT-PCR. mES cells were mock treated (control;black bars) or treated for 4 hours 5μM cisplatin (grey bars). (three independent experiments) **(B)** Relative protein levels of Cdh1, p53, centrin2 and Mark2 measured by western-blot between control (black bars) and 4 hours after 5μM cisplatin (grey bars) in mES (three independent experiments).

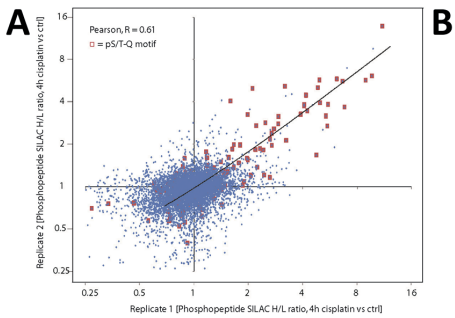

B

Gene Names	Phosphopeptide Sequence *Potential ATM/ATR substrates*	Ratio H/L Normalized Replicate 1	Ratio H/L Normalized Replicate 2
Brca1	NINENPVS(ph)QNLK	11.02	13.82
Numa1	QAASS(ph)QEPSELEELR	9.65	6.11
Hmga1	(ac)SESGSKSS(ph)QPLASK	8.91	5.68
Chek1	FSSS(ph)QPEPR	6.81	3.66
Trp53bp1	ELLEEGPQVQPSSEPEVSST(ph)QEDLFDQSSK	6.63	5.62
Rsf1	GIDSSVPDIESLS(ph)QK	6.17	5.82
Taf1c	VPPS(ph)QELTQEVWGQGVK	5.51	3.84
Rad51c	DAVVTAASS(ph)QTESSLNFR	5.47	2.69
Capd2	GMDGIEEFETGQQGGS(ph)QR	5.38	3.18
Capd2	DSPSVPEPEGS(ph)QSNDELVK	4.98	3.94
Mcm6	(ac)MDLAAAAEPGAGS(ph)QHPEVR	4.95	5.71
Smg9	(ac)SES(ph)GHS(ph)QPGLYGIER	4.75	1.67
Wdhd1	SGAVFSSS(ph)QGWVVNPFK	4.24	3.46
Palb2	SSVS(ph)QEKEDYFDTNSLALLGK	4.16	4.46
Trp53bp1	LPADSENVLVTPS(ph)QDDQVEMSQNVDK	4.08	3.83
Nsmce4a	TFEISEPVIPLSQS(ph)QQR	4.06	3.75
Non	NHAVLTVNFPVTSLS(ph)QTDEIPTLTIK	3.89	3.26
Trim28	(gl)QSGSSS(ph)QPMEVQEGYGFGSDDPYSSAEPHVSGMK	3.23	2.12
Hp1bp3	TIPAWATLSAS(ph)QLAR	3.18	5.16
Ppp1r7	GAGQQQS(ph)QEMMEVDR	2.93	3.15
Mapk14	(ac)S(ph)QERPTFYR	2.92	2.78
Pafah1b2	(ac)S(ph)QGDSNPAAIPHAAEDIQGDDR	2.77	2.57
Srrm2	SLLPNSS(ph)QDELMEVEK	2.69	2.39
Trp53bp1	LMLSTSEYS(ph)QSSK	2.64	2.18
Pdzd4	GAPDGGPGLNNS(ph)QDLDSGVGR	2.63	1.16
Ppp1	SELLVPGS(ph)QLDLGAR	2.48	2.85
Smg8	ALNSDMPLVILSSS(ph)QGR	2.44	1.21
Atm	SPTFEEGS(ph)QGTTSSLSEK	2.41	1.82
Smc1a	GTMDDISQEEGSS(ph)QGEESVSGSQR	2.31	1.86
Pds5a	AAGS(ph)QESLEAGNAK	2.21	2.71
Gclc	GLLS(ph)QGSPLSWEETQR	2.19	1.83
Srrm2	VGLFSS(ph)QK	2.11	4.97
Rbm14	LSES(ph)QLSFR	2.06	1.20
Myst3	LFGS(ph)QEIMTER	1.98	3.25
Enah	(gl)QNS(ph)QLPAQVQNGPSQEELEIQRR	1.96	1.59
Mdu1	(ac)S(ph)QDTEVDMKDVELNELEPEKQPMNAADGAAAGEK	1.77	1.47
Ercc3	QYEEEEEDEDDIPGNES(ph)QEAVPSAAGK	1.66	1.98
Pou2f1	(ac)ADGGAAS(ph)QDESSAAAAAAADSR	1.63	1.85
Psma1	AQPS(ph)QAAEEPAEKADEPMEH	1.59	4.05
Sfrs2ip	HNLDNS(ph)QSDKFLEETTESLVEHPIHAELPHKEVDQSEK	1.55	1.61

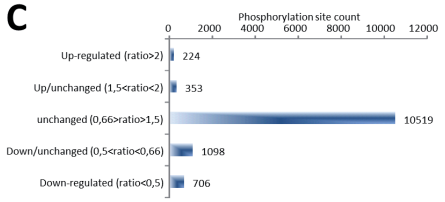

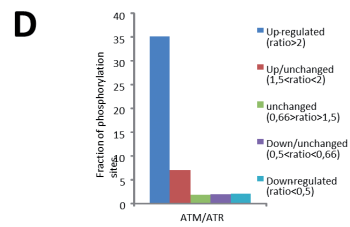

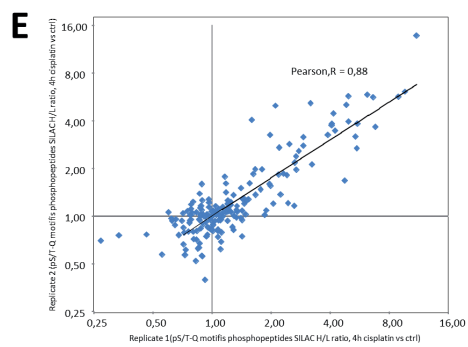

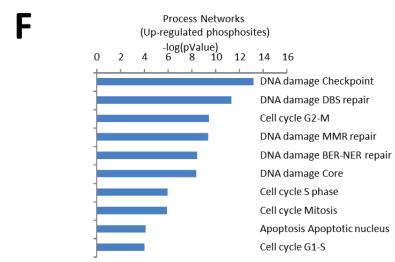

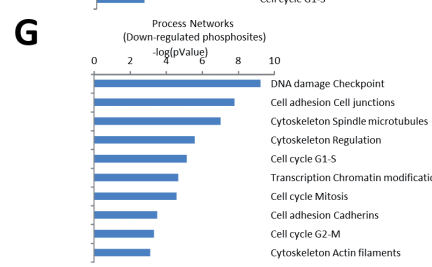

FigureS6. (A) Phosphopeptide ratio plot between the two replicate phosphopeptide experiments. ATM/ATR substrate phosphopeptides are represented in red **(B)** Top 40 ATM/ATR substrates up-regulated phosphopeptides in the two replicates. **(C)** Number of phosphopeptides up-regulated (>2), down regulated (<0.5), up/unchanged (1.5<ratio>2) and down/unchanged (0.5<ratio>0.66) (second experiment). **(D)** Consensus sequence for ATM/ATR kinases among up-regulated, down-regulated, and unmodified phosphorylation sites (second experiment). **(E)** pS/T-Q motifi phosphopeptide ratio plot between the two replicate phosphopeptide experiments. **(F)** MetaCore network analysis of proteins containing more than 2-fold up-regulated phosphorylation sites after cisplatin treatment (second experiment). **(G)** MetaCore network analysis of proteins containing more than 2-fold down-regulated phosphorylation sites after cisplatin treatment (second experiment).

6

Increased DNA damage sensitivity of Cornelia de Lange syndrome cells: Evidence for impaired recombinational repair

Mischa G. Vrouwe, Elhaam Elghalbzouri-Maghrani, Matty Meijers, Peter Schouten, Barbara C. Godthelp, Zahurul A. Bhuiyan, Egbert J.Redeker, Marcel M. Mannens, Leon H. F. Mullenders, Albert Pastink and Firouz Darroudi

Human molecular genetics. Jun 15; 16(12):1478-87. 2007

ABSTRACT

Cornelia de Lange syndrome (CdLS) is a rare dominantly inherited multisystem disorder affecting both physical and mental development. Heterozygous mutations in the *NIPBL* gene were found in about half of CdLS cases. Scc2, the fungal ortholog of the *NIPBL* gene product, is essential for establishing sister chromatid cohesion. In yeast, the absence of cohesion leads to chromosome missegregation and defective repair of DNA double-strand breaks. To evaluate possible DNA repair defects in CdLS cells, we characterized the cellular responses to DNA-damaging agents. We show that cells derived from CdLS patients, both with and without detectable *NIPBL* mutations, have an increased sensitivity for mitomycin C (MMC). Exposure of CdLS fibroblast and B-lymphoblastoid cells to MMC leads to enhanced cell killing and reduced proliferation and, in the case of primary fibroblasts, an increased number of chromosomal aberrations. After X-ray exposure increased numbers of chromosomal aberrations were also detected, but only in cells irradiated in the G_2 phase of the cell cycle when repair of double-strand breaks is dependent on the establishment of sister chromatid cohesion. Repair at the G_1 stage is not affected in CdLS cells. Our studies indicate that CdLS cells have a reduced capacity to tolerate DNA damage, presumably as a result of reduced DNA repair through homologous recombination.

INTRODUCTION

Cornelia de Lange Syndrome (CdLS; OMIM 122470) is a rare multisystem developmental disorder with characteristic facial dysmorphia, growth and cognitive retardation, malformations of the upper limbs and a variety of other abnormalities affecting a wide range of tissues and organs (Jackson et al., 1993;Van Den Berg and Francke, 1993;Ireland et al., 1993). The prevalence of CdLS is estimated to be as high as 1/10.000 to 1/30.000 and most cases are sporadic. CdLS is genetically heterogeneous and at present three disease-causing genes have been identified, all of which are implicated in sister chromatid cohesion. Approximately half of CdLS patients carry heterozygous mutations in the *NIPBL* gene (Krantz et al., 2004;Tonkin et al., 2004;Gillis et al., 2004;Borck et al., 2004;Bhuiyan et al., 2006;Schoumans et al., 2007). Recently, mutations in the X-linked *SMC1A* gene have been identified in about 5% of the CdLS cases. One CdLS patient is currently known carrying a mutation in *SMC3* (Musio et al., 2006;Borck et al., 2007;Deardorff et al., 2007). Primarily truncation mutations and amino acid substitutions have been observed. Large rearrangements of *NIPBL* do occur in CdLS but are likely to be infrequent (Bhuiyan et al., 2007). The majority of affected individuals carry *de novo* mutations and only a very few familial cases of CdLS have been reported.

The *NIPBL* gene is predicted to code for two isoforms of 2804 and 2697 amino acids, termed delangin-A and delangin-B, respectively. The human delangin proteins share homology with Nipped-B from *D. melanogaster* and Scc2 from *S. cerevisiae*. Scc2 and its orthologs have an essential role in sister chromatid cohesion, which is crucial for proper chromosome segregation during mitosis (Michaelis et al., 1997). In fungi the cohesin complex consists of two SMC (structural maintenance of chromosomes) proteins, Smc1 and Smc3 and two non-SMC proteins, Scc1/Mcd1/Rad21 and Scc3. In vertebrates Scc3 exists as two isoforms called SA1 and SA2. Live-cell imaging experiments in mammalian cells revealed that cohesin dynamically binds to DNA during most of the cell cycle, but it is during S phase that cohesin becomes stably bound to DNA to mediate cohesion of sister chromatids until segregation (Gerlich et al., 2006). The Scc2 protein in *S. cerevisiae* is not a subunit of cohesin but functions in collaboration with Scc4 as a cohesin loading complex (Ciosk et al., 2000). Analogous to the function of Scc2 and Scc4 in *S. cerevisiae* the *NIPBL* gene product, in conjunction with human Scc4, was shown to facilitate the chromatin association of cohesin subunits (Watrin et al., 2006;Seitan et al., 2006). Loading of cohesin occurs on unreplicated DNA. Establishment of cohesion between sister chromatids occurs during S-phase and is dependent on the acetyltransferase protein Eco1/Ctf7/Eso1 in yeast. Although the cohesin complex can be loaded in its absence, Eco1, via its interaction with PCNA, facilitates cohesion at the replication fork (Moldovan et al., 2006;Lengronne et al., 2006). Recently mutations in the *ESCO2* gene, one of the human *Eco1* orthologs, were shown to be associated with Roberts syndrome (OMIM 268300), a disorder with characteristics similar to CdLS (Vega et al., 2005).

Physical linkage of sister chromatids by the cohesin complex is essential for correct chromosome segregation, but is also vital for DNA double-strand break (DSB) repair by homologous recombination (HR) during the S and G_2 phase of the cell cycle (Sjogren and

Nasmyth, 2001). Inactivation of either Scc2/Scc4 or one of the cohesin subunits results in a reduced efficiency of postreplicative DSB repair in G_2/M cells. Recently, it became evident that cohesin is specifically recruited to sites of DSBs. Evidence presented by Ström *et al*. and Ünal *et al*. showed that the local enrichment of cohesin depends on the Scc2/Scc4 complex (Strom et al., 2004;Unal et al., 2004). This damage specific recruitment of the cohesin complex is however distinct from its normal chromatin binding because of the dependence on γH2AX and Mre11 proteins which are required for DSB repair (Unal et al., 2004). Based on these data it can be concluded that tethering of the broken DNA ends to the sister chromatid is required for efficient repair through HR. Also in higher organisms evidence has been obtained for a role of cohesin in DSB repair. Depletion of SCC1 in chicken DT40 cells leads to a marked increase in the formation of chromosome aberrations after exposure to ionizing radiation and reduced levels of sister chromatid exchanges after treatment with 4NQO (Sonoda et al., 2001). Local irradiation of HeLa cells showed the recruitment of cohesin to the site of damage (Kim et al., 2002). Additionally, in a recent genome wide screen in *C. elegans* for genes required for resistance to ionizing radiation, a homologue of *NIPBL*, *pqn-85*, was identified. RNAi mediated ablation of this gene resulted in increased sensitivity to radiation and cisplatin (van Haaften et al., 2006).

The implication of cohesin and delangin homologues in the DNA damage responses in yeast and higher eukaryotes raises the question if cells derived from CdLS patients display increased sensitivity to DNA-damaging agents and defects in DSB-repair. Evidence presented here shows a drastic reduced survival after exposure to the DNA interstrand cross-link inducing agent mitomycin C (MMC) as well as an increased frequency of chromosomal aberrations in response to ionizing radiation at the G_2 phase of the cell cycle.

RESULTS

Cornelia de Lange syndrome is associated with increased sensitivity to DNA-damaging agents

To determine if CdLS is associated with increased sensitivity to DNA-damaging agents at the cellular level, we obtained two fibroblast and five B-lymphoblastoid cell lines from CdLS patients. To screen for the presence of *NIPBL* mutations in these lines, exon sequences, including exon-intron junctions, were amplified and PCR products were analyzed by denaturing high performance liquid chromatography (DHPLC). Heterozygous mutations were detected in two B-cell lymphoblastoid lines. Cell line CdLS11165 harbors a three base-pair deletion in exon 16 (c.3813delGAA), leading to a lysine (p.Lys1271del) deletion in a conserved part of the protein. Line CdLS11167 contains a single nucleotide insertion (c.3940_3941ins A) causing a premature stop codon. Using multiplex ligation-dependent probe amplification (MLPA) analysis a large genomic rearrangement, resulting in a duplication of exon 11-22, was identified in cell line CdLS45. In the other four CdLS lines no mutations could be detected in the coding region of the *NIPBL* gene by DHPLC and MLPA. Screening for mutations in the *SMC1A* gene by DHPLC also did not reveal any causative genetic alterations in these four patients.

In budding yeast, the absence of the Scc2/Scc4 cohesin loading complex compromises the repair capacity for X-ray-induced DNA breaks (Sjogren and Nasmyth, 2001). However, exposure of CdLS45 and CdLS3478 fibroblast lines to increasing doses of ionizing radiation did not result in a robust increase in radiation sensitivity as was observed for radiation-sensitive cells derived from ataxia telangiectasia (AT5BIVA) and severe combined immunodeficiency (SCID) (*Artemis*-6) patients (Figure 1A). Only at the highest dose tested both CdLS fibroblasts lines displayed a decrease in survival in comparison to the control fibroblasts. At lower doses only the CdLS3478 line reproducibly showed a marginal increase in radiation sensitivity in comparison with the three fibroblast lines derived from normal individuals. Growth inhibition assays for the five lymphoblast CdLS lines also did not reveal a distinct hypersensitivity to ionizing radiation (results not shown). However, exposure to the DNA interstrand cross-link-inducing agent mitomycin C revealed a strong increase in sensitivity of all fibroblast and lymphoblast CdLS lines (Figure 1B,C). In comparison with VH25 and FN1 normal cells, the D_{10} values (dose of MMC leading to 10% survival) for both fibroblast CdLS lines are approximately three-fold lower. Surprisingly, the increased MMC-sensitivity of CdLS45 and CdLS3478 is in the range of the MMC hypersensitivity of Fanconi's anemia (FA) (Figure 1B). Likewise, all five CdLS B-lymphoblastoid cell lines exhibited enhanced sensitivity for MMC when compared to control cells (Figure 1C). Growth inhibition experiments indicate a two-fold reduction of the IC_{50} values (dose of MMC leading to a growth reduction of 50%) of the CdLS lines in comparison with both normal human B-lymphoblastoid lines. In contrast to MMC, exposure of CdLS cells to UV-C light does not cause increased sensitivity (data not shown).

CdLS cells have increased levels of chromosomal aberrations after exposure to ionizing radiation

The formation of DSBs after exposure to DNA-damaging agents is counteracted by either non-homologous end joining (NHEJ) or homologous recombination (HR). Whereas NHEJ is believed to function throughout the cell cycle, HR occurs predominantly during the S and G_2 phase, when sister chromatids are available as a template for repair synthesis (Takata et al., 1998;Rothkamm et al., 2003). The role of delangin and the cohesin complex in DNA repair is most likely to enhance linkage between damaged and undamaged chromatids, to facilitate efficient repair of the lesion, thereby allowing HR to occur. To investigate the role of cohesion in repair of DSBs at different stages of the cell cycle, we first analyzed the formation of chromosomal aberrations after exposure to X-rays at the G_1 stage of the cell cycle. Confluent normal VH10 and CdLS fibroblasts were irradiated with different doses of X-rays and the frequency of dicentric chromosomes and acentric fragments was determined. Exposure to X-rays resulted in a dose-dependent increase in dicentrics and acentric fragments in both VH10 and CdLS3478 cells (Table 1A). Both normal and CdLS fibroblast showed a very similar dose-response relation for the formation of chromosome aberrations after irradiation with different doses of X-rays (0.25 – 1 Gy).

To determine the induction of chromosome aberrations after irradiation of cells in the G_2 phase of the cell cycle, metaphase preparations were made 3 hours after exposure to X-rays. In this experimental set up, only G_2 cells were analyzed (see materials and methods

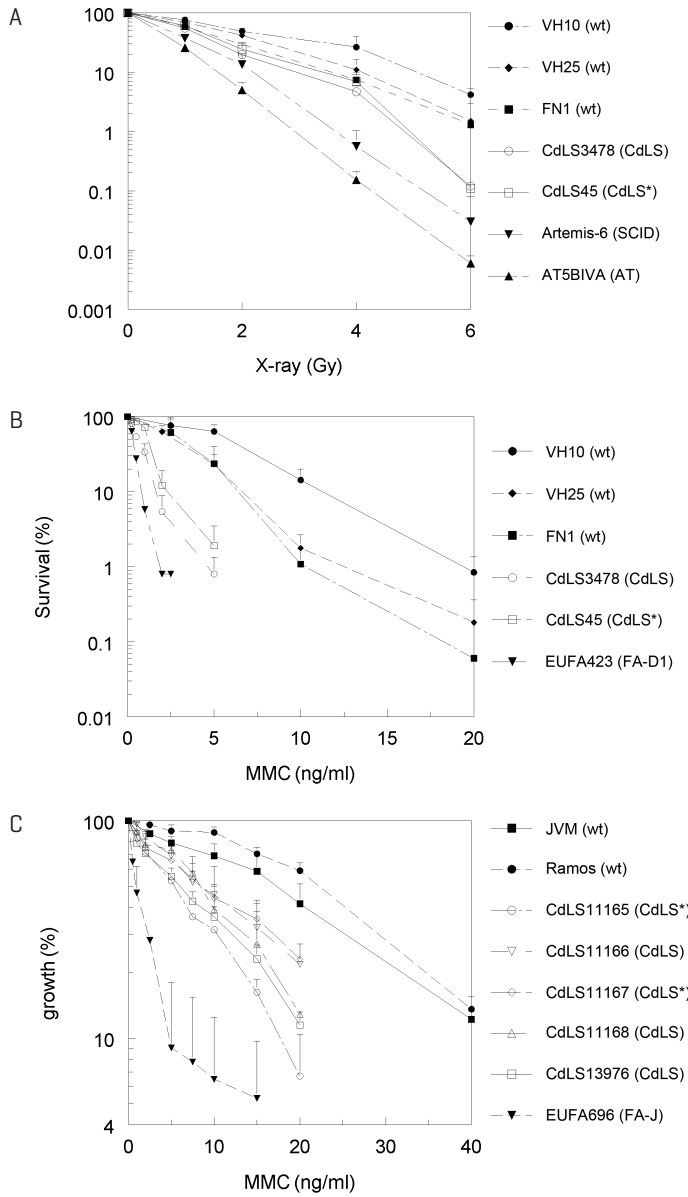

Figure 1: Survival of normal and CdLS cells after genotoxic treatment. CdLS cell lines are represented by open symbols. Data are the average of at least two independent experiments. Error bars represent the standard deviation. (A) Clonogenic survival of primary normal (VH10, VH25, FN1) and CdLS (CdLS3478, CdLS45) fibroblasts after X-ray exposure. The *Aretemis-6* (SCID) and AT5BIVA (AT) X-ray sensitive cell lines are shown for comparison. (B) Clonogenic survival of primary fibroblasts after MMC exposure. The MMC hypersensitive EUFA423 (FA-D1 / BRCA2) cell line is shown for comparison. (C) Growth inhibition assay of normal (JVM, Ramos) and CdLS (CdLS 11165, 11166, 11167, 11168, 13976) B-lymphoblastoid cells exposed to MMC. The MMC hypersensitive EUFA696 (FA-J) cell line is shown for comparison. Asterisk indicates cells with NIPBL mutation.

Table 1A. X-ray induced chromosomal aberrations in G_1 fibroblasts.

Cell line	X-ray dose (Gy)	Abnormal cells (%)	Dicentrics	Excess of acentric fragments
VH10	0	0	0	0
(wt)	0.25	3	2	1
	0.5	8	5	3
	1	13	9	6
	2	25	17	13
CdLS3478	0	1	0	1
(CdLS)	0.25	3	1	2
	0.5	7	4	3
	1	12	8	5
	2	26	18	12

Confluent primary fibroblasts were exposed to X-rays. Chromosomal aberrations are indicated per 100 cells.

for details). In mock treated cells the frequency of chromatid breaks was similar in VH10 and CdLS3478 cells. After exposure to low doses of X-rays (0.1 and 0.25 Gy), the frequency of chromatid exchanges in VH10 and CdLS3478 fibroblasts was comparable. However, an increase was observed in CdLS cells following exposure to doses of 0.5 and 1 Gy (Table 1B). Exposure to increasing doses of X-rays (0.1 to 1 Gy) also caused a strong increase in the level of residual chromatid breaks in CdLS fibroblasts when compared to control cells. At the highest dose tested (1 Gy) a four-fold difference was seen in the number of residual breaks between CdLS and normal cells. In two B-lymphoblastoid cell lines derived from CdLS patients a similar increase in radiosensitivity of G_2 cells was observed. The level of chromatid-type breaks was drastically enhanced (3–4.5 fold) in both lines tested in comparison with normal B-lymphoblastoid cells (Table 1C). In addition to ionizing radiation, we also analyzed chromatid-type aberrations after treatment with MMC. In CdLS fibroblasts the level of chromatid breaks and exchanges was found to be approximately three-fold higher than in normal cells (Table 1D). In CdLS B-lymphoblastoid cells no increase in chromatid-type aberrations was observed when compared to normal cells (data not shown) despite the strong MMC induced growth inhibition. It is known that B-lymphoblastoid cells readily go into apoptosis after inflicting DNA damage (Jha et al., 1995). Therefore severely damaged B-lymphoblastoid cells may not reach the next metaphase.

The formation of sister chromatid exchanges (SCE) reflects the occurrence of homologous recombination between sister chromatids (Sonoda et al., 1999;Wilson, III and Thompson, 2007). As repair of DSBs through homologous recombination is dependent on cohesion between sister chromatids, we reasoned that the level of SCE induction may be reduced in CdLS cells. To induce SCEs we treated B-lymphoblastoid cells with MMC and fibroblast cells with MMC or UV-C light. In contrast to X-rays both agents efficiently induce

Table 1B. X-ray induced chromosomal aberrations in G_2 fibroblasts.

			Chromatid	
Cell line	**X-ray dose (Gy)**	**Abnormal cells (%)**	**Breaks**	**Exchanges**
VH10	0	2	2	0
(wt)	0.1	8	8	0
	0.25	18	18	2
	0.5	29	28	6
	1	50	52	10
CdLS3478	0	2	2	0
(CdLS)	0.1	15	16	0
	0.25	37	46	2
	0.5	74	112	10
	1	84	220	16

Asynchronous primary fibroblasts were exposed to X-rays. Chromosomal aberrations are indicated per 100 cells.

Table 1C. X-ray induced chromosomal aberrations in G_2 B-lymphoblastoid cells.

			Chromatid	
Cell line	**X-ray dose (Gy)**	**Abnormal cells (%)**	**Breaks**	**Exchanges**
Ramos	0	0	0	0
(wt)	0.5	26	44	3
	1	52	81	6
CdLS11165	0	2	2	0
(CdLS*)	0.5	52	128	0
	1	74	286	10
CdLS13976	0	0	0	0
(CdLS)	0.5	66	158	0
	1	84	364	24

Asynchronous B-lymphoblastoid cells were exposed to X-rays. Chromosomal aberrations are indicated per 100 cells. Asterisk indicates cells with NIPBL mutation.

Table 1D. MMC induced chromosomal aberrations in primary fibroblasts.

			Chromatid	
Cell line	**MMC dose (ng/ml)**	**Abnormal cells (%)**	**Breaks**	**Exchanges**
VH10	0	0	0	0
(wt)	45	18	16	2
CdLS3478	0	0	0	0
(CdLS)	45	34	44	6

Chromosomal aberrations are indicated per 100 cells.

SCEs (Darroudi et al., 1989). As can be seen in Figure 2, SCEs were induced with equal efficiency in normal and CdLS B-lymphoblastoid cells after treatment with MMC. Similar results were obtained in fibroblasts after exposure to MMC and UV-C light (data not shown).

Normal Rad51 and γH2AX foci formation in CdLS cells

A central player in homologous recombination is the Rad51 molecule, a protein that promotes pairing and strand exchange reactions (Baumann and West, 1998). Upon treatment with DNA-damaging agents Rad51 relocalizes and forms nuclear foci, which most probably represent centers of DNA repair (Haaf et al., 1995;Tashiro et al., 2000). To determine if reduced cohesin loading affects the ability to form nuclear Rad51 foci, we exposed normal and CdLS cells to MMC and X-rays. In untreated cells between 2% and 5% of the nuclei contained five Rad51 foci or more. After treatment with X-rays or MMC between 6% and 31% of the normal and CdLS B-lymphoblastoid cells contained over five Rad51 foci (Figure 3A). This indicates that all CdLS cell lines tested are proficient for DNA damage induced foci formation although the level of induction varied between different

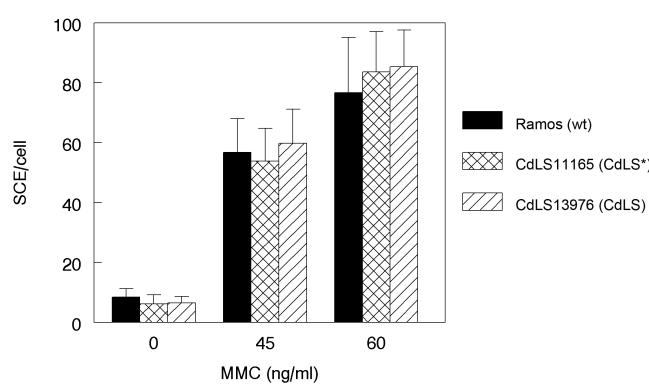

Figure 2: SCE induction in CdLS B-lymphoblastoid cells after MMC treatment. Normal (Ramos) or CdLS (CdLS11165, CdLS13976) cells were either mock treated or treated with 45 or 60 ng/ml MMC. Asterisk indicates cells with NIPBL mutation.. Error bars represent the standard error of the mean.

cell lines. A similar analysis using primary fibroblasts derived from CdLS patients also showed normal induction of Rad51 foci after MMC treatment (data not shown).

Exposure to ionizing radiation leads to phosphorylation of histone H2AX (γH2AX) near sites of DSBs which can be visualized as nuclear foci. Because the number of γH2AX foci is thought to correlate with the number of DSBs, the analysis of γH2AX foci can be used to evaluate the repair capacity of a cell (Rothkamm and Lobrich, 2003). Here we quantified the number of Rad51 and γH2AX foci per nucleus after X-ray exposure of exponentially growing CdLS and normal fibroblasts. Analysis of γH2AX foci was limited to cells that were also positive for Rad51 and presumably represent S or G_2 phase cells. No significant difference in the number of Rad51 or γH2AX foci was observed between normal and CdLS fibroblasts either 12 or 24 hours after irradiation (Figure 3B).

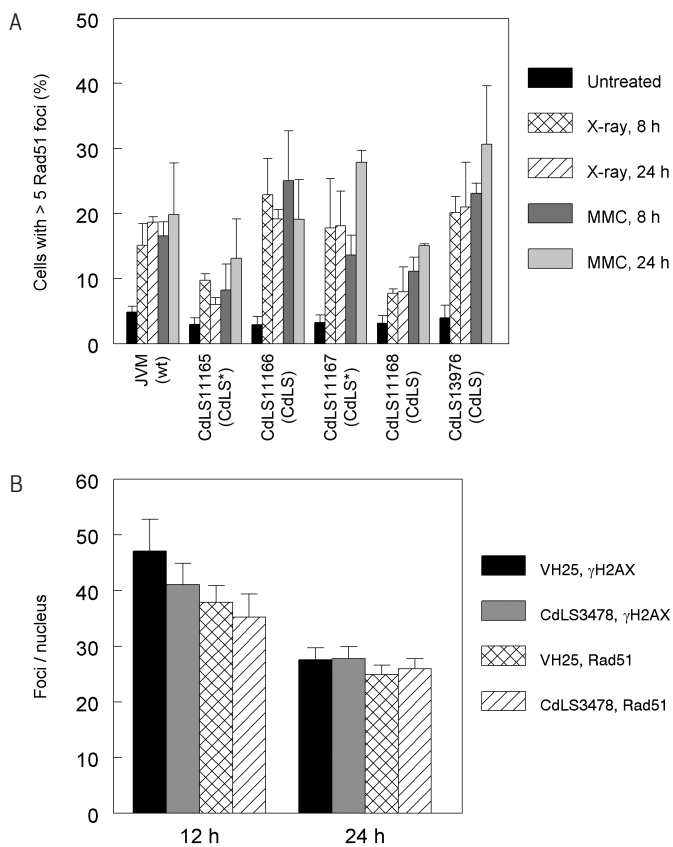

Figure 3: Rad51 and γH2AX nuclear foci formation is normal in CdLS cells. (A) Rad51 foci in normal and CdLS B-lymphoblastoid cells after X-rays (12 Gy) and MMC (2.4 μg/ml for 1 h). Cells containing more than 5 nuclear foci were considered as positive. Asterisk indicates cells with NIPBL mutation. (B) γH2AX and Rad51 nuclear foci after X-ray exposure (5 Gy). Only cells positive for Rad51 foci were analysed. Data are the means of at least 2 experiments. Error bars represent the standard error of the mean.

DISCUSSION

The Cornelia de Lange syndrome is a dominantly inherited multisystem congenital disorder and has been associated with heterozygous mutations in *NIPBL*, *SMC1A* or *SMC3* (Krantz et al., 2004;Tonkin et al., 2004;Gillis et al., 2004;Borck et al., 2004;Bhuiyan et al., 2006;Schoumans et al., 2007;Musio et al., 2006;Borck et al., 2007;Deardorff et al., 2007;Bhuiyan et al., 2007). Although the clinical manifestations of CdLS have been described in great detail, little is known about the characteristics at the cellular level. Studies in budding yeast have revealed that a complex consisting of Scc2 and Scc4 is required for loading of cohesin onto chromosomes before replication starts. Sister chromatid cohesion is established at the replication fork and involves additional proteins, including Eco1, Ctf4 and Ctf18 (Lengronne et al., 2006;Skibbens et al., 1999;Hanna et al., 2001). Establishing cohesion between sister chromatids is essential not only for correct chromosome segregation, but also for post-replicative DNA repair. Experiments in yeast have shown that repair of DSBs in S- and G_2-phase cells requires *de novo* formation of cohesion at the site of the damage (Strom et al., 2004;Unal et al., 2004). To determine if CdLS is associated with impaired repair of DSBs, we studied the survival of CdLS cell lines, the induction of chromosomal aberrations and the levels of γH2AX and Rad51 nuclear foci after treatment with DNA-damaging agents.

Pathogenic *NIPBL* mutations were identified in three (CdLS11165, CdLS11167 and CdLS45) out of seven cell lines examined. In the remaining four CdLS lines no mutations were identified in *NIPBL* or *SMC1A*, which has recently been implicated in CdLS (Musio et al., 2006;Borck et al., 2007;Deardorff et al., 2007;Bhuiyan et al., 2007). However, the screening methods used cannot exclude the presence of mutations in intronic sequences or in the promoter region of the genes. As sister chromatid cohesion involves various factors, the presence of disease-causing mutations in additional genes can also not be ruled out.

The induction of chromosomal aberrations (dicentrics and acentric fragments) after exposure of G_1 CdLS fibroblast cells to X-rays was similar to normal cells. However, both CdLS fibroblast and B-lymphoblastoid cells showed a strong dose dependent increase in the formation of chromatid exchanges and chromatid breaks when exposed to X-rays in the G_2 stage of the cell cycle. Our observations are consistent with a defect in DSB repair through HR, resulting in delayed and/or aberrant repair of DSBs. In G_1 cells X-ray-induced DSBs are repaired primarily though NHEJ, while repair of DSBs in S- and G_2-phase proceeds via NHEJ as well as via HR (Takata et al., 1998;Rothkamm et al., 2003). A G_2 specific increase in the induction of chromosomal aberrations has previously also been reported for cells derived from Bloom syndrome patients (Kuhn, 1980). BLM, the protein affected in these cells, is known to function in HR (Cheok et al., 2005), which would suggest that a bias for ionizing radiation induced chromosomal aberrations in G_2 is a general feature of cells deficient in HR. However, in spite of the clear increase in the formation of chromosomal aberrations during G_2, clonogenic survival of CdLS cells after X-ray exposure did not differ significantly from that of control cells. The absence of a hypersensitivity to X-rays in this assay might reflect the relative contributions of NHEJ and HR during the cell cycle. In an asynchronous population of primary fibroblasts, a large fraction of cells will be in G_1 or

early S and hence the role of HR in the repair of DSBs is expected to be less important. This is opposed to the situation in G_2 where the contribution of HR is significant and cannot be fully compensated by NHEJ (Godthelp et al., 2002;French et al., 2002;Godthelp et al., 2006). It should, however, be noted that an increased sensitivity was observed in hTERT immortalized human fibroblasts after RNAi mediated knockdown of *NIPBL* (van Haaften et al., 2006). Consistent with our data is the observation that mammalian cell lines containing hypomorphic mutations in *RAD51C* or *BRCA2* are hypersensitive to cross-linking agents as a consequence of impaired HR but are not or only mildly sensitive for X-rays (Godthelp et al., 2002;French et al., 2002;Godthelp et al., 2006). Although clonogenic survival assays did not reveal a dreastic increase in X-ray sensitivity of CdLS cells, a distinct MMC hypersensitivity was observed. All 7 CdLS cell lines tested displayed an increased sensitivity to MMC. Repair of cross-links is dependent on several DNA repair pathways, including nucleotide excision repair, HR and post-replication/translesion synthesis repair (Lehoczky et al., 2007). DSBs, which are presumably formed as intermediates in the repair of interstrand cross-links, are processed by HR. No difference in sensitivity was observed between CdLS lines containing pathogenic *NIPBL* mutations (CdLS11165, CdLS11167and CdLS45) and the other four CdLS lymphoblast lines without detectable *NIPBL* mutation. This suggests that these four cell lines also have a defect in the establishment of cohesion and that MMC hypersensitivity is a general feature of CdLS at the cellular level. The reduced ability to process DNA cross-links is further demonstrated by the increased frequency of chromatid exchanges and chromatid breaks that is observed in CdLS fibroblasts after MMC exposure.

The formation of SCEs signifies HR between sister chromatids and consequently defects in HR affect the induction of SCEs after exposure to DNA-damaging agents (Sonoda et al., 1999;Wilson, III and Thompson, 2007). Ablation of the cohesion factors Smc3, Scc1 or the delangin ortholog Scc2 in chicken DT40 cells or budding yeast were found to impair the formation of SCEs (Sonoda et al., 2001;Cortes-Ledesma and Aguilera, 2006). However, in contrast to these observations we observed efficient formation of SCEs in CdLS cells after exposure to UV light or MMC. One explanation for this apparent contradiction would be that the capacity to repair DNA lesions via HR is still substantial in CdLS cells. In the former studies protein levels are likely to be reduced to very low levels, whereas in CdLS cells the residual levels of delangin protein could be sufficient to induce near normal levels of SCEs. In support of this would be the recent observation that FA-D1/BRCA2 patient derived cells, despite being highly sensitive for MMC, are also proficient in SCE formation (Godthelp et al., 2006).

In the current study we observed efficient induction of Rad51 foci in all CdLS B-lymphoblastoid cells upon MMC or X-ray treatment (Figure 3A). Apparently, the redistribution of Rad51 protein to the site of the damage is not or hardly affected in CdLS cells. The variation in the induction of Rad51 foci in the various cell lines is not the result of differences in cell cycle distribution, as was shown by FACS analysis, but most likely reflects cell line specific differences (data not shown). Analysis of the number of Rad51 and γH2AX foci after X-ray exposure of fibroblasts also did not reveal a difference between CdLS3478 and control fibroblasts. The decline in the number of γH2AX foci after exposure to X-rays suggests efficient processing of DSBs in CdLS cells and is consistent with the unperturbed

clonal survival observed after X-rays. The reduction of Rad51 foci in time suggests that homologous recombination is still possible in CdLS cells. However, due to reduced levels of delangin protein, small differences in the recombination efficiency between normal and CdLS cells might exist, as implied by the G_2 specific formation of chromosomal aberrations.

In man multiple diseases are known which negatively affect the capacity of cells to repair or process DNA lesions, often resulting in a predisposition for developing tumours. The occurrence of neoplasms in CdLS individuals however appears infrequent, with only four cases being described in the literature (Sugita et al., 1986;Maruiwa et al., 1988;DuVall and Walden, 1996). Although our study clearly shows there is an increased susceptibility for CdLS cells to form chromosomal aberrations after genotoxic stress, there were no signs of chromosomal instability in untreated samples thus corroborating the low incidence of tumour development observed in CdLS individuals. Neither did we observe precocious sister chromatid separation (PSCS) in CdLS cells as was reported by Kaur et al. (Kaur et al., 2005). The most striking feature of delangin deficiency in higher eukaryotes, like *Drosophila* and *X. tropicalis*, is its impact on development. Similarly, mutations in genes involved in the establishment of sister chromatid cohesion in man (e.g. *ESCO2, NIPBL, SMC1A* and *SMC3*) result in Roberts syndrome or CdLS, disorders which are manifested by congenital malformations. Despite the recent identification of causal genes associated with these syndromes, the underlying mechanisms for the observed clinical features remain obscure. *Drosophila* Nipped-B is involved in the transcriptional regulation of *cut* and *ultrabithorax* genes, which are involved in embryonic development, in addition to its role in cohesion of sister chromatids after replication (Dorsett et al., 2005;Rollins et al., 2004;Rollins et al., 1999). It is possible that human delangin, like in *Drosophila*, is also involved in regulation of developmental genes, although at present no target genes have been identified. In this study we have shown that CdLS, in addition to the established clinical phenotype, is characterized at the cellular level by an increased sensitivity to ionizing radiation and MMC. This hypersensitivity to DNA crosslinking agents may help improve diagnosis of CdLS and other human disorders associated with defects in sister chromatid cohesion.

MATERIALS EN METHODS

Cell culture

Primary fibroblasts were cultured in DMEM (Gibco) supplemented with 10% fetal calf serum (Bodinco), penicillin (100 U/ml) and streptomycin (0.1 mg/ml). B-lymphoblastoid cells were grown in RPMI 1640 medium Dutch modification (Gibco) supplemented with glutamax (Gibco), 20 mM sodiumpyruvate (Gibco), 10% fetal calf serum (Bodinco), penicillin (100 U/ml) and streptomycin (0.1 mg/ml). The primary fibroblast lines used were normal (VH10, VH25, FN1), CdLS (GM00045 and GM03478; obtained from the Coriell Institute), ataxia telangiectasia (AT5BIVA), SCID (*Aretemis-6*), Fanconi anemia-D1 (EUFA423). B-lymphoblastoid cells used were normal (JVM, Ramos), CdLS (GM11165, GM11166, GM11167, GM11168 and GM13976; obtained from the Coriell Institute) and Fanconi anemia-J (EUFA696). Both Fanconi anemia cell lines were kindly provided by Dr. H. Joenje (VUMC, Amsterdam).

NIPBL and SMC1A mutation analysis

Genomic DNA of all CdLS cell lines was isolated and screened for mutations in the *NIPBL* coding region (exons 2-47, for primer sequences and PCR conditions see (8)). Mutational analysis of the amplimers was performed by denaturing high performance liquid chromatography (DHPLC) (Transgenomic Wave). PCR products with altered DHPLC peaks were purified using a QiaQuick PCR purification kit (Qiagen) and sequenced bidirectionally on an ABI 377 sequencer. The *NIPBL* sequence in the NCBI nucleotide database (NM_015384) was used as reference to identify mutations. MLPA analyses were performed using MLPA kits P141 and P142 (MRC-Holland) according to the manufacturers instructions. All probands negative for mutations in *NIPBL* were screened for the presence of mutations in *SMC1A* (GenBank accession number NM_006306). The complete *SMC1A* coding region was amplified in 22 fragments and analyzed by DHPLC (primer sequences and PCR conditions are available on request). Amplification products with altered chromatographic peaks were purified and sequenced bi-directionally.

Clonogenic survival and growth inhibition assays

Exponentially growing cells were trypsinized and 500-2000 cells were plated in 9 cm dishes in duplicate (controls in triplicate), and irradiated or exposed continuously to MMC, in complete medium. After 14-17 days the dishes were rinsed with 0.9% NaCl, dried, stained with methylene blue (0.25%) and colonies were counted using a light microscope. In all experiments, normal fibroblasts were treated in an identical manner to serve as controls. For growth inhibition assays B-lymphoblastoid cell cultures were seeded at a density of 5×10^4 cells/ml and exposed to X-rays or MMC. Cells were cultured for 3 to 10 days until unexposed controls had undergone 3 population doublings, at which point all parallel cultures were counted using a Z2 Coulter counter (Beckman Coulter).

Chromosomal aberrations and SCEs

For G_1 chromosome aberration analysis primary fibroblasts were grown until confluency and kept confluent for 1 week before irradiation. After exposure to 0, 0.25, 0.5, 1 and 2 Gy of X-rays, fibroblasts were subcultured and allowed to grow in the presence of BrdU (5 μM) for 52 h. Colcemid (25 μg/ml) was added to all cultures 4 h before harvesting. Air-dried preparations were made and stained with FPG (Perry and Wolff, 1974). For G_2 chromosome aberration analysis exponentially growing cells were exposed to 0, 0.1, 0.25, 0,5 and 1 Gy of X-rays followed by 3 h incubation in the presence of BrdU and colcemid before harvesting. For MMC induced chromosome aberration analysis exponentially growing normal and CdLS fibroblasts and B-lymphoblastoid cells were either mock-treated or treated with MMC (45 or 60 ng/ml) continuously during culturing. Following treatment BrdU was added to the medium. Cells were harvested for the analysis of chromosome aberrations at 28 h and for SCE analysis at 54 h after MMC treatment, including 4 h incubation with colcemid. For chromosomal aberrations 100 mitotic cells were analyzed for each dose, for SCE analysis 25 mitotic cells were scored for each dose.

Immunofluorescence labeling and microscopy

To examine γH2AX or Rad51 foci formation, primary fibroblasts were grown on sterile glass slides, resulting in sub-confluent cells at time of fixation. B-lymphoblastoid cells were grown in tissue culture flasks and transferred to 9 cm culture dishes prior to treatment at a density of 0.5×10^6 cells/ml. For Rad51 foci analysis, cells were either mock-treated or treated with MMC (2.4 μg/ml for 1 h) or X-ray irradiation (5 or 12 Gy). After an 8, 12 or 24 h recovery period, primary fibroblasts were fixed immediately using 2% formaldehyde in PBS, and permeabilized for antibody staining with PBS/0.1% Triton X-100. The (mock)-treated B-lymphoblastoid cells (1×10^6) were seeded on poly-D-lysine (Sigma) coated glass slides after an 8 or 24 h recovery period and left to attach for 15 minutes prior to fixation and permeabilization. Subsequently the slides were blocked for 30 min in PBS/BSA (0.5%)/glycin (0.15%) and incubated with rabbit anti-Rad51 antiserum (FBE2, kindly provided by Dr. F.E. Benson) or mouse anti-γH2AX (Upstate Biotechnology) for 90 min in a humidified atmosphere. The slides were washed 3 times in PBS/0.1% Triton X-100 and incubated with AlexaFluor 488-conjugated goat anti-rabbit or goat anti-mouse IgG (Molecular Probes) or Cy3 conjugated goat anti-rabbit IgG (Jackson ImmunoResearch) for 1 h at 37°C in a humidified atmosphere. After 3 washes with PBS/0.1% Triton X-100 the cells were counterstained with 4',6-diamino-2-phenylindole (DAPI; 0.1 μg/ml) in Vectashield mounting medium (Vector Laboratories).

ACKNOWLEDGEMENTS

We would like to thank Dr. R.C. Hennekam for stimulating discussions. This work was supported in part by the EU RISC-RAD project (FI6R-CT-2003-508842).

REFERENCE LIST

1. Baumann,P. and S.C.West. 1998. Role of the human RAD51 protein in homologous recombination and double-stranded-break repair. *Trends Biochem. Sci.* **23**: 247-251.
2. Bhuiyan,Z.A., M.Klein, P.Hammond, H.A.van, M.M.Mannens, I.Van Berckelaer-Onnes, and R.C.Hennekam. 2006. Genotype-phenotype correlations of 39 patients with Cornelia De Lange syndrome: the Dutch experience. *J. Med. Genet.* **43**: 568-575.
3. Bhuiyan,Z.A., H.Stewart, E.J.Redeker, M.M.Mannens, and R.C.Hennekam. 2007. Large genomic rearrangements in NIPBL are infrequent in Cornelia de Lange syndrome. *Eur. J. Hum. Genet.* **15**: 505-508.
4. Borck,G., R.Redon, D.Sanlaville, M.Rio, M.Prieur, S.Lyonnet, M.Vekemans, N.P.Carter, A.Munnich, L.Colleaux, and V.Cormier-Daire. 2004. NIPBL mutations and genetic heterogeneity in Cornelia de Lange syndrome. *J. Med. Genet.* **41**: e128.
5. Borck,G., M.Zarhrate, J.P.Bonnefont, A.Munnich, V.Cormier-Daire, and L.Colleaux. 2007. Incidence and clinical features of X-linked Cornelia de Lange syndrome due to SMC1L1 mutations. *Hum. Mutat.* **28**: 205-206.
6. Cheok,C.F., C.Z.Bachrati, K.L.Chan, C.Ralf, L.Wu, and I.D.Hickson. 2005. Roles of the Bloom's syndrome helicase in the maintenance of genome stability. *Biochem. Soc. Trans.* **33**: 1456-1459.
7. Ciosk,R., M.Shirayama, A.Shevchenko, T.Tanaka, A.Toth, A.Shevchenko, and K.Nasmyth. 2000. Cohesin's binding to chromosomes depends on a separate complex consisting of Scc2 and Scc4 proteins. *Mol. Cell* **5**: 243-254.
8. Cortes-Ledesma,F. and A.Aguilera. 2006. Double-strand breaks arising by replication through a nick are repaired by cohesin-dependent sister-chromatid exchange. *EMBO Rep.* **7**: 919-926.
9. Darroudi,F., A.T.Natarajan, and P.H.Lohman. 1989. Cytogenetical characterization of UV-sensitive repair-deficient CHO cell line 43-3B. II. Induction of cell killing, chromosomal aberrations and sister-chromatid exchanges by 4NQO, mono- and bi-functional alkylating agents. *Mutat. Res.* **212**: 103-112.
10. Deardorff,M.A., M.Kaur, D.Yaeger, A.Rampuria, S.Korolev, J.Pie, C.Gil-Rodriguez, M.Arnedo, B.Loeys, A.D.Kline, M.Wilson, K.Lillquist, V.Siu, F.J.Ramos, A.Musio, L.S.Jackson, D.Dorsett, and I.D.Krantz. 2007. Mutations in cohesin complex members SMC3 and SMC1A cause a mild variant of cornelia de Lange syndrome with predominant mental retardation. *Am. J. Hum. Genet.* **80**: 485-494.
11. Dorsett,D., J.C.Eissenberg, Z.Misulovin, A.Martens, B.Redding, and K.McKim. 2005. Effects of sister chromatid cohesion proteins on cut gene expression during wing development in Drosophila. *Development* **132**: 4743-4753.
12. DuVall,G.A. and D.T.Walden. 1996. Adenocarcinoma of the esophagus complicating Cornelia de Lange syndrome. *J. Clin. Gastroenterol.* **22**: 131-133.
13. French,C.A., J.Y.Masson, C.S.Griffin, P.O'Regan, S.C.West, and J.Thacker. 2002. Role of mammalian RAD51L2 (RAD51C) in recombination and genetic stability. *J. Biol. Chem.* **277**: 19322-19330.
14. Gerlich,D., B.Koch, F.Dupeux, J.M.Peters, and J.Ellenberg. 2006. Live-cell imaging reveals a stable cohesin-chromatin interaction after but not before DNA replication. *Curr. Biol.* **16**: 1571-1578.
15. Gillis,L.A., J.McCallum, M.Kaur, C.DeScipio, D.Yaeger, A.Mariani, A.D.Kline, H.H.Li, M.Devoto, L.G.Jackson, and I.D.Krantz. 2004. NIPBL mutational analysis in 120 individuals with Cornelia de Lange syndrome and evaluation of genotype-phenotype correlations. *Am. J. Hum. Genet.* **75**: 610-623.
16. Godthelp,B.C., P.P.van Buul, N.G.Jaspers, E.Elghalbzouri-Maghrani, A.van Duijn-Goedhart, F.Arwert, H.Joenje, and M.Z.Zdzienicka. 2006. Cellular characterization of cells from the Fanconi anemia complementation group, FA-D1/BRCA2. *Mutat. Res.* **601**: 191-201.
17. Godthelp,B.C., W.W.Wiegant, A.van Duijn-Goedhart, O.D.Scharer, P.P.van Buul, R.Kanaar, and M.Z.Zdzienicka. 2002. Mammalian Rad51C contributes to DNA cross-link resistance, sister chromatid cohesion and genomic stability. *Nucleic Acids Res.* **30**: 2172-2182.
18. Haaf,T., E.I.Golub, G.Reddy, C.M.Radding, and D.C.Ward. 1995. Nuclear foci of mammalian Rad51 recombination protein in somatic

cells after DNA damage and its localization in synaptonemal complexes. *Proc. Natl. Acad. Sci. U. S. A* **92**: 2298-2302.

19. Hanna,J.S., E.S.Kroll, V.Lundblad, and F.A.Spencer. 2001. Saccharomyces cerevisiae CTF18 and CTF4 are required for sister chromatid cohesion. *Mol. Cell Biol.* **21**: 3144-3158.
20. Ireland,M., D.Donnai, and J.Burn. 1993. Brachmann-de Lange syndrome. Delineation of the clinical phenotype. *Am. J. Med. Genet.* **47**: 959-964.
21. Jackson,L., A.D.Kline, M.A.Barr, and S.Koch. 1993. de Lange syndrome: a clinical review of 310 individuals. *Am. J. Med. Genet.* **47**: 940-946.
22. Jha,A.N., P.M.Hande, L.H.Mullenders, and A.T.Natarajan. 1995. Mimosine is a potent clastogen in primary and transformed hamster fibroblasts but not in primary or transformed human lymphocytes. *Mutagenesis* **10**: 385-391.
23. Kaur,M., C.DeScipio, J.McCallum, D.Yaeger, M.Devoto, L.G.Jackson, N.B.Spinner, and I.D.Krantz. 2005. Precocious sister chromatid separation (PSCS) in Cornelia de Lange syndrome. *Am. J. Med. Genet. A* **138**: 27-31.
24. Kim,J.S., T.B.Krasieva, V.LaMorte, A.M.Taylor, and K.Yokomori. 2002. Specific recruitment of human cohesin to laser-induced DNA damage. *J. Biol. Chem.* **277**: 45149-45153.
25. Krantz,I.D., J.McCallum, C.DeScipio, M.Kaur, L.A.Gillis, D.Yaeger, L.Jukofsky, N.Wasserman, A.Bottani, C.A.Morris, M.J.Nowaczyk, H.Toriello, M.J.Bamshad, J.C.Carey, E.Rappaport, S.Kawauchi, A.D.Lander, A.L.Calof, H.H.Li, M.Devoto, and L.G.Jackson. 2004. Cornelia de Lange syndrome is caused by mutations in NIPBL, the human homolog of Drosophila melanogaster Nipped-B. *Nat. Genet.* **36**: 631-635.
26. Kuhn,E.M. 1980. Effects of X-irradiation in G1 and G2 on Bloom's Syndrome and normal chromosomes. *Hum. Genet.* **54**: 335-341.
27. Lehoczky,P., P.J.McHugh, and M.Chovanec. 2007. DNA interstrand cross-link repair in Saccharomyces cerevisiae. *FEMS Microbiol. Rev.* **31**: 109-133.
28. Lengronne,A., J.McIntyre, Y.Katou, Y.Kanoh, K.P.Hopfner, K.Shirahige, and F.Uhlmann. 2006. Establishment of sister chromatid cohesion at the S. cerevisiae replication fork. *Mol. Cell* **23**: 787-799.
29. Maruiwa,M., Y.Nakamura, K.Motomura, T.Murakami, M.Kojiro, M.Kato, M.Morimatsu, S.Fukuda, and T.Hashimoto. 1988. Cornelia de Lange syndrome associated with Wilms' tumourandinfantilehaemangioendothelioma of the liver: report of two autopsy cases. *Virchows Arch. A Pathol. Anat. Histopathol.* **413**: 463-468.
30. Michaelis,C., R.Ciosk, and K.Nasmyth. 1997. Cohesins: chromosomal proteins that prevent premature separation of sister chromatids. *Cell* **91**: 35-45.
31. Moldovan,G.L., B.Pfander, and S.Jentsch. 2006. PCNA controls establishment of sister chromatid cohesion during S phase. *Mol. Cell* **23**: 723-732.
32. Musio,A., A.Selicorni, M.L.Focarelli, C.Gervasini, D.Milani, S.Russo, P.Vezzoni, and L.Larizza. 2006. X-linked Cornelia de Lange syndrome owing to SMC1L1 mutations. *Nat. Genet.* **38**: 528-530.
33. Perry,P. and S.Wolff. 1974. New Giemsa method for the differential staining of sister chromatids. *Nature* **251**: 156-158.
34. Rollins,R.A., M.Korom, N.Aulner, A.Martens, and D.Dorsett. 2004. Drosophila nipped-B protein supports sister chromatid cohesion and opposes the stromalin/Scc3 cohesion factor to facilitate long-range activation of the cut gene. *Mol. Cell Biol.* **24**: 3100-3111.
35. Rollins,R.A., P.Morcillo, and D.Dorsett. 1999. Nipped-B, a Drosophila homologue of chromosomal adherins, participates in activation by remote enhancers in the cut and Ultrabithorax genes. *Genetics* **152**: 577-593.
36. Rothkamm,K., I.Kruger, L.H.Thompson, and M.Lobrich. 2003. Pathways of DNA double-strand break repair during the mammalian cell cycle. *Mol. Cell Biol.* **23**: 5706-5715.
37. Rothkamm,K. and M.Lobrich. 2003. Evidence for a lack of DNA double-strand break repair in human cells exposed to very low x-ray doses. *Proc. Natl. Acad. Sci. U. S. A* **100**: 5057-5062.
38. Schoumans,J., J.Wincent, M.Barbaro, T.Djureinovic, P.Maguire, L.Forsberg, J.Staaf, A.C.Thuresson, A.Borg, A.Nordgren, G.Malm, and B.M.Anderlid. 2007. Comprehensive mutational analysis of a cohort of Swedish Cornelia de Lange syndrome patients. *Eur. J. Hum. Genet.* **15**: 143-149.
39. Seitan,V.C., P.Banks, S.Laval, N.A.Majid, D.Dorsett, A.Rana, J.Smith, A.Bateman, S.Krpic, A.Hostert, R.A.Rollins, H.Erdjument-Bromage, P.Tempst, C.Y.Benard, S.Hekimi, S.F.Newbury, and T.Strachan. 2006. Metazoan

Scc4 homologs link sister chromatid cohesion to cell and axon migration guidance. *PLoS. Biol.* **4**: e242.

40. Sjogren,C. and K.Nasmyth. 2001. Sister chromatid cohesion is required for postreplicative double-strand break repair in Saccharomyces cerevisiae. *Curr. Biol.* **11**: 991-995.
41. Skibbens,R.V., L.B.Corson, D.Koshland, and P.Hieter. 1999. Ctf7p is essential for sister chromatid cohesion and links mitotic chromosome structure to the DNA replication machinery. *Genes Dev.* **13**: 307-319.
42. Sonoda,E., T.Matsusaka, C.Morrison, P.Vagnarelli, O.Hoshi, T.Ushiki, K.Nojima, T.Fukagawa, I.C.Waizenegger, J.M.Peters, W.C.Earnshaw, and S.Takeda. 2001. Scc1/Rad21/Mcd1 is required for sister chromatid cohesion and kinetochore function in vertebrate cells. *Dev. Cell* **1**: 759-770.
43. Sonoda,E., M.S.Sasaki, C.Morrison, Y.Yamaguchi-Iwai, M.Takata, and S.Takeda. 1999. Sister chromatid exchanges are mediated by homologous recombination in vertebrate cells. *Mol. Cell Biol.* **19**: 5166-5169.
44. Strom,L., H.B.Lindroos, K.Shirahige, and C.Sjogren. 2004. Postreplicative recruitment of cohesin to double-strand breaks is required for DNA repair. *Mol. Cell* **16**: 1003-1015.
45. Sugita,K., T.Izumi, K.Yamaguchi, Y.Fukuyama, A.Sato, and A.Kajita. 1986. Cornelia de Lange syndrome associated with a suprasellar germinoma. *Brain Dev.* **8**: 541-546.
46. Takata,M., M.S.Sasaki, E.Sonoda, C.Morrison, M.Hashimoto, H.Utsumi, Y.Yamaguchi-Iwai, A.Shinohara, and S.Takeda. 1998. Homologous recombination and non-homologous end-joining pathways of DNA double-strand break repair have overlapping roles in the maintenance of chromosomal integrity in vertebrate cells. *EMBO J.* **17**: 5497-5508.
47. Tashiro,S., J.Walter, A.Shinohara, N.Kamada, and T.Cremer. 2000. Rad51 accumulation at sites of DNA damage and in postreplicative chromatin. *J. Cell Biol.* **150**: 283-291.
48. Tonkin,E.T., T.J.Wang, S.Lisgo, M.J.Bamshad, and T.Strachan. 2004. NIPBL, encoding a homolog of fungal Scc2-type sister chromatid cohesion proteins and fly Nipped-B, is mutated in Cornelia de Lange syndrome. *Nat. Genet.* **36**: 636-641.
49. Unal,E., A.Arbel-Eden, U.Sattler, R.Shroff, M.Lichten, J.E.Haber, and D.Koshland. 2004. DNA damage response pathway uses histone modification to assemble a double-strand break-specific cohesin domain. *Mol. Cell* **16**: 991-1002.
50. Van Den Berg,D.J. and U.Francke. 1993. Roberts syndrome: a review of 100 cases and a new rating system for severity. *Am. J. Med. Genet.* **47**: 1104-1123.
51. Van Haaften,G., R.Romeijn, J.Pothof, W.Koole, L.H.Mullenders, A.Pastink, R.H.Plasterk, and M.Tijsterman. 2006. Identification of conserved pathways of DNA-damage response and radiation protection by genome-wide RNAi. *Curr. Biol.* **16**: 1344-1350.
52. Vega,H., Q.Waisfisz, M.Gordillo, N.Sakai, I.Yanagihara, M.Yamada, G.D.van, H.Kayserili, C.Xu, K.Ozono, E.W.Jabs, K.Inui, and H.Joenje. 2005. Roberts syndrome is caused by mutations in ESCO2, a human homolog of yeast ECO1 that is essential for the establishment of sister chromatid cohesion. *Nat. Genet.* **37**: 468-470.
53. Watrin,E., A.Schleiffer, K.Tanaka, F.Eisenhaber, K.Nasmyth, and J.M.Peters. 2006. Human Scc4 is required for cohesin binding to chromatin, sister-chromatid cohesion, and mitotic progression. *Curr. Biol.* **16**: 863-874.
54. Wilson,D.M., III and L.H.Thompson. 2007. Molecular mechanisms of sister-chromatid exchange. *Mutat. Res.* **616**: 11-23.

7

Perspectives

RESPONDING TO DNA DAMAGE

The genetic material of cells is continually subjected to genotoxic attacks, raising the question how the cell can protect itself from the potentially harmful consequences of DNA damage. Decades of research have uncovered in increasing detail how cells, from bacteria to mammals, have dedicated mechanisms for repairing DNA by removing DNA damage and restoring the original sequence. It has also become apparent that the DNA damage signaling cascade, through protein phosphorylation, regulates the cell cycle and acts in concert with DNA repair to protect genomic integrity and cell viability. In addition, it has more recently become apparent that other post-translational modifications (PTM) such as poly(ADP-ribosyl)ation (PAR), ubiquitylation and possibly sumoylation have important roles in DNA repair. These modifications are likely to have a signaling function but might also affect protein function due to imposed structural changes. The stability of the nucleotide excision repair factor DDB2 is for example regulated by both ubiquitin as well as PAR modifications on the protein (chapter 3). The widespread use of PTM in cells in concert with the possibility to target the same protein with different types of PTM adds to the challenge of understanding protein function and regulation.

Despite the clear role of phosphorylation in the DNA damage response, results from unbiased phosphoproteomic screens suggest that other pathways which are not obviously related to DNA damage repair may also be modulated (Bennetzen et al., 2010;Pines et al., 2011). The biological significance of such changes in the phosphoproteome are, however, often unknown and require further study. Nevertheless, it is clear that the most prominent changes in the phosphoproteome after cisplatin or ionizing radiation exposure are due to activation of PI3 like kinases such as ATM and ATR. These kinases are known to respond to DNA damage and are important regulators of cell cycle progression following genotoxic stress. What has been surprising, however, is the abundance of ATM/ATR target proteins that have been identified in both unbiased screens (Bennetzen et al., 2010;Pines et al., 2011) and screens specifically directed towards ATM/ATR target identification (Matsuoka et al., 2007;Stokes et al., 2007). It can thus be conjectured that processes other than cell cycle checkpoints, replication and repair are also regulated through these kinases.

Many of the cell's proteins can be phosphorylated. However, the phosphoproteome is subject to variables such as cell type, phase of the cell cycle and other parameters such as DNA damage induced stress. The prevalence of phospho modification is reflected by the cohesion complex in which all components (i.e. Smc1α, Smc3, Rad21, SA1/2, Wapl and Pds5a/b) undergo multiple phosphorylation events. Consistent with its role in DNA repair (chapter 6), DNA damage signaling (Yazdi et al., 2002) and sister chromatid cohesion, changes in the pattern of cohesin phosphorylation were observed after cisplatin treatment (chapter 5). Although most phospho sites remain unchanged a significant increase or decrease of phosphorylation was found on Smc1α, Smc3, SA2, Pds5a/b and Wapl. The complex changes in up and down phosphorylation events, are predicted to involve multiple kinases and likely reflects cohesin's diverse role in cell biology. The observed increase in putative ATM/ATR dependent phosphorylation of Smc1α and Pds5a could relate to a DNA damage signaling function while decreased Wapl phosphorylation, likely due to lower

PLK activity, could reflect the decrease in mitotic cells after cisplatin treatment. The significance of other changes remains, however, elusive.

The wealth of information obtained from unbiased mass spectrometry based analyses can evidently be used to improve our understanding of the interconnectivity of processes and pathways and their regulation by phosphorylation. It will allow changes to be observed in an unbiased manner after for example treatment with cytostatic drugs or pharmacological inhibitors, many of the latter being inhibitors of kinases. Consequently, target proteins for kinases can be identified as well as their wider impact on the cell's phosphoproteome. Such a broad view of the changes will allow the identification of pathways that might unexpectedly be altered in response to drugs, potentially creating a compensatory effect thereby reducing drug efficacy.

FROM UV LESION TO DAMAGE SIGNALING

The most prominent response to DNA damage when considering phospho modifications relates to the activation of the ATR/ATM family of kinases. Responding to aberrant DNA configurations, i.e. double stranded DNA breaks or single stranded DNA, their activation upon exposure to DNA damaging agents is expected. Indeed these aberrant DNA structures can be induced, either directly or through processing, by a variety of DNA damaging agents such as cisplatin, UV or ionizing radiation. The manners by which UV lesions can promote ATM/ATR activation are manifold. Although it has been suggested on the basis of *in vitro* studies that UV lesions are directly recognized by components of the ATR signaling cascade (Unsal-Kacmaz et al., 2002), there is no evidence *in vivo* that ATR kinase is activated directly by UV lesions (chapter 4). It should nevertheless be stressed that kinase activation depends on processing of the UV lesions such that a DNA configuration is created that supports signaling.

A process that does lead to UV-induced ATM/ATR activation is DNA replication. As UV lesions cannot be passed by replicative polymerases, the presence of UV photolesions during replication can potentially lead to uncoupling of the polymerase from the replication fork helicase, resulting in extended single stranded DNA regions (Cotta-Ramusino et al., 2005). It is highly likely that these expanses of ssDNA lay at the base of ATR dependent UV mediated signaling during S phase (Byun et al., 2005), although other processes will also contribute. While most lesions are likely to be taken care of by DNA repair or translesion synthesis the possibility exists that the replication fork cannot recover leading to its collapse, a process that is associated with the formation of DSBs. UV lesions can therefore albeit indirectly activate ATM signaling.

Signaling is, however, not restricted to cycling cells as various mechanisms exist that evoke an ATR response in G0/G1 cells as well. One route to signaling proceeds via NER itself. Once a damage containing oligo is removed by NER the resulting structure, an approximately 35 nucleotide single stranded DNA gap bound by a single RPA moiety, should in principle be able to support ATR signaling. There are, however, two caveats: the time that such structures exist and the size of the formed gap. During the process of NER the gapped intermediates are expected to exist only transiently as they are removed by the

replicative polymerases δ or ε. Nevertheless, under certain conditions the process of gap filling might be attenuated. The abundance of factors required for gap filling such as PCNA, DNA polymerase δ/ε or ligase I is reduced in non-cycling cells (Zeng et al., 1994;Kurki et al., 1986;Moser et al., 2007). It can therefore be considered that upon high DNA lesion induction there might be an insufficient level of post-incision factors to complete repair, thus stabilizing the gapped DNA intermediates. A similar effect has previously been demonstrated in primary lymphocytes in which inhibition of repair was observed due to very low level of deoxyribonucleosides (Green et al., 1996).

A gap created by NER and covered by a single RPA unit would comply with the known structural requirements for ATR activation. Given that ssDNA patch size is a determinant for ATR activity, such minimal gaps as generated by NER are expected to promote signaling less efficiently then the large ssDNA regions formed after replication stalling (MacDougall et al., 2007). In fact, much of the ATR signaling after UV exposure of quiescent cells is dependent on the exonuclease EXO1 suggesting extension of the ssDNA gap (Sertic et al., 2011). It is unclear whether the conversion from a persistent NER gap to a resected gap is a ubiquitous event or whether it affects merely a small subset of NER gaps. The mechanism by which EXO1 would participate and is recruited to these gaps has also not been established. One possibility lies in the presence of a PCNA interaction domain (PIP-box) on EXO1 which perhaps could facilitate the recruitment to persistent gaps provided that PCNA, or any upstream components essential for PCNA loading, are not rate limiting factors.

Activation of ATR through the resection of NER induced gaps engages the G1/S checkpoint, preventing cells from entering S-phase. Such a safeguard would prevent the formation of toxic DSBs that are likely to form when replication forks encounter these gaps. It can, however, be envisioned that even in non-replicating cells the resection of gaps can lead to DSBs i.e. if during resection a ssDNA gap is encountered on the opposite DNA strand. The frequency of such events would be predicted to increase exponentially with higher DNA damage loads and could potentially lead to chromosomal rearrangements.

While repair of UV lesions via GG-NER contributes to signaling it has also become apparent that a failure to swiftly remove lesions equally is a cause for ATR activation. As already mentioned it is not the lesion per se, but rather a processed form of the lesion that underlies activation. Both in the presence and absence of GG-NER DNA damage signaling correlates with the formation of DNA breaks and in the latter case is controlled, at least in part, through APE1 dependent processing. Why APE1 acts on UV lesions is unclear. It is known that cytosine residues within UV photolesions are more prone to deamination events (Peng and Shaw, 1996) which might activate UNG glycosylase and subsequently APE1. Arguing against this, however, is the observation that XPE deficient cells that lack the capacity to remove CPD, fail to activate ATR when other GG-NER deficient cells do. Alternatively it is possible that aberrant nucleotides are a direct target for APE1 endonuclease activity as has been demonstrated *in vitro* (chapter 4, Ischenko and Saparbaev, 2002).

THE ENIGMA OF RNA POLYMERASE ARREST AND SIGNALING

An additional mechanism that activates DNA damage signaling exists which is mediated by RNA polymerase II (RNAPII) arrest (Yamaizumi and Sugano, 1994). This signaling is particularly pronounced in TC-NER deficient cells with transcription stalling lesions like UV photoproducts and is characterized by high induction of p53. It is more than 10 years ago that RNA polymerase stalling, by either DNA damage or RNAPII inhibitors, was shown to control signaling yet a mechanistic explanation for this phenomenon has remained elusive. Although it is generally assumed that the stalling of RNA polymerase itself is a determinant for signaling this has not formally been demonstrated. It would be equally possible that indirect effects of transcriptional arrest such as imbalances in RNA transcript levels, the release of incomplete transcripts or disruption of RNAPII associated processes such as splicing, are causal for the observed p53 activation. However, it has been recently been demonstrated that these signaling events are mediated by the ATR kinase (Derheimer et al., 2007) although the mechanistic basis for its activation remains unclear. The archetype structure for ATR activation based on replication stalling and *in vitro* studies is an ssDNA gap coated with RPA. The formation of such gaps would be predicted to be independent of NER mediated incisions given that XPA deficient cells strongly respond to RNAPII stalling. Moreover, the activation of p53 in CS-B cells does not necessarily coincide with the presence of DNA breaks (chapter 4) or RPA (S. Lagerwerf personal communication). Although it cannot be excluded that low frequencies of single strand breaks, not detected by the assays used, can support signaling in the context of a stalled RNA polymerase, it was also observed that p53 activation did not coincide with phosphorylation of H2AX in CS-B cells (chapter 4). When ATR is activated, either upon replication stalling or through GG-NER induced ssDNA gaps, it is capable of phosphorylating H2AX. These differences between canonical ATR activation and activation through RNA polymerase arrest suggest a mechanistically distinct mode for ATR activation in the latter situation.

REFERENCE LIST

1. Bennetzen,M.V., D.H.Larsen, J.Bunkenborg, J.Bartek, J.Lukas, and J.S.Andersen. 2010. Site-specific phosphorylation dynamics of the nuclear proteome during the DNA damage response. *Mol. Cell Proteomics.* **9**: 1314-1323.
2. Byun,T.S., M.Pacek, M.C.Yee, J.C.Walter, and K.A.Cimprich. 2005. Functional uncoupling of MCM helicase and DNA polymerase activities activates the ATR-dependent checkpoint. *Genes Dev.* **19**: 1040-1052.
3. Cotta-Ramusino,C., D.Fachinetti, C.Lucca, Y.Doksani, M.Lopes, J.Sogo, and M.Foiani. 2005. Exo1 processes stalled replication forks and counteracts fork reversal in checkpoint-defective cells. *Mol. Cell* **17**: 153-159.
4. Derheimer,F.A., H.M.O'Hagan, H.M.Krueger, S.Hanasoge, M.T.Paulsen, and M.Ljungman. 2007. RPA and ATR link transcriptional stress to p53. *Proc. Natl. Acad. Sci. U. S. A* **104**: 12778-12783.
5. Green,M.H., A.P.Waugh, J.E.Lowe, S.A.Harcourt, P.H.Clingen, J.Cole, and C.F.Arlett. 1996. Protective effect of deoxyribonucleosides on UV-irradiated human peripheral blood T-lymphocytes: possibilities for the selective killing of either cycling or non-cycling cells. *Mutat. Res.* **350**: 239-246.
6. Ischenko,A.A. and M.K.Saparbaev. 2002. Alternative nucleotide incision repair pathway for oxidative DNA damage. *Nature* **415**: 183-187.
7. Kurki,P., M.Vanderlaan, F.Dolbeare, J.Gray, and E.M.Tan. 1986. Expression of proliferating cell nuclear antigen (PCNA)/cyclin during the cell cycle. *Exp. Cell Res.* **166**: 209-219.
8. MacDougall,C.A., T.S.Byun, C.Van, M.C.Yee, and K.A.Cimprich. 2007. The structural determinants of checkpoint activation. *Genes Dev.* **21**: 898-903.
9. Matsuoka,S., B.A.Ballif, A.Smogorzewska, E.R.McDonald, III, K.E.Hurov, J.Luo, C.E.Bakalarski, Z.Zhao, N.Solimini, Y.Lerenthal, Y.Shiloh, S.P.Gygi, and S.J.Elledge. 2007. ATM and ATR substrate analysis reveals extensive protein networks responsive to DNA damage. *Science* **316**: 1160-1166.
10. Moser,J., H.Kool, I.Giakzidis, K.Caldecott, L.H.Mullenders, and M.I.Fousteri. 2007. Sealing of chromosomal DNA nicks during nucleotide excision repair requires XRCC1 and DNA ligase III alpha in a cell-cycle-specific manner. *Mol. Cell* **27**: 311-323.
11. Peng,W. and B.R.Shaw. 1996. Accelerated deamination of cytosine residues in UV-induced cyclobutane pyrimidine dimers leads to CC-->TT transitions. *Biochemistry* **35**: 10172-10181.
12. Pines,A., C.D.Kelstrup, M.G.Vrouwe, J.C.Puigvert, D.Typas, B.Misovic, G.A.de, S.L.von, B.van de Water, E.H.Danen, H.Vrieling, L.H.Mullenders, and J.V.Olsen. 2011. Global phosphoproteome profiling reveals unanticipated networks responsive to cisplatin treatment of embryonic stem cells. *Mol. Cell Biol.* **31**: 4964-4977.
13. Sertic,S., S.Pizzi, R.Cloney, A.R.Lehmann, F.Marini, P.Plevani, and M.Muzi-Falconi. 2011. Human exonuclease 1 connects nucleotide excision repair (NER) processing with checkpoint activation in response to UV irradiation. *Proc. Natl. Acad. Sci. U. S. A* **108**: 13647-13652.
14. Stokes,M.P., J.Rush, J.Macneill, J.M.Ren, K.Sprott, J.Nardone, V.Yang, S.A.Beausoleil, S.P.Gygi, M.Livingstone, H.Zhang, R.D.Polakiewicz, and M.J.Comb. 2007. Profiling of UV-induced ATM/ATR signaling pathways. *Proc. Natl. Acad. Sci. U. S. A* **104**: 19855-19860.
15. Unsal-Kacmaz,K., A.M.Makhov, J.D.Griffith, and A.Sancar. 2002. Preferential binding of ATR protein to UV-damaged DNA. *Proc. Natl. Acad. Sci. U. S. A* **99**: 6673-6678.
16. Yamaizumi,M. and T.Sugano. 1994. U.v.-induced nuclear accumulation of p53 is evoked through DNA damage of actively transcribed genes independent of the cell cycle. *Oncogene* **9**: 2775-2784.
17. Yazdi,P.T., Y.Wang, S.Zhao, N.Patel, E.Y.Lee, and J.Qin. 2002. SMC1 is a downstream effector in the ATM/NBS1 branch of the human S-phase checkpoint. *Genes Dev.* **16**: 571-582.
18. Zeng,X.R., H.Hao, Y.Jiang, and M.Y.Lee. 1994. Regulation of human DNA polymerase delta during the cell cycle. *J. Biol. Chem.* **269**: 24027-24033.

Addenda

SUMMARY

DNA is the carrier of genetic information and therefore it is important to protect its integrity in order to ensure fitness of the organism. There are many sources that generate DNA damage i.e. through cellular metabolism and through external exposure like solar UV and certain chemicals. To protect against the deleterious effects of DNA lesions cells have at their disposal two defense mechanisms. One protective mechanism is to repair damaged DNA, for which cells have multiple repair pathways to cope with a wide variety of DNA lesions. The second protective mechanism works through signaling pathways controlling cell cycle progression and apoptosis, giving cells time to repair damaged DNA or to remove damaged cells in order to protect the organism. **Chapter 1** and **chapter 2** provide an introduction to various repair pathways and DNA damage signaling.

The UV-DDB complex consisting of DDB1 and DDB2 is the primary factor that detects and binds to UV-induced DNA lesions. Consequently, defects in DDB2 result in defective nucleotide excision repair (NER). Being the first factor in the NER process as well as the factor that binds directly to DNA damage embedded in chromatin leaves open the possibility that the local chromatin environment might be subject to DDB2 dependent changes. Indeed it has been demonstrated that the UV-DDB associated Cul4/Roc1 ubiquitin ligase complex ubiquitylates histones after UV. **Chapter 3** describes the identification of PARP1 as a component of the UV-DDB complex and its possible role in UV dependent chromatin remodeling. The induction of UV lesions results in the formation of poly(ADP-ribose) (PAR) chains at sites of UV damage. The formation of PAR chains was in part due to the presence of single stranded DNA gaps as a result of NER induced incisions. However, part of the PAR formation was found to be independent of single stranded DNA yet dependent on DDB2, indicating a function during the early stages of NER. In fact, DDB2 itself is a target for PARylation and PAR negatively affects the level of ubiquitylation of DDB2. Consistently it was observed that stabilizing PAR modifications through depletion of the PAR removing enzyme PARG increased the DDB2 chromatin retention time, most likely as a result of decreased DDB2 degradation. We also found that the chromatin remodeling protein ALC1 was also recruited to UV exposed DNA in a PAR dependent manner. This recruitment was also observed in XPA deficient cells but was suppressed by DDB2 depletion or PARP inhibition. The role of ALC1 in NER was further demonstrated by depletion of ALC1 or by PARP inhibition as both treatments resulted in reduced CPD repair.

While UV lesions evoke the activation of PARP and thereby affect repair other post translational modifications, most notably phosphorylation, serve to inhibit cell cycle progression. **Chapter 4** describes the central role of the ATR kinase in activation of cell cycle checkpoints after UV exposure. Surprisingly, it was found that checkpoint proteins were activated in both normal repair proficient cells as well as in global genome NER (GG-NER) deficient cells independent of replication. Activation of p53 was rapid in normal cells with p53 levels reducing in time. In contrast, in cells with a defect in GG-NER p53 was more delayed to normal cells but, crucially, p53 levels did not diminish. Similar differences in kinetics between repair GG-NER proficient and deficient cells were also observed for phosphorylation of H2AX and suggest that the underlying cause for checkpoint activation

differs between repair proficient and deficient cells. Nonetheless, in both cases the activation of checkpoint proteins depends on the ATR kinase. Consistent with the activation of ATR, DNA breaks were detected in both normal and repair deficient cells. The latter is remarkable as the repair deficiency precludes the formation of DNA breaks as part of the NER process. The presence of breaks and their persistent nature in GG-NER deficient cells is supported by the recruitment of replication factors PCNA, polδ and polη to sites of UV damage. These data indicate that rather than being directly activated by UV lesions prior processing needs to occur. We show that APE1 exhibits endonuclease activity on UV lesions. As the incision by APE1 occurs 5' of the lesion without removing it this might result in a structure that is refractory to repair and eventually provokes ATR signaling.

While ATR and the related kinases ATM and DNA-PK_{cs} are known to respond to DNA damage and are likely to phosphorylate several hundred proteins they are not the only kinases whose activity is influenced by DNA damage. To gain insight into the dynamics of phosphorylation and dephosphorylation following DNA damage, quantitative mass spectrometry analyses were performed using the chemotherapeutic drug cisplatin (described in **chapter 5)**. We identified 183 phosphopeptides with more than 2-fold increase and 194 phosphopeptides that were more than 2-fold decreased phosphorylation levels following cisplatin treatment. As expected, many (46%) of the up regulated phosphopeptides were phosphorylated at an ATM/ATR consensus sequence. Interestingly, some proteins were found to contain both up regulated as well as down regulated sites. Possibly this differential phosphorylation signifies some form of molecular switch. We also tested the hypothesis that changes in RNA transcript levels correlate with changes in protein levels after cisplatin treatment. However, we found no clear correlation between changes in transcript and its corresponding protein. In contrast, pathway analysis based on transcriptomics, proteomics and phosphoproteomics did reveal a large overlap in affected processes. The impact of cisplatin on DNA damage repair pathways was, however, only manifested in the phosphoproteome analysis. This suggests that phosphorylation events are important for DNA repair pathway activation after genotoxic stress.

Chapter 6 describes how cells from individuals with Cornelia de Lange Syndrome (CdLS) respond to genotoxic stress. CdLS is a disease where the function of the cohesin complex has been compromised. Cohesin is important for multiple cellular functions i.e. maintaining sister chromatid cohesion, gene regulation, DNA repair and DNA damage signaling. The identification of disease causing mutations in cohesin and associated factors in CdLS individuals prompts the question whether these individuals would be at increased risk when exposed to genotoxic agents. Two fibroblast and five B-cell lymphoblastoid lines were screened for the presence of pathogenic mutations in the *NIPBL* and *SMC1A* gene. Mutations in the *NIPBL* gene were detected in one fibroblast and two B-cell lymphoblastoid lines whereas no causative genetic alterations were found in the other cell lines. Clonal survival assays indicated that CdLS cells have no clear increased sensitivity for ionizing radiation (IR). In contrast, exposure to the DNA crosslink-inducing agent mitomycin C (MMC) revealed increased sensitivity of all CdLS lines compared to normal controls. Although CdLS cells did not show decreased survival upon IR exposure

there was a marked increase in chromosomal aberrations when exposed in G2 but not when exposed in G1, suggesting homologous recombination is impaired. Chromosomal aberrations were also increased after MMC. It should be noted that the reduced survival and increased chromosomal aberrations were observed in al CdLS cells regardless of the presence or absence of *NIPBL* mutations. This study demonstrates that CdLS cells have increased sensitivity for certain DNA damaging agents highlighting potential health risk for CdLS individuals when exposed to such agents.

NEDERLANDSE SAMENVATTING

DNA is de drager van genetische informatie en het is daarom van essentieel belang om de integriteit van deze informatie te beschermen en daarmee het organisme. Beschadiging van DNA kan het gevolg zijn van vele processen zoals de vorming van schadelijke moleculen door cellulaire metabolismen en door blootstelling aan bepaalde chemicaliën in onze leefomgeving of UV-straling van de zon. Om de cel te vrijwaarden van de gevolgen van DNA veranderingen beschikt deze over beschermingsmechanismen. Een van de mechanismen is om DNA schade te herstellen. Om dit te bereiken beschikken cellen over meerdere herstelsystemen die in staat zijn om een breed scala aan DNA afwijkingen te corrigeren. Een ander beschermingsmechanisme maakt gebruik van signaaltransductie waarbij processen zoals cel cyclus progressie en apoptose (celdood) worden gereguleerd. **Hoofdstukken 1 en 2** geven een introductie in DNA schade herstelsystemen en signalering.

Het UV-DDB complex bestaat uit DDB1 en DDB2 en is de belangrijkste factor voor detectie van en binding aan UV geïnduceerde DNA schade. Defecten in DDB2 resulteren dan ook in nucleotide excisie herstel (NER) deficiëntie. De eigenschap om aan beschadigd DNA te binden in de context van chromatine opent de mogelijkheid dat het lokale chromatine onderhevig is aan UV-DDB afhankelijke modificaties. **Hoofdstuk 3** beschrijft de identificatie van PARP1 als een component van het UV-DDB complex en de mogelijke rol in UV afhankelijke chromatine veranderingen. Behandeling van cellen met UV straling resulteert in de formatie van poly(ADP-ribose) (PAR) ketens op de plaats van de schade. De vorming van PAR ketens is gedeeltelijk afhankelijk van enkelstrengs DNA formatie als gevolg van de NER reaktie. Echter, een gedeelte van de PAR formatie vindt plaats in afwezigheid van enkelstrengs DNA en hiervoor is DDB2 essentieel, indicatief voor een rol gedurende de eerste stappen van het NER proces. We tonen verder aan dat PAR belangrijk is voor de dynamiek en stabiliteit van DDB2 en de rekrutering van de chromatine remodeler ALC1. Depletie van ALC1 of inhibitie van PAR resulteert in verminderd herstel van UV schade wat de rol van ALC1 in NER onderschrijft.

Naast inductie van PAR resulteert de aanwezigheid van UV schade ook in fosforylatie, een andere eiwitmodificatie met een belangrijke rol in de regulatie van de celcyclus. **Hoofdstuk 4** beschrijft de rol van ATR kinase na blootstelling aan UV. We vinden dat activatie van checkpoint eiwitten in zowel normale als globaal genoom NER (GG-NER) deficiënte cellen plaatsvindt in een replicatie onafhankelijk proces. Zowel p53 als H2AX worden gefosforyleerd zij het met verschillende kinetiek in normale en GG-NER deficiënte cellen wat suggereert dat er verschillende processen aan ten grondslag liggen. In beide gevallen echter is de activatie afhankelijk van ATR en in overeenstemming hiermee worden DNA breuken gedetecteerd in zowel normale als GG-NER deficiënte cellen. Dit laatst is opmerkelijk aangezien de deficiëntie het ontstaan van breuken als gevolg van NER uitsluit. De aanwezigheid van de replicatiefactoren PCNA, polδ en polη bij UV beschadigd DNA is een verdere indicatie dat breuken worden gevormd. We tonen aan dat breuken gedeeltelijk het gevolg zijn van APE1 endonuclease activiteit op UV schade. Omdat de incisie plaatsvindt aan de 5' zijde van de schade zonder deze te verwijderen resulteert dit mogelijk in een structuur welke moeilijk te herstellen is en uiteindelijk leidt tot ATR activatie.

Hoewel van ATR en de gerelateerde kinasen ATM en DNA-PKcs bekend is dat ze enkele honderden eiwitten fosforyleren na DNA schade wordt de activiteit van andere kinasen ook door schade beïnvloed. Om inzicht te krijgen in de dynamiek van fosforylatie en defosforylatie is kwantitatieve massaspectrometrische analyse uitgevoerd na behandeling met het chemotherapeuticum cisplatina (**hoofdstuk 5**). We hebben 183 fosfopeptides geïdentificeerd die meer dan tweevoudig verrijkt waren en 194 fosfopeptides die meer dan tweevoudig verminderd waren in fosforylatie niveaus na cisplatina behandeling. Zoals verwacht zijn veel (46%) van de verrijkte fosfopeptides gemodificeerd op een ATM/ATR consensus sequentie. Opvallend is dat bij sommige eiwitten zowel verrijking als depletie van fosforylatie wordt gevonden binnen hetzelfde eiwit. Deze differentiële fosforylatie functioneert mogelijk als moleculaire schakelaar. De hypothese dat veranderingen in RNA transcript niveaus correleren met veranderingen in eiwit niveaus na cisplatina is ook getest. Er is echter geen eenduidige correlatie gevonden tussen veranderingen in transcript niveaus en het corresponderende eiwit. Pathway analyse gebaseerd op transcriptomics, proteomics en fosfoproteomics laat echter een grote overlap zien in processen. Het effect van cisplatina op DNA herstel mechanismen is echter alleen manifest in de fosfoproteome analyse en dit suggereert dat fosforylatie belangrijk is voor DNA herstel activatie na genotoxische stress.

Hoofdstuk 6 beschrijft hoe cellen van personen met Cornelia de Lange Syndroom (CdLS) reageren op genotoxische stress. CdLS is een ziekte waarbij het cohesin complex niet correct functioneert. Cohesin is belangrijk voor meerdere cel functies zoals het in stand houden van zuster chromatide cohesie, genregulatie, DNA herstel en DNA schade signalering. De identificatie van pathogene mutaties in cohesin en geassocieerde factoren in CdLS patiënten riep de vraag op of deze personen verhoogd risico lopen wanneer blootstelling aan genotoxische agentia plaats vind. Twee fibroblast en vijf B-cell lymphoblastoïde lijnen werden geanalyseerd op de aanwezigheid van pathogene mutaties in de *NIPBL* en *SMC1A* genen. In een fibroblast en twee B-cell lymphoblastoïde lijnen zijn *NIPBL* mutaties gevonden. In de andere lijnen zijn geen causale genetische afwijkingen gevonden. Klonale survival proeven tonen aan dat CdLS cellen niet gevoeliger zijn voor ioniserende straling (IR) dan controle cellen. Blootstelling aan het DNA crosslink agens mitomycine C (MMC) leidt echter tot verhoogde gevoeligheid vergeleken met normale cellen. Hoewel CdLS cellen een normale overleving hebben na IR vertonen ze verhoogde niveaus van chromosomale afwijkingen na blootstelling G2, maar niet na blootstelling in G1. Dit suggereert een mogelijk defect in homologe recombinatie. Chromosomale afwijkingen zijn ook na MMC verhoogd. De verminderde overleving en verhoogde chromosomale afwijkingen zijn in alle CdLS cellen present ongeacht de aan- of afwezigheid van *NIPBL* mutaties. Deze studie toont aan dat CdLS cellen een verhoogde gevoeligheid hebben voor bepaalde agentia die DNA schade induceren, wat een potentieel gezondheidsrisico kan betekenen voor CdLS patiënten.

CURRICULUM VITEA,

Mischa G. Vrouwe was born on the 30th November 1975 in Ter Aar. He attended the Christelijk Lyceum in Alphen aan den Rijn and received his HAVO diploma in 1992. From 1992 to 1996 he attended the HLO in Leiderdorp studying biotechnology. After the successful completion of the HLO he subsequently started at Leiden University reading chemistry. During his studies he performed an internship at the department of molecular genetics of the Leiden Institute of Chemistry where he worked on the purification of the Rad7/Rad16 complex from saccharomyces cerevisiae. In 2000 he successfully completed his doctoraal exam. He started his PhD. in 2000 at the department of Toxicogenetics (formerly the department radiation genetics and chemical mutagenesis) where he worked on various topics in DNA repair but focusing on UV and ionizing radiation. Between 2008 and 2009 he worked as a research technician where he helped setup an in vitro lung tissue culture system. From 2010 he works as a postdoctoral researcher studying the molecular mechanisms of transcription coupled nucleotide excision repair.

LIST OF PUBLICATIONS

1. Pines, A.*, **M.G.Vrouwe***, Jurgen A. Marteijn, Dimitris Typas, Martijn S. Luijsterburg, Medine Cansoy, Paul Hensbergen, André Deelder, Anton de Groot, Syota Matsumoto, Kaoru Sugasawa, Nicolas Thoma, Wim Vermeulen, Harry Vrieling, and Leon Mullenders. 2012. PARP1 promotes nucleotide excision repair through DDB2 stabilization and recruitment of ALC1. *J.Cell Biol*. In press
2. Luijsterburg,M.S., M.Lindh, K.Acs, **M.G.Vrouwe**, A.Pines, H.van Attikum, L.H.Mullenders, and N.P.Dantuma. 2012. DDB2 promotes chromatin decondensation at UV-induced DNA damage. *J. Cell Biol.* **197**: 267-281.
3. Lagerwerf,S., **M.G.Vrouwe**, R.M.Overmeer, M.I.Fousteri, and L.H.Mullenders. 2011. DNA damage response and transcription. *DNA Repair (Amst)* **10**: 743-750.
4. Pines,A., C.D.Kelstrup, **M.G.Vrouwe***, J.C.Puigvert*, D.Typas*, B.Misovic, A.de Groot, S.von Stechow, B.van de Water, E.H.Danen, H.Vrieling, L.H.Mullenders[+], and J.V.Olsen[+]. 2011. Global phosphoproteome profiling reveals unanticipated networks responsive to cisplatin treatment of embryonic stem cells. *Mol. Cell Biol.* **31**: 4964-4977.
5. **Vrouwe,M.G.**, A.Pines, R.M.Overmeer, K.Hanada, and L.H.Mullenders. 2011. UV-induced photolesions elicit ATR-kinase-dependent signaling in non-cycling cells through nucleotide excision repair-dependent and -independent pathways. *J. Cell Sci.* **124**: 435-446.
6. **Vrouwe,M.G.**, L.H.F.Mullenders. 2009. Nucleotide excision repair: From DNA damage processing to human disease. K.K.Khana and Y. Shiloh (Eds.) The DNA Damage response: Implications on Cancer Formation and Treatment. Springer.
7. **Vrouwe,M.G.,** E.Elghalbzouri-Maghrani, M.Meijers, P.Schouten, B.C.Godthelp, Z.A.Bhuiyan, E.J.Redeker, M.M.Mannens, L.H.Mullenders, A.Pastink*, and F.Darroudi. 2007. Increased DNA damage sensitivity of Cornelia de Lange syndrome cells: evidence for impaired recombinational repair. *Hum. Mol. Genet.* **16**: 1478-1487.

*,[+] Equal author contributions